CONTRACT NAS9-14169
DRL NO. T990
LINE ITEM NO. 4
DRD NO. MA183T
NASA CR-
147433

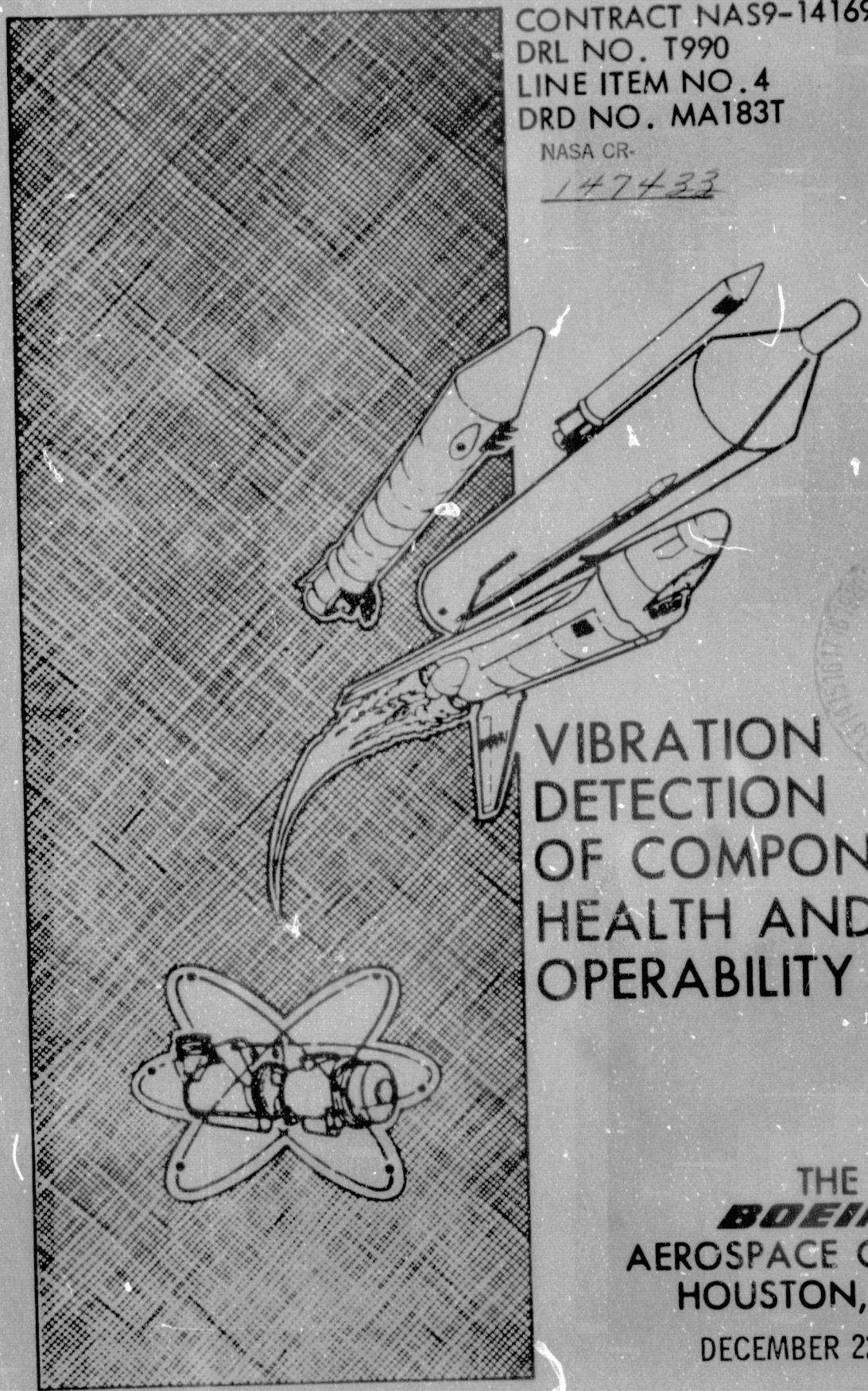

VIBRATION DETECTION OF COMPONENT HEALTH AND OPERABILITY

THE BOEING
AEROSPACE COMPANY
HOUSTON, TEXAS

DECEMBER 22, 1975

TABLE OF CONTENTS

LIST OF FIGURES

LIST OF FIGURES (Continued)

LIST OF FIGURES (Continued)

LIST OF FIGURES (Continued)

LIST OF TABLES

ABSTRACT

In order to prevent catastrophic failure and eliminate unnecessary periodic maintenance in the Shuttle Orbiter Program environmental control system components, some means of detecting incipient failure in these components is required. This study investigated the utilization of vibrational/acoustic phenomena as one of the principal physical parameters on which to base the design of this instrumentation. Baseline vibration/acoustic data was collected from three aircraft type fans and two aircraft type pumps over a frequency range from a few hertz to greater than 300 KHz. The baseline data included spectrum analysis of the baseband vibration signal, spectrum analysis of the detected high frequency bandpass acoustic signal, and amplitude distribution of the high frequency bandpass acoustic signal. A total of eight bearing defects and two unbalancings were introduced into the five test items. All defects were detected by at least one of a set of vibration/acoustic parameters with a margin of at least 2:1 over the worst case baseline. The design of a portable instrument using this set of vibration/acoustic parameters for detecting incipient failures in environmental control system components is described.

DEFINITIONS

BVRMS-1: Baseband Vibration Root Mean Square-1

Ratio of the baseband vibration RMS signal level after the defect is introduced to the maximum baseline vibration RMS signal level. The minimum baseband frequency bandwidth used for the test item is used for BVRMS-1.

RMS-1: Root Mean Square-1

Ratio of the RMS signal level in the high frequency pass band after the defect is introduced to the maximum baseline RMS signal level.

SABVS-5: Spectrum Analysis of the Baseband Vibration Signal-5

Ratio of the defect produced baseband vibration maximum spectral line amplitude at the fundamental frequency associated with the defect, ±3%, to the baseline maximum spectral line amplitude in the same frequency band. This is an important parameter to consider when the baseline contains a major spectral line in the near vicinity of the defect fundamental frequency as the result of other mechanical phenomena. Inexact knowledge as to the correct defect frequency or inaccuracies in processing electronics of any portable component health monitor could easily result in these near spectral lines being mistaken as defect originated. The minimum spectrum analyzer bandwidth used for the test item is uded for SABVS-5.

SABVS-6: Spectrum Analysis of the Baseband Vibration Signal-6

Ratio of the defect produced baseband vibration maximum spectral line amplitude at any frequency contained within the frequency band bounded by the antifriction bearing's three major ball passing frequencies f_o, f_b, and f_i, ± 3%, to the baseline maximum spectral line amplitude in the same frequency band. The minimum spectrum analyzer bandwidth used for the test item is used for SABVS-6.

SADAS-1: Spectrum Analysis of the Detected Acoustic Signal-1

Ratio of the defect produced high frequency bandpass detected signal spectral line amplitude at the fundamental frequency associated with the defect to the baseline spectral line amplitude at the same frequency. The minimum spectrum analyzer bandwidth used for the test item is used for SADAS-1.

SADAS-2: Ratio of the defect produced high frequency bandpass detected signal spectral line amplitude at the fundamental frequency associated with the defect to the baseline maximum spectral line amplitude at any frequency within the minimum SADAS baseband frequency range used for the test item. The minimum spectrum analyzer bandwidth used for the test item is used for SADAS-2.

SADAS-3: Spectrum Analysis of the Detected Acoustic Signal-3

Ratio of the defect produced high frequency bandpass detected signal spectral line amplitude at the frequency associated with the defect to the baseline maximum spectral line amplitude at any frequency within the maximum SADAS baseband frequency range used for the test item. The maximum spectrum analyzer bandwidth used for the test item is used for SADAS-3.

SADAS-4: Spectrum Analysis of the Detected Acoustic Signal-4

Ratio of the defect produced high frequency bandpass detected signal maximum spectral line amplitude at any frequency within the minimum SADAS baseband frequency range to the maximum baseline spectral line amplitude in the same frequency band. This is similar to SADAS-2, differing only in that the defect produced spectral line does not have to be at the fundamental defect frequency. Thus, if a defect results in increased rattling at the shaft frequency, and this is the maximum spectral line in the band, then it is used in calculating SADAS-4. The minimum spectrum analyzer bandwidth used for the test item is used for SADAS-4.

SADAS-5: Spectrum Analysis of the Detected Acoustic Signal-5

Ratio of the defect produced high frequency bandpass detected signal maximum spectral line amplitude at the fundamental frequency associated with the defect, ±3%, to the baseline maximum spectral line amplitude in the same frequency band. SADAS-5 is the high frequency bandpass detected signal equivalent of SABVS-5. The minimum spectrum analyzer bandwidth used for the test item is used for SADAS-5.

SADAS-6: Spectrum Analysis of the Detected Acoustic Signal-6

Ratio of the defect produced high frequency bandpass detected signal maximum spectral line amplitude at any amplitude contained within the frequency band bounded by the antifriction bearing's three major ball passing frequencies f_o, f_b, and f_i, ±3%, to the baseline maximum spectral line amplitude in the same frequency band. SADAS-6 is the high frequency bandpass detected signal equivalent of SABVS-6. The minimum spectrum analyzer bandwidth used for the test item is used for SADAS-6.

SANDAS-1 to 6: Spectrum Analysis of the Normalized Detected Acoustic Signal-1 to 6

These are the normalized versions of SADAS-1 to 6, respectively. Normalization is made with respect to the high frequency bandpass RMS signal levels.

SEACOST-1: Spike Energy Above Constant Sigma Threshold-1

Ratio of the 3σ (RMS level = 1σ) spike voltage level determined after the defect is introduced to that determined from the worst case baseline.

TCCFR-1: Threshold for Constant Count to Frequency Ratio-1

Ratio of the threshold required to obtain a Counts/Minute rate of 1.5 x center frequency which is determined after the defect is introduced to that determined from the worst case baseline.

TCCFR-2: Threshold for Constant Count to Frequency Ratio-2

Ratio of the threshold required to obtain a Counts/Minute rate of 5×10^{-3} x center frequency which is determined after the defect is introduced to that determined from the worst case baseline.

RESULTS

A total of eight bearing defects and two unbalance defects were introduced into the five test items. All the defects were detected with a margin of at least 2:1 by at least one of the vibration/acoustic processed parameters. Table I provides a SUMMARY OF RESULTS. The vibration/acoustic parameters shown in this table are a set of parameters around which the design of instrumentation for detecting incipient defects in Environmental System Components could be based. Five high frequency passbands with approximately equal logarithmic separation are shown in the table for the high frequency parameters. In actuality, the 20 KHz bandpass frequency was not optimum for any of the defects but was included in the set of frequencies to maintain the approximate equal spacing. A 20 KHz frequency would probably be optimum for detecting a bearing defect which would be a cross between a small spall and a brinelled indentation.

The most significant parameter value shown in Table I is the margin by which the most successful single parameter from the set exceeds its worst case baseline value. The easiest defect to detect was an outer race simulated spall for the Rotron Fan for which the most significant parameter varied from 157 to 438. The hardest defect to detect was the water lubricated bearing in the Hydrokinetics Pump for which the most significant parameter for the vibration accelerometer was 2.02. The most significant parameter value varied from 4.21 to 120 for the other bearing defects and from 3.08 to 8.63 for the unbalance defects.

TABLE I. SUMMARY OF RESULTS

TEST ITEM	FAULT	TRANSDUCER	MOST SIGNIFICANT PARAMETER VALUE	HIGH FREQUENCY BANDPASS VALUE AT MOST OPTIMUM FREQUENCY OF 5 FREQUENCIES (8,20,50,125,300KHz)			BASEBAND VIBRATION VALUE		
				RMS-1	SEACOST-1	SADAS-6	BVRMS-1	SABVS-5 f_s	SABVS-5 f_o
Rotron Aximax 2-464-YS Fan	Brg. Outer Race Defect	B100-2	219	20.1	53.9	219	-	-	-
		B100-3	157	23.5	56.8	157	-	-	-
	Brg. O.R. Def. + Unbalance	B100-2	438	17.4	58.2	438	-	-	-
		B100-3	222	14.0	64.0	222	-	-	-
	Unbalanced	B100-2	3.55	-	-	-	1.44	3.55	-
		B100-3	4.85	-	-	-	1.37	4.85	-
		22-AD25	3.16	-	-	-	1.31	3.16	-
TRW 19A532 Fan	Brg. Ball Defect	B100-0	11.4	1.43	11.4	3.59	-	-	-
		B100-1	6.36	1.42	6.36	2.09	-	-	-
	Brg. Ball Def. if Unbalanced	B100-0	6.36	1.43	6.36	1.83	-	-	-
		B100-1	4.29	1.42	4.29	1.00	-	-	-
	Unbalanced	B100-0	3.73	-	-	-	3.73	3.40	-
		B100-1	3.08	-	-	-	2.30	3.08	-
		2222B-DF83	8.63	-	-	-	6.00	8.63	-
		2222B-DF81	3.82	-	-	-	2.90	3.82	-
Dyn. Air. Eng C050L Fan	Brg. Inner Race Defect	B100-9	16.4	3.09	1.05	16.4	-	-	-
Micropump 10-71-316-1367 Pump	3000# Brinnelled Brg.	B100-5	120	27.6	1.16	120	-	-	-
	1000# Brinnelled Brg.	B100-5	7.41	4.63	2.81	7.41	-	-	-
Hydrokinetics 10461 Pump	Water Lubricated Brg.	B100-8	1.47	1.06	1.15	1.12	.95	-	1.47
		113-342	2.02	-	-	-	.69	-	2.02
	Corroded Bearing	B100-8	4.21	2.72	1.14	3.02	.88	-	4.21
		113-342	9.01	-	-	-	.94	-	9.01
	Bearing Internal Clearance Reduced	B100-8	20.1	5.61	-	20.1	-	-	-
		113-342	84.06	-	-	-	10.25	-	84.06

CONCLUSIONS

The results of this study indicate that it is feasible to utilize mechanical vibration or structure-borne acoustics as one of the principle physical parameters on which the design of instrumentation for determining incipient failures in the Shuttle Orbiter's dynamic components could be based. In order for this instrumentation to be successful, however, it must provide the following capabilities.

1. Provide spectrum analysis of both the low frequency vibration signal and the detected high frequency bandpass acoustic signal.

2. Determine parameters associated with the amplitude distribution of the high frequency bandpass acoustic signal.

3. Process more than a single pass band of high frequencies.

RECOMMENDATIONS

1. Vibration/Acoustic Monitoring of ECS Components During Life Testing

   The main objective of this investigation was to determine a set of vibration/acoustic parameters which would form the basis for the design of instrumentation for detecting incipient failures in environmental control system components. This was done by examining the effect that induced defects in three aircraft type fans and two aircraft type water pumps had on many vibration/acoustic parameters. A set of parameters which was successful at detecting all induced defects in these test items was selected as the basis for the design of the portable instrument described in the DATA ASSESSMENT paragraph. Although the design of the instrument discussed in that paragraph is more flexible than that required to detect the induced defects in the test items, so that it would be capable of detecting most incipient defects in all rotating equipment, more failure data directly related to the environmental system components would be highly desirable in order to optimize the design. The most expedient method for doing this is to monitor the environmental control system components during life testing. Any failures which occur in the ECS components during this life testing would also provide information on vibration/acoustic parameter variation as a function of fault growth and also data on the time between first detection and eventual catastrophic failure, if the failure is allowed to progress that far.

2. Prototype Vibration/Acoustic Portable Instrument

   A prototype vibration/acoustic portable monitoring instrument similar to that described in the DATA ASSESSMENT paragraph should be developed since this was the main purpose of this study. The design of the instrument should reflect the results obtained in the ECS component life testing.

3. Vibration/Acoustic Sensor Development

   The Boeing B-100 IFD sensors which were used in this study were not developed so as to withstand the Space Shuttle environment or maintain a stable sensitivity over the temperature range imposed by the ECS components. A transducer should be developed which will meet these requirements and still provide the required sensitivity versus frequency response. As an alternate to the transducer development, presently available vibration accelerometers and acoustic emission sensors should be investigated as possible candidates for a suitable operational component health monitoring sensor.

INTRODUCTION

Present spacecraft design requires that sufficient redundancy be provided to allow mission completion or assure a safe abort following a component failure. Component design life has been normally fixed by planned mission duration, where mission lengths are relatively short (<30 days).

The requirements for multiple missions using the same hardware in the Shuttle Orbiter Program impose operational lifetime requirements on dynamic components which may require periodic hardware replacement to preclude flight failures. The present state-of-the-art requires that components be disassembled to determine if abnormalities exist which would necessitate hardware replacement. In order to be able to avoid equipment disassembly, which often introduces abnormalities into hardware, it is necessary to have instrumentation capable of determining incipient hardware failures.

The objective of this study was to investigate the feasibility of utilizing mechanical vibration or structure-borne acoustics as one of the principle physical parameters on which the design of this incipient failure instrumentation could be based. This investigation was to be accomplished by examining the effect of introducing incipient faults into the antifriction bearings of three fans and two water pumps which were typical of the Shuttle Orbiter environmental control system components. The vibration/acoustic signal from each of these test items after the fault was introduced was to be compared with the worst case baseline signal from the non-faulted device to determine the changes which could be attributed to the fault. The vibration/acoustic signals from the test items were to be examined by measuring various statistical parameters associated with the signals. If the induced fault resulted in increasing one or more of these statistical parameters by a significant amount over its worst case baseline value, then those parameters would be considered to be good indicators of the induced fault. After analyzing the results from all the faults it was expected that a family of measurable statistical parameters could be selected, out of which at least one parameter from the family would provide a significant detectability of each of the induced incipient defects. Instrumentation could then be designed which would measure this family of statistical parameters for actual Shuttle Orbiter dynamic components and compare them against stored baseline values resulting in a high probability of detecting incipient hardware failure.

HARDWARE TYPES (reference paragraph 3.2.1 of SOW)

Photographs of the hardware items which were tested are shown in Figures 1 through 5. A list of the operating specifications for each test item is given in Table II, and a list of the bearing types with their specifications is shown in Table III. These hardware items were selected after an extensive search of available or easily modified fans and pumps. They represent a good cross section of manufacturers and operating speeds. All items used 115 VAC, 400 Hz, single phase power and could be easily disassembled for fault injection.

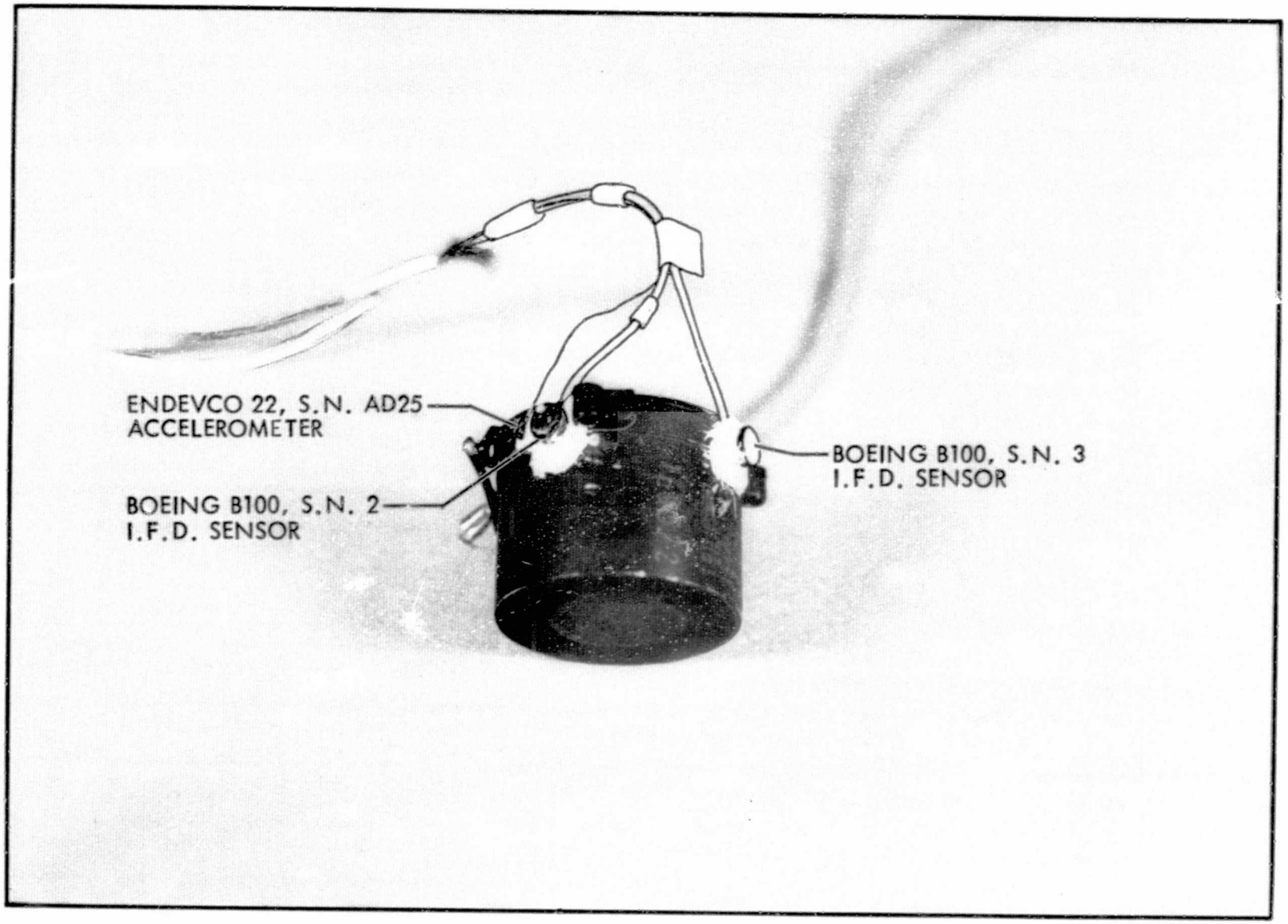

FIGURE 1 ROTRON AXIMAX 2-464-YS FAN

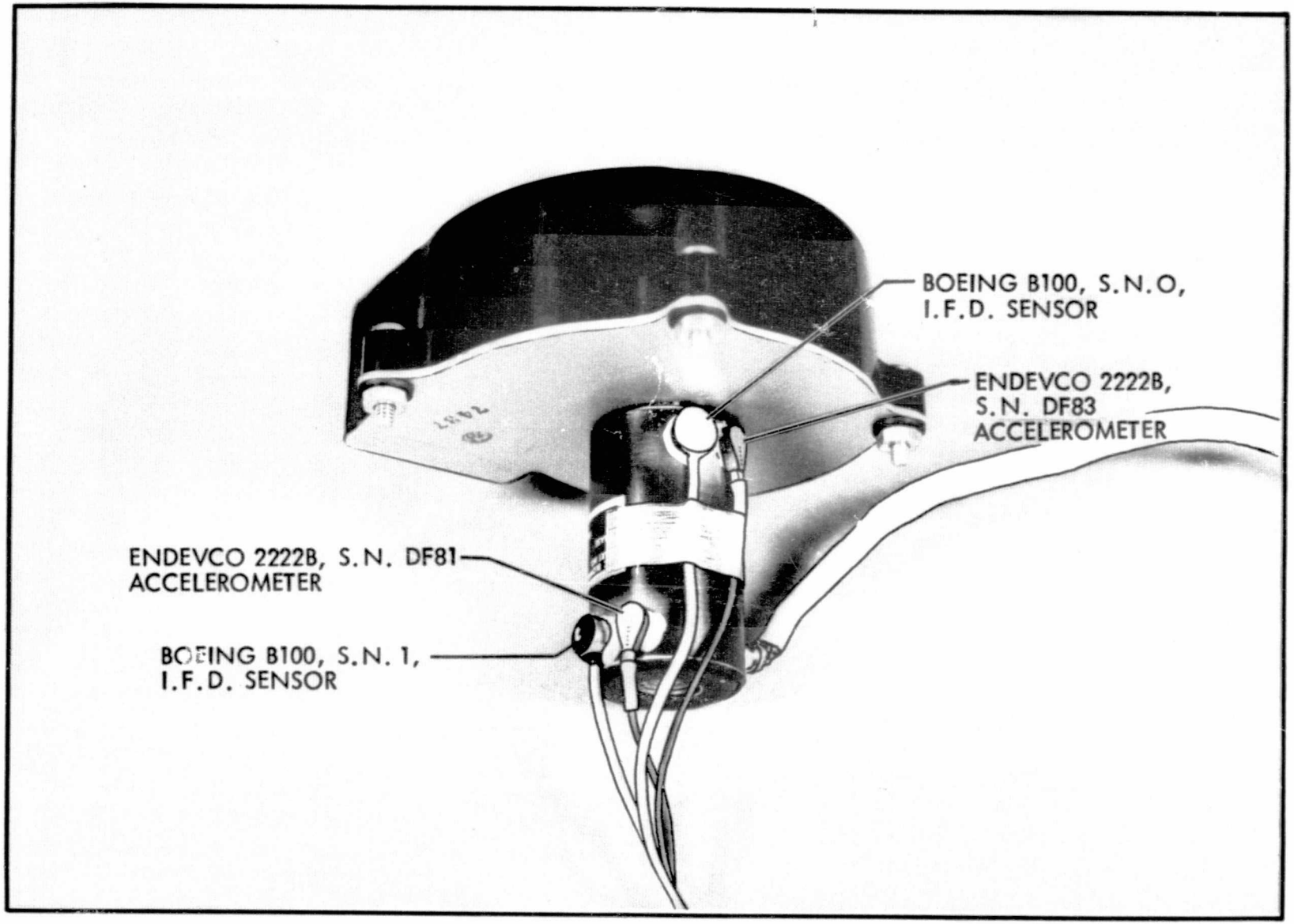

FIGURE 2 TRW GLOBE 19A532 FAN

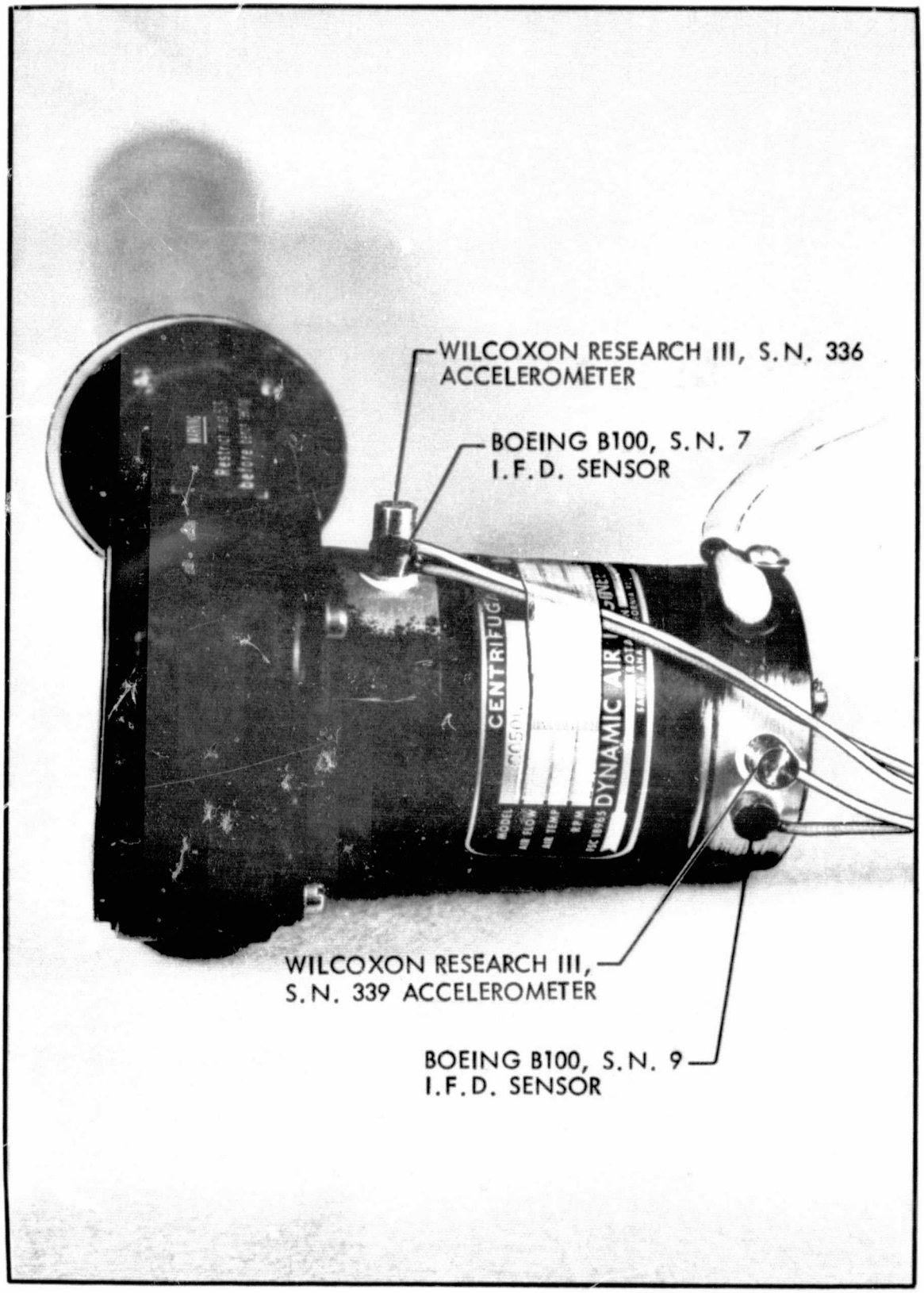

FIGURE 3 DYNAMIC AIR ENGINEERING C050L FAN

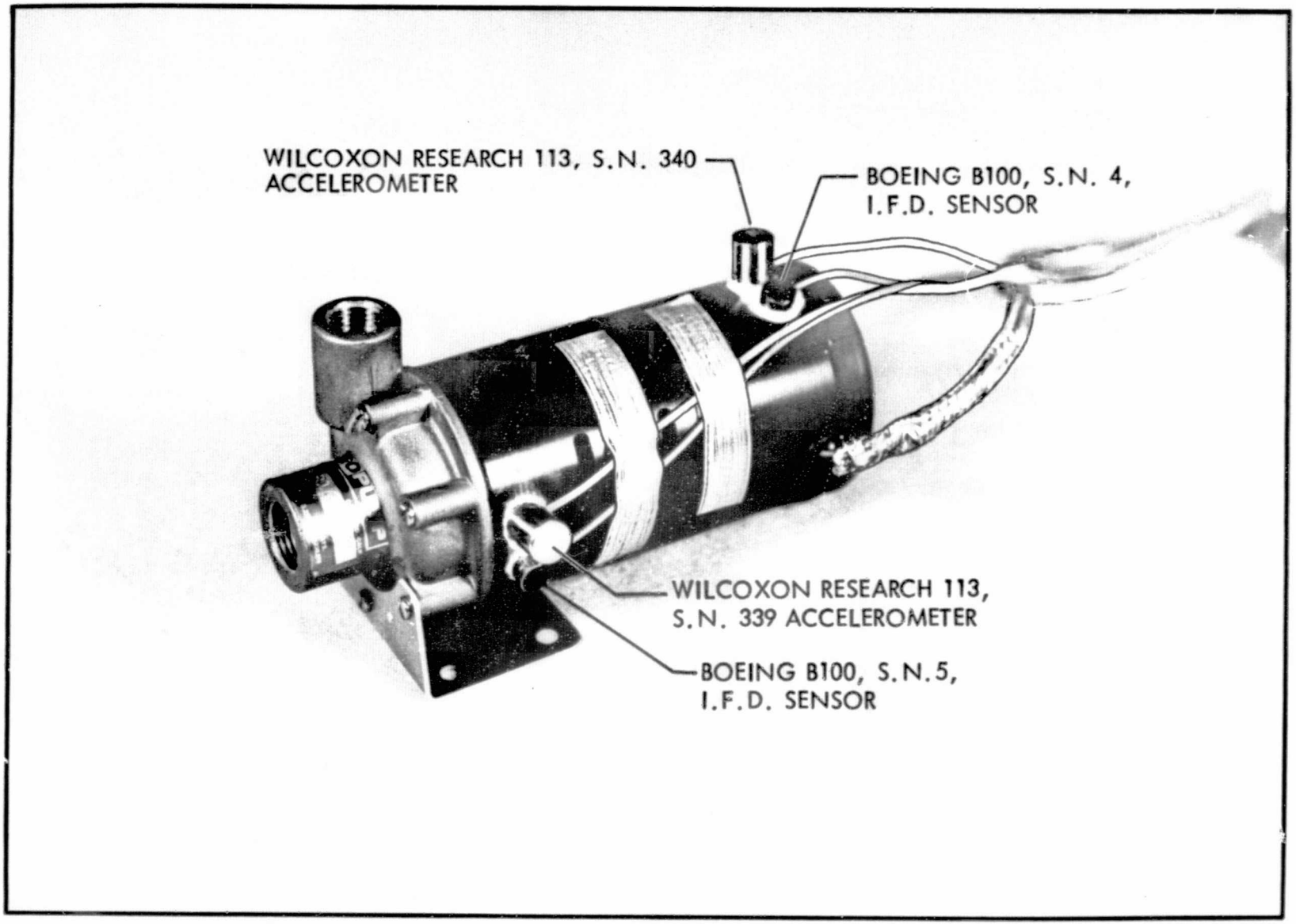

FIGURE 4 MICROPUMP 10-71-316-1367 PUMP

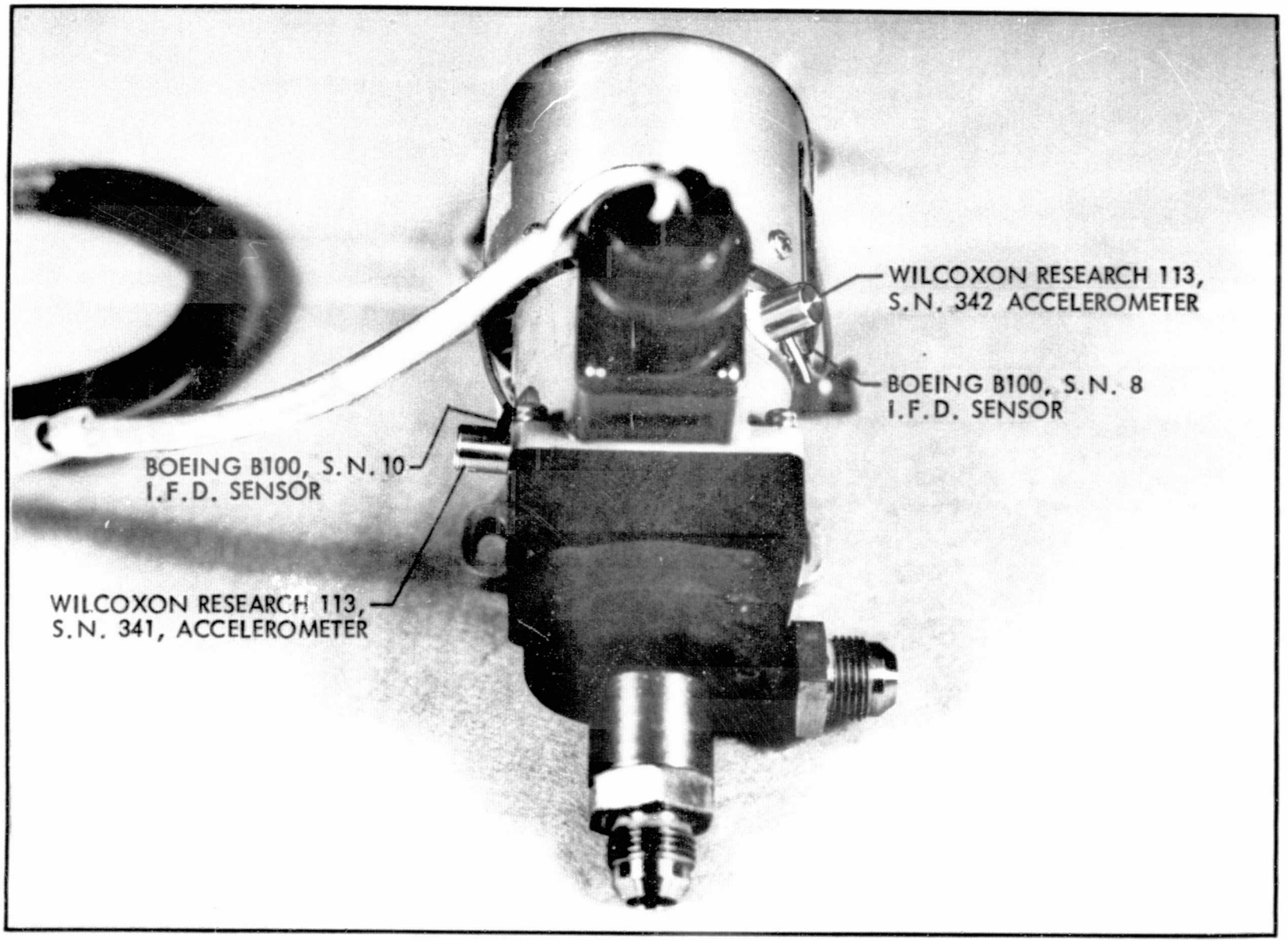

FIGURE 5 HYDROKINETICS 10461 PUMP

TABLE II. TEST HARDWARE OPERATING SPECIFICATIONS

HARDWARE TYPE	MANUFACTURER	MANUFACTURER DESIGNATION	SHAFT SPEED RPM	FLOW RATE M^3/SEC (FT^3/MIN) [GAL./MIN]	DIFFERENTIAL PRESSURE PASCAL (IN. H_2O) [PSI]	INPUT CURRENT AMPERE	PHASE ANGLE RADIAN	INPUT POWER WATT
AXIAL BLOWER	ROTRON MFG. WOODSTOCK N.Y.	AXIMAX 2-464-YS	10900	8.85×10^{-3} (18.75)	186 (.747)	.113	.576	10.9
SQUIRREL CAGE BLOWER	TRW GLOBE IND. DAYTON, OHIO	19A532	5790	9.59×10^{-3} (20.3)	206 (.827)	.361	.838	27.8
CENTRIFUGAL BLOWER	DYNAMIC AIR ENGINEERING SANTA ANA, CALIF.	C050L	23470	1.89×10^{-2} (40.0)	4360 (17.5)	2.02	.158	229
CENTRIFUGAL PUMP (LOW) (PRESSURE)	MICROPUMP CO. CONCORDE, CALIF.	10-71-316-1367	10250	7.5×10^{-5} [1.2]	157000 [22.8]	.677	.402	71.6
CENTRIFUGAL PUMP (HIGH) (PRESSURE)	HYDROKINETICS INC. OCEANSIDE, CALIF.	10461	23310	7.5×10^{-5} [1.2]	647000 [93.8]	3.35	.035	385

TABLE III. TEST HARDWARE BEARING SPECIFICATIONS

TEST ITEM	BEARING CLOSEST TO IMPELLER					BEARING FARTHEST FROM IMPELLER				
	TYPE	NO. BALLS	PITCH DIAMETER METER (INCH)	BALL DIAMETER METER (INCH)	CONTACT ANGLE RADIAN	TYPE	NO. BALLS	PITCH DIAMETER METER (INCH)	BALL DIAMETER METER (INCH)	CONTACT ANGLE RADIAN
Rotron Aximax 2-464-YS	Barden VSR2-5SS4C	6	5.753×10^{-3} (.2265)	1.524×10^{-3} (.060)	0	Barden VSR2-5SS4C	6	5.753×10^{-3} (.2265)	1.524×10^{-3} (.060)	0
TRW 19A532	Globe 15D013A056	7	7.938×10^{-3} (.3125)	2.381×10^{-3} (.09375)	0	Globe 15D013A056	7	7.938×10^{-3} (.3125)	2.381×10^{-3} (.09375)	0
Dynamic Air Eng. C050L	D.A.E. K271D-38SSEL	7	1.471×10^{-2} (.5790)	3.969×10^{-3} (.15625)	.1728	D.A.E. K271D-R4SSEL	8	1.102×10^{-2} (.4340)	2.381×10^{-3} (.09375)	.2234
Micropump 10-71-316-1367	Fafnir SIKDD7	8	1.089×10^{-2} (.4288)	2.381×10^{-3} (.09375)	0	Fafnir SIKDD7	8	1.089×10^{-2} (.4288)	2.381×10^{-3} (.09375)	0
Hydrokinetics 10461	Barden 38SSTX2-K5G32	7	1.471×10^{-2} (.5790)	3.969×10^{-3} (.15625)	.1728	Barden R4ASSTA-5G32	6	1.250×10^{-2} (.4920)	3.572×10^{-3} (.14063)	.1815

TEST RIG (reference paragraph 3.2.2 of SOW)

Photographs of the two test rigs are shown in Figures 6 and 7 and the test rig schematics are shown in Figure 8. The design philosophy for the test rigs was to insure that removal and replacement of the test article did not compromise data repeatability. Different mounting configurations for the test items were tried, varying from special shock isolated fixtures to simply laying the test item on layers of two inch thick foam rubber. The best repeatability results occurred for all test items, with the exception of the Rotron Aximax fan, when the test item was mounted on two inch thick layers of foam rubber with the top layer contoured out to support the test item in the proper operating position. Best repeatability for the Aximax fan occurred with the fan mounted in a two inch length of two inch diameter rubber hose which was mounted to the end of the test rig's air duct.

The A. C. power supply and throttling valves were used to set the controlled operating parameters for each test item. Both the frequency and voltage of the power supply could be varied. During nominal testing the power supply voltage was set to 115 volts and its frequency to 400 Hz. For all test items, with the exception of the TRW Globe 19A532 fan, the throttling valves were used to set the flow rate shown in Table II. Since the flow rate tended to vary significantly during testing of the TRW fan the throttling valve, in this case, was used to set the differential pressure shown in Table II. During off-nominal testing the voltage and frequency of the A.C. power supply were varied ±10%. The throttling valves were used to vary either the flow rate or differential pressure by a minimum of ±10% and a maximum of +47/-63%.

Instrumentation used exclusively for measuring the test item's operating parameters and environmental conditions and for powering the test item are shown in Table IV. An optical tachometer was used for measuring the test item's RPM for both the Rotron and Globe fans. Since there was no convenient point on the Micropump pump to affix a piece of reflecting tape, which is required when using the optical tachometer, RPM measurements on this item were made by simply filtering the signal from one of the vibration accelerometers with a bandpass filter set at the specified shaft frequency and measuring the resulting filtered signal with an electronic counter. This proved to be just as accurate and simpler to implement than the optical tachometer and thus was used on all further tests.

Table V is a list of the instrumentation sensors used during this study, and Table VI lists some of the accelerometer specifications. The accelerometers, which will provide low frequency, longitudinal mode vibration data, all use piezoelectric ceramics and operate in the shear mode. Their selection was based on their sensitivity, high mounted resonant frequency, low transverse and base strain sensitivities and small size with respect to the test item on which they were used. The Boeing B-100 Incipient Failure Detection (IFD) sensor is a multiple axis vibration/acoustic transducer that was specifically developed for this study and has a non-flat frequency response over a wide frequency range from a few Hertz to several hundred KHz. This sensor was used for providing both low and high frequency vibration/acoustic data. Four sensors were used for each test item, except for the

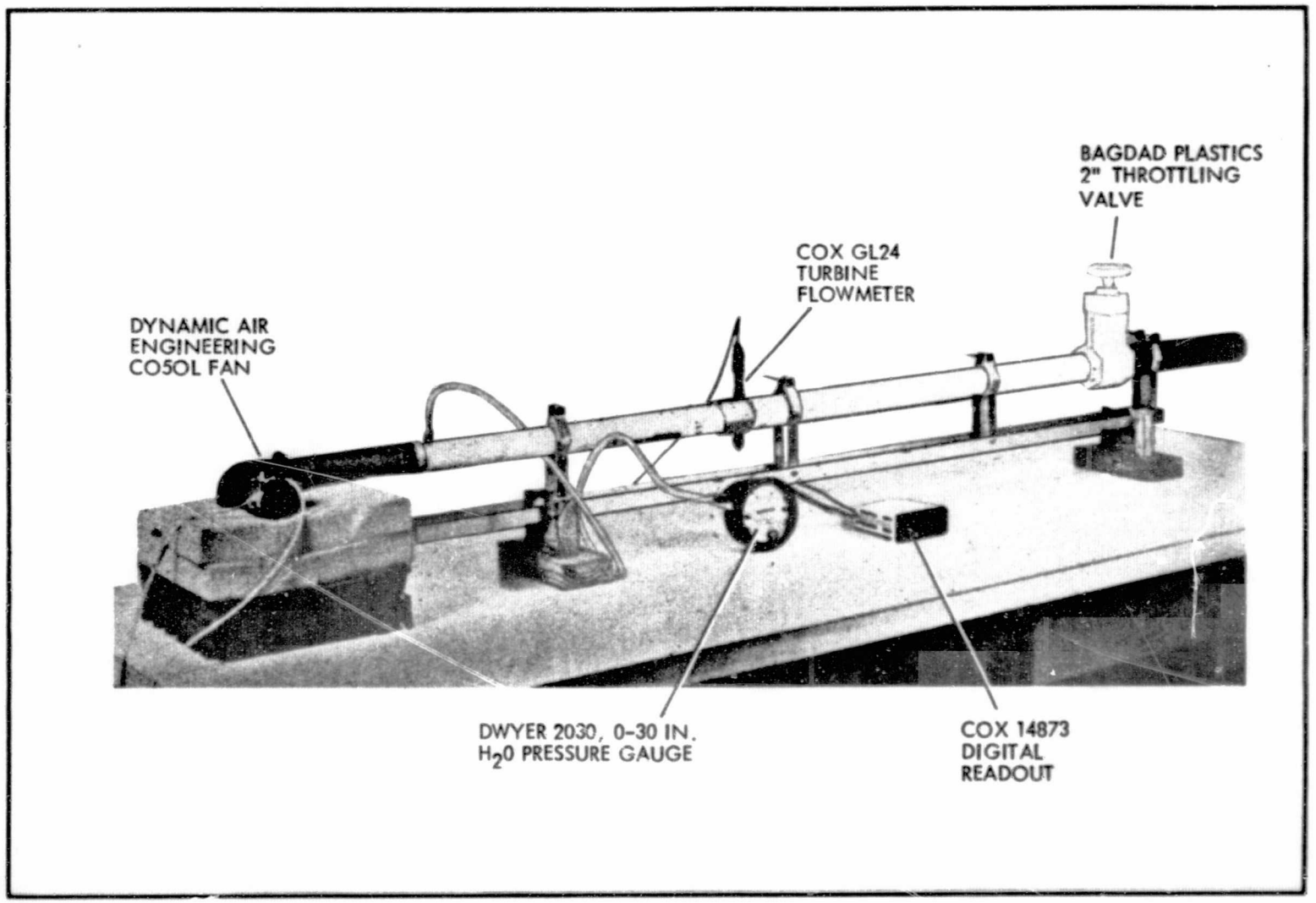

FIG. 6 FAN TEST RIG TYPICAL SETUP

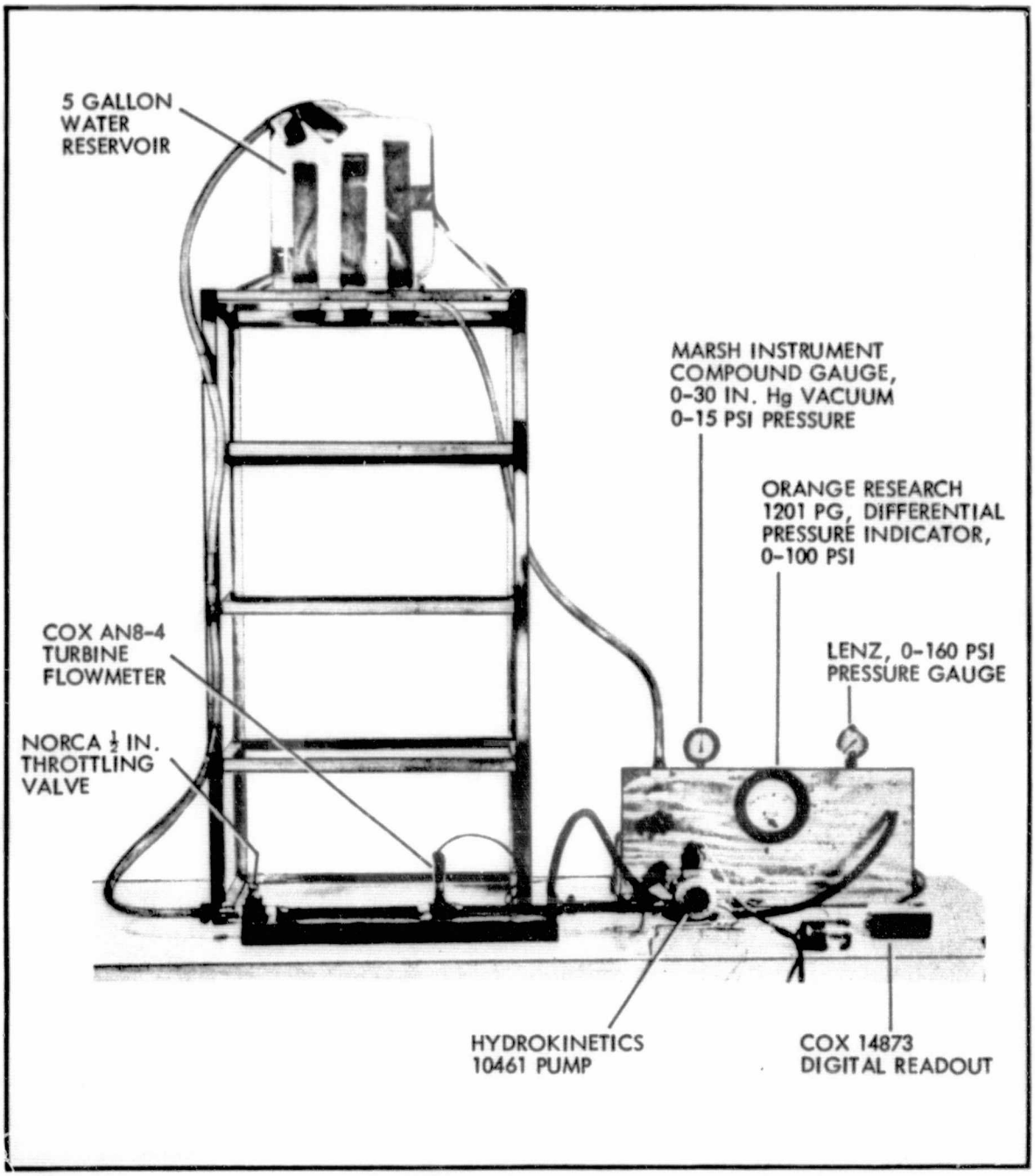

FIG. 7 WATER PUMP TEST RIG
TYPICAL SETUP

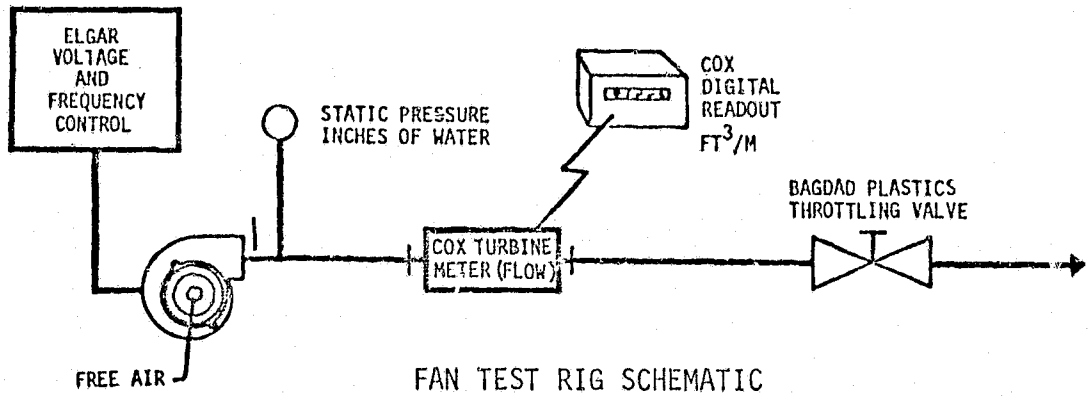

FAN TEST RIG SCHEMATIC

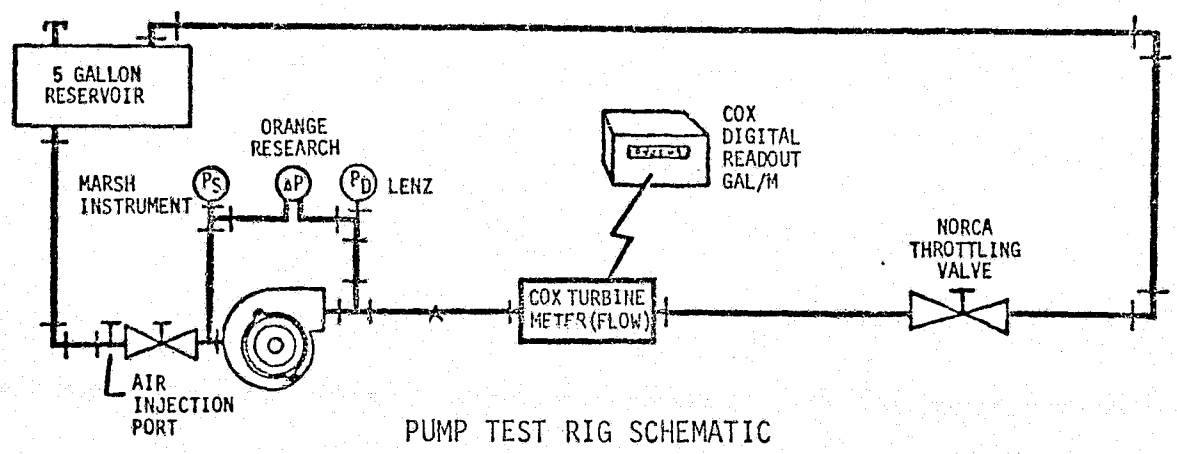

PUMP TEST RIG SCHEMATIC

FIG. 8 TEST RIG SCHEMATICS

TABLE IV. TEST HARDWARE SUPPORT EQUIPMENT

MANUFACTURER	MODEL NO.	DESCRIPTION	USE
ELGAR	501A	500 Watt A.C. Power Source	Power Test Items
ELGAR	400V	Variable Frequency Oscillator	Drive Elgar 501A Power Source
KATO	5EF9P	5000 Watt A.C. Generator	Start up Dynamics Air Fan & Hydrokinetics Pump which were then switched to Elgar P.S.
TAYLOR	-	Thermometer-Barometer	Measure Room Temp. - Barometric Pressure
TEKTRONIX	5103N-D10	Oscilloscope	Measure Phase Angle
TEKTRONIX	5A15N	Amplifier	Measure Phase Angle
TEKTRONIX	5B10N	Time Base/Amplifier	Measure Phase Angle
GEN. RADIO	1432P	Decade Resistor	Rotron Fan 1 ohm Current Sampling Resistor
BOEING	-	.901 Ohm Resistor	Globe Fan & Micropump Pump Current Sampling
BOEING	-	.0527 Ohm Resistor	Dynamic Air Fan & Hydrokinetics Pump Current Sampling
H. P.	400H	RMS Voltmeter	Measure Operating Voltage and Current
BAGDAD PLASTICS	-	2 Inch Throttling Valve	Control Air Flow Rate and Dirrerential Pressure
GLASS INNOVATIONS	-	0-2 IN. H_2O Inclined Manometer	Measure Air Diff. Pressure for Rotron and Globe Fans
DWYER	2030	0-30 In. H_2O Pressure Gauge	Measure Air Diff. Pressure for Dynamic Air Fan
COX	GL24	Turbine Flowmeter	Measure Air Flow Rate for All Fans
COX	14873	Digital Readout	Digital Readout for Cox GL24 Flowmeter
NORCA	-	½ Inch Throttling Valve	Control Water Flow Rate and Differential Pressure
MARSH INSTRUMENT	-	Compound Gauge, 0-30 In. Hg. Vacuum, 0-15 psi Pressure	Measure Suction Pressure for Pumps
LENZ	-	Pressure Gauge, 0-160 psi	Measure Discharge Pressure for Pumps
ORANGE RESEARCH	1201 PG	Differential Pressure Indicator 0-100 psi	Measure Differential Pressure for Pumps
COX	AN8-4	Turbine Flowmeter	Measure Water Flow Rate for Pumps
COX	14873	Digital Readout	Digital Readout for Cox AN8-4 Flowmeter
GRAHAM & WHITE	25	Optical Tachometer	Measure RPM of Rotron and Globe Fans
H.P.	5301A	Counter	Measure RPM

TABLE V. INSTRUMENTATION SENSORS

TEST ITEM	VIBRATION ACCELEROMETER				BOEING B-100 IFD SENSOR S.N.	
	MANUFACTURER	MODEL	S.N.			
			#1	#2	#1	#2
ROTRON AXIMAX 2-464-YS	ENDEVCO	22	AD25	AC88	2	3
TRW 19A532	ENDEVCO	2222B	DF83	DF81	0	1
DYNAMIC AIR. ENG. C050L	WILCOXON RESEARCH	111	336	339	7	9
MICROPUMP 10-71-316-1367	WILCOXON RESEARCH	113	339	340	5	4
HYDROKINETICS 10461	WILCOXON RESEARCH	113	341	342	10	8

TABLE VI. ACCELEROMETER SPECIFICATIONS

MANUFACTURER	MODEL #	OPERATING MODE	WEIGHT (GRAMS)	DIAMETER (IN.)	HEIGHT (IN.)	VOLTAGE SENSITIVITY (mv/g)	CAPACITANCE (pf)	MOUNTED RES. FREQ. (KHz)	TRANSVERSE SENSITIVITY (%)	BASE STRAIN SENSITIVITY (g/μ in.)
ENDEVCO	22	Shear	0.14	0.141	0.095	1.75-1.79	246-259	54	2.2-3.5	.008
ENDEVCO	2222B	Shear	0.5	0.25	0.125	2.7 - 3.6	450-469	32	1.1	.040
WILCOXON RESEARCH	111	Shear	1.0	0.31	0.38	5.75-5.8	240-250	55	5	.002
WILCOXON RESEARCH	113	Shear	4.0	0.41	0.50	22.6-23.5	215-225	36	2-5	.002

TABLE VII. TEST INSTRUMENTATION

A_1	Hewlett Packard Model 465A, 0-20-40 dB Variable Gain Amplifier, S.N. 0970A02701
A_2	Hewlett Packard Model 465A, 0-20-40 dB Variable Gain Amplifier, S.N. 0970A02682
A_3	Hewlett Packard Model 465A, 0-20-40 dB Variable Gain Amplifier, S.N. 0970A02698
Attenuator #1	Boeing Model IFD-10002, 0-43.2 dB Variable Attenuator
Attenuator #2	Kay Model 439 Variable Attenuator, S.N. 32-34
Band Pass Filter	Krohn Hite Model 3202 Variable Band Pass Filter, S.N. 1651
Counter	Hewlett Packard Model 5301A Counter, 19.4 mv Avg. Sensitivity, S.N. 1104A00116
Digital D.C. Voltmeter	Hewlett Packard Model 3440A, S.N. 606-05430
High Pass Filter	Spencer Kennedy Lab Model 302 Variable High Pass Filter, S.N. 796
Low Pass Filter	Spencer Kennedy Lab Model 302 Variable Low Pass Filter, S.N. 796
Oscilloscope	Tektronix Model RM45, S.N. 471 with CA Plug In, S.N. 68255
Precision Detector	Boeing Model IFD-10089
RMS Voltmeter	Hewlett Packard Model 400H, S.N. 001-08389
Signal Generator	Interstate Electronics Corp., Model F55A Function Generator, S.N. 1595
Spectrum Analyzer	Saicor Model SAI-52B 400-Line Spectrum Analyzer/Digital Integrators, S.N. 5111212
Spike Signal Detector	Boeing Model IFD-10088, 3 volt threshold
Strip Chart Recorder	Esterline Angus Model M04A01A4-000 Minigraph Recorder
Tape Recorder	Bell and Howell Model CPR-4010
X-Y Recorder	Houston Instruments Model 2000 X-Y Recorder, S.N. R-5724-1

Rotron fan. Only one accelerometer was used for this item since a special coaxial cable which was used with the Endevco Model 22, S.N. AC88 accelerometer shorted out during mounting repeatability tests and a new cable was not received until after baseline tests were completed. It was suggested from the start of the study, and later confirmed by the test results, that only one B-100 I.F.D. sensor would be required for each test item. However, in order to compare the low frequency performance of the I.F.D. sensors against standard accelerometers and in order to satisfy the SOW, which required a sensor adjacent to each bearing assembly, four sensors were used.

A list of the test instrumentation used in this study is shown in Table VII.

TESTING (PHASE I) (reference paragraph 3.2.3 of SOW)

During Phase I of this study, various statistical parameters associated with the baseline vibration/acoustic signal from each of the non-faulted test items were recorded. The statistical parameters which were recorded can be grouped into four major categories, as follows:

1. Spectrum Analysis of the Detected Bandpassed Vibration/Acoustic Signal

2. Amplitude Distribution of the Bandpassed Vibration/Acoustic Signal

3. Spectrum Analysis of the Baseband Vibration/Acoustic Signal

4. Overall RMS Level of the Baseband Vibration/Acoustic Signal

An understanding of how these statistical parameters can be related to incipient failure in rotating machinery can best be obtained by examining the relationship between these parameters and a typical machinery defect. The defect selected for this example is a spall on the outer race of a ball bearing. Consider the spall just starting to form underneath the outer race rolling surface. As crack propagation takes place beneath the surface, weak acoustic emission pulses are generated. The generation of these acoustic emission pulses could be in a random manner or they could be correlated with the times at which the balls pass over the area where the crack propagation is taking place. These pulses are of very short time duration and thus contain energy over a very wide frequency band. If there were no other source of background noise in the bearing or associated instrumentation, it should be possible to detect these pulses in any frequency band by an examination of the amplitude distribution of the bandpassed or broadband vibration/acoustic signal. However, normal vibration and low frequency background noise makes this impossible for the low frequencies. At high frequencies, this becomes possible as long as the friction produced background signal is low, which usually means the bearing cannot be rotating faster than a few hundred RPM. Generally this is not the case for small aircraft pumps and fans and thus it probably is not possible to detect this very early stage of a bearing defect for this type of component. Eventually crack propagation reaches the surface, resulting

in a surface spall. When this occurs, the balls in the bearing impact the spall at the ball passing rate and generate repetitive vibration/acoustic impulses. Again these pulses contain energy over a very wide frequency range from the low ball passing frequency into the megahertz region. At some frequency within this broad frequency band the ratio of the signal generated by this defect to the normal background signal will be a maximum. This optimum frequency depends on many parameters such as the geometry of the spall and bearing components, the velocity at which the balls impact the spall, signal attenuation of the defect signal from the point of generation to the sensor, background signal characteristics and their attenuation from their sources to the sensor, instrumentation noise characteristics, etc. For a typical incipient spall this optimum detection frequency usually is greater than 10 KHz. Even at this frequency the ratio may be so small that the defect cannot be detected by examining the amplitude distribution of the resulting signal because the defect is so small. Any change in the amplitude distribution of the resultant signal may be swamped by normal statistical variations in the amplitude distribution. However, it still may be possible to detect the effect of the defect on the overall signal by examining a different statistical parameter of this bandpassed signal than just its amplitude distribution. Since the action of the balls impacting the spall generate repetitive vibration/acoustic pulses at the ball passing rate, the amplitude of the bandpassed signal also varies at the ball passing rate. A spectral analysis of the amplitude detected bandpass signal will yield an increase in the spectral line associated with the ball passing frequency. This statistical parameter usually provides the best defect detectability of incipient spalls.

As the spall grows in size, this spectral line also grows in size. The optimum frequency may also change since the spall's geometry is changing. The amplitude distribution of the bandpass signal will also change, by such an extent that they cannot be explained away as normal statistical variations in the amplitude distribution. Since the spall generally results in a pulse type signal, the first recognizable changes in the amplitude distribution of the bandpass signal is in the energy contained in the higher σ levels. As the spall continues to grow, the RMS (root mean square, RMS = 1σ) level will increase beyond the normal statistical variation. Still further increases in spalling may cause the ball passing frequency spectral line associated with the low frequency baseband vibration signal to increase beyond its normal statistical levels. Eventually spalling becomes so bad that increased unbalance occurs and the overall baseband vibration signal will increase beyond its normal limits.

The preceding example has attempted to depict the effect that one type of defect has on the four major categories of statistical parameters that were evaluated in this study. For this particular example, the sensitivity of the parameters at detecting this defect are as previously listed. One may wonder why it was necessary to examine all four categories rather than just the spectrum analysis of the detected bandpass vibration/acoustic signal since this was the most sensitive at detecting this defect. However, in some instances in rotating machinery, a defect produced signal is not repetitive at a constant rate but occurs at a random rate so that the spectral line associated with the defect is reduced in amplitude and broadened out. For this type of defect, variations in the amplitude

distribution of the bandpassed vibration/acoustic signal often provide an earlier indication of an incipient defect. When gross defects such as unbalance occur in a machine the parameters associated with the baseband vibration signal normally provide a better indication than do the bandpassed parameters which usually are non-responsive to this type of defect. Thus, it is important that all four parameter categories be examined in order to achieve the highest probability of detecting all faults.

For the actual data collection the transducers were installed in the locations shown in the photographs in Figures 1 through 5. All transducers were mounted using L. D. Caulk Co. Grip cement which was found to be highly successful at holding the transducers on during the course of the testing.

All test items were operated at 115 VAC, 400 Hz, and at the flow rate or differential pressures shown in Table II and discussed in the paragraph TEST RIG. Following baseline data collection, which will be discussed subsequently, the test items were subjected to the controlled parameter variations shown in Tables VIII through XII with no apparent resonances or anti-resonances noted.

Table XIII is a summary of the baseline data which was collected and processed for all the test items. For the Micropump pump a second set of baseline data was collected since too large of a fault was introduced into an original bearing in the pump and the bearing had to be replaced with a spare bearing. The baseline data taken for the replacement bearing was also made at lower bandpass frequencies since preliminary data for the type of fault which was to be introduced into this bearing indicated that optimum detection would occur at a lower frequency.

The second and third columns of Table XIII show the normal variation in the high frequency (greater than 50 KHz) RMS signal output from a Boeing B100 IFD sensor for a 16 hour or more period, and the number of separate baseline data runs which were conducted on each test item, respectively. After each test item's mounting arrangement was finalized to obtain good data repeatability, the test item was run for a 16 hour or more period, at the controlled nominal parameters, to determine the normal variation in high frequency signal level. It was considered that if this high frequency signal level variation was excessive, then too few baseline runs could result in interpreting normal baseline changes as due to fault insertions when the fault data was collected. Only one test item was found to have excessive variations in the high frequency baseline RMS signal level, the Rotron Aximax fan. For this fan a total of five separate baseline runs were conducted. For all other test items, a total of two baseline runs were considered to be sufficient.

In order to determine the effects of disassembly/reassembly on the measured vibration/acoustic parameters the test items were disassembled as completely as necessary and then reassembled between baseline runs. Exceptions to complete disassembly are shown in Table XIV.

For the Rotron Aximax 2-464-YS and TRW 19A532 fans baseline data was collected and processed for both the Boeing IFD sensors. This was found

TABLE VIII. ROTRON AXIMAX-2-464YS FAN
OFF-NOMINAL OPERATION

CONTROLLED PARAMETER CONDITIONS			RESULTING VARIABLE TEST PARAMETER CONDITIONS				
Voltage (Volts)	Frequency (Hertz)	Flow Rate (m^3/sec)	Current (amp)	Phase Angle (radian)	Power (watts)	RPM	ΔPress (Pascal)
103.5-126.5	400.0	8.35×10^{-3}	.103-.121	.506-.576	9.32-12.84	10,698 -11,106	179.1-196.8
115	360.0-440.0	8.35×10^{-3}	.103-.126	.628-.401	9.58-13.34	9,924 -11,958	149.4-230.6
115	400.0	7.50×10^{-3} -9.20×10^{-3}	.111-.112	.559-.541	10.83-11.04	11,004 -10,920	194.0-181.3

TABLE IX. TRW GLOBE 19A532 FAN

OFF-NOMINAL OPERATION

CONTROLLED PARAMETER CONDITIONS			RESULTING VARIABLE TEST PARAMETER CONDITIONS				
VOLTAGE (Volts)	FREQUENCY (Hertz)	Δ PRESS (Pascal)	CURRENT (Amp)	PHASE ANGLE (Radian)	POWER (Watt)	RPM	FLOW RATE (m^3/sec)
103.5-126.5	400.0	206	.311 - .422	.855	21.1 - 35.0	5,580-6,000	7.87×10^{-3} - 1.111×10^{-2}
115	360.0 - 440.0	206	.400 - .355	.855 - .803	30.2 - 28.4	5,700-5,820	9.19×10^{-3} - 9.83×10^{-3}
115	400.0	124-288	.361	.838	27.8	5,100-6,600	1.028×10^{-2} - 9.19×10^{-3}

TABLE X - MICROPUMP 10-71-316-1367 CENTRIFUGAL PUMP

OFF NOMINAL OPERATION

CONTROLLED PARAMETER CONDITIONS			RESULTING VARIABLE TEST PARAMETER CONDITIONS						
VOLTAGE (Volts)	FREQUENCY (Hertz)	FLOW RATE (m^3/sec)	CURRENT (Amp)	PHASE ANGLE (Radian)	POWER (Watt)	RPM	SECTION PRESSURE (Pascal)	DISCHARGE PRESSURE (Pascal)	ΔP (Pascal)
103.5-126.5	400.0	7.5×10^{-5}	.721-.644	.401-.314	68.7-77.5	9290-10710	6900	138,000-179,000	131,000-172,000
115	360.0-440.0	7.5×10^{-5}	.566-.832	.489-.349	57.5-89.9	9650-10340	6900	145,000-165,000	138,000-158,000
115	400.0	2.8×10^{-5} - 11.0×10^{-5}	.622-.733	.314-.367	68.0-78.7	10550-9930	3500-10300	179,000-152,000	175,000-142,000

TABLE XI - DYNAMIC AIR ENGINEERING CO50L FAN OFF-NOMINAL OPERATION

CONTROLLED PARAMETER CONDITIONS			RESULTING VARIABLE TEST PARAMETER CONDITIONS				
VOLTAGE (VOLTS)	FREQUENCY (HERTZ)	FLOW RATE (M^3/SEC)	CURRENT (AMP)	PHASE ANGLE (RADIAN)	POWER (WATT)	RPM	Δ PRESSURE (PASCAL)
103.5-126.5	400.0	1.89×10^{-2}	2.20 - 1.90	.175 - .192	224 - 236	23,280 - 23,520	4230 - 4330
115	360.0-440.0	1.89×10^{-2}	1.73 - 2.47	.349 - .087	187 - 283	21,200 - 25,580	3490 - 5280
115	400.0	1.33×10^{-2} - 2.46×10^{-2}	1.68 - 2.31	.140 - .175	191 - 262	23,570 - 23,320	4780 - 3810

TABLE XII - HYDROKINETICS 10461 CENTRIFUGAL PUMP

OFF NOMINAL OPERATION

CONTROLLED PARAMETER CONDITIONS			RESULTING VARIABLE TEST PARAMETER CONDITIONS						
VOLTAGE (Volts)	FREQUENCY (Hertz)	FLOW RATE (m^3/sec)	CURRENT (Amp)	PHASE ANGLE (Radian)	POWER (Watt)	RPM	SECTION PRESSURE (Pascal)	DISCHARGE PRESSURE (Pascal)	ΔP (Pascal)
103.5-126.5	400.0	7.5×10^{-5}	3.32-3.53	- .175 - + .244	338 - 433	23140 - 23390	6900	648,000 - 665,000	641,000 - 658,000
115	360.0-440.0	7.5×10^{-5}	3.17-4.04	+ .401 - - .279	336-447	21090 - 25410	6900	541,000 - 783,000	534,000 - 776,000
115	400.0	2.8×10^{-5} - 11.0×10^{-5}	2.98-3.34	.035	342-384	23360 - 23240	3500 - 10300	672,000 - 648,000	669,000 - 638,000

TABLE XIII. SUMMARY OF BASELINE DATA COLLECTED AND PROCESSED

TEST ITEM	High Freq. Variation	No. Baseline Test Runs	Transducer	Bandpass Center Frequency (KHz)													SADAS Baseband Frequency					Baseband Spectrum Frequency						
				2	3	5	8	12.5	20	30	50	80	125	200	300	500	0-500 Hz	0-1 KHz	0-2 KHz	0-5 KHz	0-10 KHz	0-500 Hz	0-1 KHz	0-2 KHz	0-5 KHz	0-10 KHz	0-50 KHz	0-1 MHz
ROTRON AXIMAX 2-464-YS	±5.0db	5	B100-2						x	x	x	x	x	x	x			x		x			x		x	x	x	x
			B100-3						x	x	x	x	x	x	x			x		x			x		x	x	x	x
			22-AD25																				x		x			
TRW 19A532	±1.5db	2	B100-0						x	x	x	x	x	x	x		x		x			x		x		x	x	x
			B100-1						x	x	x	x	x	x	x		x		x			x		x		x	x	x
			2222B-DF83																			x		x				
			2222B-DF81																			x		x				
DYNAMIC AIR ENG. C050L	±0.8db	2	B100-9				x	x	x	x	x	x	x	x	x	x			x		x			x		x	x	x
			111-336																					x		x		
			111-339																					x		x		
MICROPUMP 10-71-316 -1367 1st Brg.	±0.7db	2	B100-5						x	x	x	x	x	x	x			x		x			x		x	x	x	x
			113-339																				x		x			
			113-340																				x		x			
MICROPUMP 10-71-316- -1367 2nd Brg.	-	2	B100-5	x	x	x	x	x	x	x								x		x			x		x	x	x	x
			113-339																				x		x			
			113-340																				x		x			
HYDROKI-NETICS 10461	±2.2db	2	B100-8				x	x	x	x	x	x	x	x	x	x			x		x			x		x	x	x
			113-342																					x		x		

TABLE XIV. DISASSEMBLY RESULTS

TEST ITEM	DISASSEMBLY/ REASSEMBLY AFTER RUN #	EXCEPTIONS TO COMPLETE DISASSEMBLY
ROTRON AXIMAX 2-464-YS	1, 3	None
TRW 19A532	1	None
DYNAMIC AIR ENG. C050L	1	Bearing farthest from impeller was not removed out of its housing or off the shaft. The bearing was forcefitted on the shaft and in the housing and could not be removed with an ordinary bearing puller. Not considered necessary since other bearing was selected to be defected.
MICROPUMP 10-71-316-1367 1st Bearing	1	Bearings were not removed since they were forcefitted on the rotor shaft and removal may have caused them to be damaged.
MICROPUMP 10-71-316-1367 2nd Bearing	1	Bearing farthest from pump's impeller not removed. Not considered necessary since there was no need to remove this bearing from the shaft during fault introduction since the other bearing had been selected as the one to be defected.
HYDROKINETICS 10461	1	Bearing closest to impeller not removed since it was forcefitted on the shaft and could not be removed with an ordinary bearing puller without fear of brinelling the bearing.

to be very time consuming and did not result in any truly significant difference in fault detectability between the two sensors. In order to reduce the amount of test and processing time for the other three test items, a different procedure was followed. As before, during baseline testing, data was collected from all four transducers. However, only that data associated with the two accelerometers and one B100 IFD sensor was processed. During fault testing it was intended that fault data for the other B100 IFD sensor not be collected. However, if it had turned out that the two accelerometers and the single B100 sensor were not capable of detecting the induced fault, baseline data for the other B100 sensor would have been processed and fault data for that sensor would have been collected and processed. This turned out not to be necessary. Baseline data was not reported for the Wilcoxon 113, S.N. 341 accelerometer since it was thought this device had failed after initial data collection. The supposed failure was evidenced by large increases in minimum baseband spectrums. It was later determined, after baseline tests were completed, that the signal from this accelerometer had just increased sufficiently, from normal variations, to cause clipping to occur in the output of the first amplifier. This clipping resulted in the unorthodox baseband spectrum.

Table XIII lists the bandpass center frequencies which were used for collecting the spectrum analysis of the detected acoustic signal (SADAS) data as well as the bandpassed acoustic signal amplitude distribution data. For the Rotron and TRW fans, bandpassed center frequencies from 20 KHz to 300 KHz were used. From past experience, 20 KHz was considered a low enough frequency to determine the optimum band for detecting all bearing defects. The IFD sensors' outputs approached the input noise level of the first amplifier at a frequency slightly greater than 300 KHz. Considering that a 45% bandpass (Bandwidth = 0.45 x Center Frequency) was used throughout the study the number of frequency steps was also considered sufficient to determine an optimum frequency. Following tests on the two fans, the Micropump pump was tested. The same limitation on frequency range was used for this pump as was used for the two fans. However, after fault tests were run on the pump with the initial bearing, and it was determined that bandpass data had not been taken at sufficiently low frequencies, baseline data for the replacement bearing was taken from 2 KHz to 30 KHz. Following baseline tests on the Micropump pump, baseline tests were run on the Dynamic Air Engineering fan and Hydrokinetics pump. Since the optimum frequency for the Micropump pump defect was found to be greater or equal to 8 KHz, baseline data for these two test items was taken at 8 KHz and 12.5 KHz in addition to the higher frequency data. The upper limit of 500 KHz for these two items was a result of the IFD sensor approaching the input noise level of the first amplifier at a frequency higher than this.

Figure 9 is a block diagram of the test setup used for measuring the spectrum analysis of the detected acoustic signal (SADAS). Equipment details are listed in Table VII. An input 22K ohm resistor was used for these measurements, when the bandpass filter was set at 20 KHz and higher, to reject the low frequency signals from the IFD sensor. This was done in order to avoid saturating the first amplifier. Similarly, the high pass filter was used to further reject the lower frequencies in order to avoid saturating the second amplifier. The bandpass filter shown

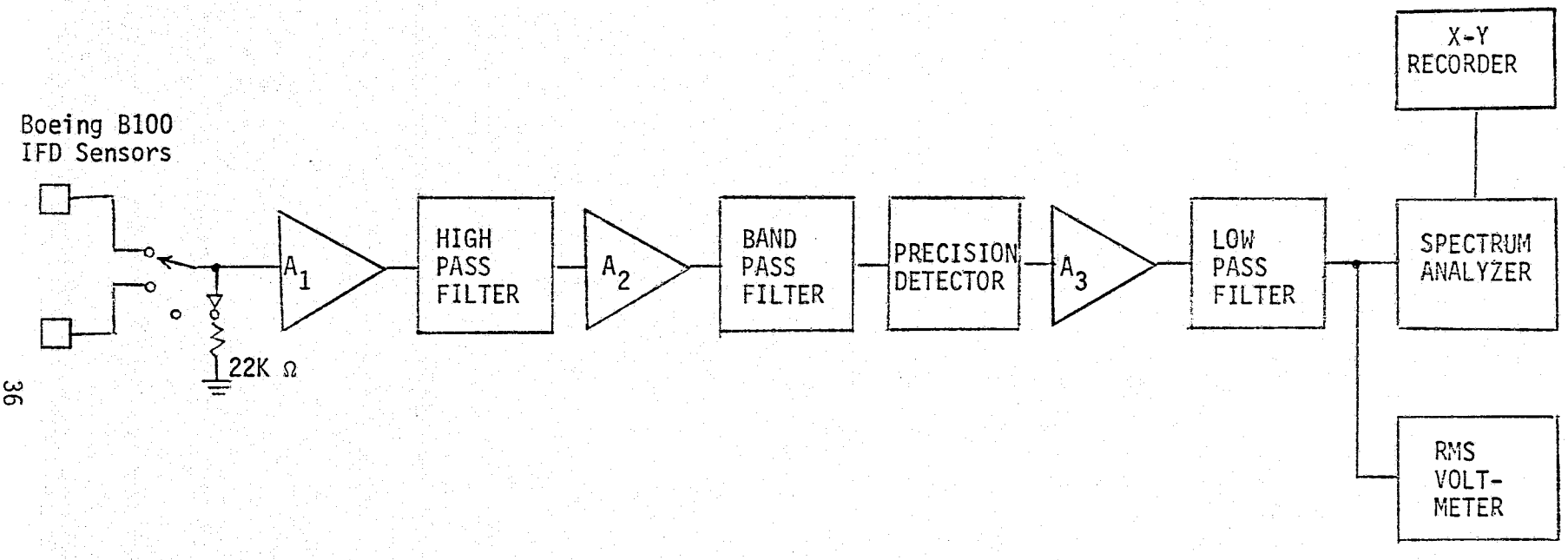

FIGURE 9. VIBRATION/ACOUSTIC PROCESSING CHANNEL FOR MEASURING THE SPECTRUM ANALYSIS OF THE DETECTED ACOUSTIC SIGNAL (SADAS)

in the test setup was actually a Krohn-Hite Model 3202 combination High Pass/Low Pass filter which has a 45% bandwidth when the high pass and low pass sections are both set to the same frequency. Detection of the band-passed signal is done by the precision detector, which has a dynamic range of 40 db. A low pass filter is used after the precision detector to limit the voltage measured by the RMS voltmeter to the frequency range being analyzed by the spectrum analyzer. All signal level measurements made with this setup were referenced to the input of the spectrum analyzer.

Spectrum data for all but the Rotron fan baseline runs were recorded on a single 8-1/2 x 13 inch plot using two different colored inks. For the Rotron fan the five runs were recorded on two sets of 8-1/2 x 13 inch plots using three different colored inks. The plots were then hand traced to another 8-1/2 x 13 inch plot using a (-----) line to indicate the maximum limits and a (——·——·) line to indicate the minimum limits which were determined from the baseline runs. A table listing the hardware operational parameters and the processing equipment parameters and a 30 db scale extension were added to this and the total layout was reduced 39% to an 8-1/2 x 11 inch format on a Xerox machine. The 30 db scale extension was added because it was determined that the original scale was not sufficient to cover the entire dynamic range required by the baseline and fault data. These plots then became the baseline plots on which future fault data would be recorded. Several samples of these baseline plots are shown in Figures 10 through 16.

The hardware operational parameters shown in these figures are in standard S.I. units which are as follows:

Power Supply Voltage	- Voltage	- Volts
Power Supply Frequency	- P.S. Freq.	- Hertz
Flow Rate		- $Meter^3/second$
Current	- I	- Ampere
Phase Angle	- $\phi<$	- Radian
Power	- Pwr	- Watt
Revolutions per min.	- RPM	- --
Suction Pressure	- P_S	- Pascal
Discharge Pressure	- P_D	- Pascal
Differential Pressure	- ΔP	- Pascal
Ambient Temperature	- Temp	- Kelvin
Barometric Pressure	- Baro	- Pascal

Tables XV through XIX are lists of calculated and measured vibration frequencies associated with the test items which may be found in the SADAS plots. The bearing frequencies were calculated using the following equations, which assume a fixed outer race.

$$f_{co} = \frac{f_s}{2} \left(1 - \frac{D_b}{D} \cos \beta\right) \quad (1)$$

$$f_{ci} = \frac{f_s}{2} \left(1 + \frac{D_b}{D} \cos \beta\right) \quad (2)$$

$$f_{sp} = \frac{D}{D_b} \frac{f_s}{2} \left[1 - \left(\frac{D_b}{D} \cos \beta\right)^2\right] \quad (3)$$

$$f_o = nf_{co} \quad (4)$$

$$f_i = nf_{ci} \quad (5)$$

$$f_b = 2f_{sp} \quad (6)$$

f_{co} = fundamental frequency of cage with respect to outer race

f_{ci} = fundamental frequency of cage with respect to inner race

f_{sp} = fundamental ball spin frequency

f_o = fundamental frequency due to flaw in outer race

f_i = fundamental frequency due to flaw in inner race

f_b = fundamental frequency due to flaw in ball

n = number of rolling elements/row

f_s = shaft speed (rps)

D_b = Ball diameter

D = Pitch diameter

β = contact angle

Figure 10, a SADAS plot for the Micropump pump with a bandpass center frequency of 300 KHz, depicts close to the ideal type of spectrum which one would expect from a good, properly preloaded antifriction bearing where rolling friction is the major acoustic source. The acoustic signal generated by this rolling friction usually has an amplitude distribution which is very close to Gaussion with only the minor number of spikes

TABLE XV. FREQUENCIES ASSOCIATED WITH ROTRON FAN

		Frequency (Hertz)
f_w	: thought to be associated with the whirl of the air inside the fan	33
f_{co}	: cage with respect to outer race	66.6-67.0
f_{ci}	: cage with respect to inner race	114.6-115.3
f_s	: shaft	181.2-182.3
$2f_s$	: 2nd harmonic of shaft	362.4-364.6
f_o	: outer race	399.6-402.0
f_L	: power line	400.0
$3f_s$	: 3rd harmonic of shaft	543.6-546.9
$2f_L-f_s$	: beat of 2nd harmonic of line and shaft	617.7-618.8
f_b	: ball	636.0-639.9
$4f_s-2f_w$	: (number of rotor blades x shaft freq.) - $2f_w$	658.8-663.2
f_i	: inner race	687.6-691.8
$4f_s-f_w$	: (number of rotor blades x shaft freq.) - f_w	691.8-696.2
$4f_s$	: number of rotor blades x shaft freq.	724.8-729.2
$2f_L$	: 2nd harmonic power line - torque pulsations	800.0
$5f_s$	: number of stator blades x shaft freq.	906 -911.5
$2f_L+f_s$	: beat of 2nd harmonic of line and shaft	981.2-982.3
$20f_s$	: number of rotor blades x number of stator blades x shaft freq.	3624 - 3646

TABLE XVI - FREQUENCIES ASSOCIATED WITH TRW GLOBE FAN

			Freq. (Hz)
f_{co}	:	cage with respect to outer race	32.9 - 34.7
f_o-2f_s	:	beat of outer race and 2nd harmonic of shaft	42.4 - 44.6
$f_o'-2f_s$	:	beat of suspected outer race & 2nd harmonic of shaft	50 - 53
f_{ci}	:	cage with respect to inner race	61.1 - 64.3
f_s	:	shaft	94.0 - 99.0
f_o-f_s	:	beat of outer race and shaft	136.4 -143.6
$f_o'-f_s$	:	beat of suspected outer race and shaft	145 - 152
$2f_s$	:	2nd harmonic of shaft	188.0 - 198.0
f_o	:	outer race	230.4 - 242.6
f_o'	:	suspected outer race	239 - 251
$3f_s$	:	3rd harmonic of shaft	282.0 - 297.0
f_b	:	ball	285.3 - 300.5
f_o+f_s	:	beat of outer race and shaft	324.4 - 341.6
$f_o'+f_s$	:	beat of suspected outer race and shaft	333 - 350
$4f_s$	:	4th harmonic of shaft	376.0 - 396.0
f_l	:	power line	400.0
f_i	:	inner race	427.6 - 450.4
$5f_s$	:	5th harmonic of shaft	470.0 - 495.0
$2f_l-f_s$	:	beat of 2nd harmonic of power line and shaft	701 - 706
$2f_l$	:	2nd harmonic power line - torque pulsations	800.0
$2f_l+f_s$	:	beat of 2nd harmonic of power line & shaft	894 - 899
$2f_l+3f_s$	:	beat of 2nd harmonic of power line & 3rd harmonic of shaft	1082 - 1097
$2f_l+4f_s$	:	beat of 2nd harmonic of power line and 4th harmonic of shaft	1176 - 1197
$4f_l-f_s$	:	beat of 4th harmonic of power line and shaft	1501 - 1506
$4f_l$	:	4th harmonic of power line	1600
$4f_l+f_s$	:	beat of 4th harmonic of power line & shaft	1694 - 1699

TABLE XVII - FREQUENCIES ASSOCIATED WITH DYNAMIC AIR ENGINEERING COSOL FAN

		Frequency (Hz)
f_{co1}	: Cage with respect to outer race for #1 bearing	143.4 - 143.7
f_{co2}	: Cage with respect to outer race for #2 bearing	154.2 - 154.5
f_{ci2}	: Cage with respect to inner race for #2 bearing	236.4 - 237.0
f_{ci1}	: Cage with respect to inner race for #1 bearing	247.2 - 247.8
f_s	: Shaft	390.6 - 391.5
f_L	: Power line	400.0
f_{sp1}	: Ball spin for #1 bearing	672.7 - 674.2
$2f_s$	: 2nd harmonic of shaft	781.2 - 783.0
$2f_L$	: 2nd harmonic power line - torque pulsations	800.0
f_{sp2}	: Ball spin for #2 bearing	863.8 - 865.8
f_{s1}	: Outer race for #1 bearing	1004 - 1006
$3f_s$	: 3rd harmonic of shaft	1172 - 1175
f_{o2}	: Outer race for #2 bearing	1233 - 1236
f_b1	: Ball impact for #1 bearing	1345 - 1349
$4f_s$	: 4th harmonic of shaft	1562 - 1566
f_{b2}	: Ball impact for #2 bearing	1728 - 1732
fi_1	: Inner race for #1 bearing	1731 - 1735
fi_2	: Inner race for #2 bearing	1892 - 1896
$5f_s$	: 5th harmonic of shaft	1953 - 1958
$9f_s$	: Number of impeller blades x shaft frequency	3515 - 3524
$18f_s$	: 2nd harmonic of number of impeller blades x shaft frequency	7031 - 7047

TABLE XVIII - FREQUENCIES ASSOCIATED WITH

MICROPUMP PUMP

			Frequency (Hz)
f_x	:	Unidentified - delta frequency between shaft frequency harmonics and sideband structure	33
f_{co}	:	Cage with respect to outer race	66.7 - 66.8
f_{ci}	:	Cage with respect to inner race	103.9 -104.1
f_s	:	Shaft	170.6 -170.9
$2f_s$	:	2nd harmonic of shaft	341.2 -341.8
f_L	:	Power line	400.0
$3f_s$	:	3rd harmonic of shaft	511.8 -512.7
f_o	:	Outer race	533.2 -534.1
$4f_s$	:	4th harmonic of shaft	682.4 -683.6
f_b	:	Ball	743.0 -744.3
$2f_L$	:	2nd harmonic power line - torque pulsations	800.0
f_i	:	Inner race	831.6 -833.1
$5f_s$	:	5th harmonic of shaft	853.0 -854.5
$17f_s-2f_L$	:	Beat of 2nd harmonic of line and 17th harmonic of shaft	2100 - 2105
$17f_s$	:	17th harmonic of shaft	2900 - 2905

TABLE XIX- FREQUENCIES ASSOCIATED WITH HYDROKINETICS 10461 PUMP

			Frequency (Hz)
f_{co2}	:	Cage with respect to outer race for #2 bearing	139.4 - 139.8
f_{co1}	:	Cage with respect to outer race for #1 bearing	144.3 - 144.8
f_{ci1}	:	Cage with respect to inner race for #1 bearing	243.6 - 244.2
f_{ci2}	:	Cage with respect to inner race for #1 bearing	248.5 - 249.2
f_s	:	Shaft	387.9 - 389.0
f_L	:	Power line	400.0
f_{sp2}	:	Ball spin for #2 bearing	624.9 - 626.7
f_{sp1}	:	Ball spin for #1 bearing	671.7 - 673.6
$2f_s$	:	2nd harmonic of shaft	775.8 - 778.0
$2f_L$	:	2nd harmonic power line - torque pulsations	800.0
f_{o2}	:	Outer race for #2 bearing	836.6 - 838.9
f_{o1}	:	Outer race for #1 bearing	1010 - 1013
$3f_s$	:	3rd harmonic of shaft	1164 - 1167
$f_x - f_{co1}$	:	Unknown freq. - Cage with respect to outer race #1 bearing	1224 - 1227
f_{b2}	:	Ball impact for #2 bearing	1250 - 1253
f_{b1}	:	Ball impact for #1 bearing	1343 - 1347
f_x	:	Unknown freq.	1368 - 1372
f_{i2}	:	Inner race for #2 bearing	1491 - 1495
$f_x + f_{co1}$	:	Unknown freq. + Cage with respect to outer race #1 bearing	1512 - 1516
$4f_s$	:	4th harmonic of shaft	1552 - 1556
$4f_L$	:	4th harmonic of power line	1600
f_{i1}	:	Inner race for #1 bearing	1705 - 1710
$5f_s$	:	5th harmonic of shaft	1940 - 1945
$6f_s$	:	Number of impeller vanes x shaft freq.	2327 - 2334

TEST ITEM	Micropump Model 10-71-316-1367 Centrifugal Pump
PLOT NO.	29
TRANSDUCER	B100-5

CONTROLLED TEST PARAMETERS	
VOLTAGE	115
P.S. FREQ.	400.0
FLOW RATE	7.5×10^{-5} (1.2)

VARIABLE TEST PARAMETERS	BASELINE	FAULT
DATE	4/23,5/10	
I	.677	
ϕ_z	.384-.419	
PWR	71.1-72.2	
RPM	10240-10250	
P_S	6900	
P_D	162000-165000	
ΔP	155000-158000	
TEMP	295-297	
BARO	100300-101900	

PROCESSING CHANNEL PARAMETERS	
INPUT RESISTANCE	22Kn
AMPLIFIER GAINS (DB)	
A_1	40
A_2	—
A_3	20
FILTER FREQUENCIES (KHZ)	
BAND PASS	300
HIGH PASS	200
LOW PASS	1

SPECTRUM ANALYZER PARAMETERS	BASELINE	FAULT
INPUT V. (MV)	8	

GAIN SETTINGS (0 DB REF)	
ANALYZER GAIN	20
INPUT ATTEN.	10
INTEGRATION	
LINEAR 32°/BIN COSINE WEIGHT	D.C. COUPLE INTERNAL SAMPLE

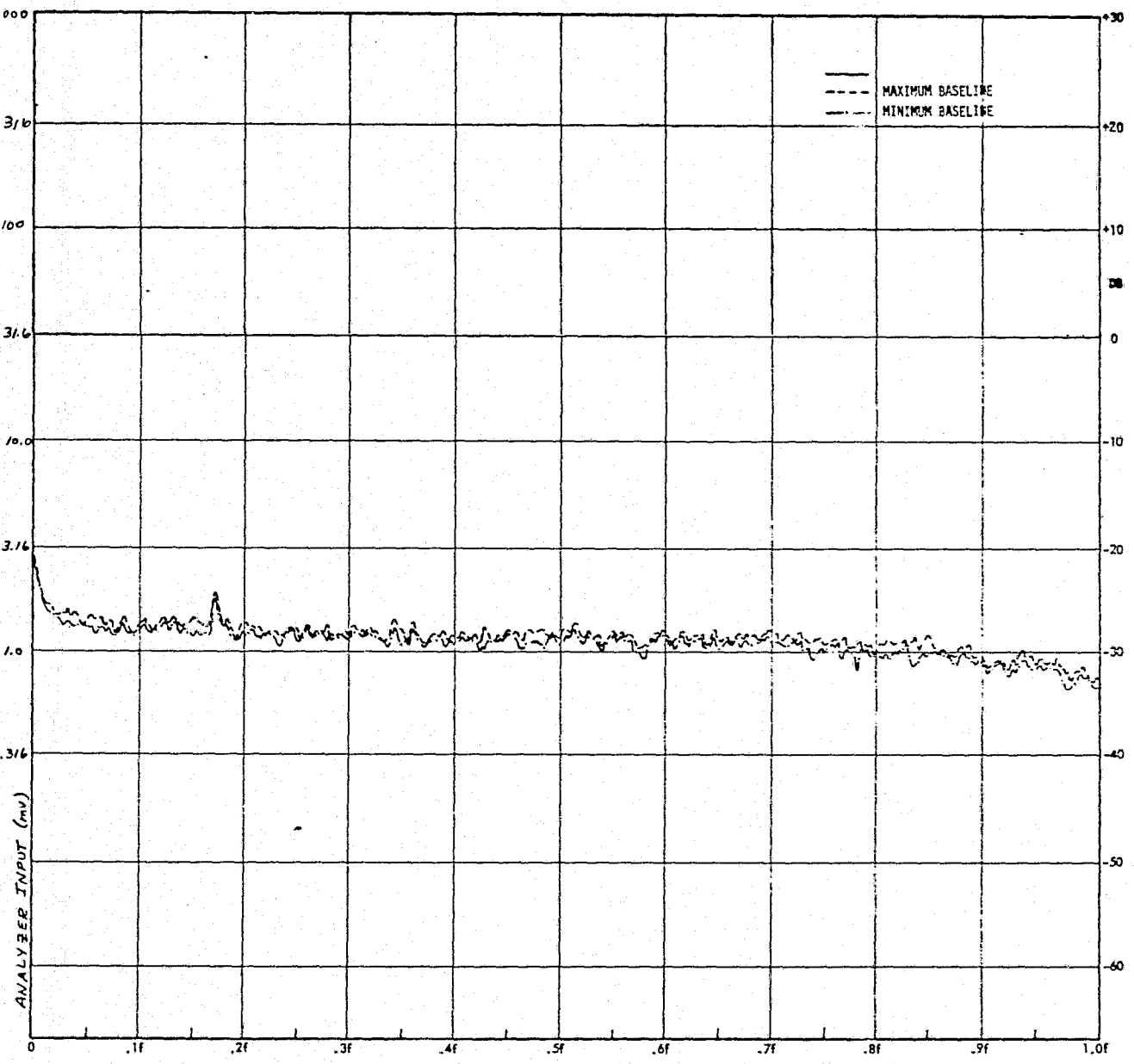

FIG. 10 FREQUENCY SPECTRUM FOR MICROPUMP 10-71-316-1367 PUMP

which one would expect from Gaussion noise. A very small spectral line exists at the shaft frequency, 170 Hz, which could be attributable to vibration modulation of the friction signal at the shaft frequency. However, the actual acoustic signal from which the SADAS plot shown in Figure 10 was made was an extremely spikey signal since the predominant signal source for this pump, at this frequency, was the turbulent water flow. Turbulent water flow at these high frequencies generates very high acoustic spikes. However, the spikes occur at random time invervals which results in the SADAS plot being very flat.

Figure 11 is a SADAS plot for the same pump at a lower bandpass center frequency, 30 KHz. At this lower frequency the bearing signal represents a greater percentage of total signal from the pump since there is considerable spike reduction. This plot illustrates the large spectral lines which can occur in the SADAS plots at the fundamental and harmonics of the shaft frequency as a result of 1) vibration modulation of the bearing's friction signal; 2) ball clatter due to bearing looseness or insufficient preloading. The spectral lines, which may be normal for the machine, are significant obstacles in the design and use of instrumentation to automatically detect incipient failures in hardware. These shaft frequency related spectral lines can exist at all bandpass frequencies. Figure 12 shows their existence at 300 KHz for the Rotron fan. For this fan the total acoustic signal was almost all from the bearings since the contribution from the air flow is very small. This figure also demonstrates the wide variation between maximum and minimum baseline spectrums which were experienced for the Rotron fan. The shaft frequency related spectral lines can be significant at one bandpass frequency, as shown in Figure 12, and be relatively insignificant at another bandpass frequency, as shown in Figure 13, which was also for the Rotron fan but at a lower frequency, 50 KHz.

Other spectral lines, besides those directly related to the fundamental and harmonics of the shaft frequency, can exist in the baseline SADAS data which can provide obstacles to the design and use of instrumentation to automatically detect incipient failures in hardware. Figure 14 for the TRW Globe fan and Figure 15 for the Dynamic Air Engineering fan both have spectral lines at a bearing's outer race ball passing frequency, 245 Hz and 1230 Hz, respectively. These spectral lines are due to a friction signal modulation which results as the balls roll pass the transducers at the outer race frequency. Figure 16, for the Hydrokinetics pump, shows another effect which results in multiple spectral lines in the SADAS plots. The cyclic type of spectrum shown here is due to non-linear effects produced by waviness in the bearings raceways. This effect was predominant in the Micropump pump brinelled bearing fault data.

Figure 17 is a block diagram of the test setup used for measuring the amplitude distribution parameters for the bandpassed vibration/acoustic signals. The parameters which were chosen to be measured were as follows:

1. Root mean square (RMS) value of the bandpassed signal referenced to the output of the IFD sensor

2. Count distribution of the bandpassed signal vs. σ (1σ = RMS level) threshold

TEST ITEM	Microbump Model 10-71-316-1367 Centrifugal Pump
PLOT NO.	19
TRANSDUCER	B100-5

CONTROLLED TEST PARAMETERS	
VOLTAGE	115
P.S. FREQ.	400.0
FLOW RATE	7.5×10^{-5} (1.2)

VARIABLE TEST PARAMETERS	BASELINE	FAULT
DATE	4/23,5/10	
I	.677	
ϕ_L	.384-.419	
PWR	71.1-72.2	
RPM	10240-10250	
P_S	6900	
P_D	162000-165000	
ΔP	155000-158000	
TEMP	295-297	
BARO	100900-101900	

PROCESSING CHANNEL PARAMETERS	
INPUT RESISTANCE	22 KΩ
AMPLIFIER GAINS (DB)	
A_1	40
A_2	—
A_3	20
FILTER FREQUENCIES (KHZ)	
BAND PASS	30
HIGH PASS	20
LOW PASS	1

SPECTRUM ANALYZER PARAMETERS	BASELINE	FAULT
INPUT V. (MV)	11-16	
GAIN SETTINGS (0 DB REF)		
ANALYZER GAIN	10	
INPUT ATTEN.	10	
INTEGRATION		
LINEAR 32ε/BIN COSINE WEIGHT	D.C. COUPLE INTERNAL SAMPLE	

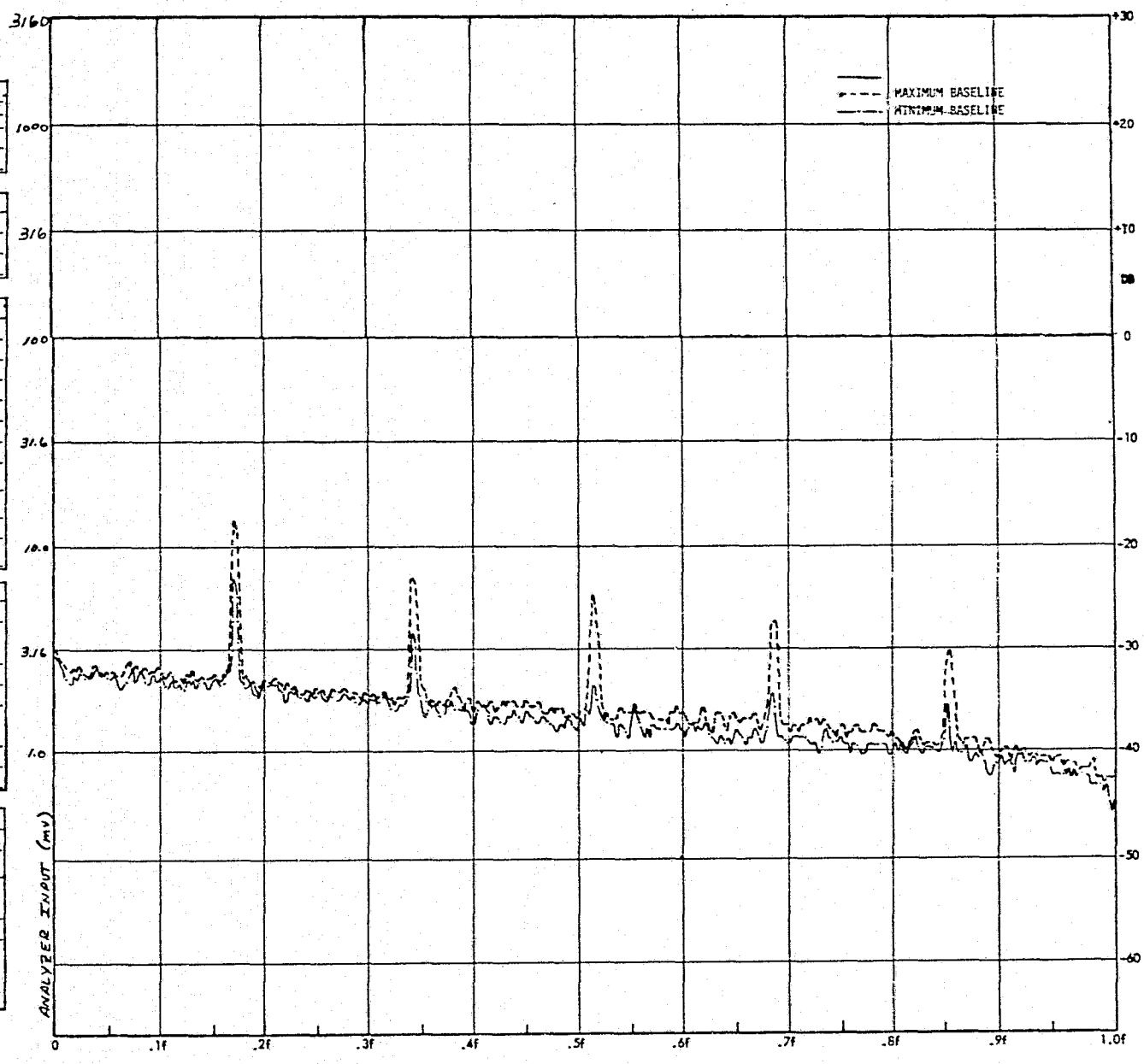

FIG. 11 FREQUENCY SPECTRUM FOR MICROPUMP 10-71-316-1367 PUMP

TEST ITEM AXIMAX-2-464YS
PLOT NO. 87
TRANSDUCER B100-3

CONTROLLED TEST PARAMETERS
VOLTAGE 115
P.S. FREQ. 400.0
FLOW RATE 8.85×10^{-3} (18.75)

VARIABLE TEST PARAMETERS		
	BASELINE	FAULT
DATE	12/12-2/17	
I	.112-.114	
$\phi <$	.576	
PWR	10.8-11.0	
RPM	10,870-10,940	
ΔP	186.1 (.747)	
TEMP	292.4°-295.3°	
BARO	100381-102540	

PROCESSING CHANNEL PARAMETERS
INPUT RESISTANCE 22kΩ
AMPLIFIER GAINS (DB)
A_1 40
A_2 40
A_3 20
FILTER FREQUENCIES (KHZ)
BAND PASS 300
HIGH PASS 200
LOW PASS 1

SPECTRUM ANALYZER PARAMETERS		
	BASELINE	FAULT
INPUT V. (MV)	10-35	
GAIN SETTINGS (0 DB REF)		
ANALYZER GAIN 10		
INPUT ATTEN. 0		
INTEGRATION		
LINEAR		
32 SUMS PER BIN		
COSINE WEIGHT		
D.C. COUPLE		
INTERNAL SAMPLE		

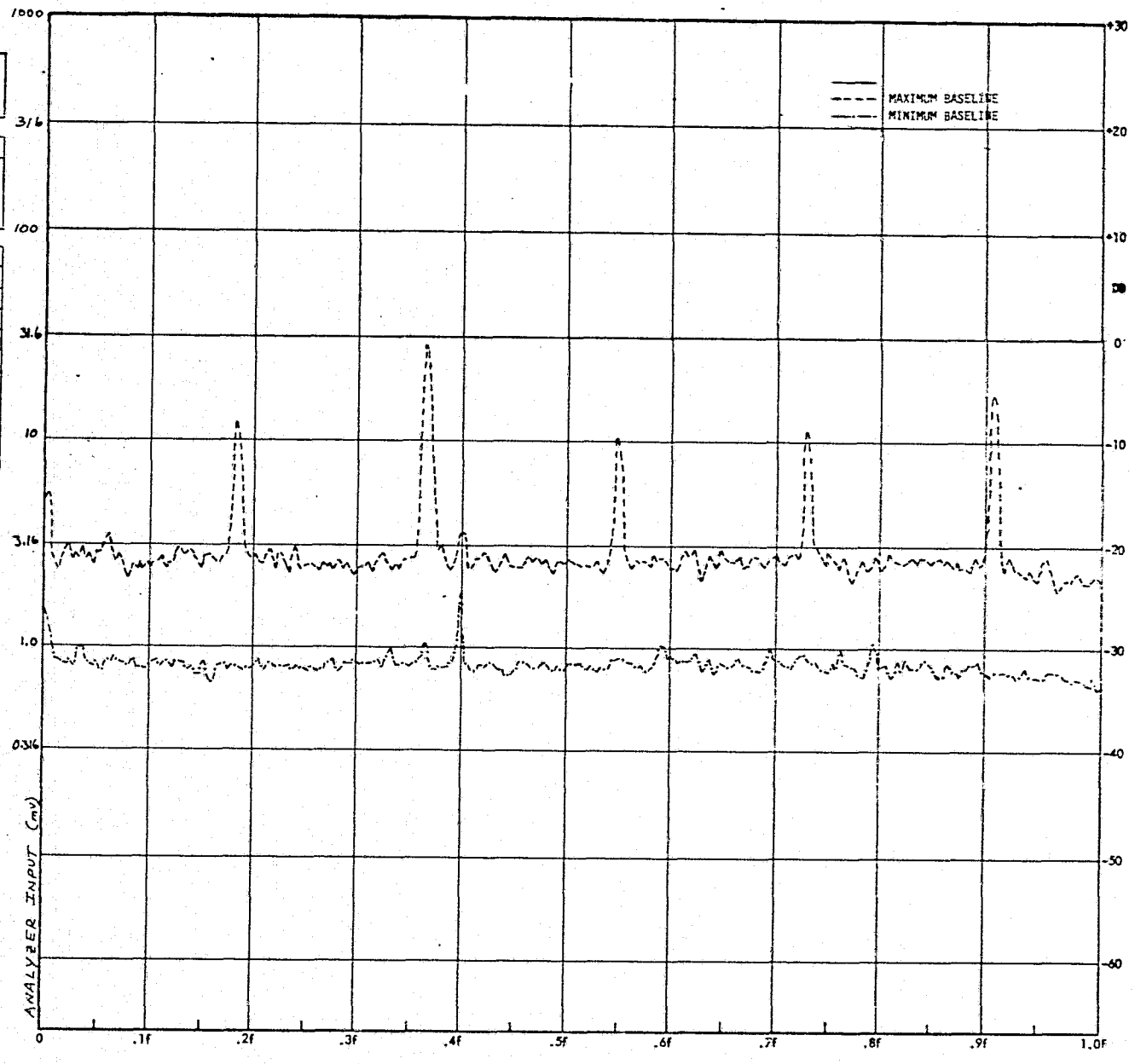

FIG. 12 FREQUENCY SPECTRUM FOR ROTRON AXIMAX-2-464 YS FAN

TEST ITEM	AXIMAX-2-464YS
PLOT NO.	67
TRANSDUCER	B100-3

CONTROLLED TEST PARAMETERS	
VOLTAGE	115
P.S. FREQ.	400.0
FLOW RATE	8.85×10^{-3} (18.75)

VARIABLE TEST PARAMETERS	BASELINE	FAULT
DATE	12/12-2/17	
I	.112-.114	
φ<	.576	
PWR	10.8-11.0	
RPM	10,870-10,940	
ΔP	186.1 (.747)	
TEMP	292.4°-296.3°	
BARO	100981-102540	

PROCESSING CHANNEL PARAMETERS	
INPUT RESISTANCE	22 KΩ
AMPLIFIER GAINS (DB)	
A_1	40
A_2	20
A_3	20
FILTER FREQUENCIES (KHZ)	
BAND PASS	50
HIGH PASS	50
LOW PASS	1

SPECTRUM ANALYZER PARAMETERS	BASELINE	FAULT
INPUT V. (P/)	16-34	
GAIN SETTINGS (0 DB REF)		
ANALYZER GAIN	10	
INPUT ATTEN.	10	
INTEGRATION		
LINEAR		
32 SUMS PER BIN		
COSINE WEIGHT		
D.C. COUPLE		
INTERNAL SAMPLE		

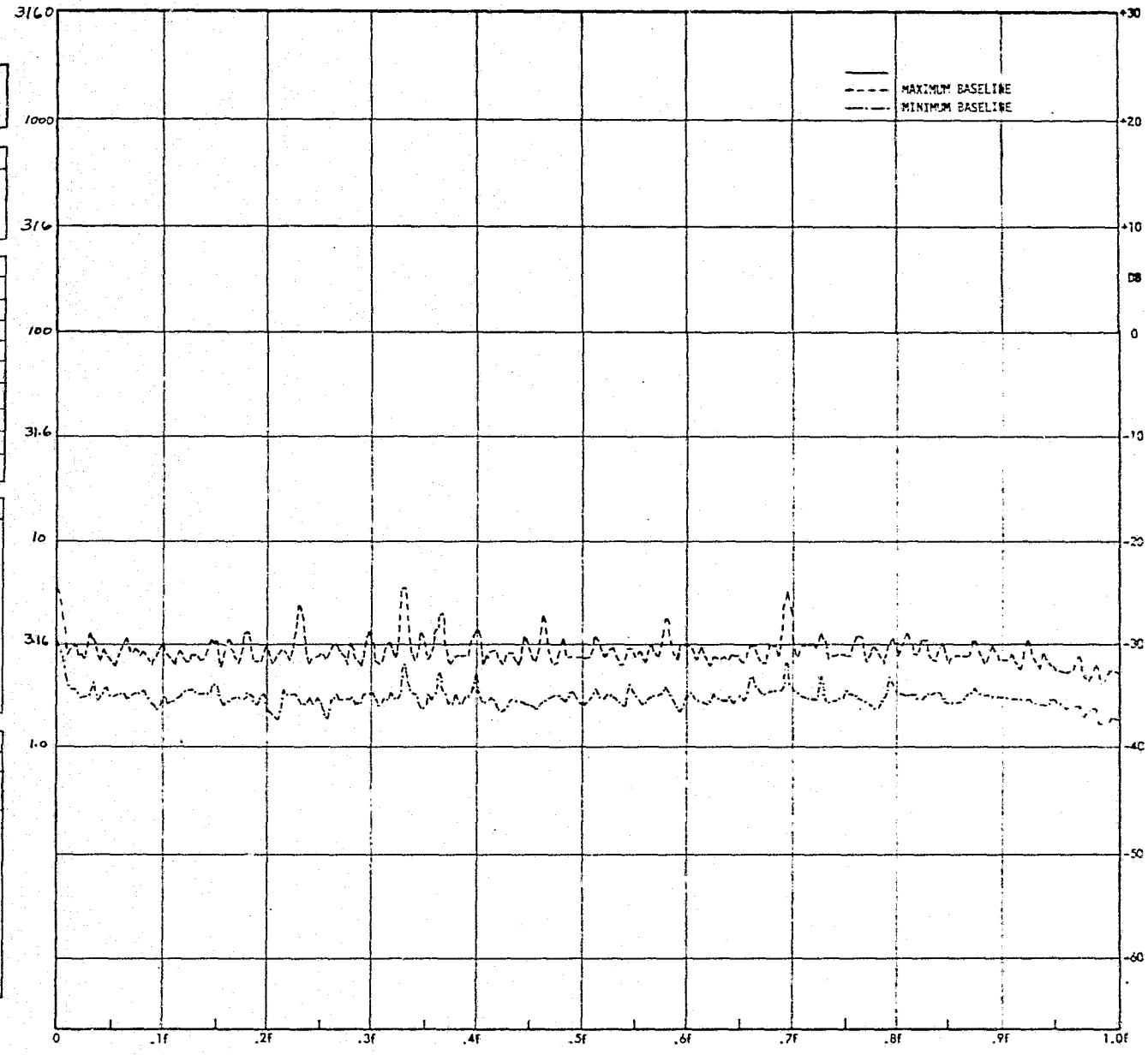

FIG. 13 FREQUENCY SPECTRUM FOR ROTRON AXIMAX-2-464 YS FAN

TEST ITEM	TRW Globe 19A532
PLOT NO.	53
TRANSDUCER	B100-1

CONTROLLED TEST PARAMETERS	
VOLTAGE	115
P.S. FREQ.	400.0
ΔP	206 (.827)

VARIABLE TEST PARAMETERS	BASELINE	FAULT
DATE	3/11-3/20	
I	.360-.361	
φ<	.838	
PWR	27.7-27.8	
RPM	5640-5940	
FLOW RATE	9.44×10^{-3} - 9.74×10^{-3}	
TEMP	293.0-296.3	
BARO	100891-102540	

PROCESSING CHANNEL PARAMETERS	
INPUT RESISTANCE	22K
AMPLIFIER GAINS (DB)	
A_1	40
A_2	20
A_3	20
FILTER FREQUENCIES (KHZ)	
BAND PASS	125KHz
HIGH PASS	50
LOW PASS	0.5

SPECTRUM ANALYZER PARAMETERS	BASELINE	FAULT
INPUT V. (MV)	6-9	
GAIN SETTINGS (0 DB REF)		
ANALYZER GAIN	10	
INPUT ATTEN.	0	
INTEGRATION		
LINEAR		
32 SUMS PER BIN		
COSINE WEIGHT		
D.C. COUPLE		
INTERNAL SAMPLE		

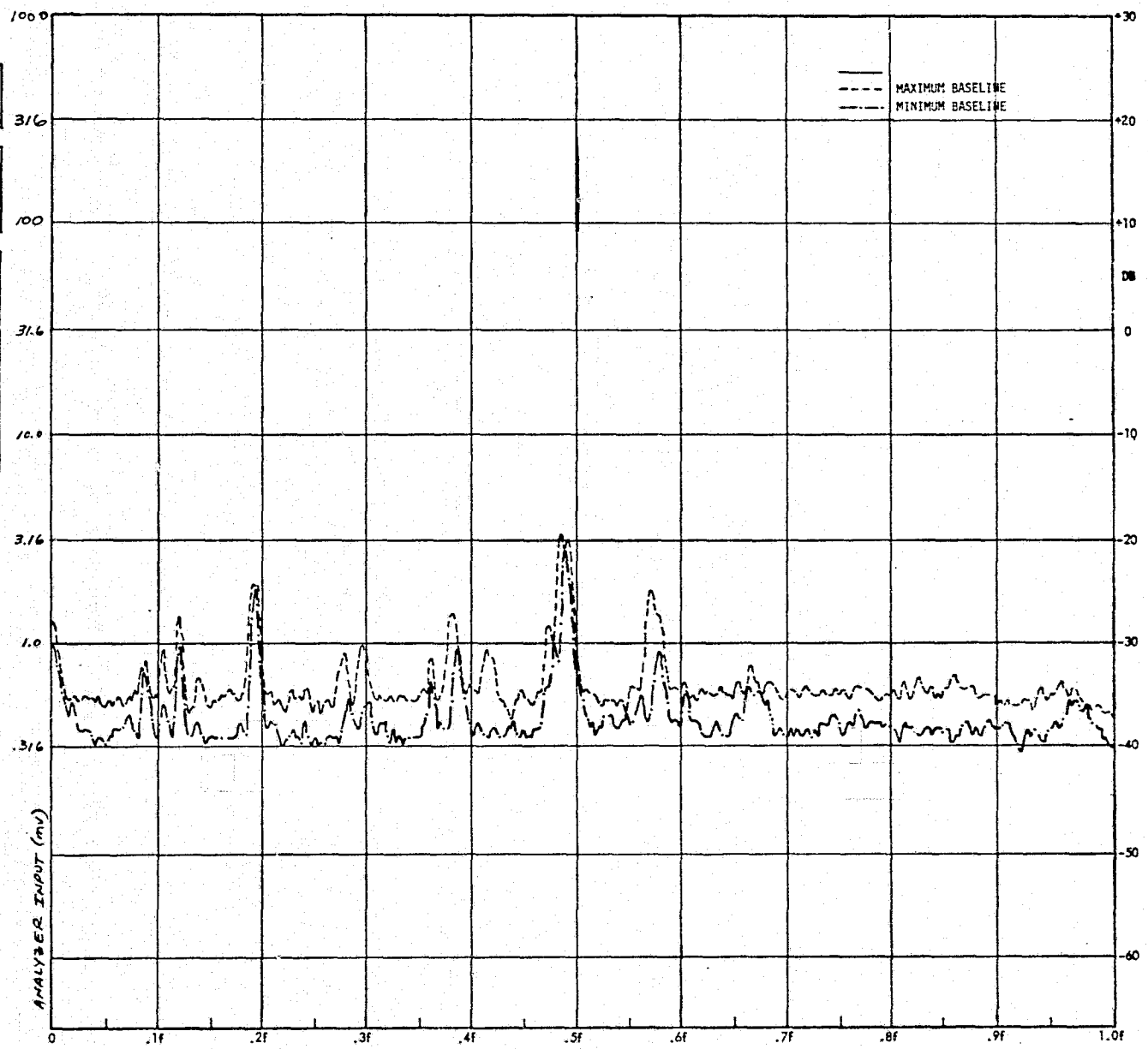

FIG. 14 FREQUENCY SPECTRUM FOR TRW GLOBE 19A532 FAN

DYNAMIC AIR ENGINEERING

TEST ITEM	COSOL FAN
PLOT NO.	51
TRANSDUCER	B100-9

CONTROLLED TEST PARAMETERS	
VOLTAGE	115
P.S. FREQ.	400.0
FLOW RATE	1.89×10^{-2} (40.0)

VARIABLE TEST PARAMETERS	BASELINE	FAULT
DATE	6/3 - 6/13	
I	2.01 - 2.03	
ε<	.150 - .175	
PWR	223 - 231	
RPM	23440 - 23490	
ΔP	4280 - 4430	
TEMP	295 - 297	
BARO	101000 - 101500	

PROCESSING CHANNEL PARAMETERS	
INPUT RESISTANCE	22 Kn
AMPLIFIER GAINS (DB)	
A_1	20
A_2	20
A_3	20
FILTER FREQUENCIES (KHZ)	
BAND PASS	300
HIGH PASS	150
LOW PASS	2

SPECTRUM ANALYZER PARAMETERS	BASELINE	FAULT
INPUT V. (MV)	15-30	

GAIN SETTINGS (0 DB REF)	
ANALYZER GAIN	10
INPUT ATTEN.	10
INTEGRATION	
LINEAR	
32 SUMS PER BIN	
COSINE WEIGHT	
D. C. COUPLE	
INTERNAL SAMPLE	

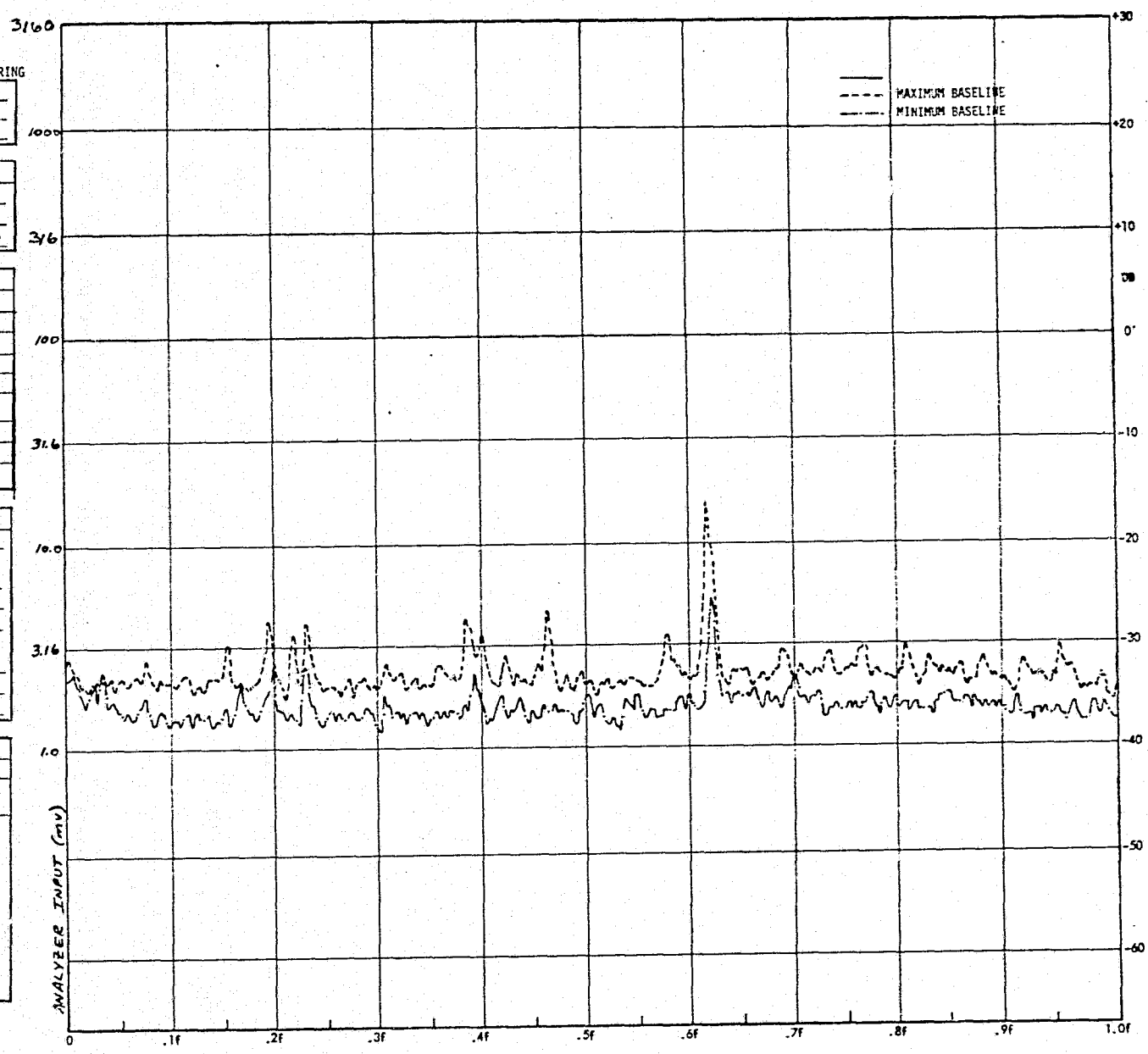

FIG. 15

FREQUENCY SPECTRUM FOR DYNAMIC AIR ENGINEERING COSOL FAN

TEST ITEM	HYDROKINETIC 10461 PUMP
PLOT NO.	35
TRANSDUCER	8100-8

CONTROLLED TEST PARAMETERS	
VOLTAGE	115
P.S. FREQ.	400.0
FLOW RATE	7.5×10^{-5} (1.2)

VARIABLE TEST PARAMETERS	BASELINE	FAULT
DATE	7/19-7/22	
I	3.2-3.5	
ϕ<	.035	
PWR	368-402	
RPM	23270-23340	
P_S	6900	
P_D	652000 - 655000	
ΔP	645000 - 648000	
TEMP	296-298	
BARO	101500 - 101700	

PROCESSING CHANNEL PARAMETERS	
INPUT RESISTANCE	22K Ω
AMPLIFIER GAINS (DB)	
A_1	20
A_2	20
A_3	—
FILTER FREQUENCIES (KHZ)	
BAND PASS	80
HIGH PASS	50
LOW PASS	2

SPECTRUM ANALYZER PARAMETERS	BASELINE	FAULT
INPUT V (MV)	50-80	
GAIN SETTINGS (0 DB REF)		
ANALYZER GAIN	10	
INPUT ATTEN.	10	
INTEGRATION		
LINEAR	D.C. COUPLE	
32t/BIN	INTERNAL SAMPLE	
COSINE WEIGHT		

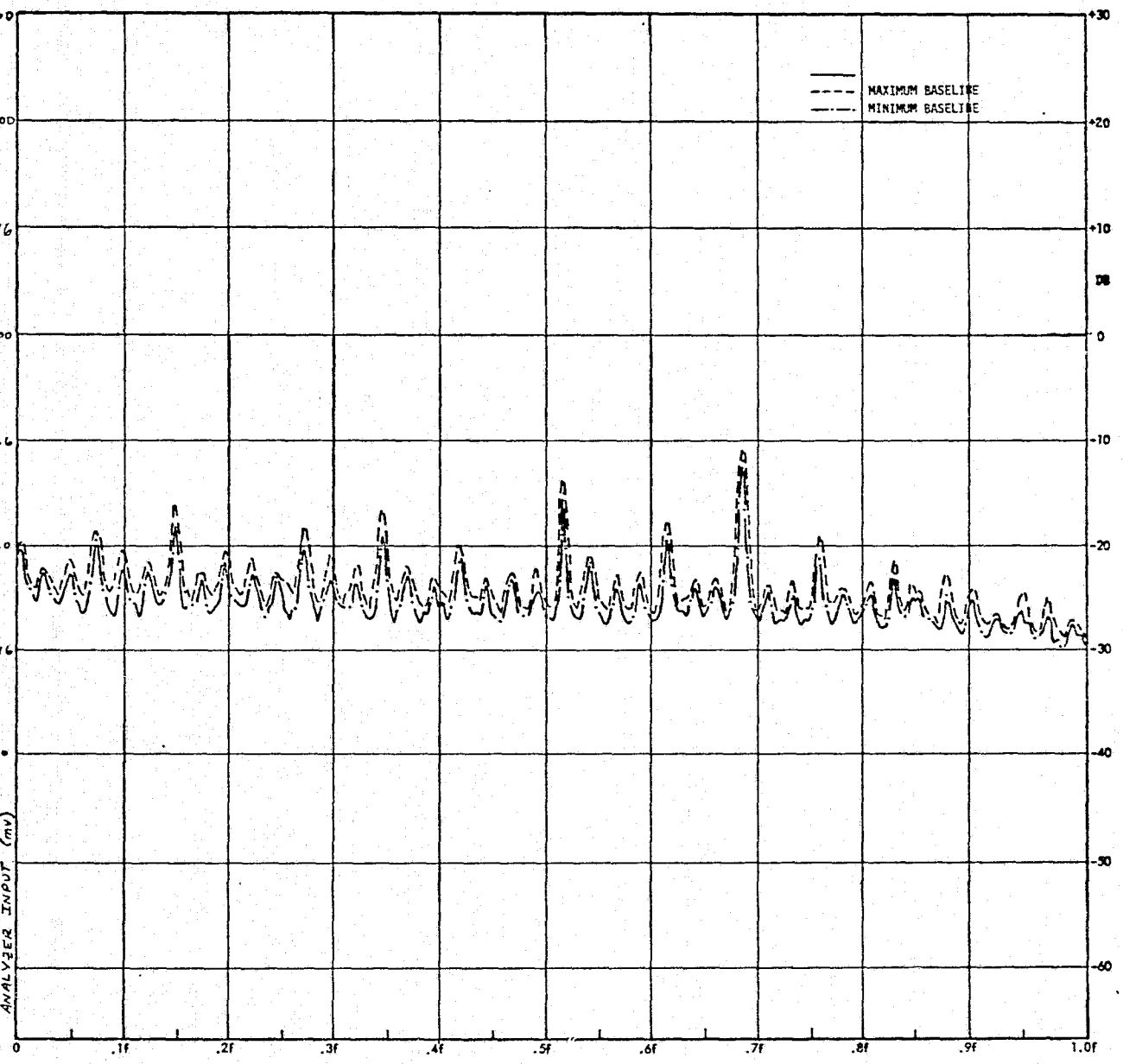

FIG. 16 FREQUENCY SPECTRUM FOR HYDROKINETICS 10461 PUMP

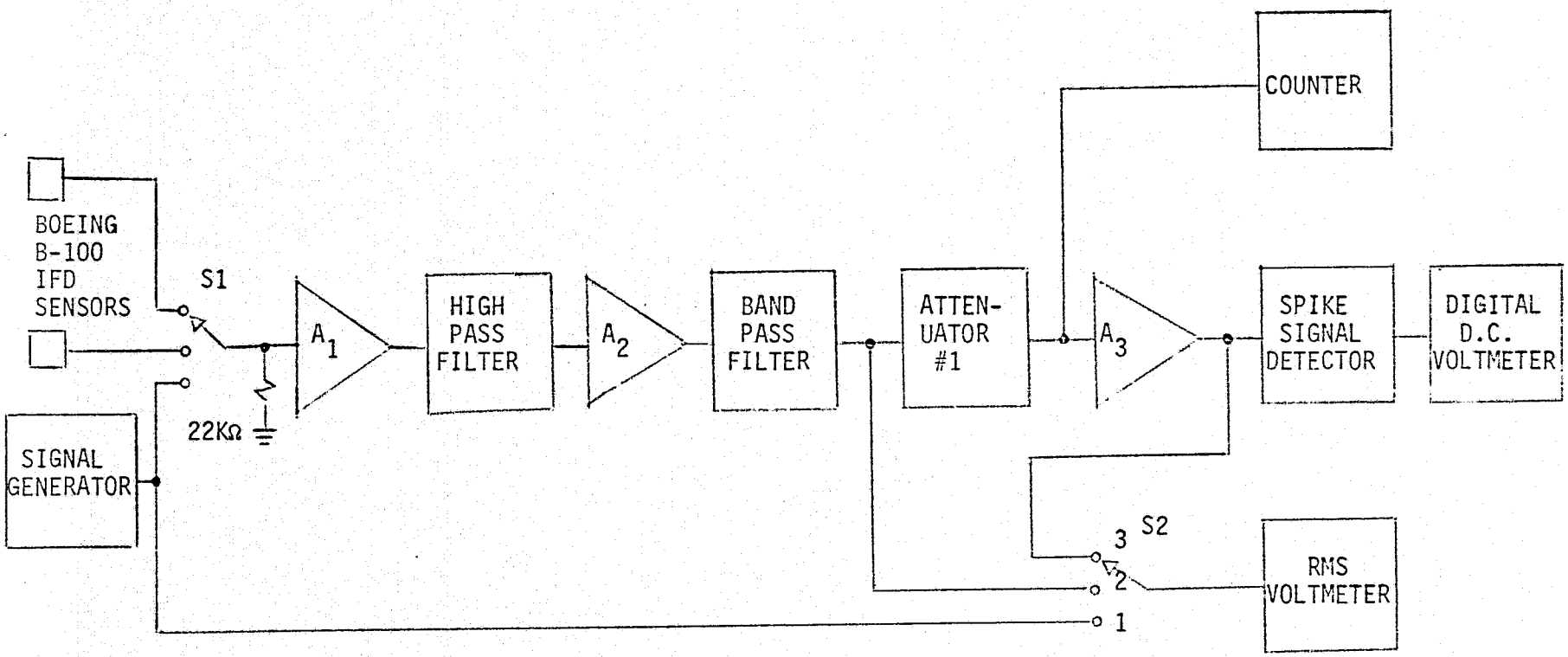

FIGURE 17 - VIBRATION/ACOUSTIC PROCESSING CHANNEL FOR BROAD BAND RMS SIGNAL LEVEL AND SPIKE AND COUNT DATA

3. Normalized integrated spike signal level above the 3σ level

The function of the 22K Ω resistor, amplifiers A_1 and A_2 and the high pass and bandpass filters is the same as for the test setup used to collect SADAS data. The bandpass center frequencies chosen for examining the amplitude distribution parameters were the same as those used for the SADAS plots and are shown in Table XIII. Attenuator #1 was used to set the input to the spike signal detector at 1 volt RMS for 3 σ spike signal detection and to adjust the input to the counter for measuring count distributions. The threshold of the spike signal detector was set at 3 volts and the threshold of the counter was set at 19.4 mv. The spike signal detector was equipped with a switch which would set its threshold to 0 volts. With a 1 volt RMS input and the threshold set to 0 volts, the output D.C. voltage from the spike signal detector was 1 volt.

A signal generator set at the bandpass filter's center frequency was used to determine the gain of the setup so that the RMS output, which was measured with switch S_2 in the #2 position, could be referenced to the output of the IFD sensor. With switch S_2 in the #3 position the RMS voltmeter was used to measure the input to the spike signal detector and the amplified input to the counter. The σ level for count distribution measurement was calculated using the following equation.

$$\sigma \text{ level} = \frac{19.4 \times 10^{\left(\frac{G3}{20}\right)}}{V} \qquad (7)$$

G_3 = Gain of A_3 - db
V = RMS Voltmeter reading - mv

Figure 18 contains a plot of the maximum RMS outputs for the Hydrokinetics 10461 Pump and a plot of the minimum RMS output for the TRW 19A532 fan. These plots represent the range in RMS signal levels which can be expected from the B100 IFD sensor for these types of test items.

Similarly, Figure 19 contains a plot of the maximum 3 σ spike outputs for the Micropump 10-71-316-1367 Pump, and a plot of the minimum 3 σ spike output for the Dynamics Air Engineering C050L Fan. As before, these plots represent the range in 3 σ spike levels which can be expected for these types of test items. The high speed level for the Micropump pump, as mentioned before, is predominantly from turbulent water flow in the pump's impeller.

Figures 20 through 22 are plots of the maximum count rate for the Micropump 10-71-316-1367 pump and the minimum count rate for the Dynamics Air Engineering C050L Fan for three frequencies, 20 KHz, 80 KHz, and 300 KHz. Note, that shifts of the count distribution curves to the right result in higher values of the normalized integrated 3 σ spike signal level.

Figure 23 is a block diagram of the test setup used for measuring the frequency spectrum and the RMS level of the baseband vibration/acoustic signal. The function of the components is similar to that which was used in the previous two setups. The total baseband spectrum from 0-1 MHz had

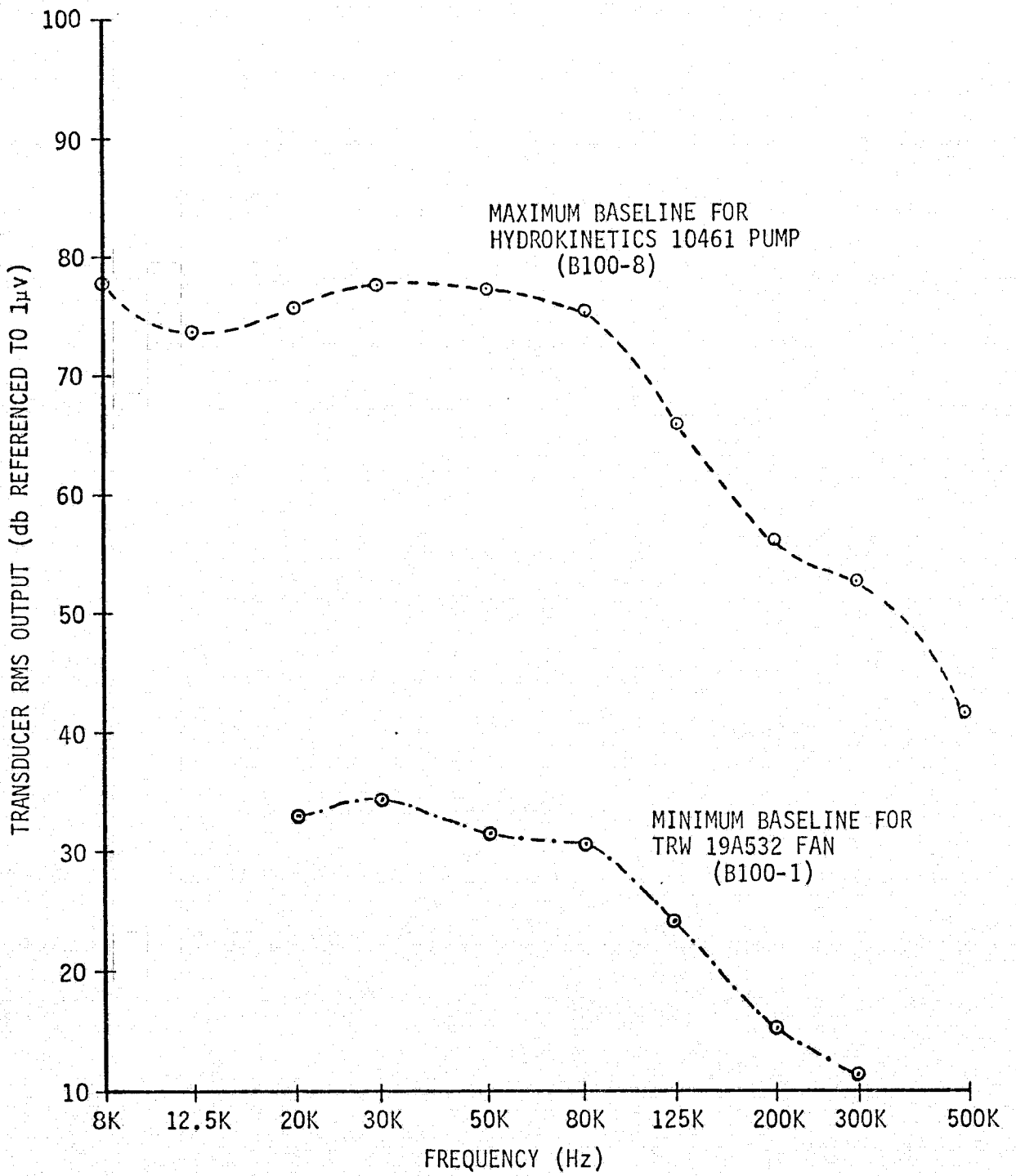

FIG. 18 RANGE OF BASELINE RMS SIGNAL LEVELS FOR THE FIVE TEST ITEMS

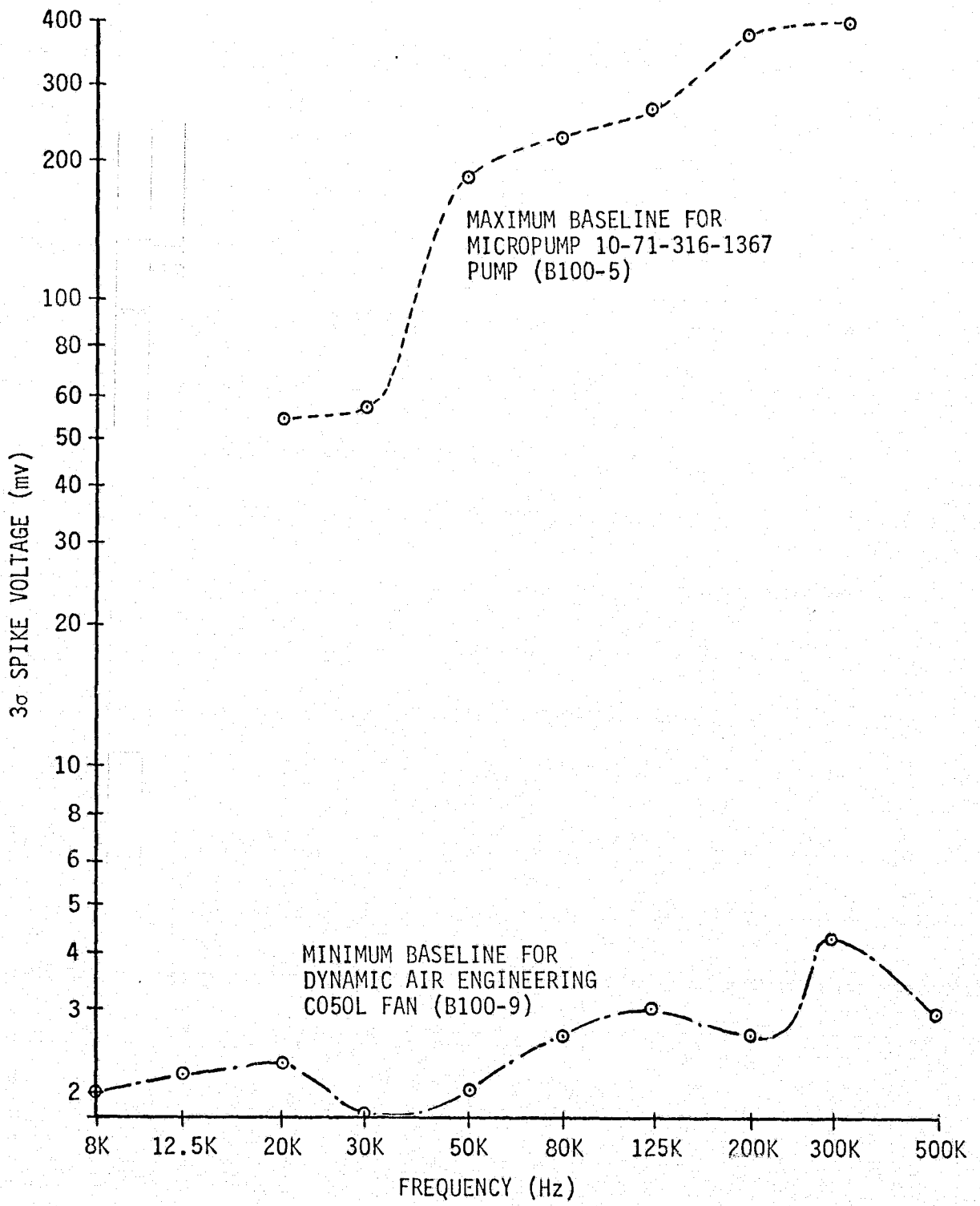

FIG. 19 RANGE OF BASELINE 3σ SPIKE VOLTAGE LEVELS FOR THE FIVE TEST ITEMS

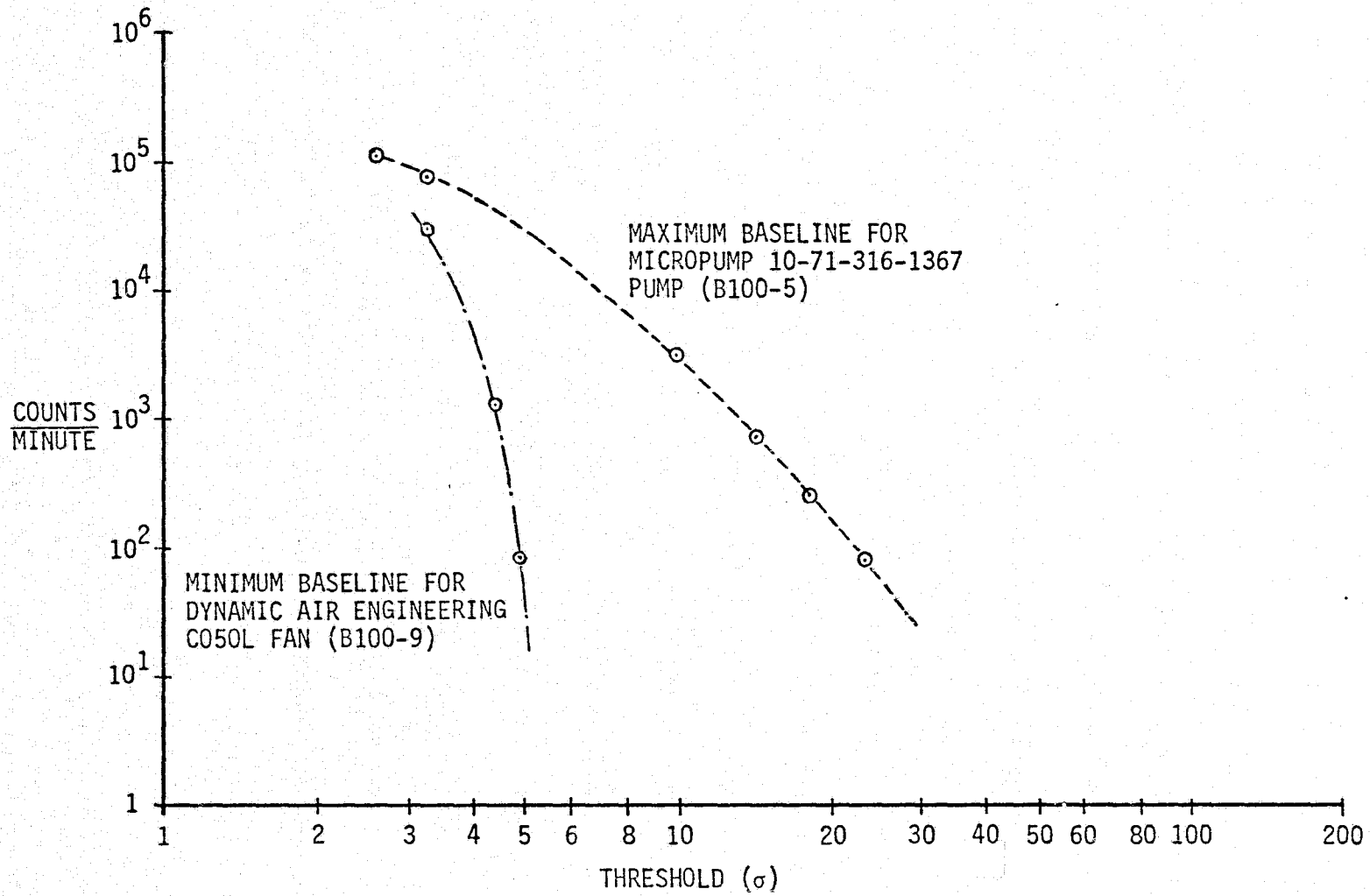

FIG. 20 RANGE OF COUNT DISTRIBUTION DATA AT 20 KHz FOR THE FIVE TEST ITEMS

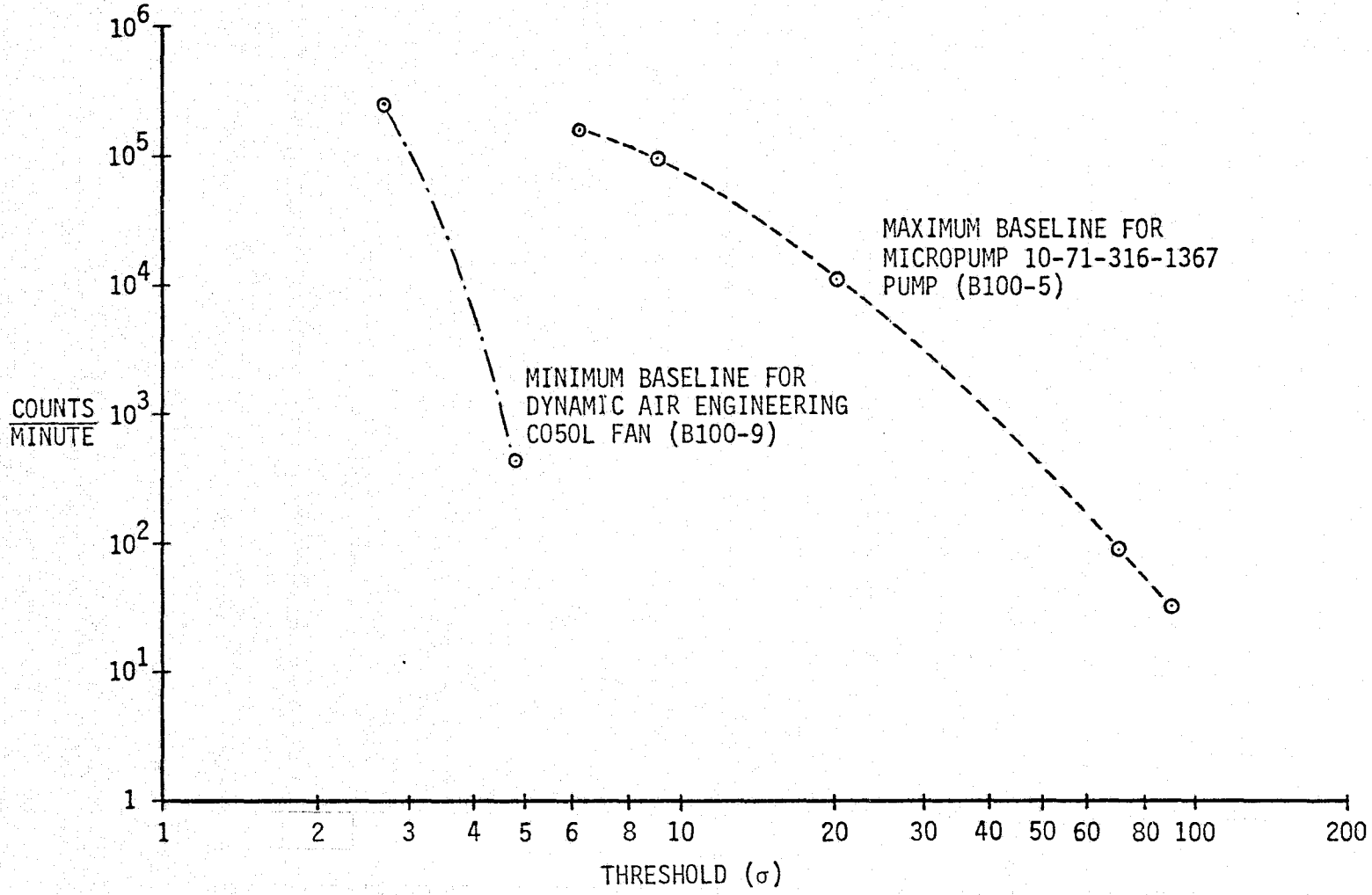

FIG. 21 RANGE OF COUNT DISTRIBUTION DATA AT 80 KHz FOR THE FIVE TEST ITEMS

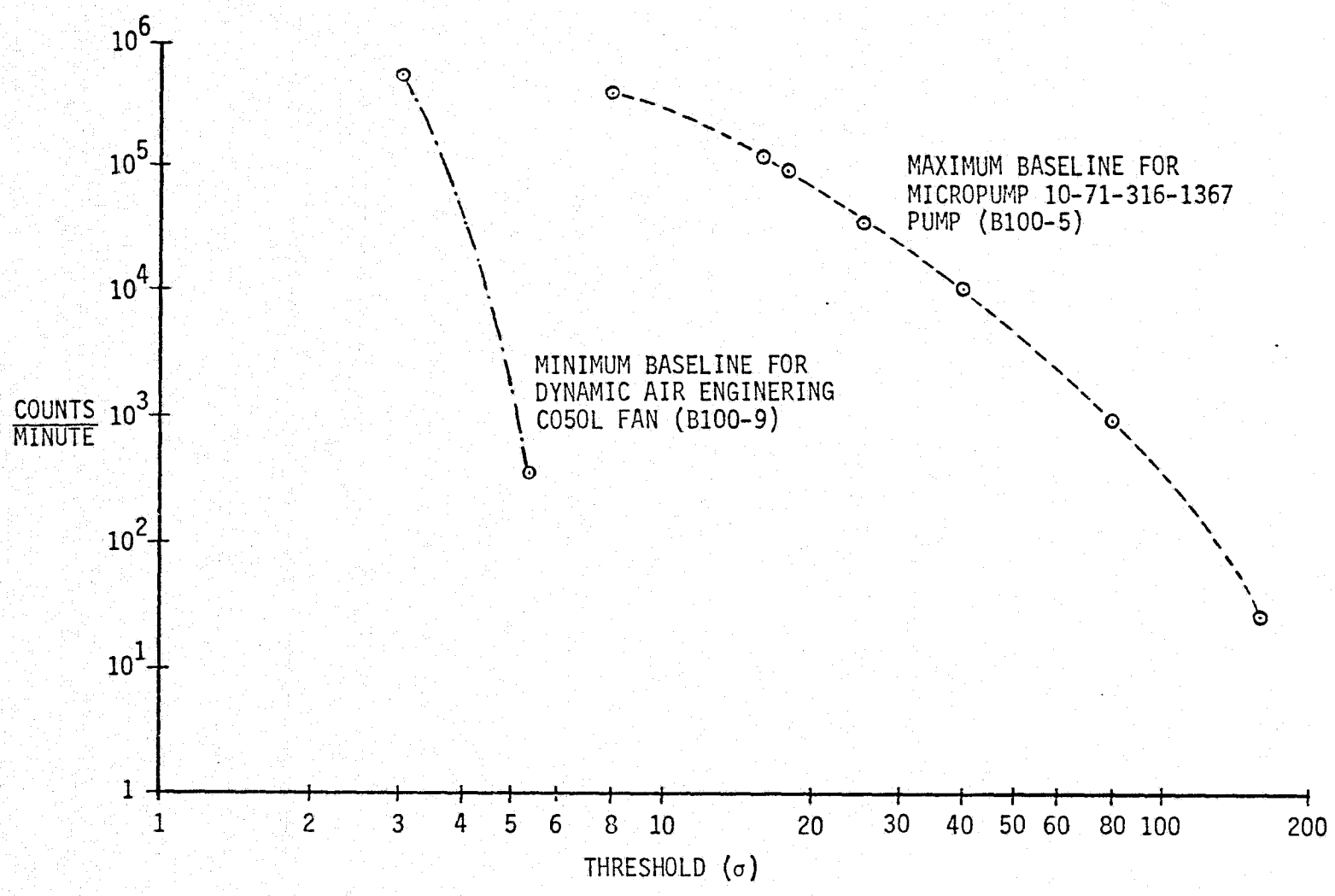

FIG. 22 RANGE OF COUNT DISTRIBUTION DATA AT 300 KHz FOR THE FIVE TEST ITEMS

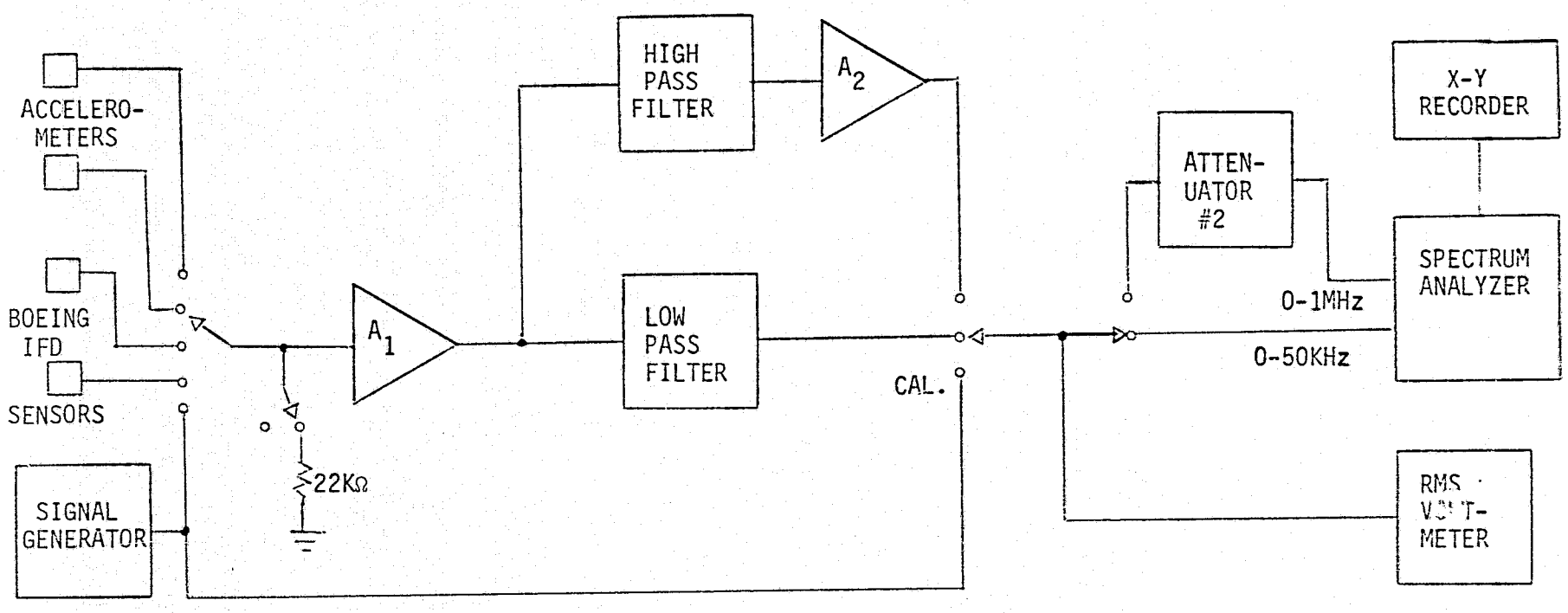

FIGURE 23 - VIBRATION/ACOUSTIC PROCESSING CHANNEL FOR BASEBAND FREQUENCY SPECTRUM DATA

had to be collected for each test item in several steps because of the limited dynamic range of the spectrum analyzer and the lower resolution at the higher frequencies. Typically, two baseband frequency ranges were selected for each test item for each transducer. These frequency ranges were the same as the SADAS baseband frequency ranges. The lowest of these two ranges for each item was sufficient to cover all the bearing ball passing frequencies for that item, and the highest of the two ranges was either 4 or 5 times the lower frequency range. Other ranges selected were for the IFD sensors and were 10 KHz, 50 KHz, and 1 MHz. The 22K Ω resistor and/or high pass filter shown in Figure 23 were used at these higher frequencies to reject the lower frequencies in order to operate within the restricted dynamic range of the spectrum analyzer. Attenuator #2 was used in the 0-1 MHz range since the spectrum analyzer does not have an internal attenuator for this range.

A typical set of baseband vibration/acoustic spectrum data is shown in Figures 24 through 28 for the TRW 19A532 Fan.

All collected baseline data was analyzed to determine the maximum and minimum values of each measured vibration/acoustic parameter. This data was then submitted as Boeing IFD reports numbers 248, 256, 263, 268 and 276 which are included in references 1-5. All the baseline data was examined by cognizant Boeing personnel before submittal and there did not appear to be any abnormalities existing in the non-faulted test items.

FAULT INJECTION (reference paragraph 3.2.4 of SOW)

Rotron Aximax 2-464-YS Fan

The first fault which was to be introduced into this fan was a bearing outer race defect. The fan was disassembled using the procedure established during baseline testing. The Barden VSR2-5SS4C ball bearing closest to the fan's air intake side and terminal ring was removed and placed in a disassembly jig. The bearing's two shields were indexed with respect to the outer race so they could be reassembled in the same position. Also one side of the inner race was indexed to avoid the possibility of reversing its position when it was reassembled. The snap rings holding the shields in place were removed and the shields removed. The one piece cage was indexed with the outer race and then removed. The six balls were next removed and located in a container with the cage so that their position in the cage could not be changed. Finally the inner race was removed. Care was taken during this procedure to minimize the removal of grease from the bearing's components and to keep dust particles from getting on them. The outer race was placed in a lab vise under a 30 power magnifier. Grease was removed from a small section of the outer race. A carbide scribe was then worked back and forth in this section across the race to make the scratch shown in Figure 29. The scratch was made at the same circumferential position around the race as the index mark on the outside of the race. Plowed up metal and loose particles were removed and the edges smoothed using an X-acto knife. The bearing was then reassembled making sure all balls were in their same relative position in the cage. The fan was reassembled with the bearing defect positioned as shown in Figure 30, following the procedure established during baseline testing.

TEST ITEM	TRW Globe 19A532
PLOT NO.	21
TRANSDUCER	B100-0

CONTROLLED TEST PARAMETERS	
VOLTAGE	115
P.S. FREQ.	400.0
ΔP	206 (.827)

VARIABLE TEST PARAMETERS	BASELINE	FAULT
DATE	3/11-3/20	
I	.360-.361	
ϕ<	.838	
PWR	27.7-27.8	
RPM	5640-5940	
FLOW RATE	9.44×10^{-3} - 9.74×10^{-3}	
TEMP	293.0-296.3	
BARO	100881-102540	

PROCESSING CHANNEL PARAMETERS	
INPUT RESISTANCE	—
AMPLIFIER GAINS (DB)	
A_1	20
A_2	—
A_3	—
FILTER FREQUENCIES (KHZ)	
BAND PASS	—
HIGH PASS	—
LOW PASS	0.5

SPECTRUM ANALYZER PARAMETERS	BASELINE	FAULT
INPUT V. (HV)	45-55	
GAIN SETTINGS (0 DB REF)		
ANALYZER GAIN	10	
INPUT ATTEN.	12	
INTEGRATION		
LINEAR		
32 SUMS PER BIN		
COSINE WEIGHT		
D.C. COUPLE		
INTERNAL SAMPLE		

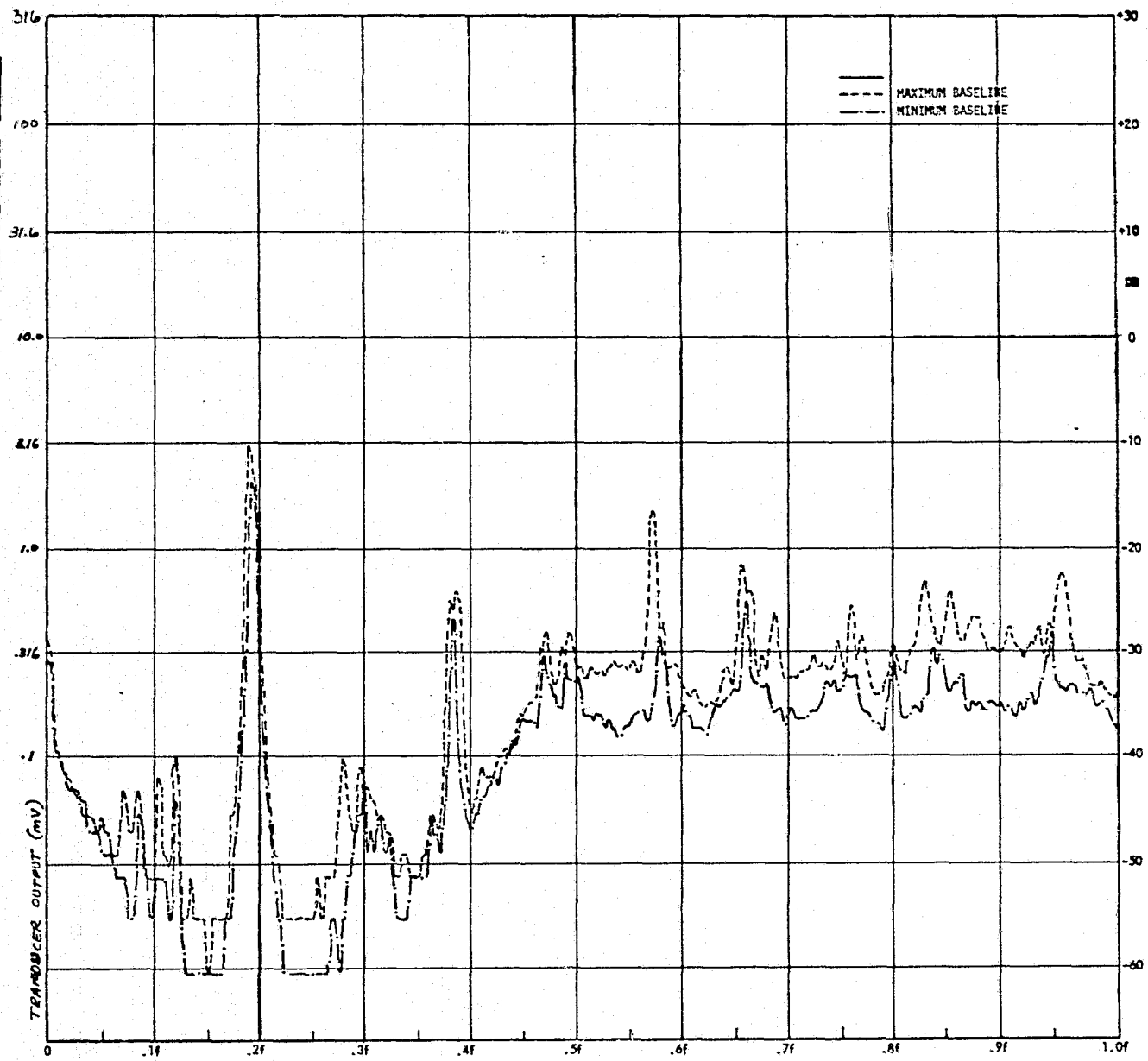

FIG. 24 FREQUENCY SPECTRUM FOR TRW GLOBE 19A532 FAN

TEST ITEM	TRW Globe 19A532
PLOT NO.	23
TRANSDUCER	B100-0

CONTROLLED TEST PARAMETERS	
VOLTAGE	115
P.S. FREQ.	400.0
ΔP	206 (.827)

VARIABLE TEST PARAMETERS	BASELINE	FAULT
DATE	3/11-3/20	
I	.360-.361	
ϕ<	.838	
PWR	27.7-27.8	
RPM	5640-5940	
FLOW RATE	9.44×10^{-3} - 9.74×10^{-3}	
TEMP	293.0-296.3	
BARO	100881-102540	

PROCESSING CHANNEL PARAMETERS	
INPUT RESISTANCE	—
AMPLIFIER GAINS (DB)	
A_1	20
A_2	—
A_3	—
FILTER FREQUENCIES (KHZ)	
BAND PASS	—
HIGH PASS	—
LOW PASS	2

SPECTRUM ANALYZER PARAMETERS	BASELINE	FAULT
INPUT V. (MV)	48-55	
GAIN SETTINGS (0 DB REF)		
ANALYZER GAIN	10	
INPUT ATTEN.	12	
INTEGRATION		
LINEAR		
32 SUMS PER BIN		
COSINE WEIGHT		
D.C. COUPLE		
INTERNAL SAMPLE		

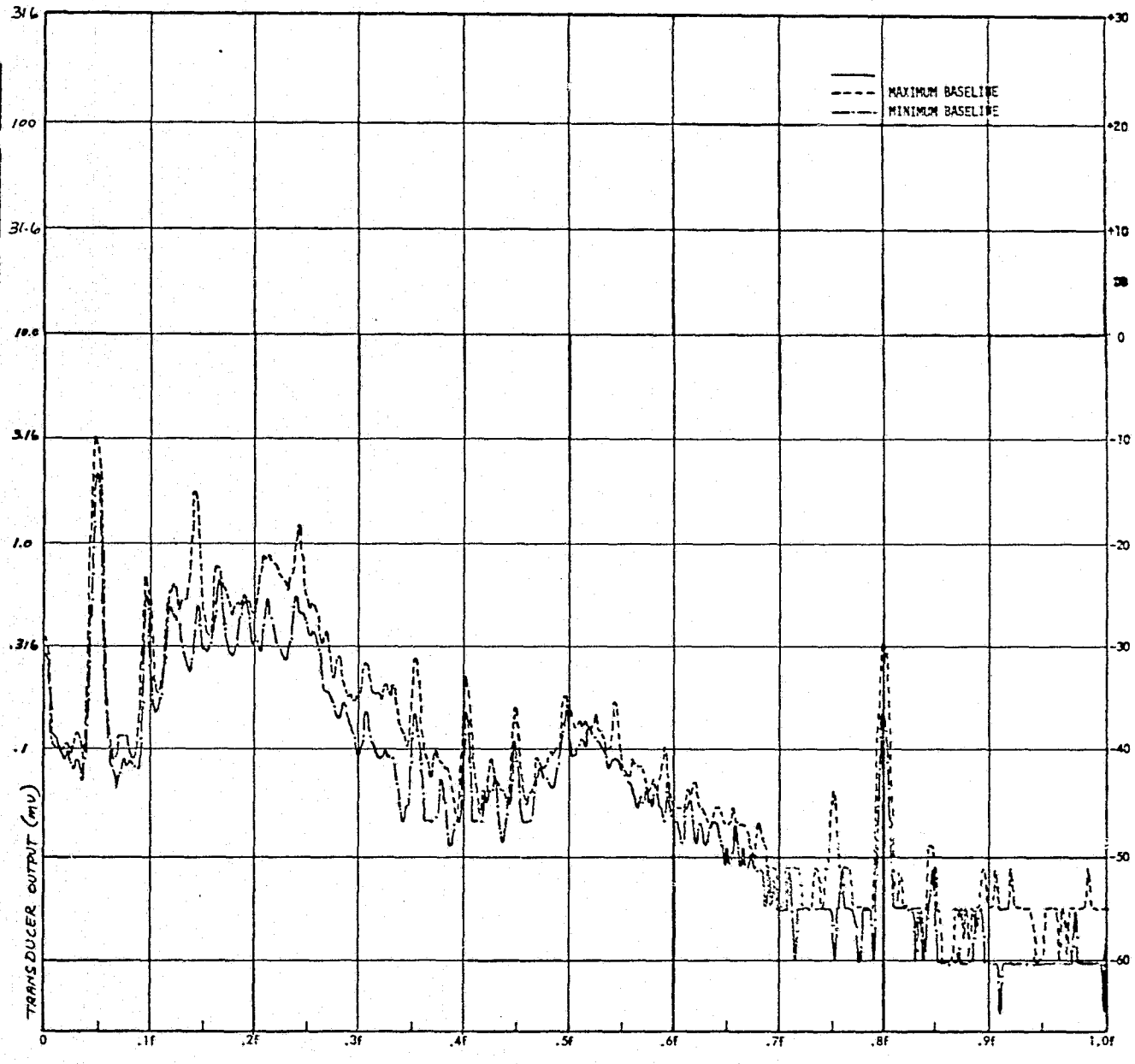

FIG. 25 FREQUENCY SPECTRUM FOR TRW GLOBE 19A532 FAN

TEST ITEM	TRW Globe 19A532
PLOT NO.	27
TRANSDUCER	B100-C

CONTROLLED TEST PARAMETERS	
VOLTAGE	115
P.S. FREQ.	400.0
ΔP	206 (.827)

VARIABLE TEST PARAMETERS	BASELINE	FAULT
DATE	3/11-3/20	
I	.360-.361	
ϕ<	.838	
PWR	27.7-27.8	
RPM	5640-5940	
FLOW RATE	9.44x10-3 - 9.74x10-3	
TEMP	293.0-296.3	
BARO	100681-102540	

PROCESSING CHANNEL PARAMETERS	
INPUT RESISTANCE	—
AMPLIFIER GAINS (DB)	
A_1	40
A_2	—
A_3	—
FILTER FREQUENCIES (KHZ)	
BAND PASS	—
HIGH PASS	1 KHz
LOW PASS	—

SPECTRUM ANALYZER PARAMETERS	BASELINE	FAULT
INPUT V. (MV)	80-90	
GAIN SETTINGS (0 DB REF)		
ANALYZER GAIN	10	
INPUT ATTEN.	12	
INTEGRATION		
LINEAR		
32 SUMS PER BIN		
COSINE WEIGHT		
D.C. COUPLE		
INTERNAL SAMPLE		

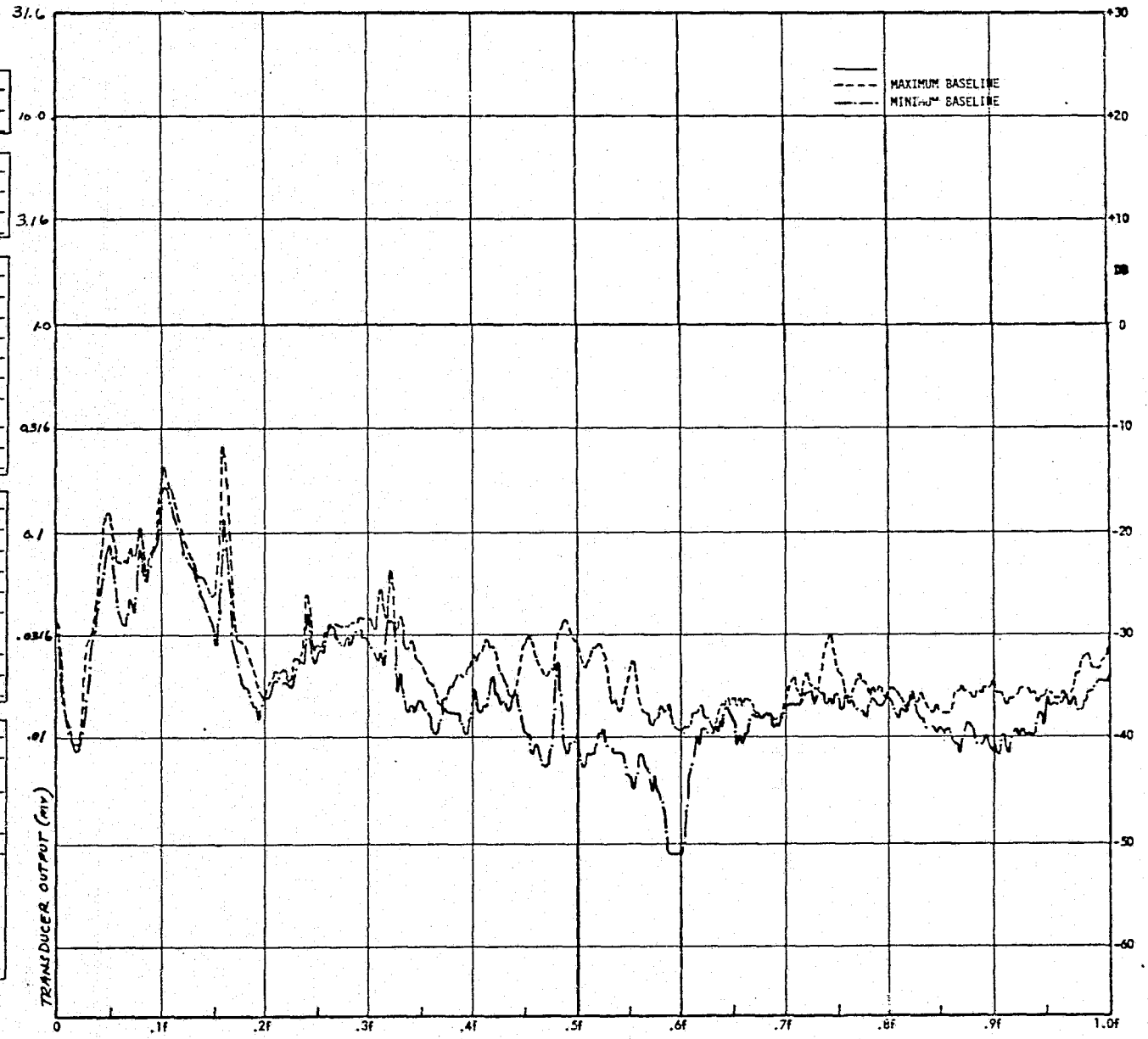

FIG. 26 FREQUENCY SPECTRUM FOR TRW GLOBE 19A532 FAN

TEST ITEM	TRW Globe 19A532
PLOT NO.	29
TRANSDUCER	8100-0

CONTROLLED TEST PARAMETERS	
VOLTAGE	115
P.S. FREQ.	400.0
ΔP	206 (.827)

VARIABLE TEST PARAMETERS	BASELINE	FAULT
DATE	3/11-3/20	
I	.360-.361	
ϕ<	.838	
PWR	27.7-27.8	
RPM	5640-5940	
FLOW RATE	9.44x10-3 - 9.74x10-3	
TEMP	293.0-296.3	
BARO	100381-102540	

PROCESSING CHANNEL PARAMETERS	
INPUT RESISTANCE	—
AMPLIFIER GAINS (DB)	
A_1	40
A_2	—
A_3	—
FILTER FREQUENCIES (KHZ)	
BAND PASS	—
HIGH PASS	5
LOW PASS	—

SPECTRUM ANALYZER PARAMETERS	BASELINE	FAULT
INPUT V. (MV)	40-57	
GAIN SETTINGS (0 DB REF)		
ANALYZER GAIN	10	
INPUT ATTEN.	12	
INTEGRATION		
LINEAR		
32 SUMS PER BIN		
COSINE WEIGHT		
D.C. COUPLE		
INTERNAL SAMPLE		

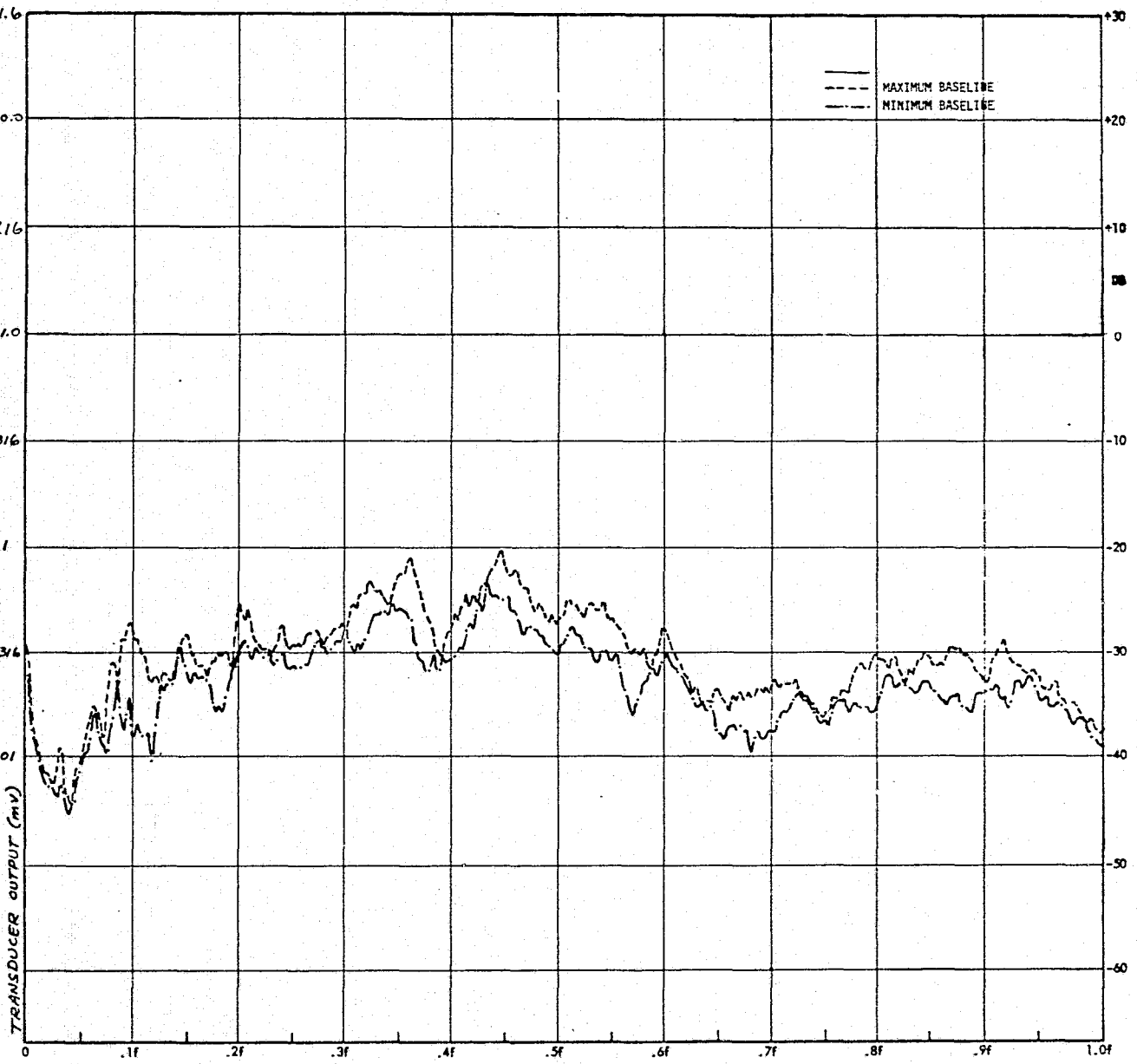

FIG. 27 FREQUENCY SPECTRUM FOR TRW GLOBE 19A532 FAN

ORIGINAL PAGE IS
OF POOR QUALITY

TEST ITEM	TRW Globe 19A532
PLOT NO.	31
TRANSDUCER	A100-0

CONTROLLED TEST PARAMETERS	
VOLTAGE	115
P.S. FREQ.	400.0
ΔP	206 (.827)

VARIABLE TEST PARAMETERS	BASELINE	FAULT
DATE	3/11-3/20	
I	.360-.361	
ϕ<	.838	
PWR	27.7-27.8	
RPM	5640-5940	
FLOW RATE	9.44x10-3 - 9.74x10-3	
TEMP	293.0-296.3	
BARO	100881-102540	

PROCESSING CHANNEL PARAMETERS	
INPUT RESISTANCE	22K
AMPLIFIER GAINS (DB)	
A_1	40
A_2	20
A_3	—
FILTER FREQUENCIES (KHZ)	
BAND PASS	—
HIGH PASS	50
LOW PASS	—

SPECTRUM ANALYZER PARAMETERS	BASELINE	FAULT
INPUT V. (MV)	220-250	
GAIN SETTINGS (0 DB REF)		
ANALYZER GAIN	10	
INPUT ATTEN.	12	
INTEGRATION		
LINEAR		
32 SUMS PER BIN		
COSINE WEIGHT		
D.C. COUPLE		
INTERNAL SAMPLE		

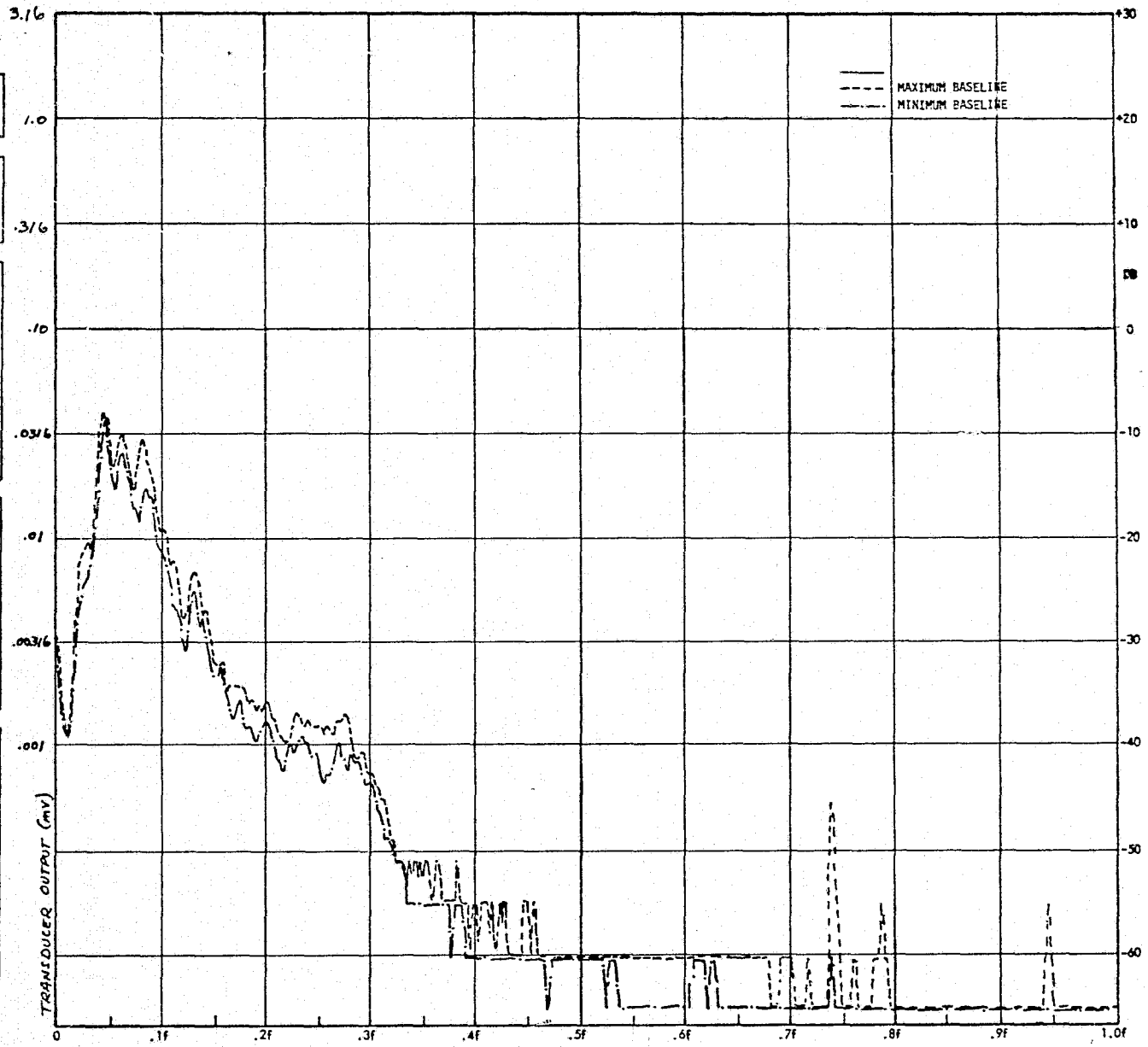

FIG. 28 FREQUENCY SPECTRUM FOR TRW GLOBE 19A532 FAN

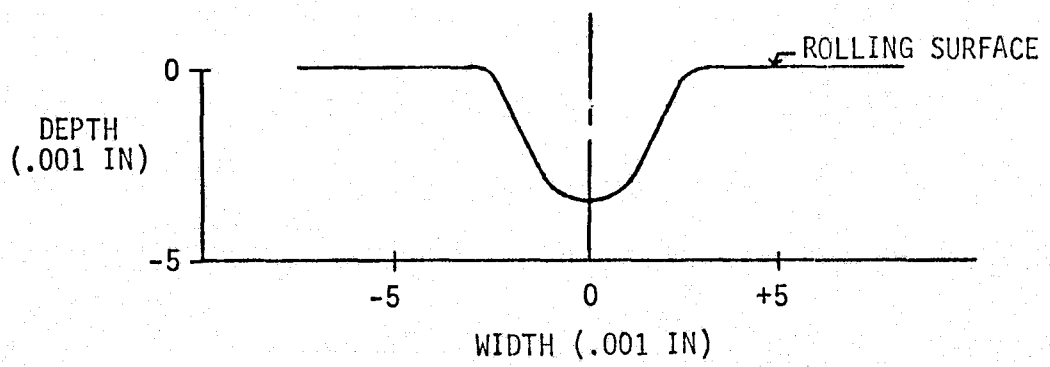

FIG. 29 BEARING ROLLING SURFACE SCRATCH CONTOUR

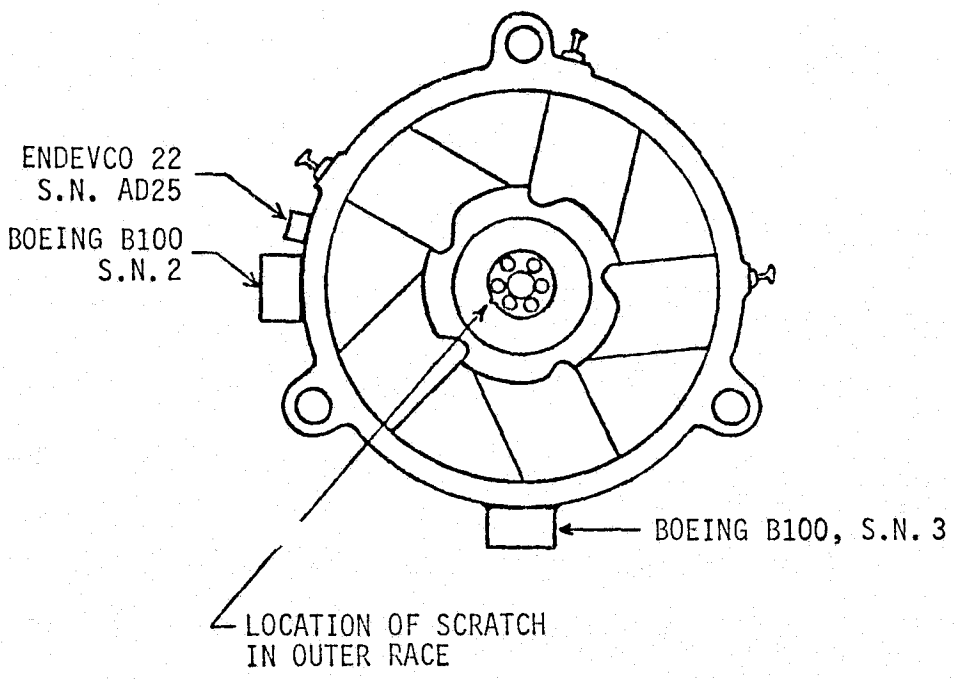

FIG. 30 BEARING OUTER RACE DEFECT POSITION IN ROTRON FAN

The fan did not have to be disassembled for the second fault condition since it was only required to unbalance the fan and the faulted bearing did not have to be replaced. The fan was unbalanced by placing a small drop (.0223 grams) of dental cement on one of the rotor blades as shown in Figure 31.

TRW Globe 19A532 Fan

The first fault which was introduced into this fan was unbalancing. The purpose of injecting this fault into the fan was twofold. First, it was necessary to determine if the Boeing acoustic sensor would detect the unbalance condition. Second it was important to determine how unbalancing might affect the high frequency processed parameters which could make it more difficult to detect a bearing incipient failure. The fan was unbalanced by wrapping a 1.75×10^{-2} meter length of #16 gauge copper solid wire around one of the squirrel cage fan's blades and soldering together the two open ends. The added weight amounted to 5.36×10^{-4} kilograms.

The second fault which was introduced into the fan was a bearing ball defect. The unbalancing weight which was previously added was removed. Disassembly of the fan was done using the procedure established during baseline testing. The TRW Globe #15D013A056 ball bearing closest to the fan's squirrel cage was removed and placed in a disassembly jig. The bearing's two shields were indexed with respect to the outer race so they could be reassembled in the same position. Also one side of the inner race was indexed to avoid the possibility of reversing its position when it was reassembled. The snap rings holding the shields in place were removed and the shields removed. Since it appeared it would be very difficult to fault a ball while it was still in the bearing, it was decided to remove a ball from the bearing and fault it externally. This required removing a two piece cage which was held together by seven fingers on one of the cage halves. The cage halves were indexed with the outer race, the seven fingers carefully pried up, and the two cage halves removed. The inner race was moved to one side and a single ball out of the seven selected. The ball was cleaned, cemented to a block using Eastman 910, and placed under a 30 power magnifier. A carbide scribe was then worked back and forth over a 180 degree arc around the circumference of the ball to make the scratch contour shown in Figure 29. Plowed up metal and loose particles were removed and the edges smoothed using an X-acto knife. The decision to make a 180 degree scratch around the ball instead of just a small point defect was made in order to avoid the possibility of the ball rolling in such a manner as to completely avoid rolling over the defect. This would result in inconclusive results. The bearing was then reassembled, taking care to reposition the fingers as close to their original position as feasible.

Dynamic Air Engineering C050L Fan

The fault which was to be introduced into this fan was a bearing inner race defect. The fan was disassembled using the procedure established during baseline testing. The K271D-38SSEL ball bearing closest to the fan's impeller was removed and placed in a disassembly jig. The bearing's two shields were indexed with respect to the outer race so they could be reassembled in the same position. Also one side of the inner race was indexed to avoid the possibility of reversing its position when it was reassembled. The snap rings holding the shields in place were removed and the shields removed. The two cage halves were indexed with the outer

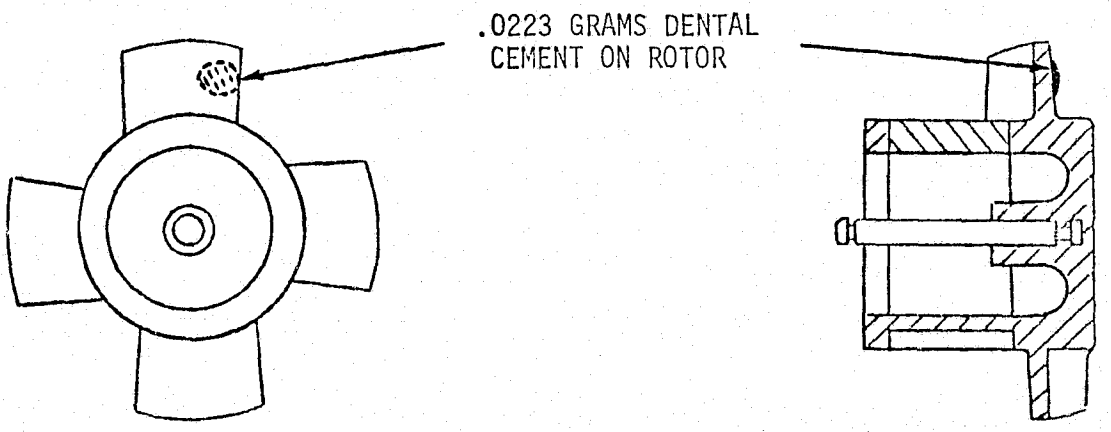

FIGURE 31 LOCATION OF .0223 GRAMS DENTAL CEMENT USED TO UNBALANCE ROTRON FAN'S ROTOR

race, the seven fingers which were holding the cage halves together were carefully pried up, and the cage halves were removed. The seven balls were moved to one side along the outer race, and the inner race was then removed. Care was taken during this procedure to minimize the removal of grease from the bearing's components and to keep dust particles from getting on them. The inner race was placed in a lab vise under a 30 power magnifier. Grease was removed from a small section of the inner race. A carbide scribe was then worked back and forth in this section across the race to make the scratch shown in Figure 29. Plowed up metal and loose particles were removed and the edges smoothed using an X-acto knife. The bearing was then reassembled, taking care to reposition the fingers as close to their original position as feasible. The fan was reassembled following the procedure established during baseline testing.

Micropump 10-71-316-1367 Pump

The fault which was to be introduced into the Micropump 10-71-316-1367 pump was a brinelling of the Fafnir SIKDD7 bearing closest to the pump's impeller. A test fixture was constructed which would hold the bearing in place so that it could be loaded radially in tension by an Instron Model TT-D Universal Testing instrument. Spare bearings were loaded to 4,450 newtons (1000 pounds), 8,900 newtons (2000 pounds) and 17,790 newtons (4000 pounds) and later examined to determine the extent of the brinelling. An attempt was made to load the bearing previously loaded to 17,790 newtons (4000 pounds) to 35,580 newtons (8000 pounds), however two balls sheared in half at a load of 16,680 newtons (3,750 pounds). Another spare bearing was loaded to 20,100 newtons (4,520 pounds) at which point a ball cracked. After the preliminary fault injection testing was completed, it was decided to load the bearing closest to the pump's impeller to 13,350 newtons (3000 pounds).

Disassembly of the pump was done using the procedure established during baseline testing. The Fafnir SIKDD7 ball bearing closest to the pump's impeller was removed and placed in the loading fixture. The fixture was placed in the Instron Tester and the bearing loaded in tension to 13,350 newtons (3000 pounds). After failure injection, the pump was reassembled and a complete set of fault data collected. The results of the fault testing indicated that the induced fault was too large, and that a less brinelled bearing could be detected. To determine to what extent the bearing should be brinnelled in order to appear as an incipient failure, the faulted bearing was replaced with a spare bearing which had been brinelled by loading it to 4,450 newtons (1000 pounds). The resulting spectrum test data showed a large increase in RMS signal level between 2 KHz and 19 KHz, and very little change for signals greater than 20 KHz. Whereas, the defect did show up in the spectral analysis of the detected 20 KHz acoustic signal it was much more pronounced in lower frequency detected signal spectrum plots. Since no baseline data had been taken for this bearing, nor at these lower frequencies, it was necessary to replace the second faulted bearing with a good spare bearing and collect additional baseline data. This third bearing was then brinelled by loading it to 4,450 newtons (1000 pounds), reinstalled in the pump, and a complete set of lower frequency fault data taken.

After all fault testing was completed the three faulted bearings were destructively disassembled to examine the degree of brinelling which had been introduced into each one. A description of the amount of brinelling follows.

For the original bearing, loaded to 13,350 newtons (3000 pounds), brinell indentations appeared at two places on both the inner and outer races. All indentations were oval in shape, were approximately 6.35×10^{-4} meters (.025 inches) wide (along rolling direction) and extended across the width of the rolling surfaces, which was about 1.905×10^{-3} (.075 inches). Two balls were also distorted so that their dimensions were $+2.03 \times 10^{-5}$ meters (.0008 inches) and -4.57×10^{-5} meters (.0018 inches) of nominal.

For the first replacement bearing, loaded to 4,450 newtons (1000 pounds), brinell indentations appeared at three places on both the inner and outer races. All indentations were oval in shape. The center indentation was approximately 3.05×10^{-4} meters (.012 inches) wide and the two outer indentations were about 2.54×10^{-4} meters (.010 inches) wide. All indentations extended across the width of the rolling surfaces. No measurable amount of distortion could be found among the eight balls.

For the second replacement bearing, loaded to 4,450 newtons (1000 pounds), brinell indentations appeared at one place on both the inner and outer races. The indentation was oval in shape, was approximately 3.81×10^{-4} meters (.015 inches) wide, and extended about 85% across the width of the rolling surfaces. No measurable amount of distortion could be found among the eight balls.

Hydrokinetics 10461 Pump

The fault which was to be introduced into the Hydrokinetics 10461 pump was a dry Barden 38SSTX2K5G32 bearing which is located closest to the impeller. This seemed to be a natural type of fault for this pump since a leaking seal experienced prior to baseline testing almost resulted in this problem occurring. The pump was disassembled using the procedure established prior to baseline testing up to the point where it became necessary to remove this bearing from its housing. During baseline testing this was simply done by removing the four screws holding the rear motor plate and pulling on the plate. This resulted in the removal of the rotor and front bearing from its housing. However, during disassembly to introduce the fault the front bearing came off the rotor shaft and stuck in its housing. When an attempt was made to push on the bearing's inner race to remove it from its housing, the bearing housing, which was press fitted into the motor case, came undone. No more attempts were made to remove the bearing from its housing. Instead the rear shield of the bearing was removed and the bearing washed out with Varsol and acetone and blown dry with compressed air. The rear shield was then reinstalled and the pump reassembled following the procedure established prior to baseline testing.

When the pump was first turned on to collect fault data the seal leak problem experienced prior to baseline testing reoccurred. The pump's impeller housing and impeller were removed and the seal repositioned, which resulted in stopping the leak. Because of the leak, water had gotten into the dry faulted bearing. However, since this closely approached an actual problem for a pump like this, and because of the difficulty encountered in removing the front bearing to dry it out, it was decided to run the fault test under these conditions.

Because of the use of a tape recorder for collecting fault data during this test, which is discussed in the next section, the total pump run time for all the fault tests was 78 minutes. The first fault test run to collect data for what was considered to be a water lubricated bearing lasted only six minutes and was done on 8-5-75. On 8-11-75 the pump was run for six short runs for a total of 72 minutes to generate and collect other fault data. On 8-13-75 the pump was once again disassembled to determine the degree of deterioration of the faulted bearing. During this 8-day period there had been no evidence of any further leaking of the pump. When the faulted bearing was inspected on 8-13-75, there was moisture on the inside of the bearing and on the inside of the pump housing. Since it appears this moisture could only have gotten into the bearing when the pump leaked prior to the fault test run on 8-5-75, it can safely be hypothesized that the faulted bearing had water lubrication when the first fault test was run.

After fault data for the water lubricated bearing was compared against the worst case baseline data, there appeared to be only a minor difference between the two. Because of this it was decided to run the pump in an attempt to try and dry the bearing out or to damage it in some other fashion. When an attempt was made to start the pump, it would not turn over. Hand turning of the pump shaft indicated an initial resistance which was assumed to be caused by corrosion having taken place inside the faulted bearing. After a few rotations of the pump shaft by hand were completed, the pump was started in the normal fashion. Data was recorded for what was considered to be a corroded bearing. When the bearing was inspected on 8-13-75, the assumption that the bearing was corroded was confirmed. All seven balls in the bearing were thoroughly covered with oxidation. The outer race exhibited the second most severe amount of oxidation, primarily on the area where the phenolic cage was in close proximity to the outer race which resulted in the retention of water in this area. The inner race was the least affected of the bearing components, since the cage is not in close proximity to it and thus could not hold water against it. The bearing components were cleaned to remove the surface oxidation and determine the extent of surface pitting. The entire surface of all balls were covered with minute surface pits with the largest pitting around the two areas of each ball where it had rested in contact with the two raceways, especially in the areas where the balls had rested in the six day period between the two test runs.

When the pump was first turned on on 8-11-75, the high frequency (>85 KHz) RMS signal level was approximately three times its previous level due to the corrosion effect. After about half an hour of running, the high frequency RMS signal level fell to its approximate normal value indicating that the corrosion effects had been worn away. After approximately 37 minutes more running time had elapsed, the pump started emitting a high pitched

audible noise. The tape recorder, which was not in operation at the time, was turned on, but the pump started drawing more current than normal and caused the 400 Hz power supply to drop out before sufficient data could be collected for proper processing. After 5 minutes, the pump was restarted and ran for 5 minutes before the high pitch audible noise started again. The recorder was restarted and 11 seconds of data recorded, sufficient to do RMS, count, and spectrum data analysis, before the power supply dropped out. It was assumed that the bearing had overheated in these two instances thus reducing internal clearances in the bearing and causing internal overloading which caused the high pitched audible noise. The frequency of the noise was later determined to be 982 Hz, which for the slower shaft speed of 22,620 RPM experienced during these instances, turned out to be the outer race ball passing frequency of the faulted bearing, f_{o1}. Later examination of the bearing on 8-13-75 showed that the balls had lost their shininess, which indicated they had overheated.

PHASE II TESTING (reference paragraph 3.2.5 of SOW)

In order to summarize the Phase II test data, several processed parameters were chosen, most of which are shown in Table XX. The terminology for these parameters is contained in the paragraph entitled DEFINITIONS. The table lists those parameters which were processed for each defect by identifying the frequency range over which each parameter was processed. A (——) in the table signifies that that parameter was not processed for the particular defect. Plots of SADAS-6 and SANDAS-6 for the fans are not included in the text of the report since these are multiple defect parameters and only single defects were inserted into the fan's bearings. The SADAS-6 parameter was calculated for the Summary of Results (Table I) however, since this appears to be one of the most useful design parameters for an actual test instrument.

In addition to the parameters shown in Table XX the high frequency bandpass parameters RMS-1, TCCFR-1, TCCFR-2, and SEACOST-1 were determined for each of the defects for which the SADAS parameters were determined. An exception to this is the reduced bearing internal clearance defect for the Hydrokinetics pump. In this case, SEACOST-1 data could not be determined because of the short data sample.

Rotron Aximax 2-464-YS Fan

The outer race defect in the bearing was expected to generate a train of narrow vibration/acoustic pulses with a repetitive frequency equal to the outer race ball passing frequency of 399.6 - 402.0 Hz. This bearing defect could not be detected with any significant degree of certainty by an examination of the low frequency baseband vibration/acoustic spectrum, as is evident in Figure 32. Notice that the spectral line associated with the outer race ball passing frequency did not exceed the maximum baseline value. However, the defect was detected at every high bandpass frequency examined and by every processed parameter. An example of this is shown in Figure 33, which is a SADAS plot for a 300 KHz bandpass frequency. The SADAS parameters at this frequency provided the greatest fault detectability of all the processed parameters.

TABLE XX. PROCESSED PARAMETERS

TEST ITEM	FAULT	FREQ. RANGE (Hz) USED FOR COMPARING DEFECT DATA WITH MAXIMUM BASELINE								
		HIGH FREQUENCY BANDPASS PARAMETERS						LOW FREQUENCY PARAMETERS		
		SADAS-1 & SANDAS-1	SADAS-2 & SANDAS-2	SADAS-3 & SANDAS-3	SADAS-4 & SANDAS-4	SADAS-5 & SANDAS-5	SADAS-6 & SANDAS-6	BVRMS-1	SABVS-5	SABVS-6
ROTRON AXIMAX 2-464-YS FAN	BEARING OUTER RACE DEFECT	399.6 - 402.0	0 - 1000	0 - 5000	-	-	387 - 713	-	-	-
	BRG O.R. DEF. & UNBALANCE	399.6 - 402.0	0 - 1000	0 - 5000	-	-	387 - 713	-	-	-
	UNBALANCED	-	-	-	-	-	-	0 - 1000	175-188 + 350-376	
TRW 19A532 FAN	BEARING BALL DEFECT	285.3 - 300.5	-	-	0 - 500	276 - 310	223 - 464	-	-	-
	BRG BALL DEF. IF UNBALANCED	-	-	-	0 - 500	276 - 310	223 - 464	-	-	-
	UNBALANCED	94.0 - 99.0	-	-	-	-	-	0 - 500	91-102 + 182-204	-
DYN. AIR ENG. CO5OL FAN	BEARING INNER RACE DEFECT	-	0 - 2000	-	-	1679 - 1787	973 - 1787	-	-	-
MICROPUMP 10-71-316-1367 PUMP	3000# BRINNELLED BRG.	-	-	-	0 - 1000	-	517 - 858	-	-	-
	1000# BRINNELLED BRG.	-	-	-	0 - 1000	-	517 - 858	-	-	-
HYDROKINETICS 10461 PUMP	WATER LUBRICATED BRG.	-	-	-	-	-	979 - 1764	0 - 2000	979 - 1045	979 - 1764
	CORRODED BEARING	-	-	-	-	979 - 1045	979 - 1764	0 - 2000	979 - 1045	979 - 1764
	BRG. INTERNAL CLEAR. REDUCED	-	-	-	-	979 - 1045	979 - 1764	0 - 2000	979 - 1045	979 - 1764

ORIGINAL PAGE IS
OF POOR QUALITY

TEST ITEM	AXIMAX-2-464YS
PLOT NO.	37
TRANSDUCER	Sloo-3

CONTROLLED TEST PARAMETERS	
VOLTAGE	115
P.S. FREQ.	400.0
FLOW RATE	8.85×10^{-3} (18.75)

VARIABLE TEST PARAMETERS	BASELINE	FAULT
DATE	12/12-2/17	4/17
I	.112-.114	.113
ϕ	.576	.558
PWR	10.8-11.0	11.0
RPM	10,870-10,940	10,956
ΔP	186.1 (.747)	186.1
TEMP	292.49-296.39°	293.6-295.8
BARO	100581-102540	101592

PROCESSING CHANNEL PARAMETERS	
INPUT RESISTANCE	—
AMPLIFIER GAINS (DB)	
A_1	20
A_2	—
A_3	—
FILTER FREQUENCIES (KHZ)	
BAND PASS	—
HIGH PASS	—
LOW PASS	1

SPECTRUM ANALYZER PARAMETERS	BASELINE	FAULT
INPUT V. (MV)	21-35	26
GAIN SETTINGS (0 DB REF)		
ANALYZER GAIN	20	
INPUT ATTEN.	21	
INTEGRATION		
LINEAR		
32 SUMS PER BIN		
COSINE WEIGHT		
D.C. COUPLE		
INTERNAL SAMPLE		

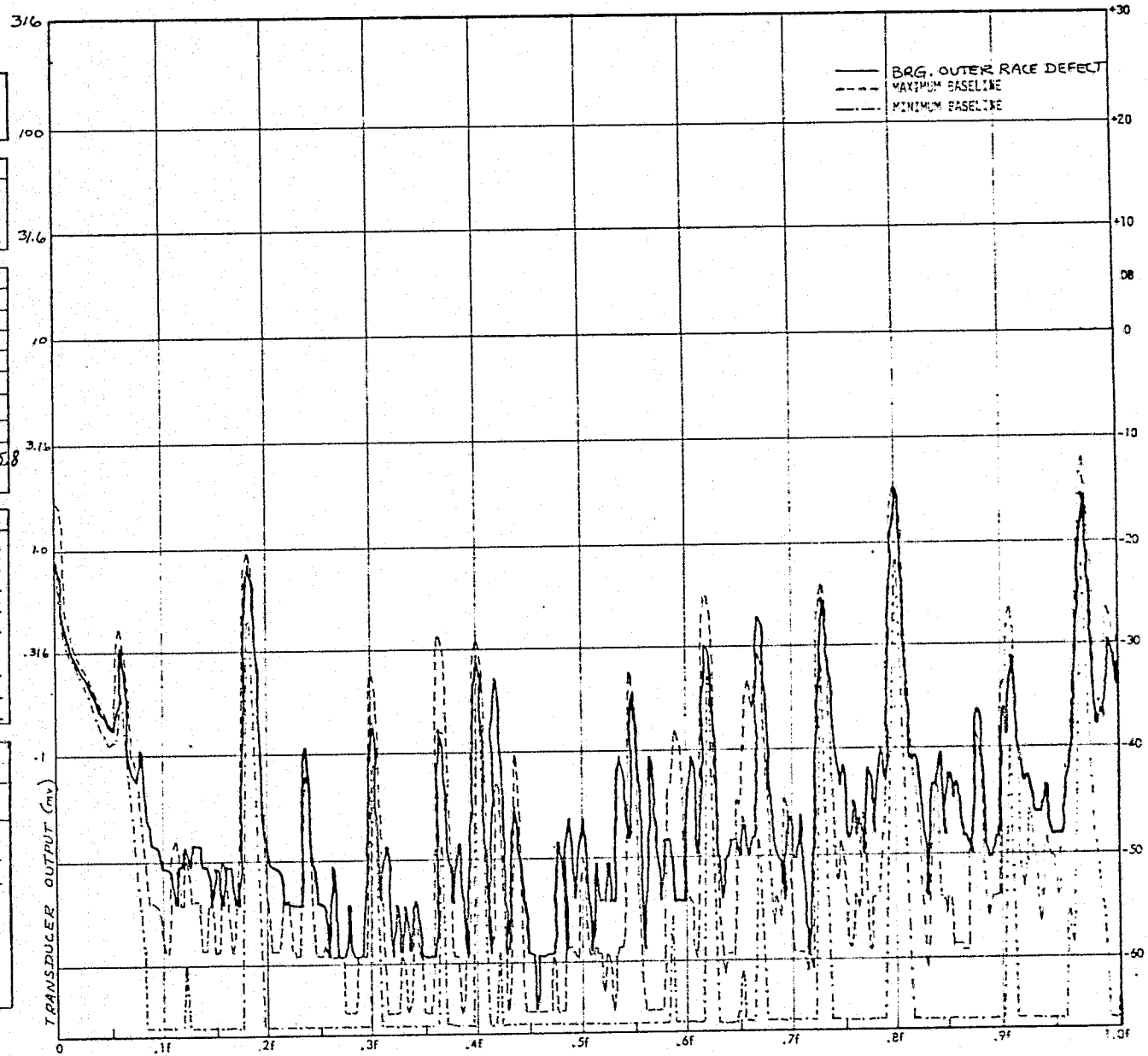

FIG. 32

FREQUENCY SPECTRUM FOR ROTRON AXIMAX-2-464 YS FAN

TEST ITEM	AXIMAX-2-464YS
PLOT NO.	87
TRANSDUCER	8100-3

CONTROLLED TEST PARAMETERS	
VOLTAGE	115
P.S. FREQ.	400.0
FLOW RATE	8.85×10^{-3} (18.75)

VARIABLE TEST PARAMETERS	BASELINE	FAULT
DATE	12/12-2/17	4/18
I	.112-.114	.113
ϕ<	.576	.558
PWR	10.8-11.0	11.0
RPM	10,870-10,940	10,946
ΔP	186.1 (.747)	186.1
TEMP	292.49-296.3°	293.6-295.8
BARO	100581-100643	101592

PROCESSING CHANNEL PARAMETERS	
INPUT RESISTANCE	22kΩ
AMPLIFIER GAINS (DB)	
A_1	40
A_2	40
A_3	20
FILTER FREQUENCIES (KHZ)	
BAND PASS	300
HIGH PASS	200
LOW PASS	1

SPECTRUM ANALYZER PARAMETERS	BASELINE	FAULT
INPUT V. (MV)	10-55	2200
GAIN SETTINGS (0 DB REF)		
ANALYZER GAIN	10	
INPUT ATTEN.	0	
INTEGRATION		
LINEAR		
32 SUMS PER BIN		
COSINE WEIGHT		
D.C. COUPLE		
INTERNAL SAMPLE		

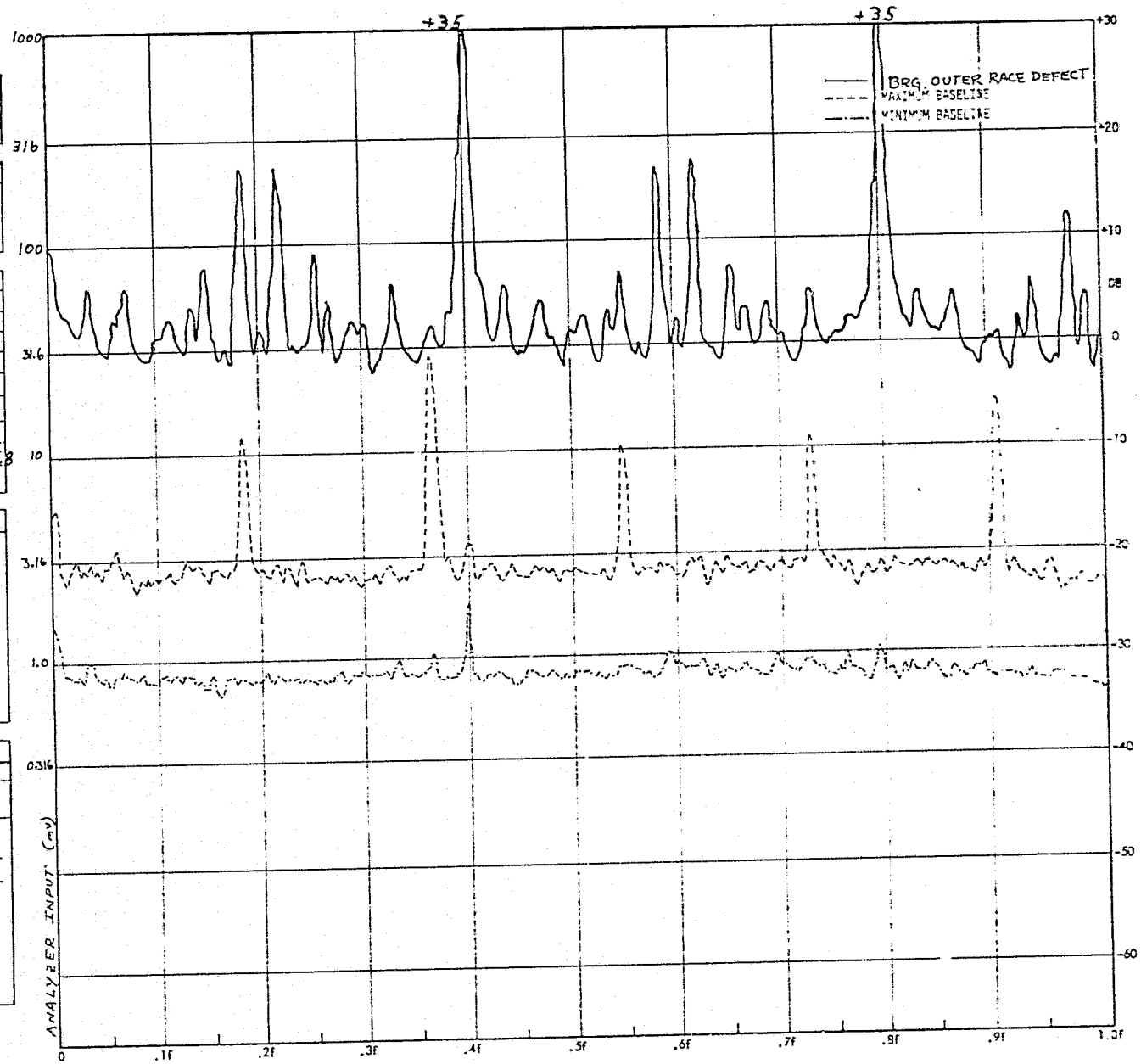

FIG. 33 FREQUENCY SPECTRUM FOR ROTRON AXIMAX-2-464 YS FAN

A comment on how the frequency spectrum fault data was collected is in order here. During the initial baseline runs, test equipment gains, such as the amplifier gains and the spectrum analyzer's input attenuator and analyzer gain, were adjusted so that spectral lines for baseband spectrums could increase at least 10 db without distortion and spectral lines for SADAS plots could increase at least 20 db without distortion. The difference in the two was set because the baseband spectrums usually required more dynamic range for recording that do the SADAS data, and the SADAS data usually increases much more when a fault is injected than do the baseband spectrums. The usable dynamic range of the SAICOR spectrum analyzer, without showing too coarse a structure (1 db resolution) is 42 db. Thus, this allowed a 32 db dynamic range for collection of the baseband baseline spectrums and 22 db for collection of the SADAS baseline data. Additional baseline runs may have been higher than the original runs, in which case they used up some of the 10 db or 20 db dynamic range allowed for the fault data. When the first fault data was run for the Rotron fan it was found that while the 10 db allowed for baseband spectrums was sufficient, the 20 db allowed for SADAS data was not nearly so. Because of this, the additional 30 db scale was added on to the composite baseline plots, as discussed previously. The fault data for the Rotron fan was so large that it saturated the test equipment. Because of this, gains were decreased to eliminate this distortion. The amount the gain was decreased was either 10, 20 or 30 db. To compensate for this gain reduction, the X-Y recorder zero reference, which was set to 0 db for all the baseline runs, was increased to +10, +20, or +30 db, respectively. In a few cases, such as shown in Figures 33 and 41, even this was not sufficient to eliminate saturation of the spectrum analyzer as can be seen by saturation of the spectral lines at 400 and 800 Hz. In these cases, the actual amplitude of these spectral lines, in db, was recorded by the line.

The high frequency bandpass summarized results for the bearing outer race defect are shown in Figures 34 through 37. Figures 34 and 35 are non-normalized processed parameters for transducers B100 - S.N. 2 and B100 - S.N. 3, respectively. All four parameters show a general increasing trend up to approximately 200 KHz. From this data it would appear that 200 KHz would be an optimum operating frequency for detecting this type of defect in the Aximax fan. However, the defect introduced into the fan was unintentionally relatively large compared to the dimensions of the bearing which resulted in the large increase in RMS level. It most likely would have been possible to detect a much smaller defect which would not have affected the RMS level. Some insight as to what might have resulted from a smaller defect can be obtained from the normalized spectrum data (SANDAS-1, 2, 3) in Figures 36 and 37.. For this data the equivalent RMS level remains constant since the data is normalized. The SANDAS data indicate a more optimum frequency of operation would be 50 - 80 KHz for smaller defects.

The SEACOST-1 parameter turned out to be the best normalized processed parameter for detecting this particular defect. The 3 σ spike voltage, shown in Figure 38, is very sensitive to the large spikes generated by this type of defect and tends to approach the RMS voltage level for very large spikes.

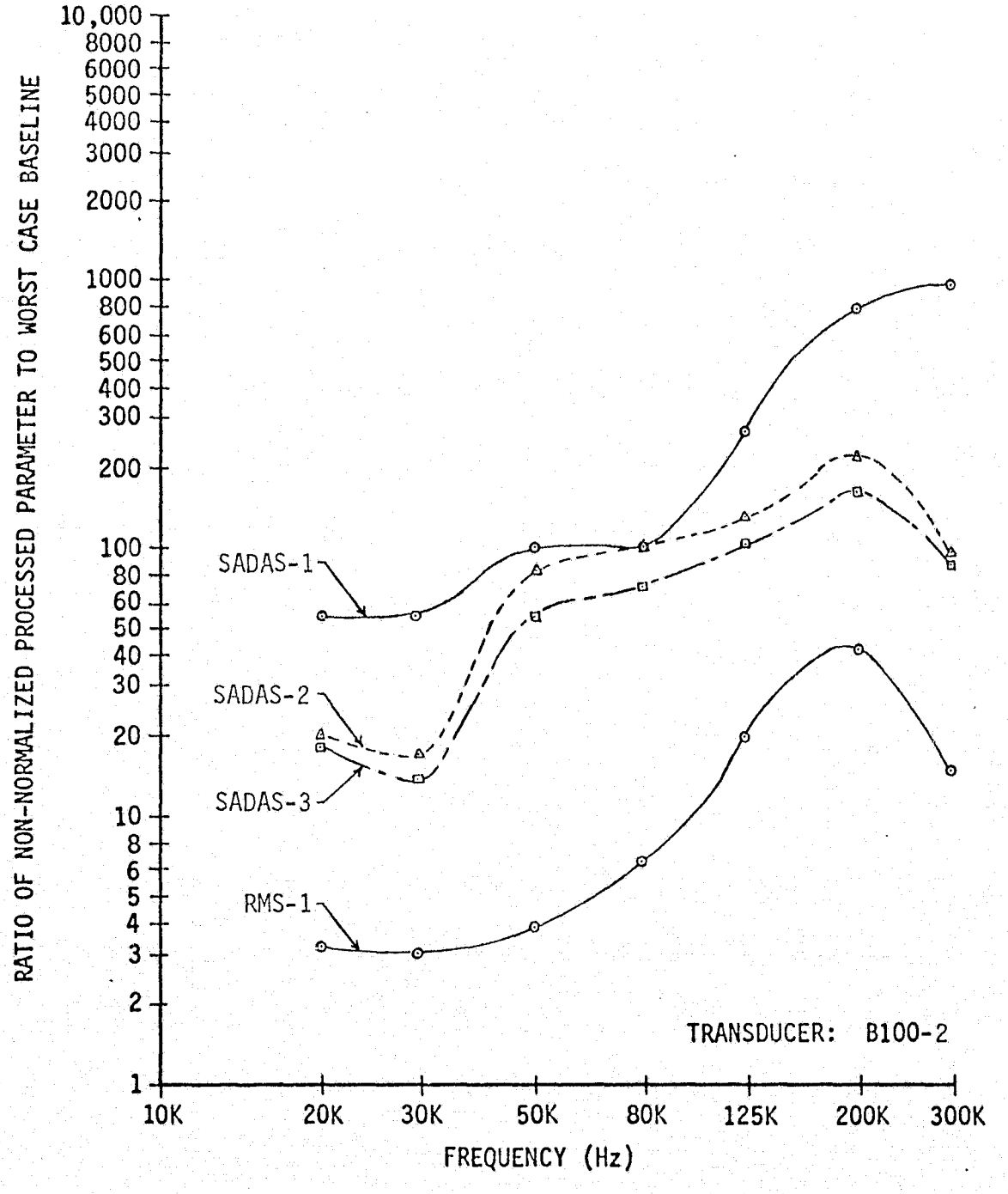

FIG. 34 NON-NORMALIZED PROCESSED PARAMETER CHANGES DUE TO BEARING OUTER RACE FLAW IN ROTRON 2-464-YS FAN

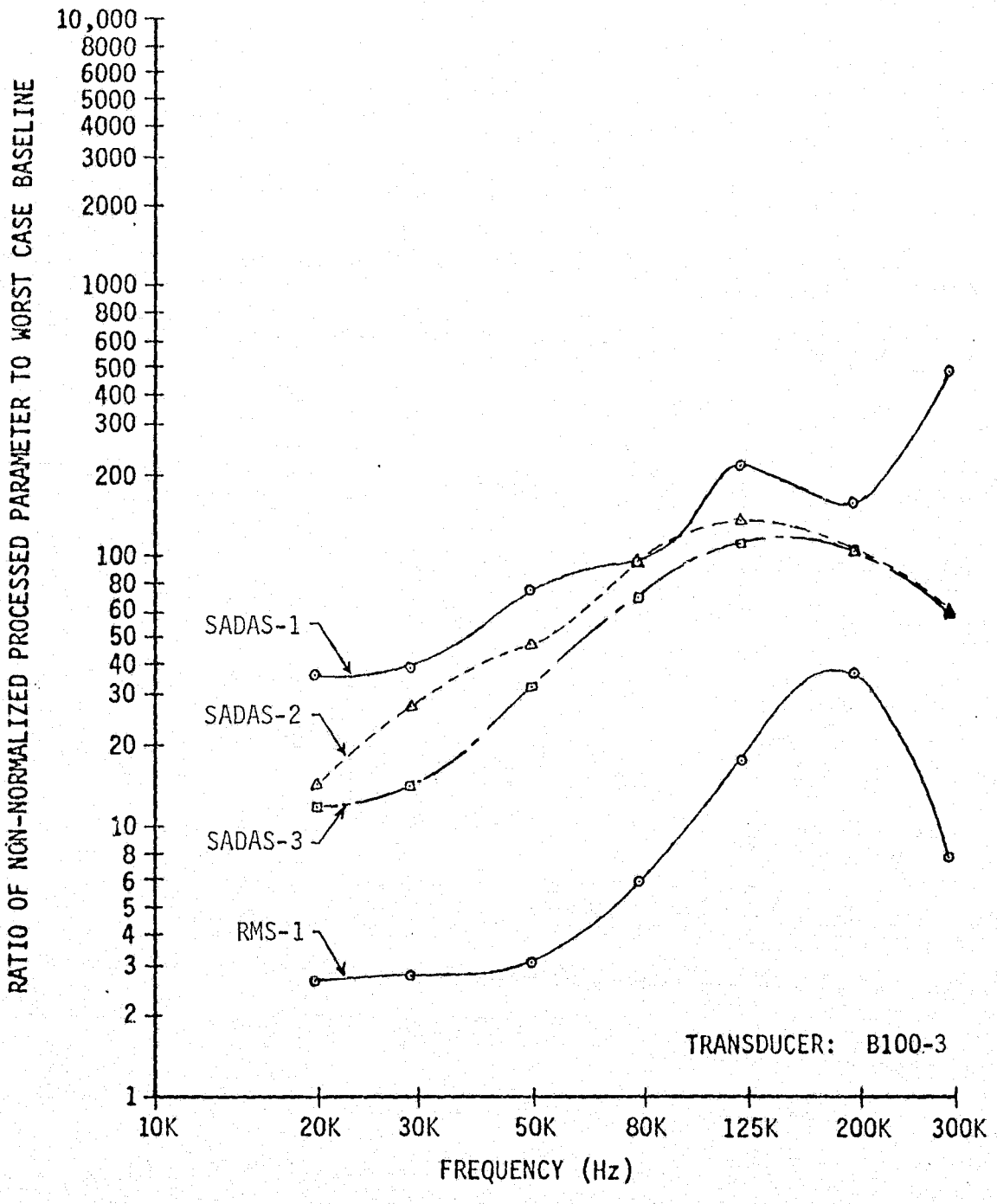

FIG. 35 NON-NORMALIZED PROCESSED PARAMETER CHANGES DUE TO BEARING OUTER RACE FLAW IN ROTRON 2-464-YS FAN

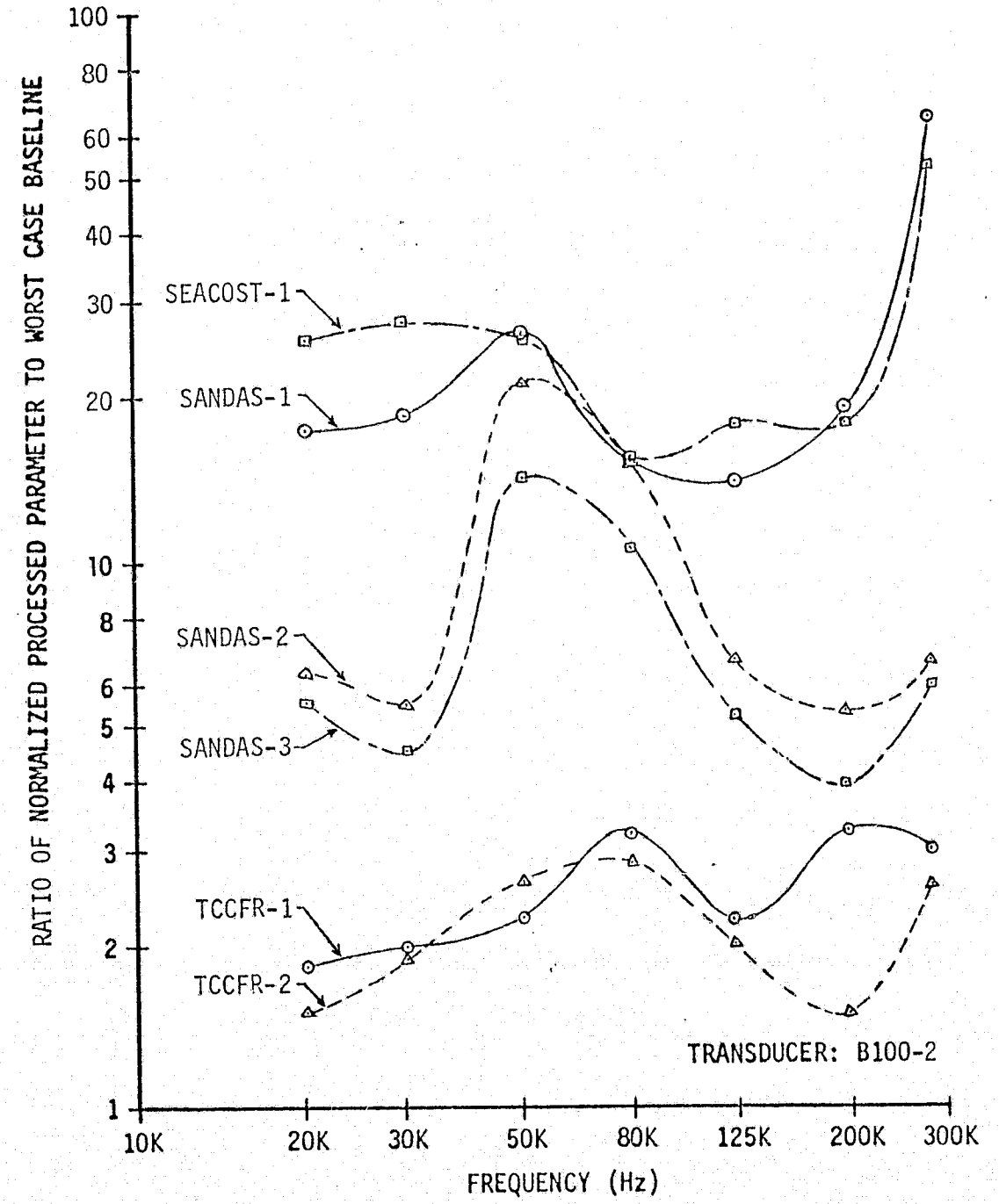

FIG. 36 NORMALIZED PROCESSED PARAMETER CHANGES DUE TO BEARING OUTER RACE FLAW IN ROTRON 2-464-YS FAN

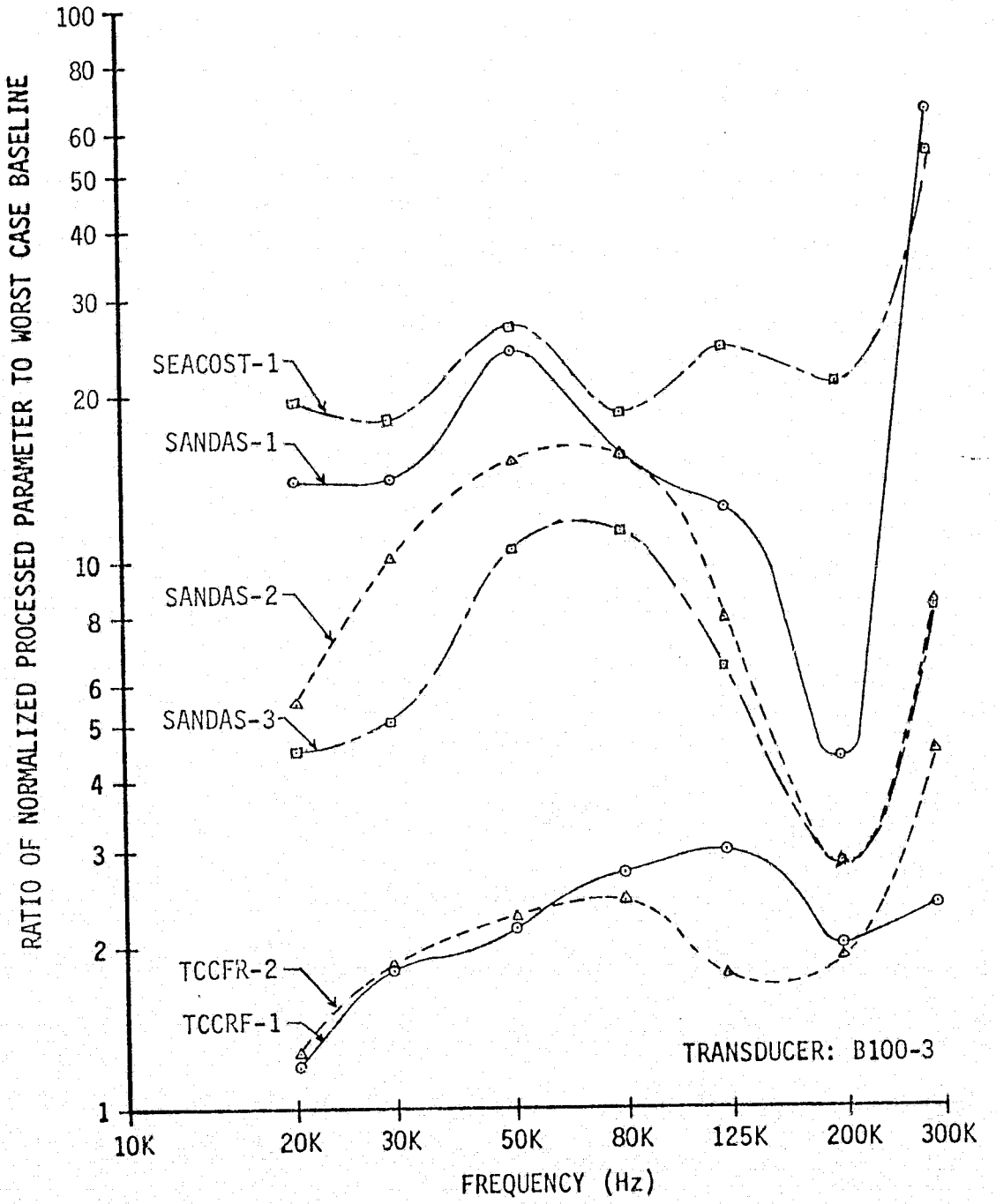

FIG. 37 NORMALIZED PROCESSED PARAMETER CHANGES DUE TO BEARING OUTER RACE FLAW IN ROTRON 2-464-YS FAN

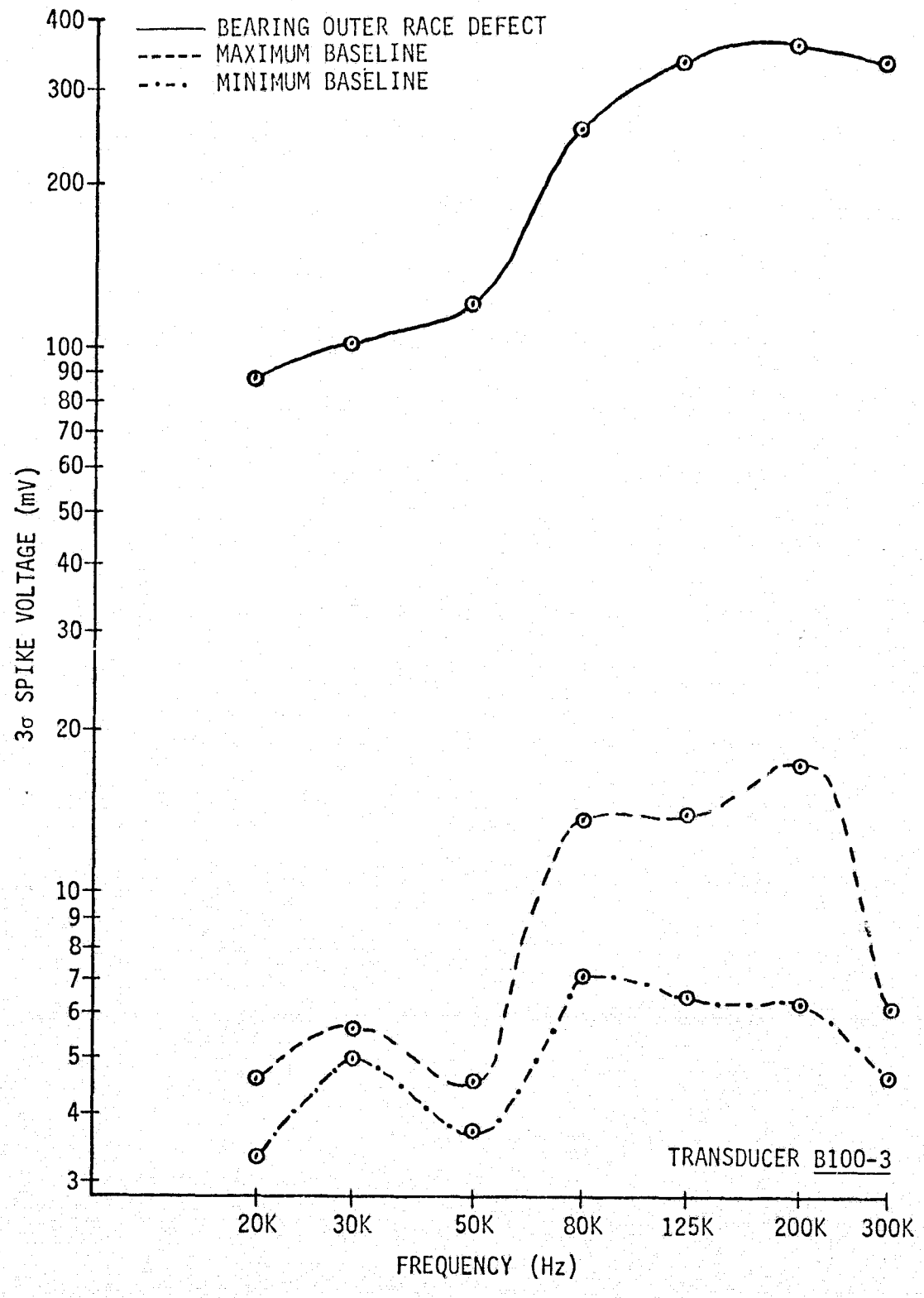

FIGURE 38 3σ SPIKE DATA FOR ROTRON FAN

The TCCFR parameters are not as sensitive to this particular type of defect as the SEACOST parameter and thus did not increase as significantly. However, they still exhibited a minimum increase of 2.4:1 at 80 KHz, as can be seen in Figure 39.

Table XXI summarizes the changes in three low frequency parameters which resulted from the bearing defect and from the unbalancing and the bearing defect combination. Note that the bearing defect alone did not cause the average value of any of the three parameters to exceed their worst case baseline condition whereas all three parameters exceeded the worst case baseline when unbalancing was added.

Figure 40 is the spectrum of the baseband vibration/acoustic signal for the combination bearing outer race defect and unbalance. It shows the increase in the spectral line associated with the shaft frequency, 181.2 - 182.3 Hz. Note that the spectral line associated with the outer race ball passing frequency still did not exceed the maximum baseline value. Figure 41 is a SADAS plot for the combination bearing defect and unbalance for a 300 KHz bandpass frequency. This plot is similar to that shown in Figure 33. Figures 42 through 45 are the high frequency summarized results for the unbalance and bearing defect combination. The data did not change significantly from that determined with the bearing defect alone and thus it can be assumed that the unbalance had little effect on the ability to detect the bearing defect.

TRW Globe 19A532 Fan

Unbalancing of the TRW Globe fan was expected to increase the overall low frequency vibration level and specifically the spectral line associated with the fundamental shaft frequency. The baseline SADAS data showed significant spectral lines at the fundamental shaft frequency of 94.0 to 99.0 Hz and its harmonics. These spectral lines associated with the high frequency data are usually caused by looseness in the bearing or machine parts, which results in a rattling or hammering effect in synchronism with the shaft. Although it is often desirable to detect this effect, these signals represent a source of interference when one is trying to detect a bad bearing. Machine unbalance just accentuates these hammering effects and thus makes it more difficult to detect a defective bearing. An interference signal of particular significance in this test is the third harmonic of the shaft frequency (282.0 - 297.0 Hz) which is very close to the frequency associated with the ball defect (285.3 - 300.5 Hz). Thus, it was expected that unbalancing the fan might make it difficult to detect a defective ball in the bearing.

Figures 46 through 49 are the high frequency bandpass summarized results for the unbalance condition. Whereas, the RMS level at all high frequencies did not change that much (a maximum of 66% at 40 KHz for B100-0) the increase in SADAS-1 and SANDAS-1 due to the rattling or hammering effect discussed previously did increase significantly. This is illustrated in the SADAS plots shown in Figure 50 and 51. Changes of this extent due to unbalance might make it difficult to detect incipient bearing failures using the SADAS-4 processed parameter. Using this parameter, which detects the maximum spectral line in the total SADAS baseband, one would not know

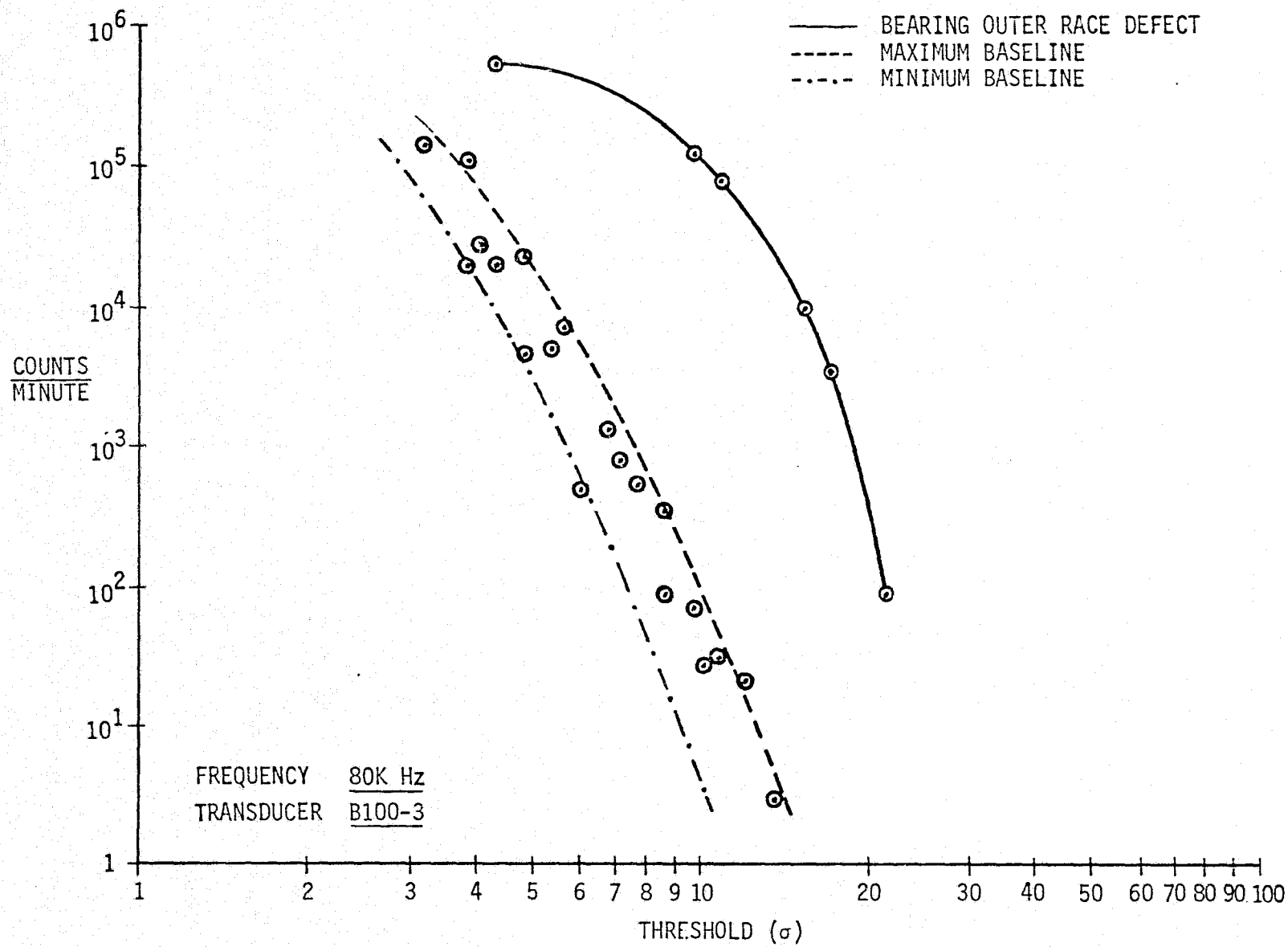

FIG. 39 COUNT DATA FOR ROTRON FAN

TABLE XXI. LOW FREQUENCY TEST RESULTS FOR ROTRON FAN

SENSOR	VBRMS-1		SABVS-5 (f_s)		SABVS-5 ($2f_s$)	
	BEARING O.R. DEFECT	UNBALANCED & BRG. DEFECT	BEARING O.R. DEFECT	UNBALANCED & BRG. DEFECT	BEARING O.R. DEFECT	UNBALANCED & BRG. DEFECT
ENDEVCO MODEL 22 S.N. AD-25	.75	1.31	.86	3.16	2.05	8.61
BOEING MODEL B100 S.N. 2	.69	1.44	.94	3.55	.76	1.52
BOEING MODEL B100 S.N. 3	.74	1.37	.99	4.85	.37	1.60
AVERAGE OF 3	.73	1.37	.93	3.79	.83	2.76

TEST ITEM	AXIMAX-2-464YS
PLOT NO.	37
TRANSDUCER	3100-3

CONTROLLED TEST PARAMETERS	
VOLTAGE	115
P.S. FREQ.	400.0
FLOW RATE	8.85×10^{-3} (18.75)

VARIABLE TEST PARAMETERS	BASELINE	FAULT
DATE	12/12-2/17	4/21
I	.112-.114	.113
ε<	.576	.558
PWR	10.8-11.0	11.0
RPM	10,870-10,940	10,932
ΔP	186.1 (.747)	186.1
TEMP	292.40-296.3°	293-295
BARO	100891-100540	102300

PROCESSING CHANNEL PARAMETERS	
INPUT RESISTANCE	—
AMPLIFIER GAINS (DB)	
A_1	20
A_2	—
A_3	—
FILTER FREQUENCIES (KHZ)	
BAND PASS	—
HIGH PASS	—
LOW PASS	1

SPECTRUM ANALYZER PARAMETERS	BASELINE	FAULT
INPUT V. (MV)	21-35	48
GAIN SETTINGS (0 DB REF)		
ANALYZER GAIN	20	
INPUT ATTEN.	21	
INTEGRATION		
LINEAR		
32 SUMS PER BIN		
COSINE WEIGHT		
D.C. COUPLE		
INTERNAL SAMPLE		

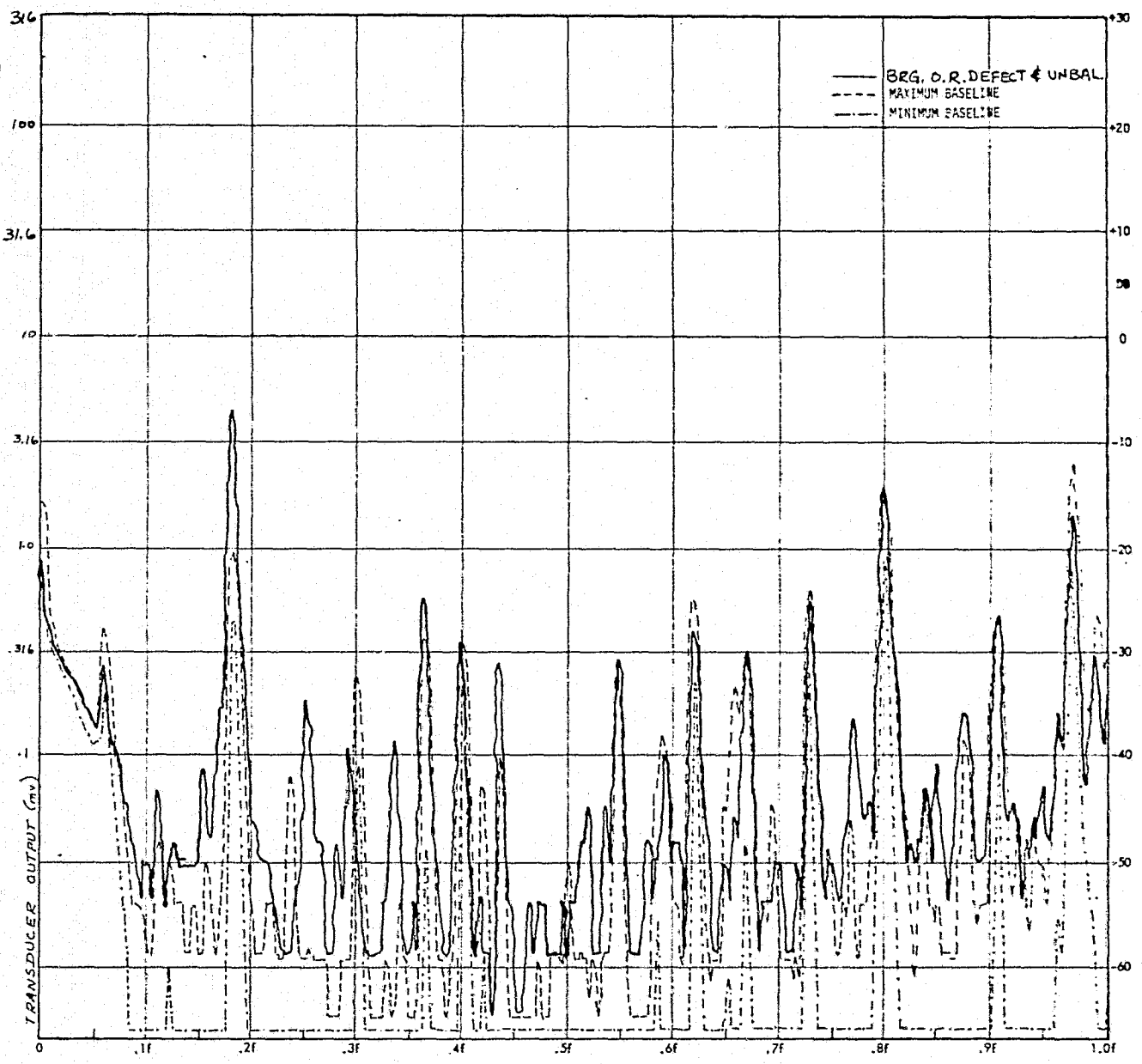

FIG. 40 FREQUENCY SPECTRUM FOR ROTRON AXIMAX-2-464YS FAN

TEST ITEM	AXIMAX-2-464YS
PLOT NO.	87
TRANSDUCER	8100-3

CONTROLLED TEST PARAMETERS	
VOLTAGE	115
P.S. FREQ.	400.0
FLOW RATE	8.85×10^{-3} (18.75)

VARIABLE TEST PARAMETERS	BASELINE	FAULT
DATE	12/12-2/17	4/21
I	.112-.114	.113
ϕ	.576	.558
PWR	10.8-11.0	11.0
RPM	10,870-10,940	10,932
ΔP	186.1 (.747)	186.1
TEMP	292.49-296.3°	293-295
BARO	100881-102540	102300

PROCESSING CHANNEL PARAMETERS	
INPUT RESISTANCE	22kΩ
AMPLIFIER GAINS (DB)	
A_1	40
A_2	40
A_3	20
FILTER FREQUENCIES (KHZ)	
BAND PASS	300
HIGH PASS	200
LOW PASS	1

SPECTRUM ANALYZER PARAMETERS	BASELINE	FAULT
INPUT V. (MV)	10-55	2800
GAIN SETTINGS (0 DB REF)		
ANALYZER GAIN	10	
INPUT ATTEN.	0	
INTEGRATION		
LINEAR		
32 SUMS PER BIN		
COSINE WEIGHT		
D.C. COUPLE		
INTERNAL SAMPLE		

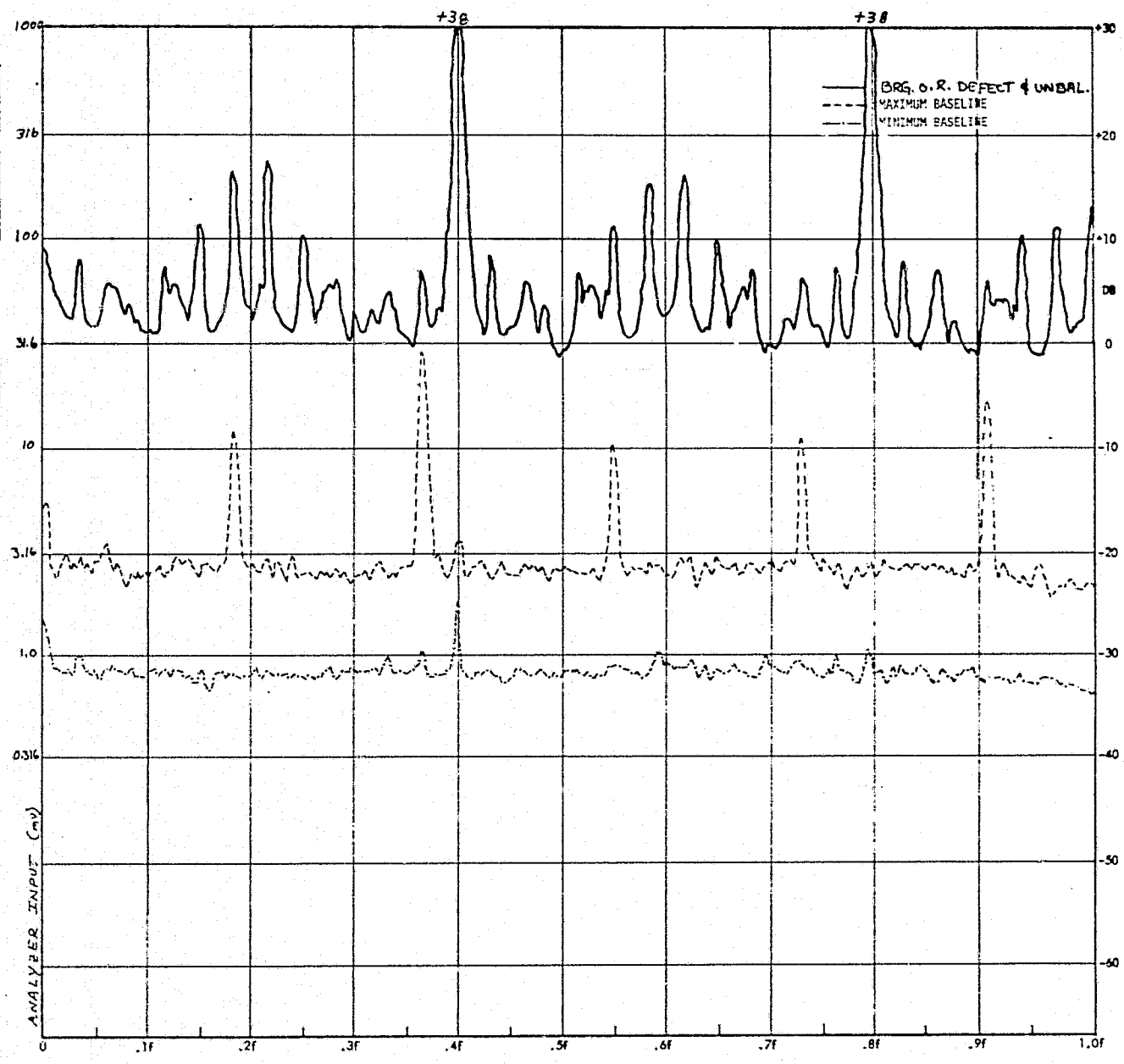

FIG. 41 FREQUENCY SPECTRUM FOR ROTRON AXIMAX-2-464 YS FAN

87

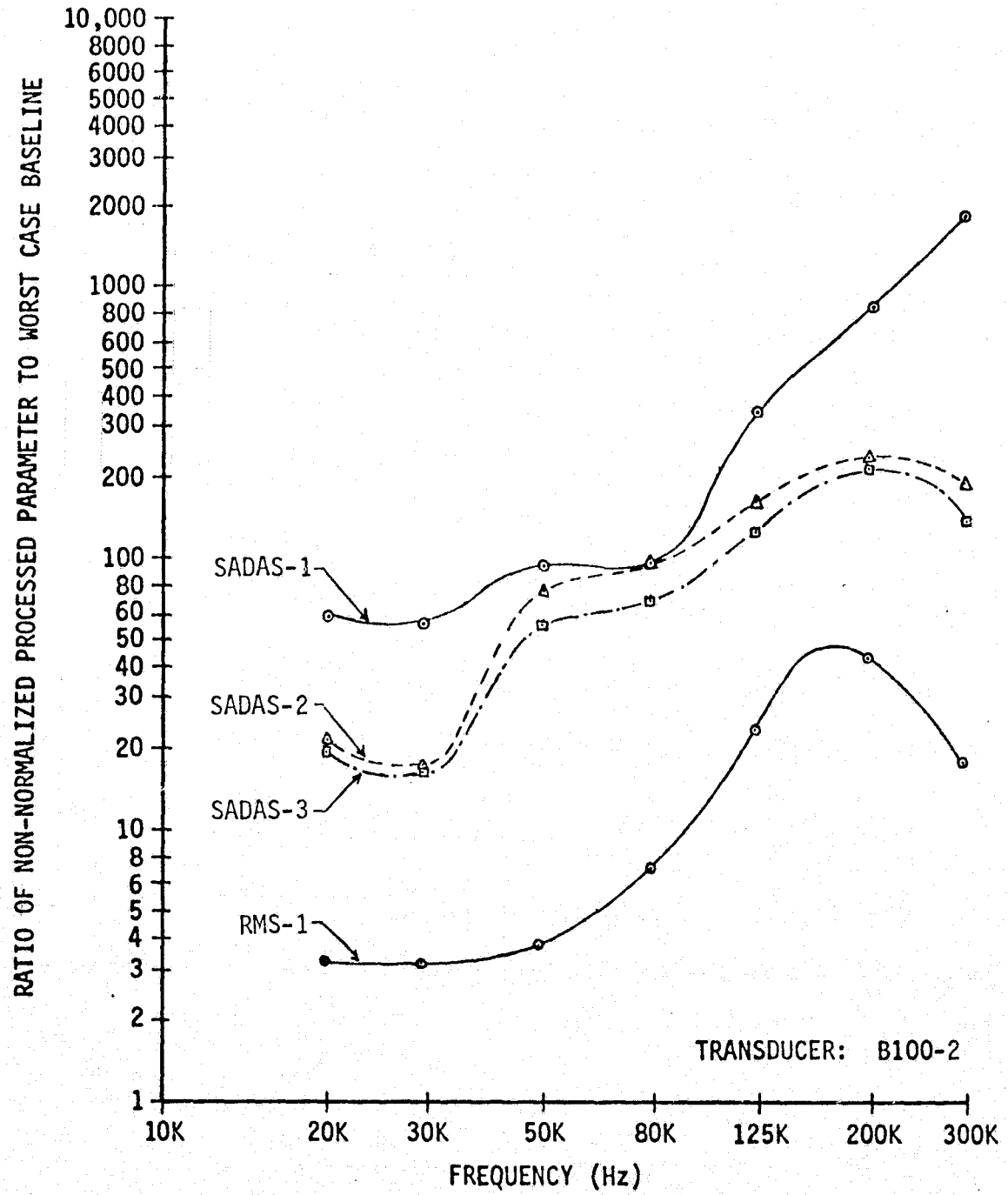

FIG. 42 NON-NORMALIZED PROCESSED PARAMETER CHANGES DUE TO UNBALANCE AND BEARING OUTER RACE FLAW - ROTRON 2-464-YS FAN

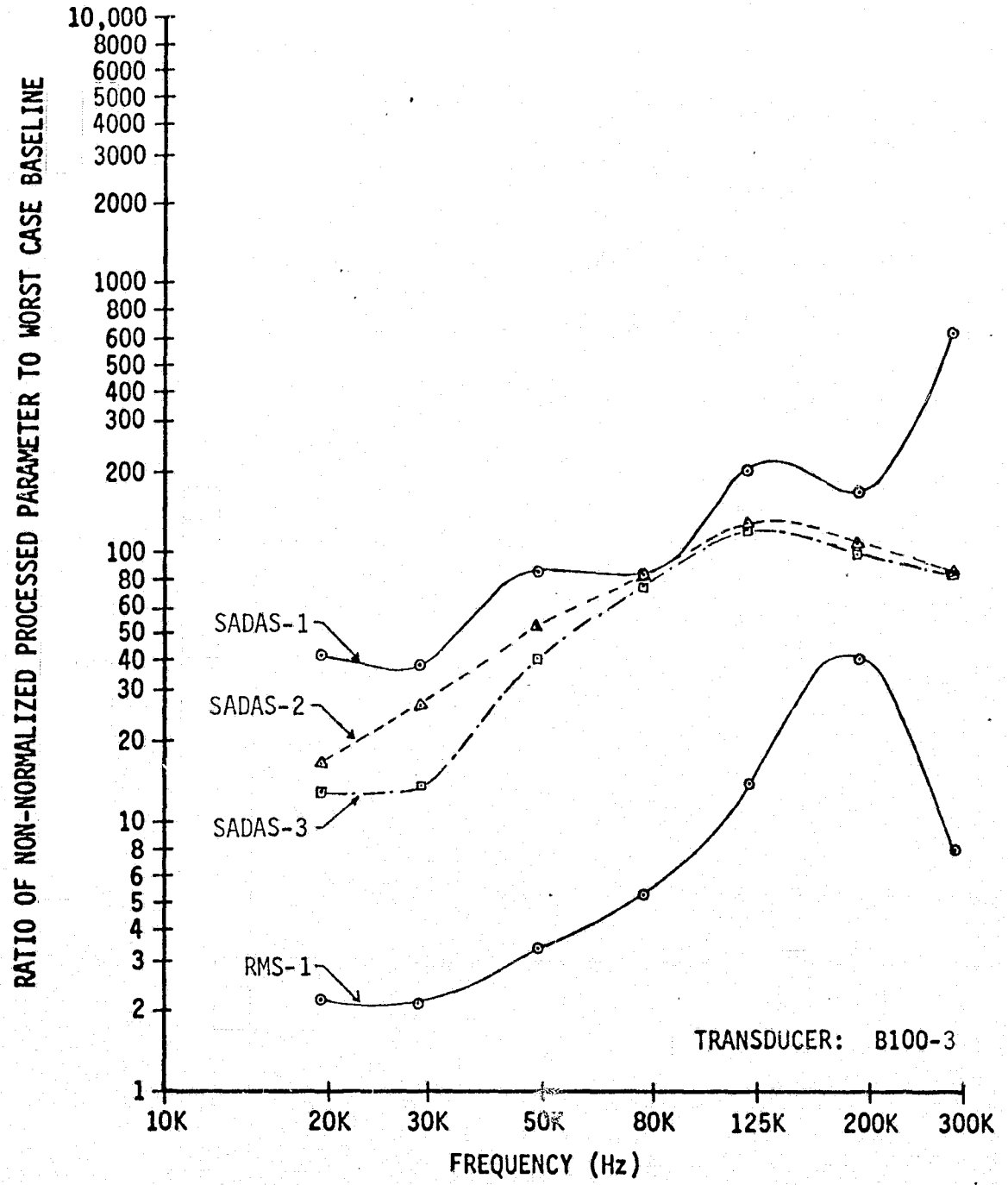

FIG. 43 NON-NORMALIZED PROCESSED PARAMETER CHANGES DUE TO UNBALANCE AND BEARING OUTER RACE FLAW - ROTRON 2-464-YS FAN

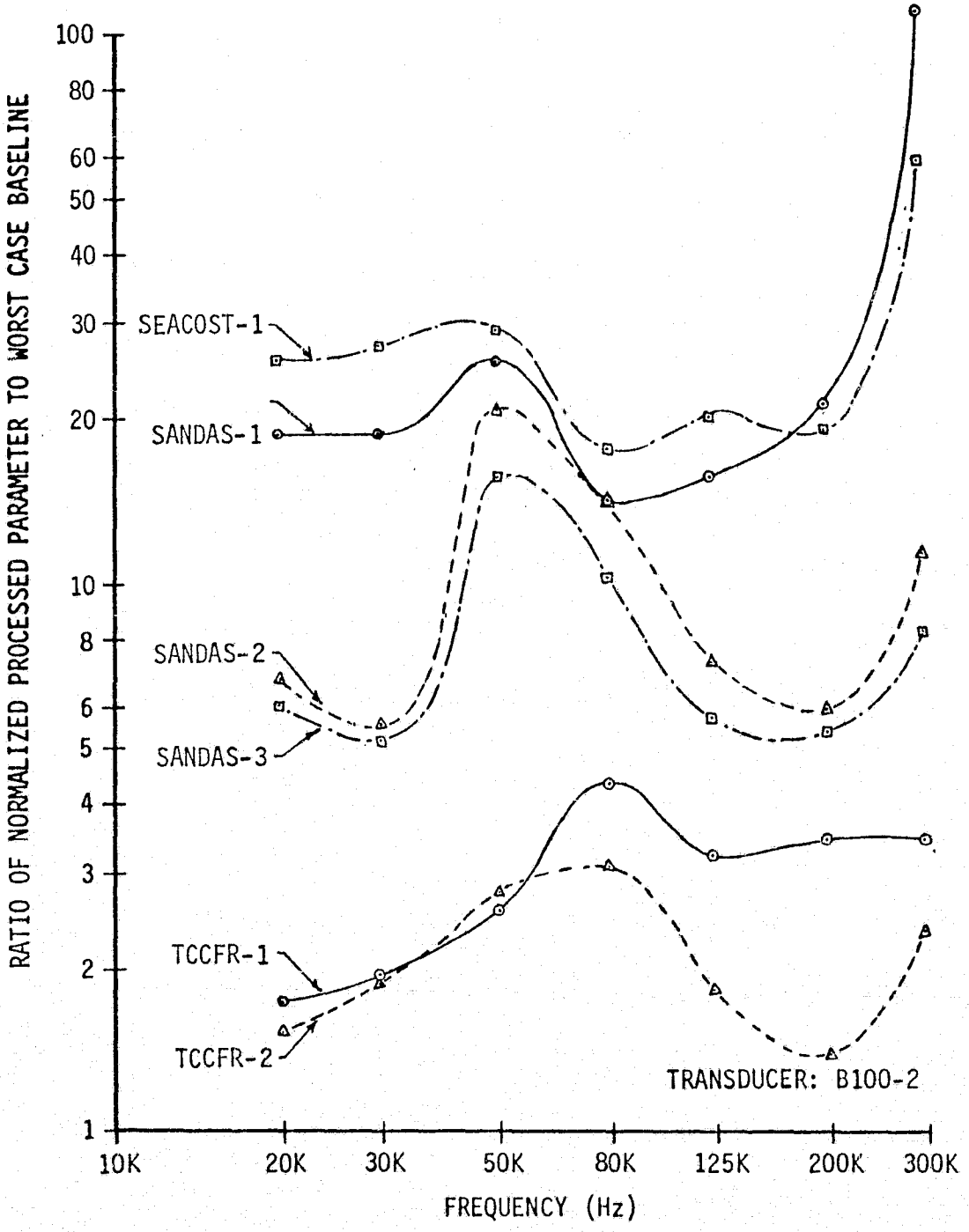

FIG. 44 NORMALIZED PROCESSED PARAMETER CHANGES DUE TO UNBALANCE AND BEARING OUTER RACE FLAW - ROTRON 2-464-YS FAN

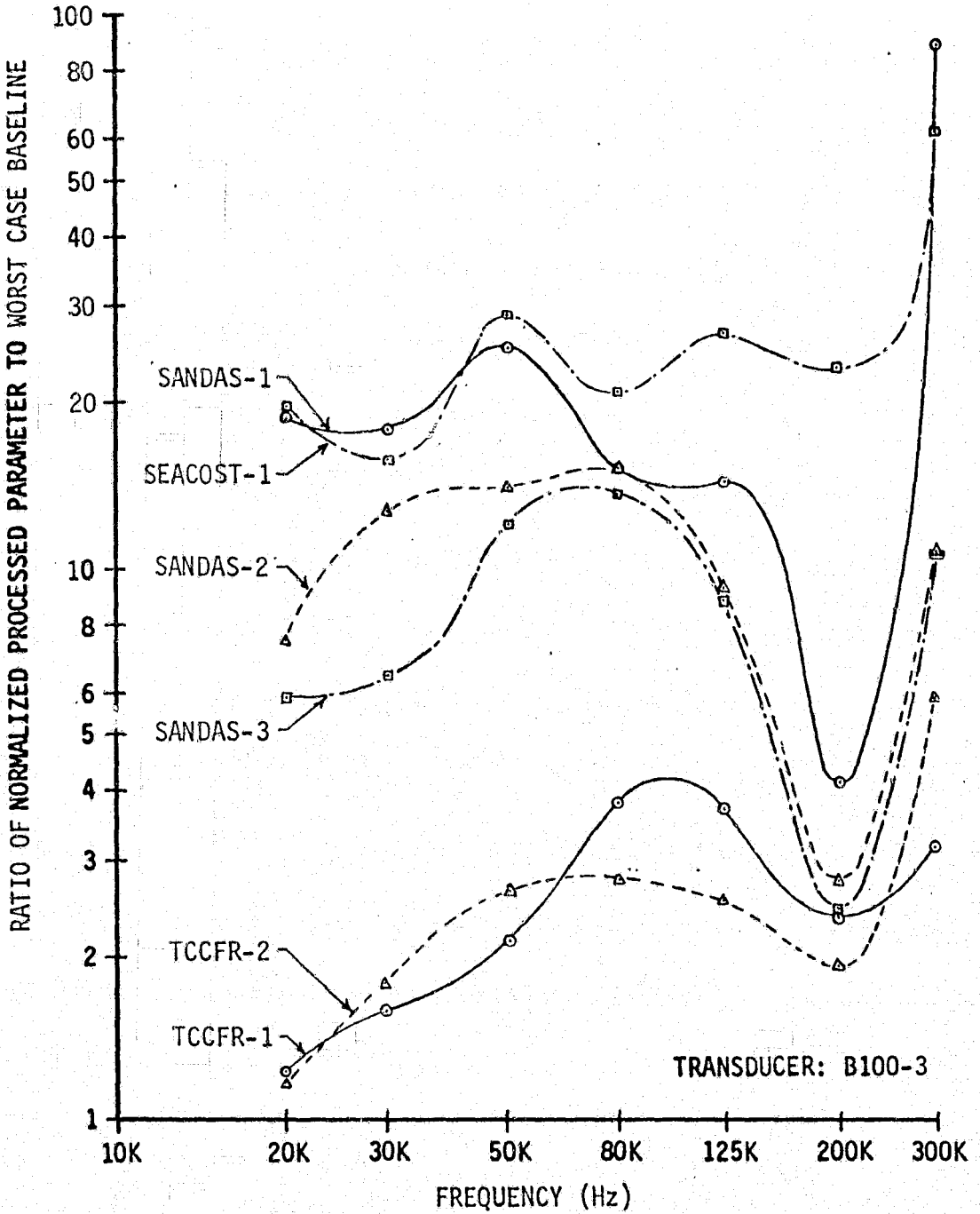

FIG. 45 NORMALIZED PROCESSED PARAMETER CHANGES DUE TO UNBALANCE AND BEARING OUTER RACE FLAW - ROTRON 2-464-YS FAN

C. 2

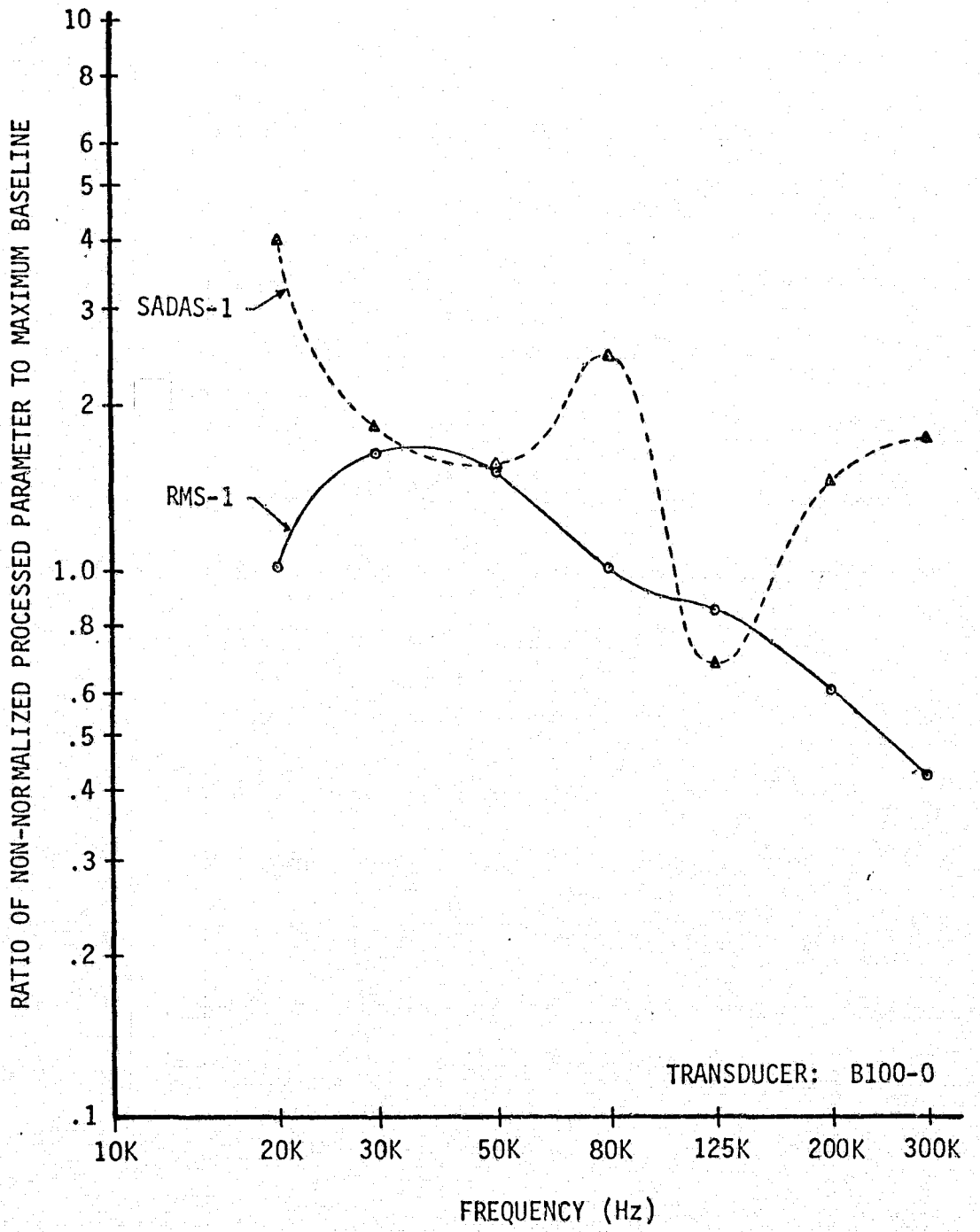

FIG. 46 NON-NORMALIZED PROCESSED PARAMETER CHANGES DUE TO UNBALANCE IN TRW GLOBE 19A532 FAN

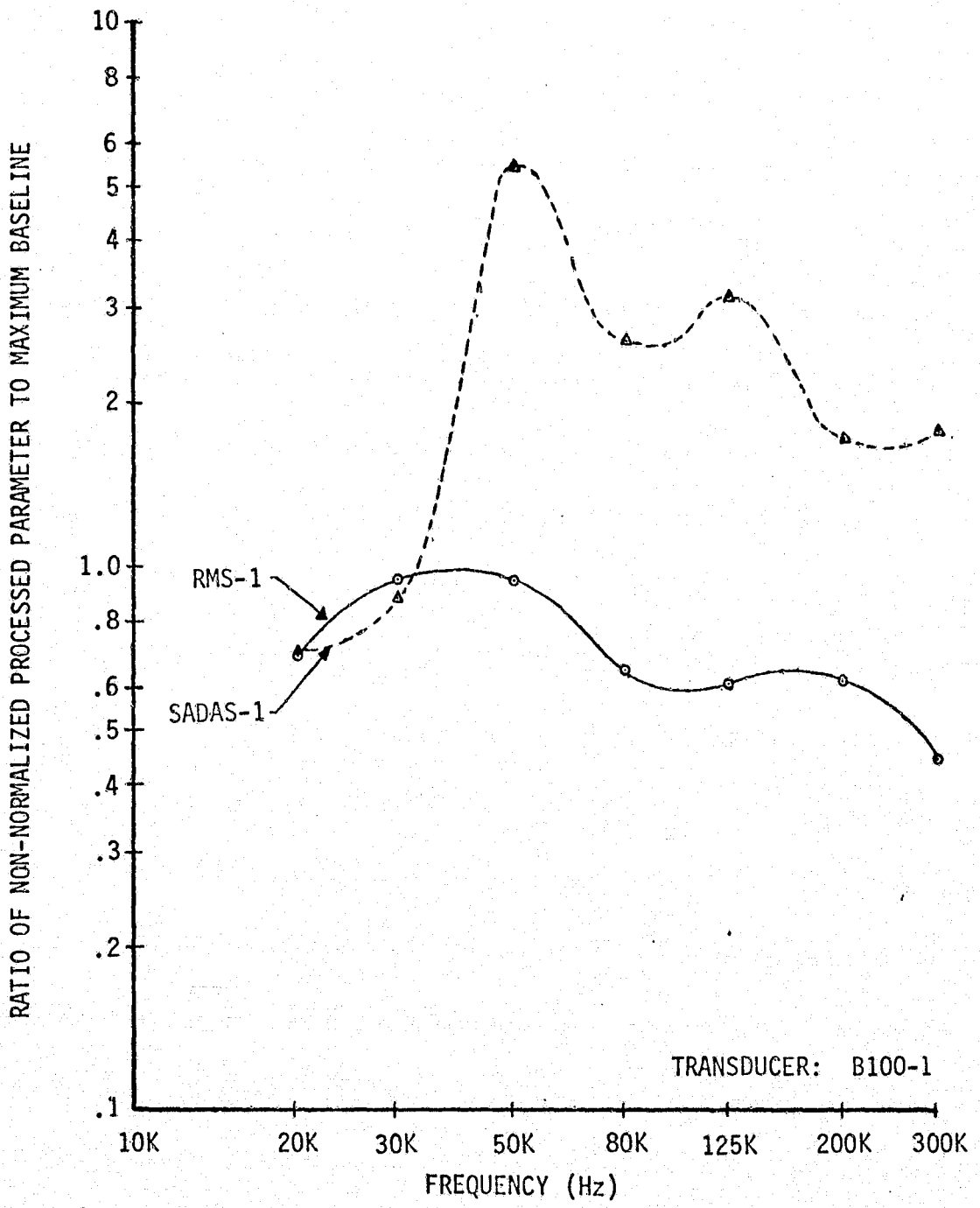

FIG. 47 NON-NORMALIZED PROCESSED PARAMETER CHANGES DUE TO UNBALANCE IN TRW GLOBE 19A532 FAN

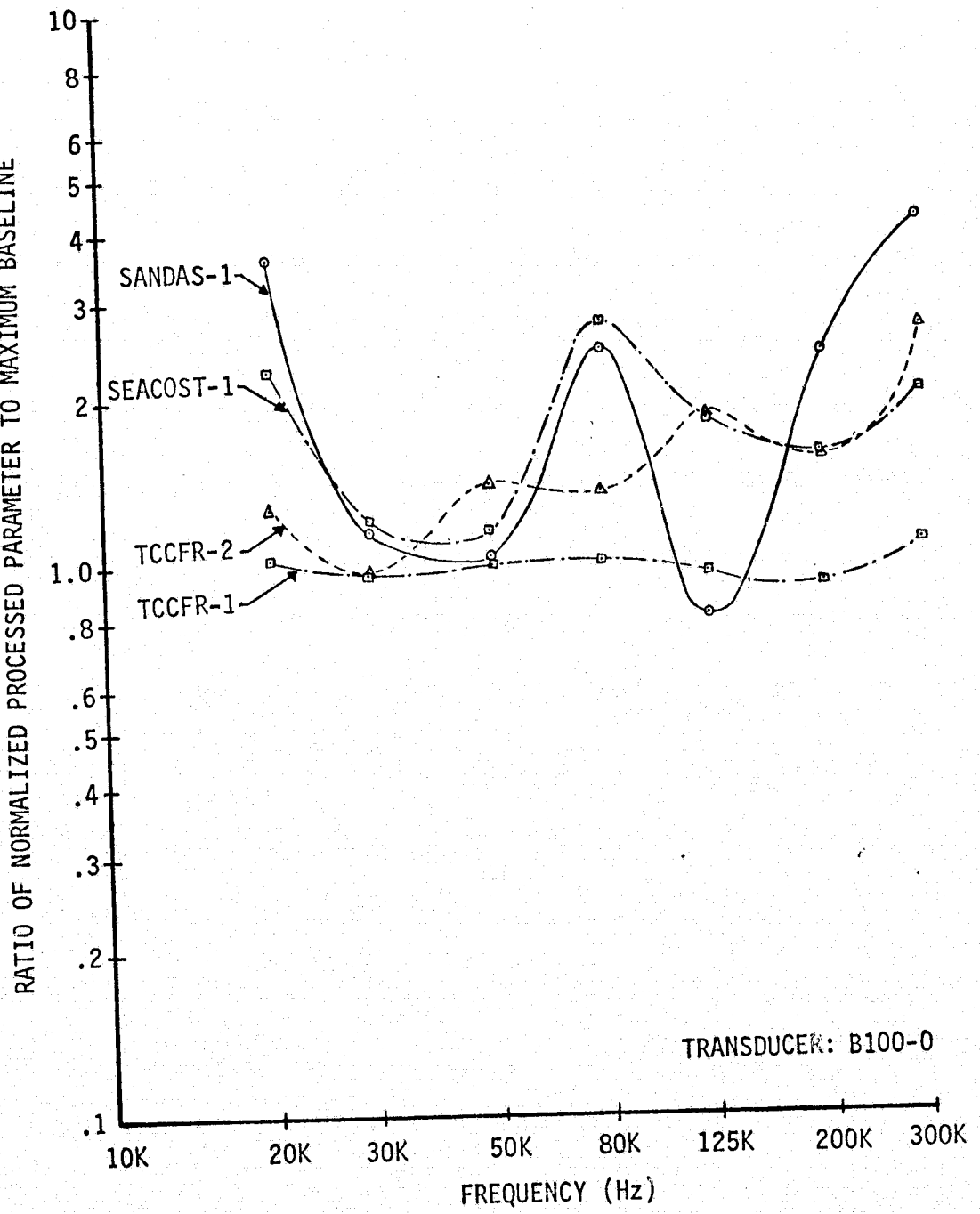

FIG.48 NORMALIZED PROCESSED PARAMETER CHANGES DUE TO UNBALANCE IN TRW GLOBE 19A532 FAN

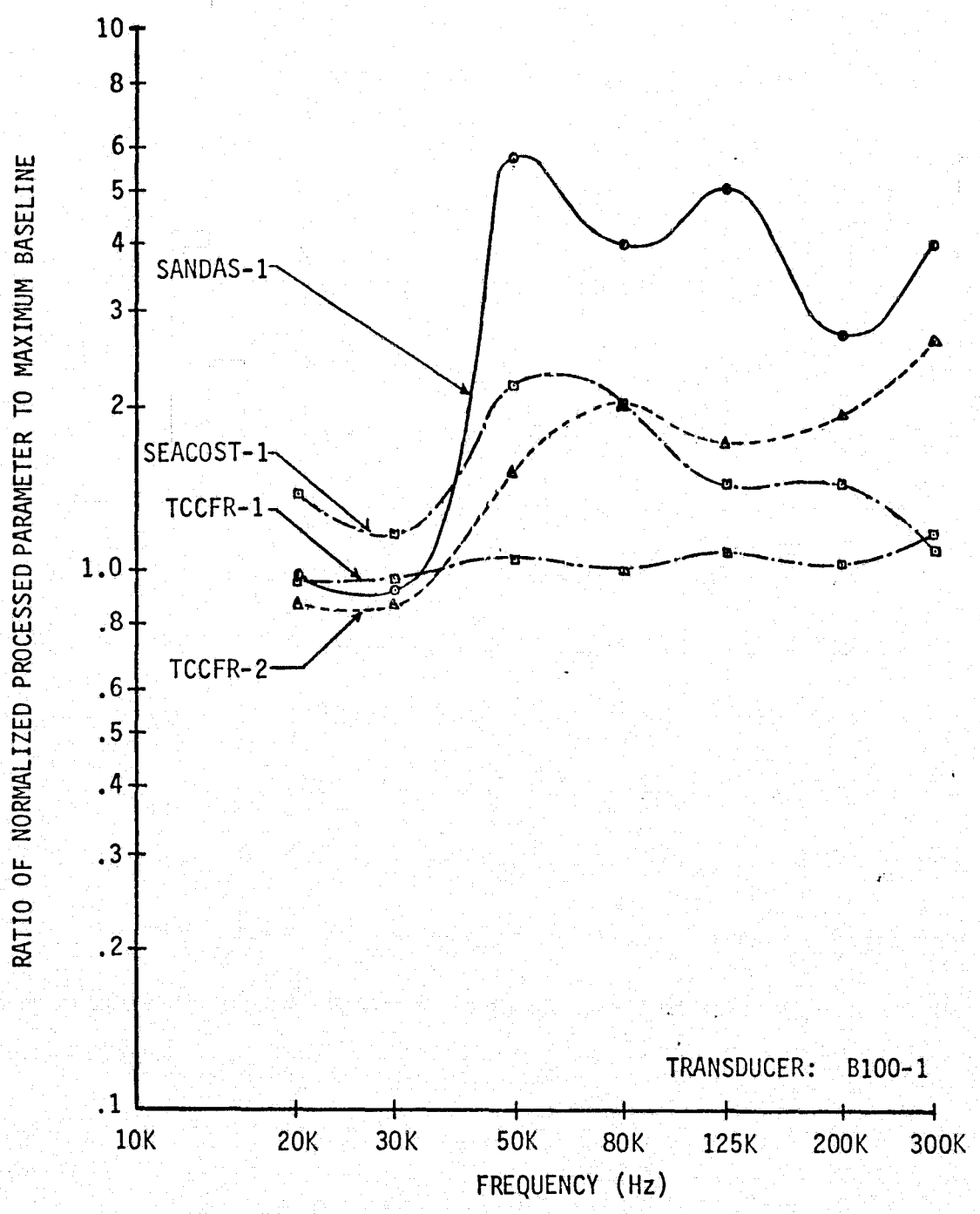

FIG. 49 NORMALIZED PROCESSED PARAMETER CHANGES DUE TO UNBALANCE IN TRW GLOBE 19A532 FAN

TEST ITEM	TRW Globe 19A532
PLOT NO.	43
TRANSDUCER	8100-2

CONTROLLED TEST PARAMETERS	
VOLTAGE	115
P.S. FREQ.	400.0
ΔP	206 (.827)

VARIABLE TEST PARAMETERS	BASELINE	FAULT
DATE	3/11-3/20	5/17
I	.360-.361	.355
ϕ<	.838	.838
PWR	27.7-27.8	27.3
RPM	5640-5940	5820
FLOW RATE	9.45x10-3 - 9.74x10-3	9.44×10^{-3}
TEMP	293.0-296.3	295
BARO	100881-102540	101000

PROCESSING CHANNEL PARAMETERS	
INPUT RESISTANCE	22K
AMPLIFIER GAINS (DB)	
A_1	40
A_2	20
A_3	20
FILTER FREQUENCIES (KHZ)	
BAND PASS	50
HIGH PASS	50
LOW PASS	0.5

SPECTRUM ANALYZER PARAMETERS	BASELINE	FAULT
INPUT V. (MV)	40-70	105
GAIN SETTINGS (0 DB REF)		
ANALYZER GAIN	20	
INPUT ATTEN.	10	
INTEGRATION		
LINEAR		
32 SUMS PER BIN		
COSINE WEIGHT		
D.C. COUPLE		
INTERNAL SAMPLE		

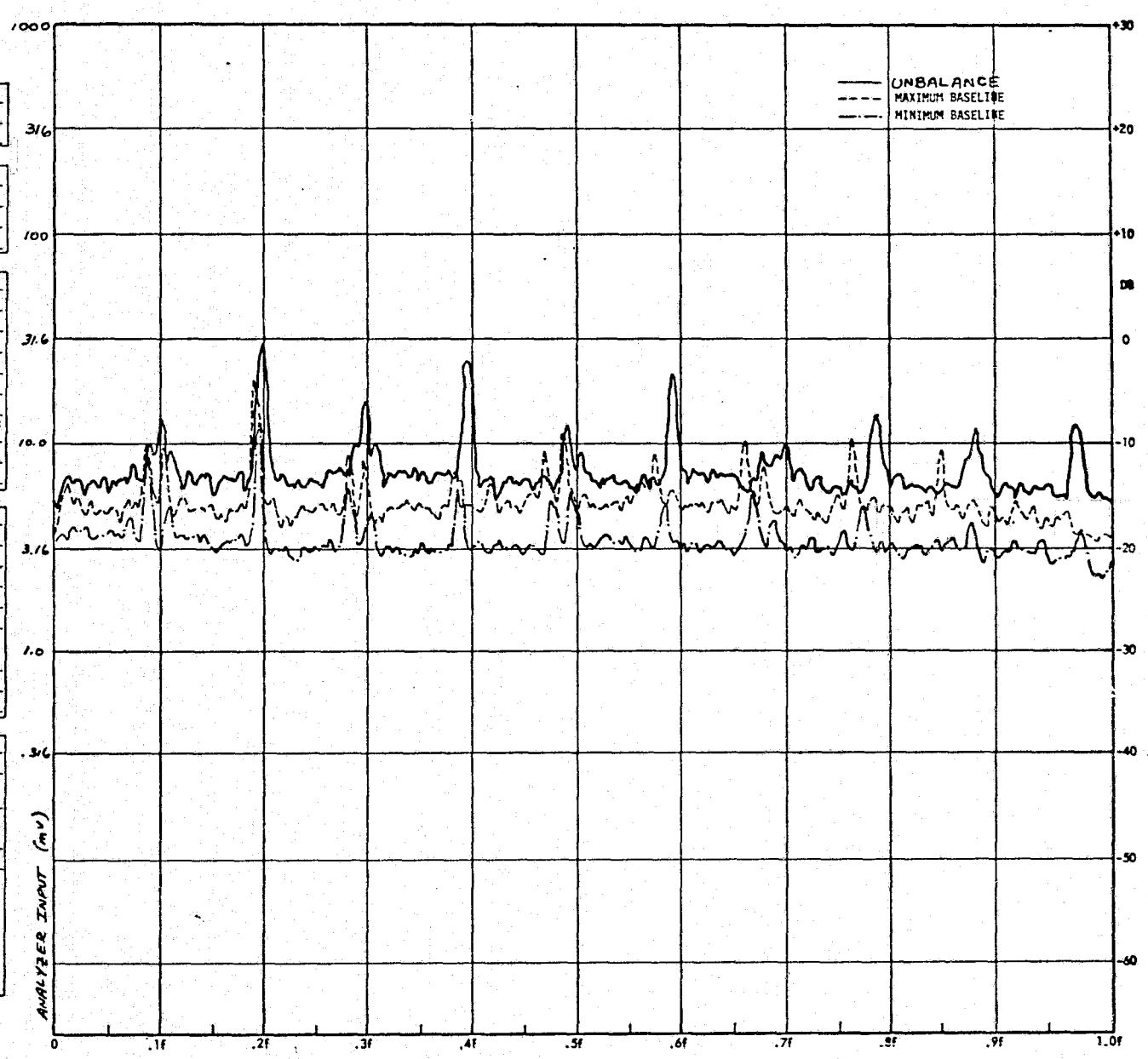

FIG. 50 FREQUENCY SPECTRUM FOR TRW GLOBE 19A532 FAN

TEST ITEM	TRW Globe 19A532
PLOT NO.	44
TRANSDUCER	3100-0

CONTROLLED TEST PARAMETERS	
VOLTAGE	115
P.S. FREQ.	400.0
ΔP	206 (.827)

VARIABLE TEST PARAMETERS	BASELINE	FAULT
DATE	3/11-3/20	5/17
I	.360-.361	.355
ϕ<	.838	.838
PWR	27.7-27.8	27.3
RPM	5640-5940	5820
FLOW RATE	9.44×10^{-3} - 9.74×10^{-3}	9.44×10^{-3}
TEMP	293.0-296.3	295
BARO	100881-102540	101000

PROCESSING CHANNEL PARAMETERS	
INPUT RESISTANCE	22K
AMPLIFIER GAINS (DB)	
A_1	40
A_2	20
A_3	20
FILTER FREQUENCIES (KHZ)	
BAND PASS	50
HIGH PASS	50
LOW PASS	2

SPECTRUM ANALYZER PARAMETERS	BASELINE	FAULT
INPUT V. (MV)	60-100	150
GAIN SETTINGS (0 DB REF)		
ANALYZER GAIN	20	
INPUT ATTEN.	10	
INTEGRATION		
LINEAR		
32 SUMS PER BIN		
COSINE WEIGHT		
D.C. COUPLE		
INTERNAL SAMPLE		

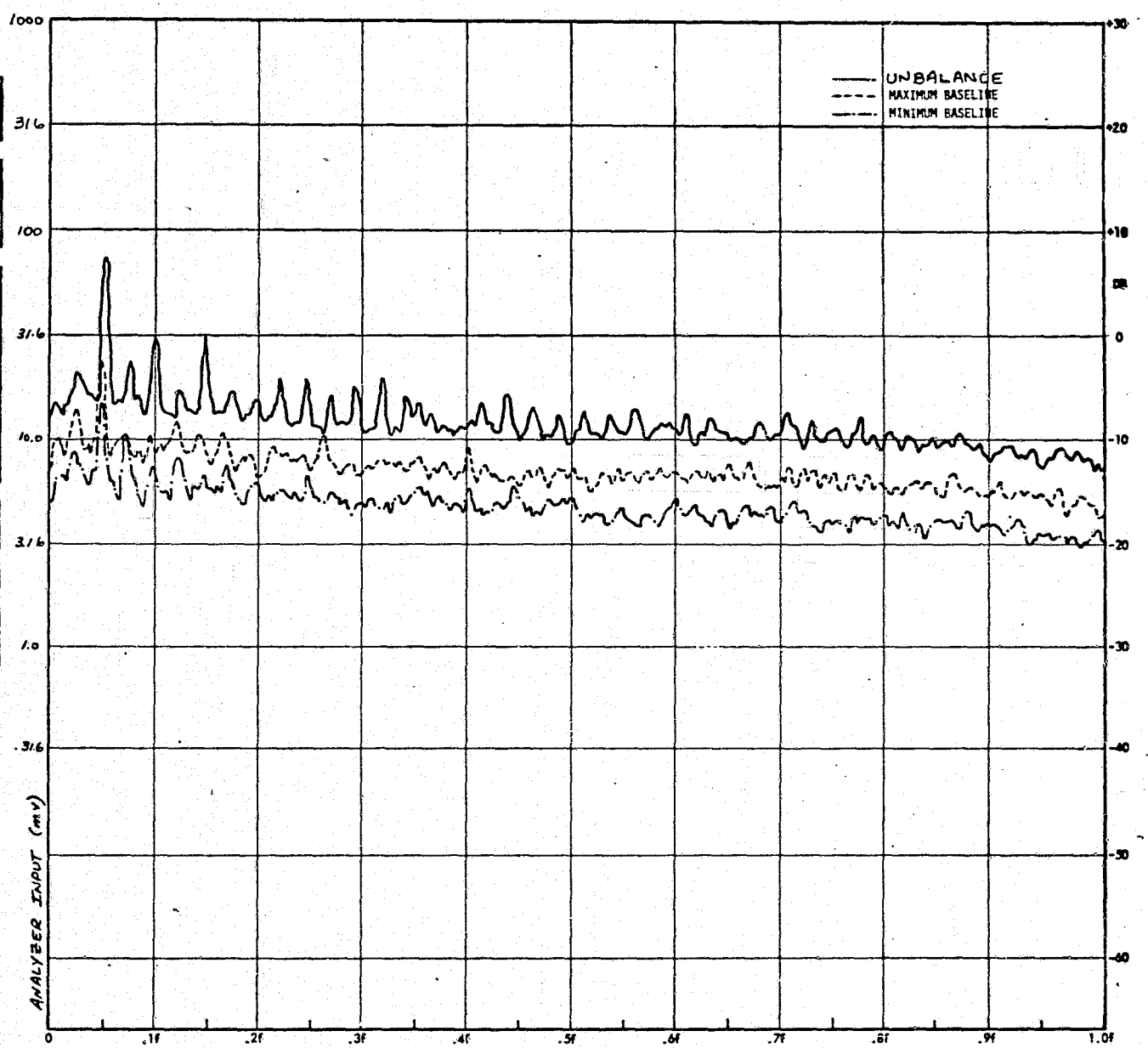

FIG. 51 FREQUENCY SPECTRUM FOR TRW GLOBE 19A532 FAN

if the defect was coming from a bearing or just unbalance. Other high frequency parameters which were affected by the unbalance are those which are associated with the amplitude distribution of the signal, namely SEACOST-1, TCCFR-1, and TCCFR-2. The maximum increase in all these parameters was limited to 2.7 to 1. Figure 52 shows the increase in the 3 σ spike voltage due to the unbalance condition and Figure 53 shows the change in the count distribution at 125 KHz. Further discussion on the effects of this unbalance condition as to the ability to detect the ball defect will be covered subsequently.

Figure 54 is the spectrum of the baseband vibration/acoustic signal for the unbalanced condition and shows the increase in the spectral line associated with the shaft frequency, 94 - 99 Hz.

Table XXII summarizes the changes in three low frequency parameters which resulted from unbalancing and also from the ball defect. All transducers showed increases greater than 133% for the three parameters due to the unbalance condition. Note that the bearing defect alone did not cause the average value of either the 0 - 500 Hz baseband RMS or fundamental shaft frequency spectral line amplitude to exceed their worst case baseline condition. The amplitude of the average value of the second harmonic of the fundamental shaft frequency spectral line exceeded the worst case baseline value by 27% for the ball defect principally because of the large increase from the Endevco DF83 sensor.

The ball defect in the bearing was expected to generate a train of narrow vibration/acoustic pulses with a repetitive frequency equal to the ball frequency, f_b, of 283.3 - 300.5 Hz. As the ball spins about its roll axis, the defect generates one acoustic pulse when it impacts the outer race and another when it impacts the inner race. The impact against the inner race also causes the ball to react against the outer race. Usually, the acoustic pulse reaching the transducer which comes from the direct impact with the outer race is larger than that which comes from the direct impact against the inner race and secondary impact against the outer race. If this difference is large the train of pulses will appear to have a repetitive frequency equal to the ball spin frequency, f_{sp}, which is half the ball impact frequency. In this case f_{sp} would be 141.7 - 150.3 Hz. Since the pulses in the train are reasonably narrow, a considerable amount of 2nd harmonic of f_{sp}, which is the same frequency as f_b, appears in a spectrum analysis of the signal.

The bearing ball defect could not be detected with any significant degree of certainty by an examination of the low frequency baseband vibration/acoustic spectrum, as is evident in Figure 55. Notice that the spectral line associated with the ball impact frequency (283.3 - 300.5 Hz) did not exceed the maximum baseline value. However, the defect was detected using the high frequency techniques but not as significantly as the outer race defect in the Rotron fan. Figures 56 through 59 show the high frequency processed parameter data for the bearing ball defect. SADAS-1 and SANDAS-1 provide the best degree of certainty in defect detectability of the six spectrum analysis parameters, as expected, having minimum values of 6.2 and 4.6 respectively at 50 KHz. The primary reason for the ratios being much

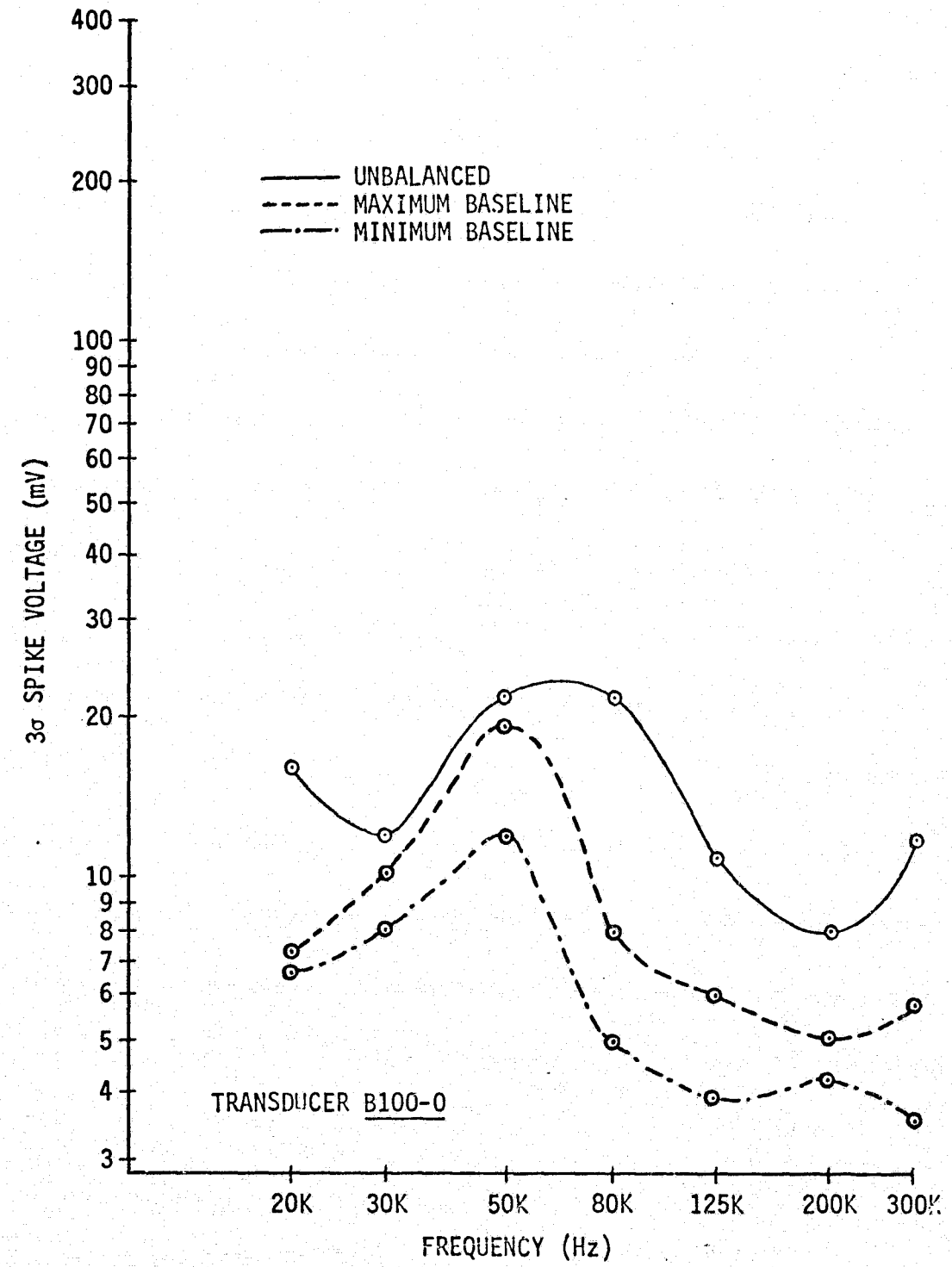

FIGURE 52 3σ SPIKE DATA FOR TRW GLOBE 19A532 FAN

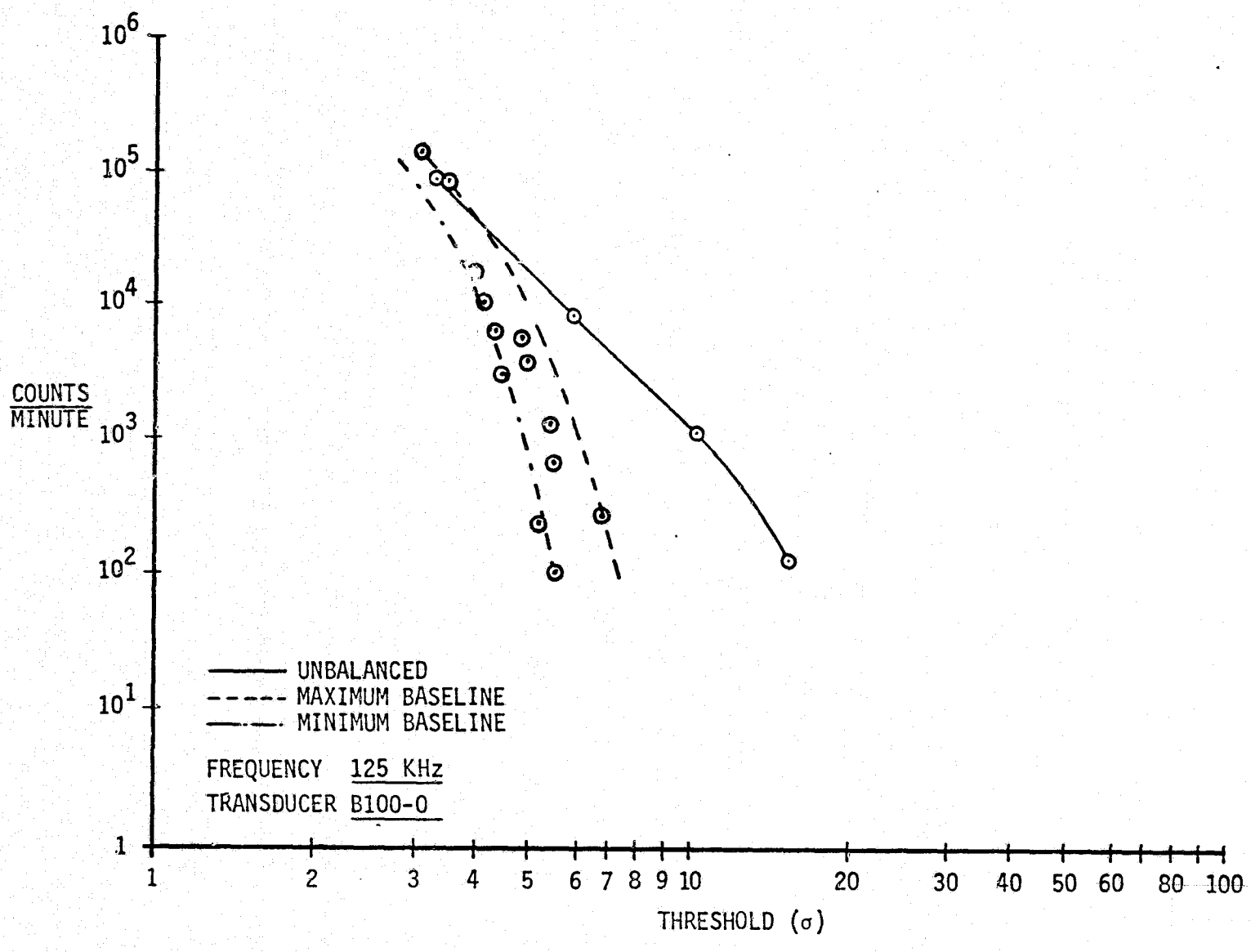

FIGURE 53 COUNT DATA FOR TRW GLOBE 19A532 FAN

TEST ITEM	TRW Globe 19A532
PLOT NO.	21
TRANSDUCER	B100-0

CONTROLLED TEST PARAMETERS	
VOLTAGE	115
P.S. FREQ.	400.0
ΔP	206 (.827)

VARIABLE TEST PARAMETERS	BASELINE	FAULT
DATE	3/11-3/20	5/17
I	.360-.361	.355
ϕ<	.838	.836
PWR	27.7-27.8	27.3
RPM	5640-5940	5820
FLOW RATE	9.44x10-3 - 9.74x10-3	9.44×10^{-3}
TEMP	293.0-296.3	295
BARO	100881-102540	101,000

PROCESSING CHANNEL PARAMETERS	
INPUT RESISTANCE	—
AMPLIFIER GAINS (DB)	
A_1	20
A_2	—
A_3	—
FILTER FREQUENCIES (KHZ)	
BAND PASS	—
HIGH PASS	—
LOW PASS	0.5

SPECTRUM ANALYZER PARAMETERS	BASELINE	FAULT
INPUT V. (MV)	45-55	205
GAIN SETTINGS (0 DB REF)		
ANALYZER GAIN	10	
INPUT ATTEN.	12	
INTEGRATION		
LINEAR		
32 SUMS PER BIN		
COSINE WEIGHT		
D.C. COUPLE		
INTERNAL SAMPLE		

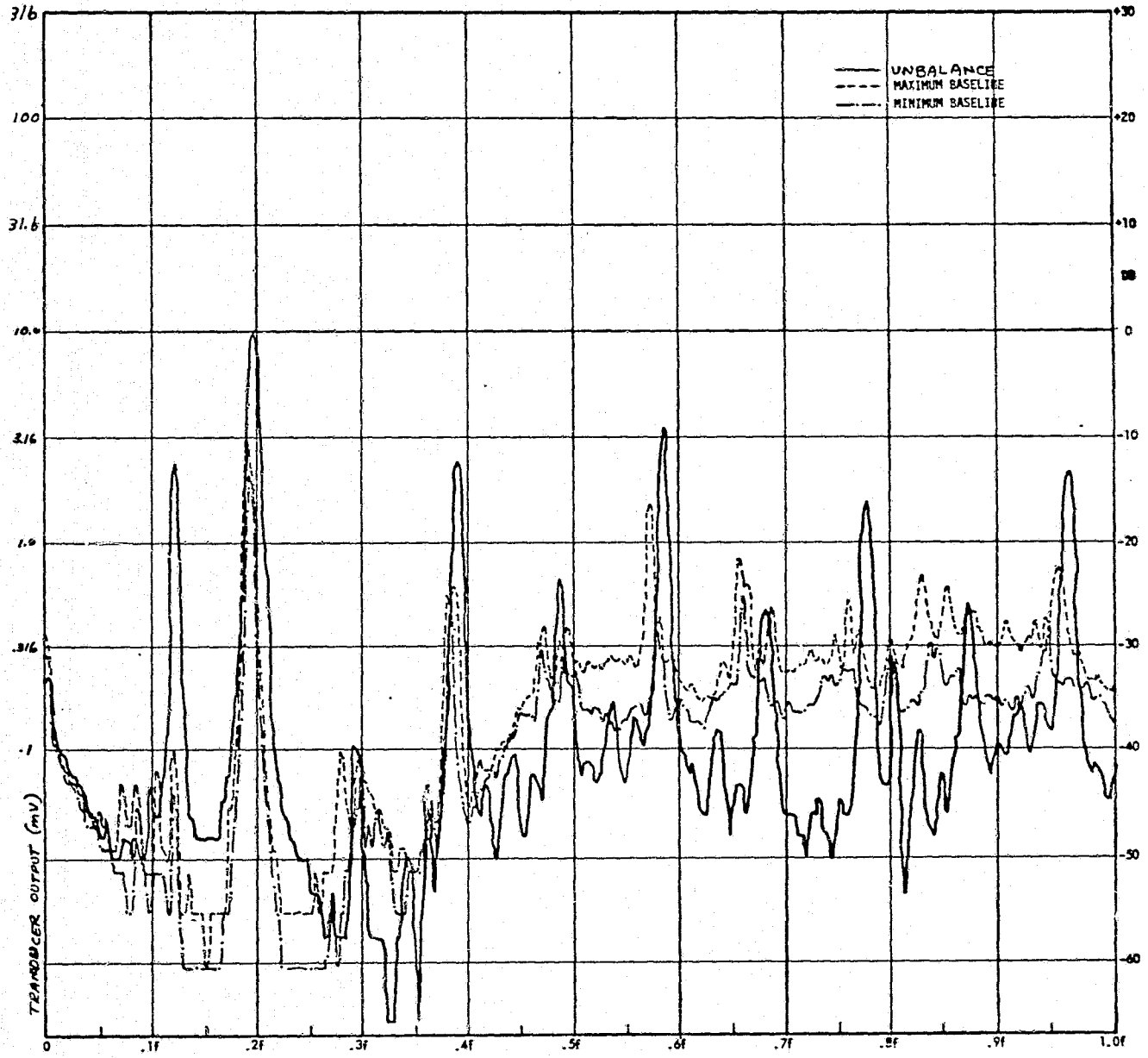

FIG. 54 FREQUENCY SPECTRUM FOR TRW GLOBE 19A532 FAN

TABLE XXII. LOW FREQUENCY TEST RESULTS FOR TRW 19A532 FAN

SENSOR	VBRMS		SABVS-5 (f_s)		SABVS-5 ($2f_s$)	
	UNBALANCE	BEARING BALL DEFECT	UNBALANCE	BEARING BALL DEFECT	UNBALANCE	BEARING BALL DEFECT
ENDEVCO MODEL 2222B S.N. DF83	6.00	0.78	8.63	1.24	9.42	4.66
ENDEVCO MODEL 2222B S.N. DF81	2.90	0.46	3.82	0.58	2.39	1.03
BOEING MODEL B100 S.N. 0	3.73	0.40	3.40	0.44	4.22	0.60
BOEING MODEL B100 S.N. 1	2.33	0.44	3.08	0.16	15.85	0.89
AVERAGE OF 4 SENSORS	3.51	0.50	4.31	0.47	6.23	1.27

TEST ITEM	TRW Globe 19A532
PLOT NO.	21
TRANSDUCER	B100-0

CONTROLLED TEST PARAMETERS	
VOLTAGE	115
P.S. FREQ.	400.0
ΔP	206 (.827)

VARIABLE TEST PARAMETERS	BASELINE	FAULT
DATE	3/11-3/20	5/28
I	.360-.361	.364
ϕ<	.838	.838
PWR	27.7-27.8	28.0
RPM	5640-5940	5700
FLOW RATE	9.44x10-3 - 9.74x10-3	9.69×10^{-3}
TEMP	293.0-296.3	298
BARO	100881-102540	101300

PROCESSING CHANNEL PARAMETERS	
INPUT RESISTANCE	—
AMPLIFIER GAINS (DB)	
A_1	20
A_2	—
A_3	—
FILTER FREQUENCIES (KHZ)	
BAND PASS	—
HIGH PASS	—
LOW PASS	0.5

SPECTRUM ANALYZER PARAMETERS	BASELINE	FAULT
INPUT V. (MV)	45-55	22
GAIN SETTINGS (0 DB REF)		
ANALYZER GAIN	10	
INPUT ATTEN.	12	
INTEGRATION		
LINEAR		
32 SUMS PER BIN		
COSINE WEIGHT		
D.C. COUPLE		
INTERNAL SAMPLE		

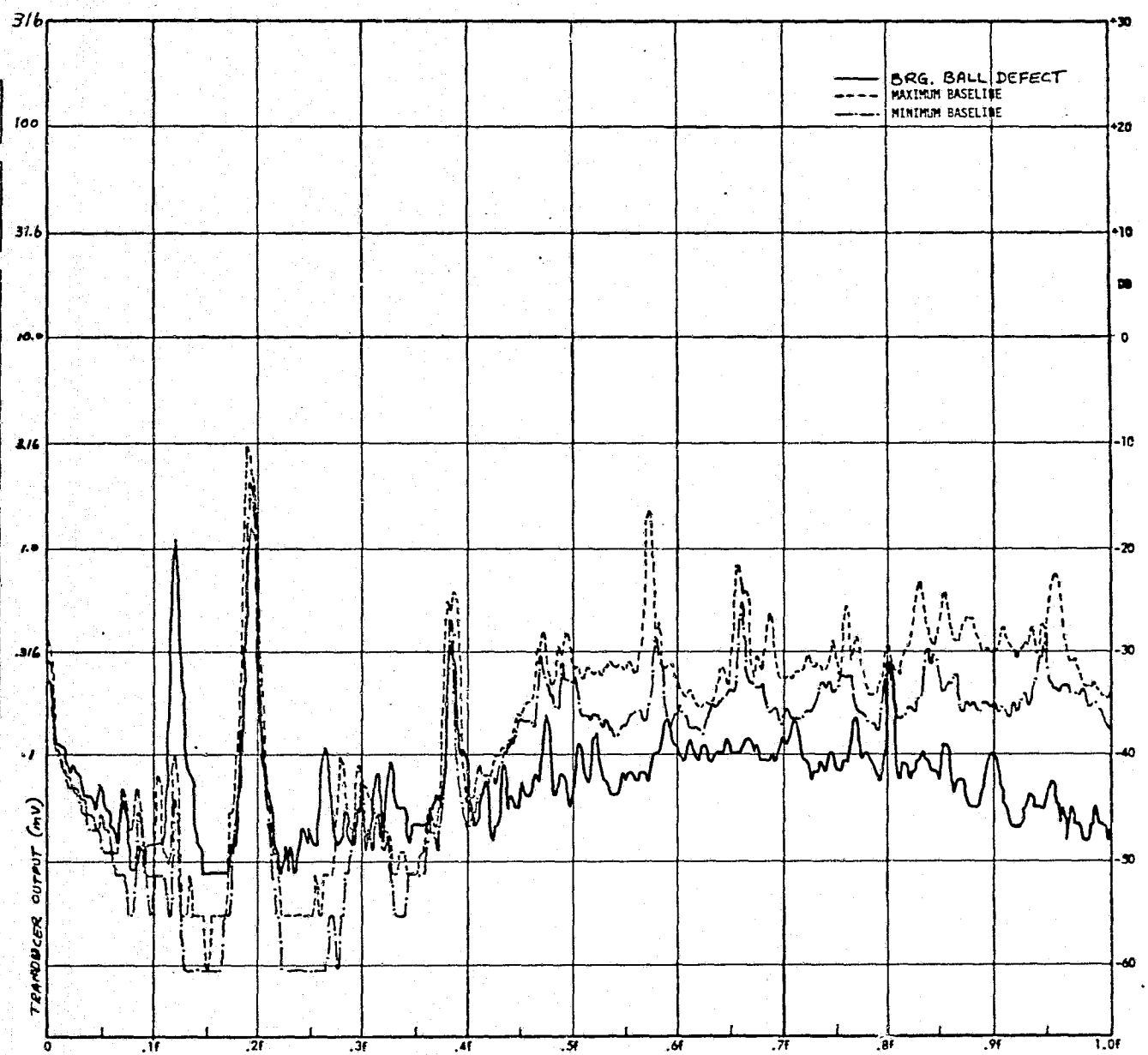

FIG. 55 FREQUENCY SPECTRUM FOR TRW GLOBE 19A532 FAN

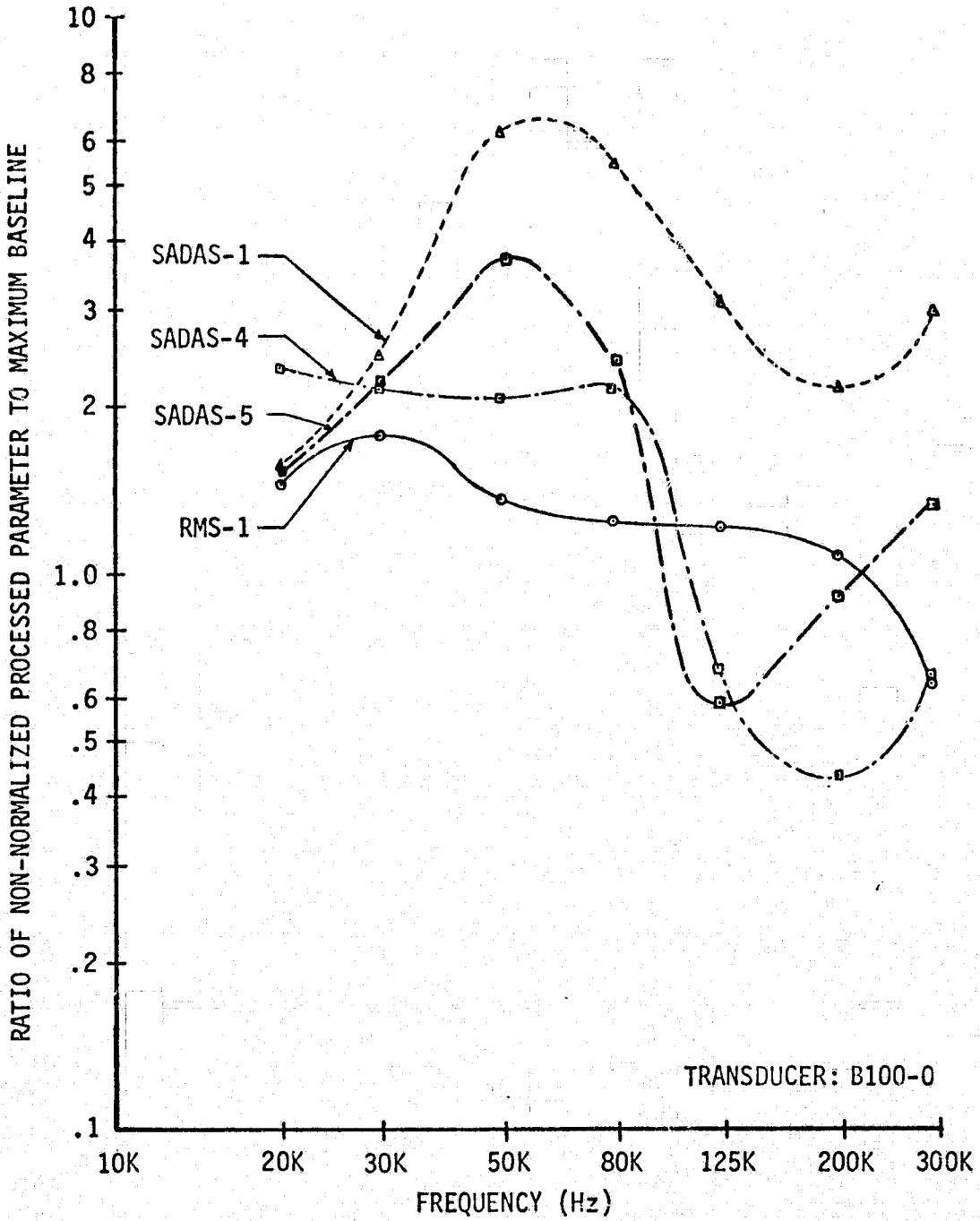

FIG. 56 NON-NORMALIZED PROCESSED PARAMETER CHANGES DUE TO BEARING BALL DEFECT IN TRW GLOBE 19A532 FAN

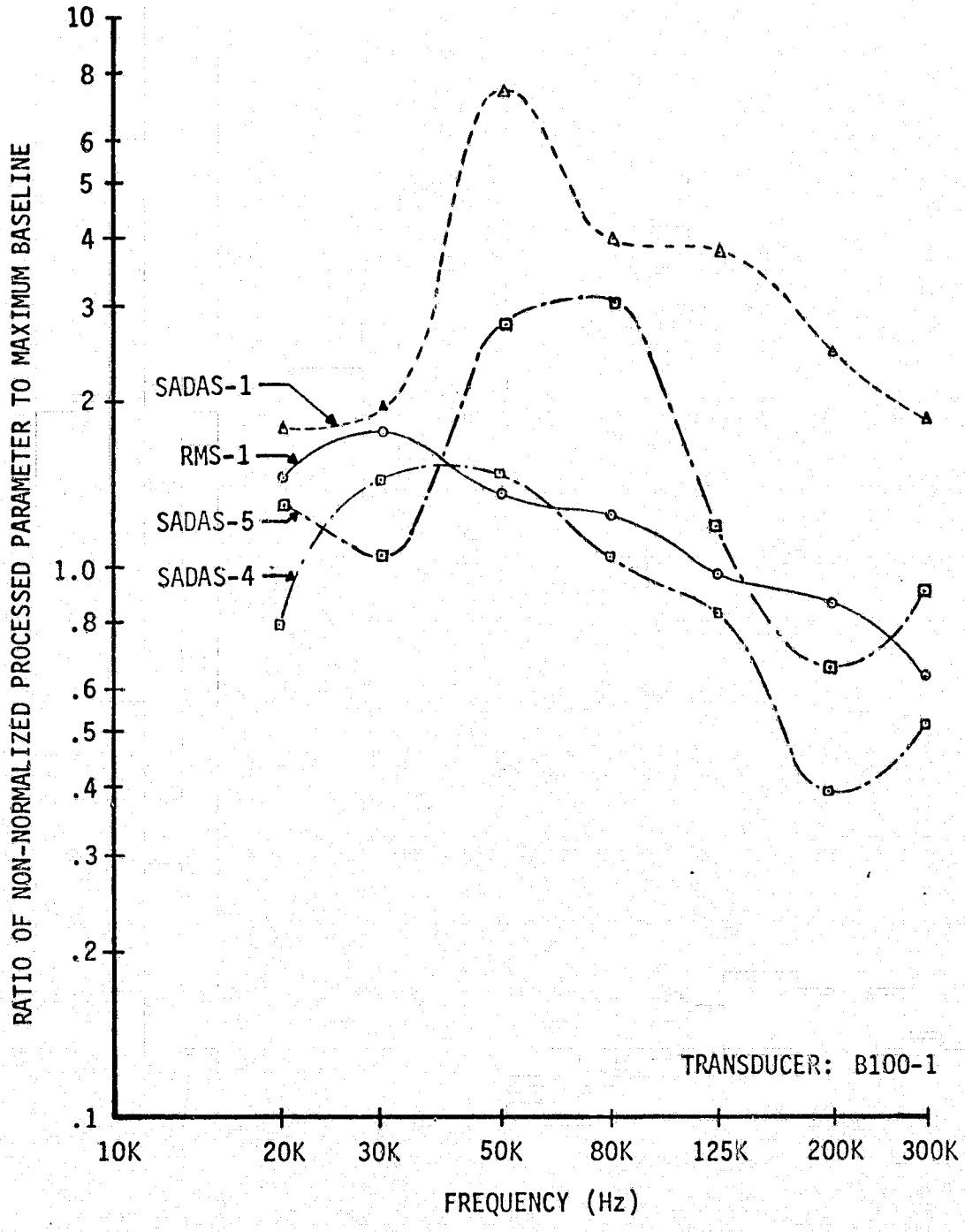

FIG.57 NON-NORMALIZED PROCESSED PARAMETER CHANGES DUE TO BEARING BALL DEFECT IN TRW GLOBE 19A532 FAN

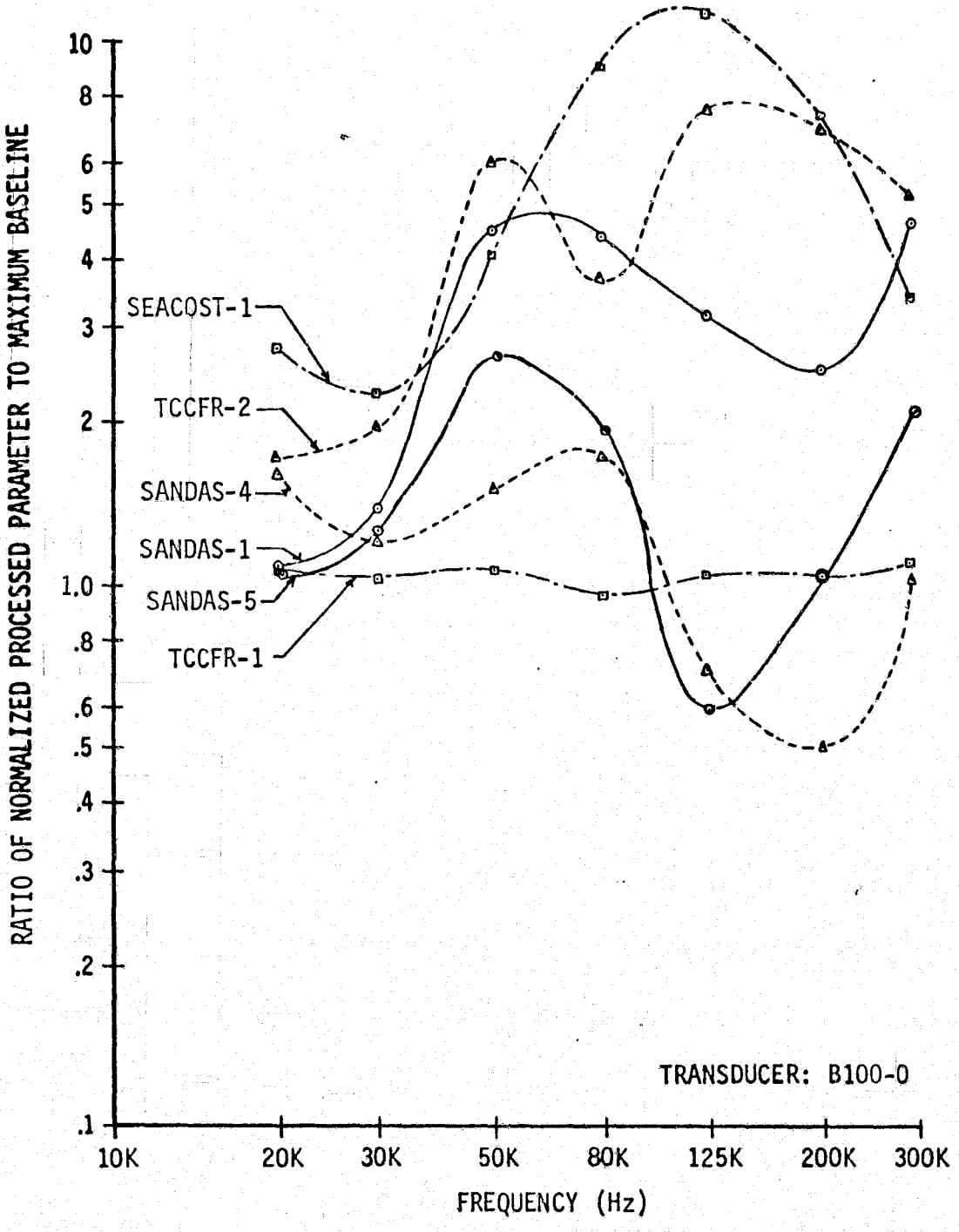

FIG. 58 NORMALIZED PROCESSED PARAMETER CHANGES DUE TO BEARING BALL DEFECT IN TRW GLOBE 19A532 FAN

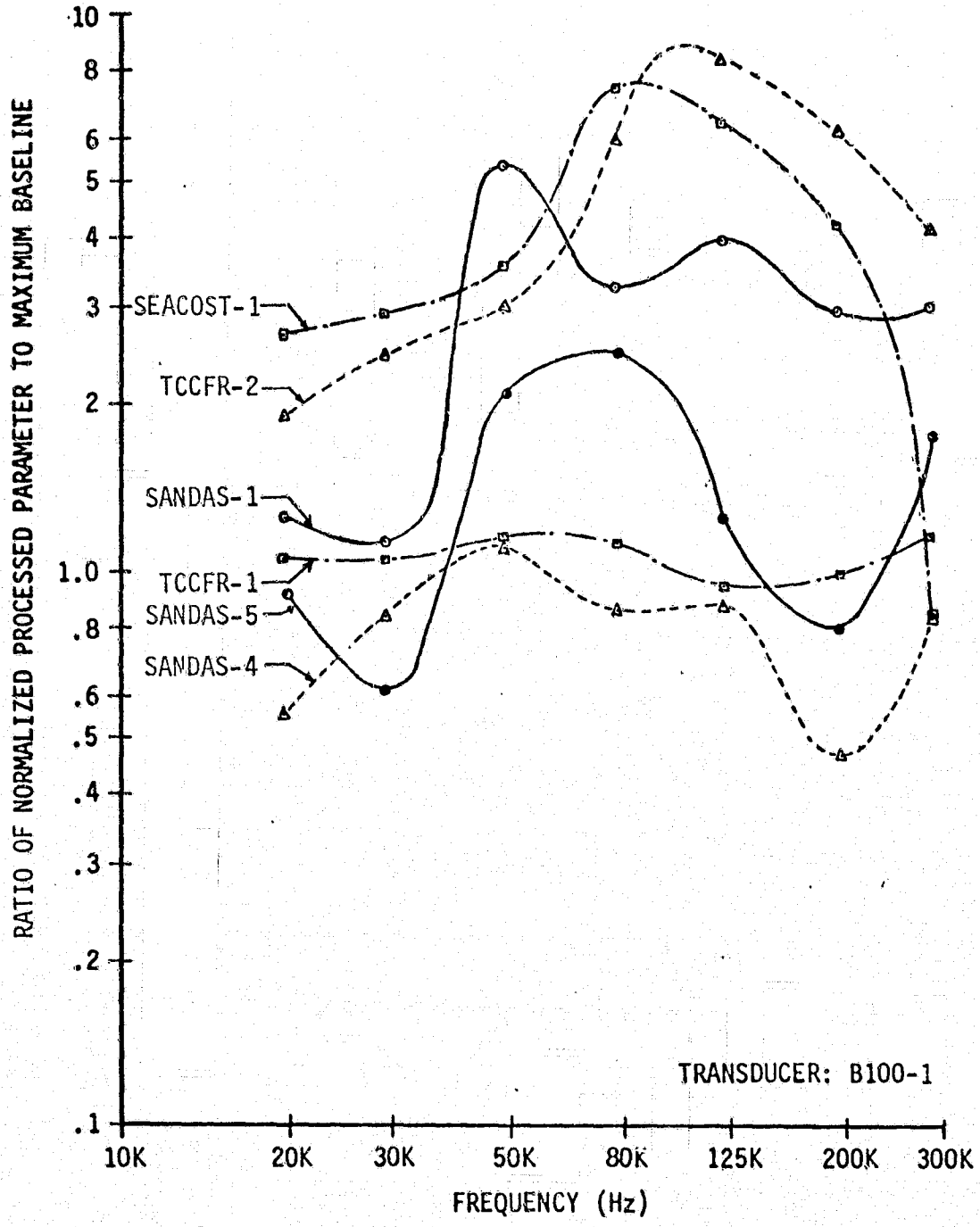

FIG. 59 NORMALIZED PROCESSED PARAMETER CHANGES DUE TO BEARING BALL DEFECT IN TRW GLOBE 19A532 FAN

smaller than those determined for the Rotron fan is probably due to the defective ball side-spinning in a random manner in addition to spinning in a forward direction. When this occurs the defect makes contact with the raceways at a more non-periodic rate. Since the time between impacts is not held constant, but is now varying, the spectrum line associated with the defect is no longer sharp, but tends to spread out. This can readily be seen by viewing the 50 KHz SADAS plots, Figures 60 and 61. The 2 KHz full scale plot, Figure 61, illustrates this quite dramatically. It shows the fundamental plus 5 harmonics of this spread spectrum. To further illustrate this phenomena, the fan motor was run under the following conditions:

A. Shaft pointing down - no load

B. Shaft pointing up - no load

C. Shaft pointing down - squirrel cage attached to shaft

D. Shaft pointing up - squirrel cage attached to shaft

SADAS plots of these four conditions are shown in Figure 62. These plots demonstrate several interesting items, the first and foremost being that if the test was performed with the fan's shaft pointing down instead of up, much better results would have been achieved. For conditions A and B, with no load, the shaft speed is 12,000 RPM, the calculated ball spin frequency is 303.5 Hz, and the ball impact frequency is 607 Hz.

Curve A is for the shaft pointing down which places the rotor weight against the defected bearing. This load against the defected bearing reduces the ball random side-spin and results in a sharp spectral line at the ball spin frequency and its harmonics. The defect appears at the ball spin frequency instead of the ball impact frequency because of the reasons previously discussed. The high amplitude of the spectral line in comparison to the other plots is due to the load and high impact speed. The fact that the spectral line is shifted up in frequency from its calculated value by approximately 12% was not resolved, but it could be due to the ball experiencing a controlled side-spin which causes the rate of defect impacts to increase. Other factors such as ball skidding would tend to decrease the spin frequency.

Curve B is for a no load condition with the shaft pointing up which removes the rotor weight against the defective bearing. This reduction of load decreases the amplitude of the spectrum lines and increases the random side-spin which results in a spreading of the spectral line. Note also that the peak center of the spectral lines approach the calculated values and that the amplitude of the ball spin spectral line is lower than the ball impact spectral line.

Curve C is for the shaft pointing down with a squirrel cage attached which places the weight of the rotor and squirrel cage against the defective bearing. The load on the motor causes the shaft speed to be reduced to 8240 RPM and the calculated ball spin and ball impact frequencies for this shaft speed are 208.4 Hz and 416.8 Hz respectively. The load against the defective bearing again reduces the ball random side-spin and a sharp spectral line at the ball spin frequency and its harmonics is achieved.

TEST ITEM	TRW Globe 19A532
PLOT NO.	43
TRANSDUCER	B100-D

CONTROLLED TEST PARAMETERS	
VOLTAGE	115
P.S. FREQ.	400.0
ΔP	206 (.827)

VARIABLE TEST PARAMETERS	BASELINE	FAULT
DATE	3/11-3/20	5/23
I	.360-.351	.364
ϕ<	.838	.838
PWR	27.7-27.8	28.0
RPM	5640-5940	5700
FLOW RATE	9.44×10^{-3} - 9.74×10^{-3}	9.69×10^{-3}
TEMP	293.0-296.3	298
BARO	100881-102540	101300

PROCESSING CHANNEL PARAMETERS	
INPUT RESISTANCE	22K
AMPLIFIER GAINS (DB)	
A_1	40
A_2	20
A_3	20
FILTER FREQUENCIES (KHZ)	
BAND PASS	50
HIGH PASS	50
LOW PASS	0.5

SPECTRUM ANALYZER PARAMETERS	BASELINE	FAULT
INPUT V. (MV)	40-70	120
GAIN SETTINGS (0 DB REF)		
ANALYZER GAIN	20	
INPUT ATTEN.	10	
INTEGRATION		
LINEAR		
32 SUMS PER BIN		
COSINE WEIGHT		
D.C. COUPLE		
INTERNAL SAMPLE		

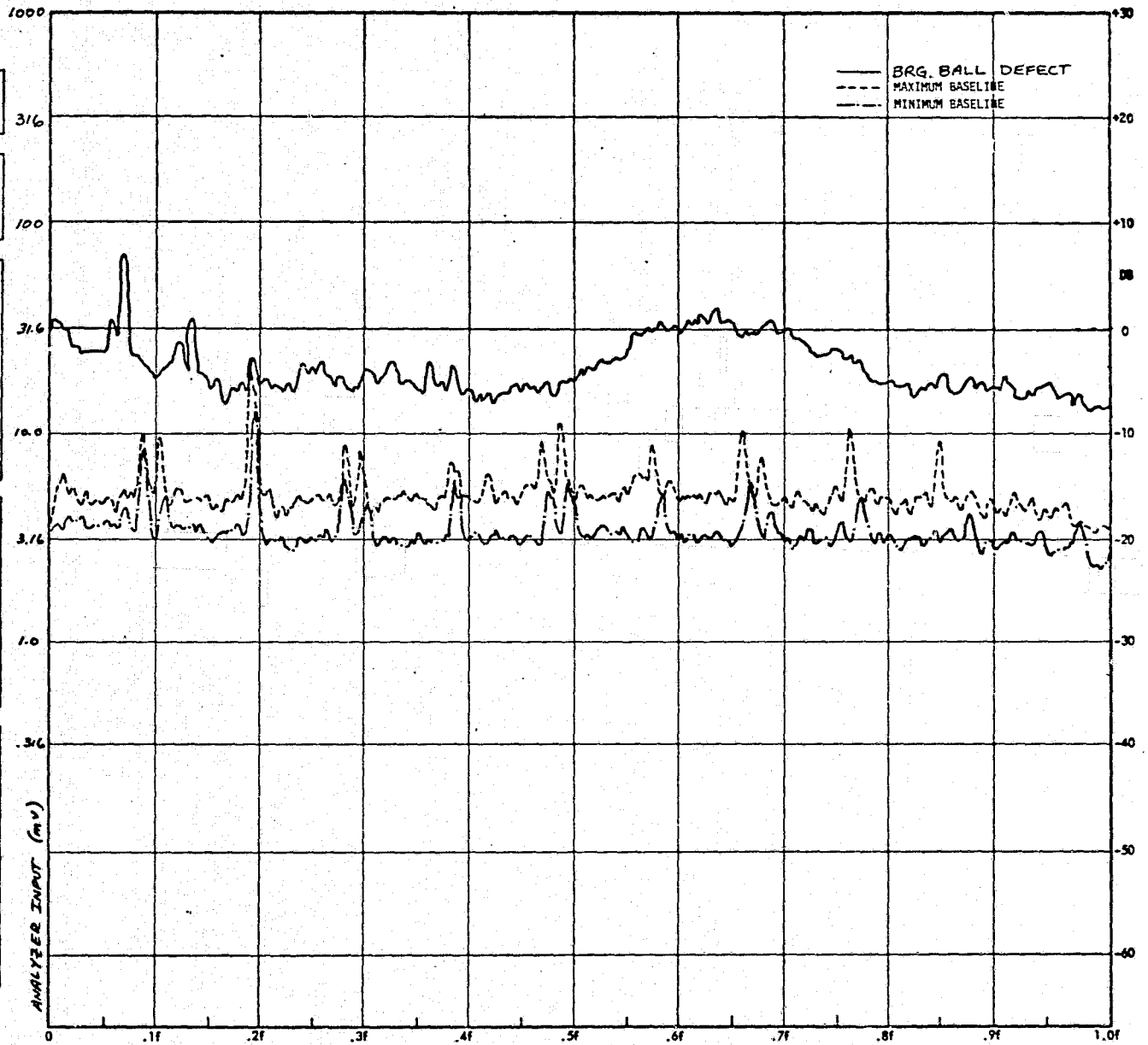

FIG. 60 FREQUENCY SPECTRUM FOR TRW GLOBE 19A532 FAN

TEST ITEM	TRW Globe 19A532
PLOT NO.	44
TRANSDUCER	3100-0

CONTROLLED TEST PARAMETERS	
VOLTAGE	115
P.S. FREQ.	400.0
ΔP	206 (.827)

VARIABLE TEST PARAMETERS	BASELINE	FAULT
DATE	3/11-3/20	5/23
I	.360-.361	.364
ϕ<	.838	.838
PWR	27.7-27.8	28.0
RPM	5640-5940	5700
FLOW RATE	9.44×10^{-3} - 9.74×10^{-3}	9.69×10^{-3}
TEMP	293.0-296.3	298
BARO	100881-102540	101300

PROCESSING CHANNEL PARAMETERS	
INPUT RESISTANCE	22K
AMPLIFIER GAINS (DB)	
A_1	40
A_2	20
A_3	20
FILTER FREQUENCIES (KHZ)	
BAND PASS	50
HIGH PASS	50
LOW PASS	2

SPECTRUM ANALYZER PARAMETERS	BASELINE	FAULT
INPUT V. (MV)	60-100	150
GAIN SETTINGS (0 DB REF)		
ANALYZER GAIN	20	
INPUT ATTEN.	10	
INTEGRATION		
LINEAR		
32 SUMS PER BIN		
COSINE WEIGHT		
D.C. COUPLE		
INTERNAL SAMPLE		

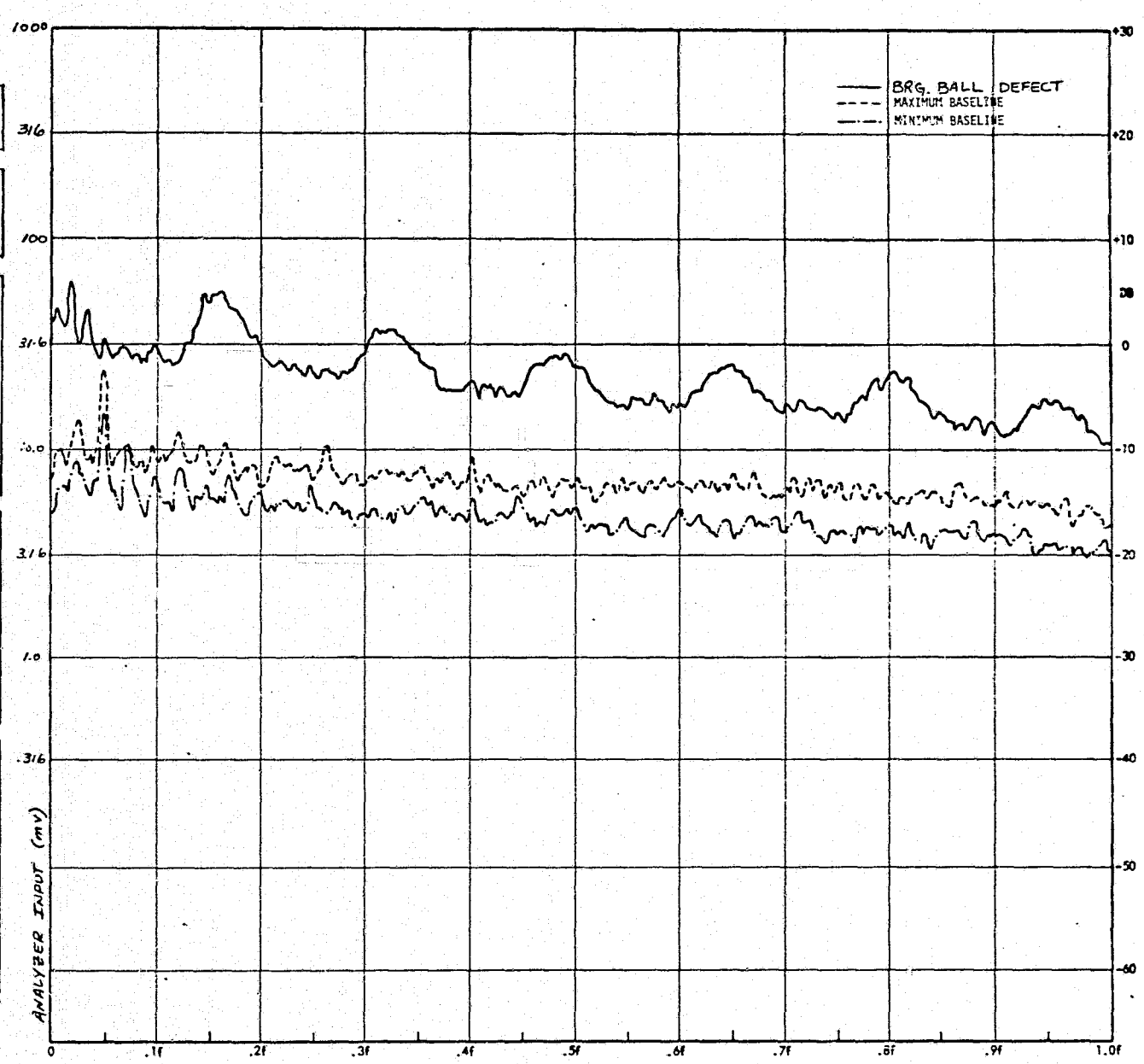

FIG. 61 FREQUENCY SPECTRUM FOR TRW GLOBE 19A532 FAN

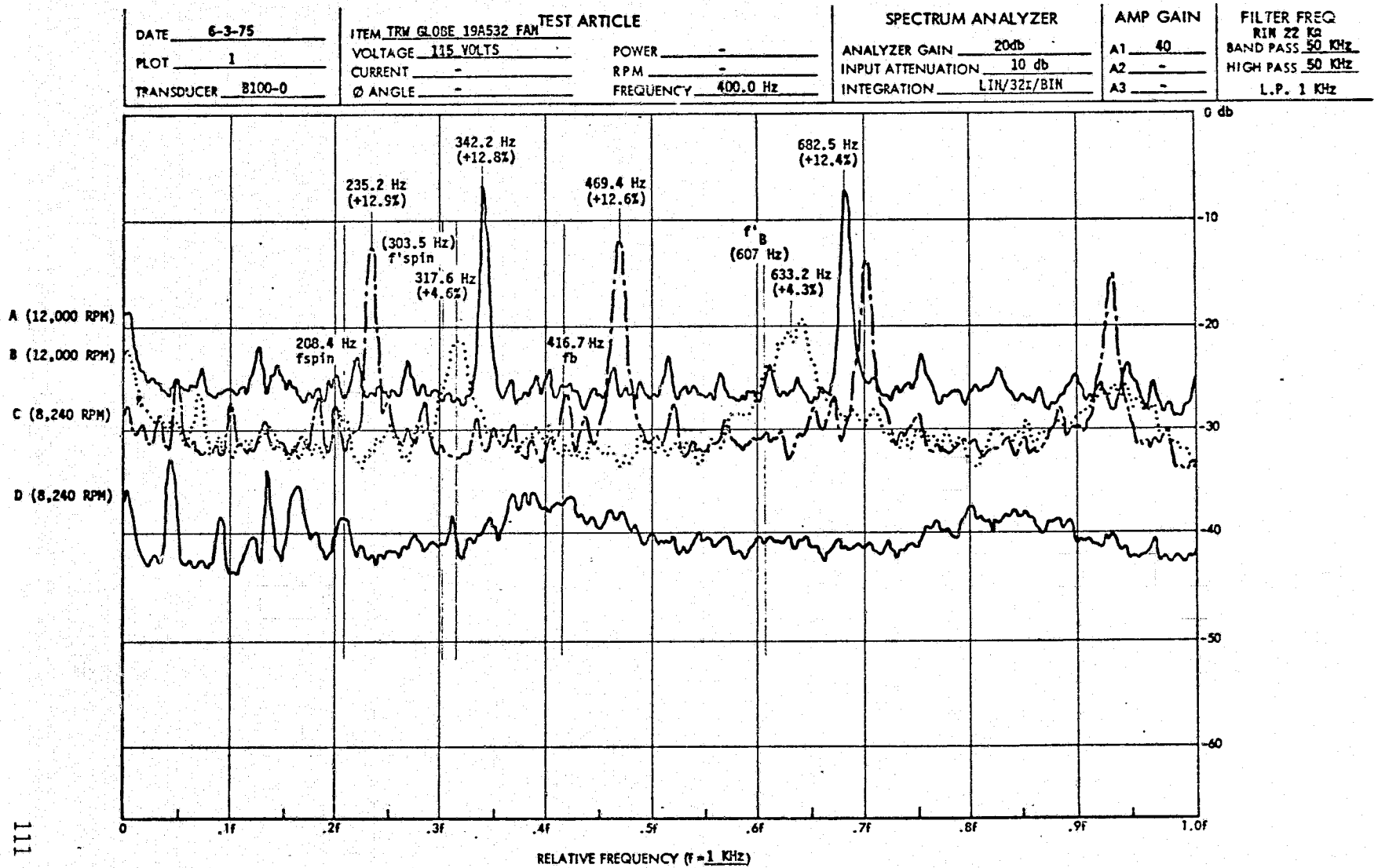

FIG. 62 FREQUENCY SPECTRUM FOR TRW GLOBE 19A532 SQUIRREL CAGE FAN

The amplitude of the spectral lines is lower than that for Curve A since the impact speed is reduced even though the load is increased. Note once again that the spectral line is shifted up in frequency from its calculated value by approximately 12%.

Curve D approaches the situation that was encountered during all of fault testing. The motor is operated with the shaft pointing up and a squirrel cage attached so, as in Curve B, there is probably very little load on the defective bearing. This reduction of load and reduced shaft speed further decreases the amplitude of the ball impact frequency spectral line, broadens it out, and essentially makes the ball spin frequency spectral line disappear.

The SADAS-4 and SANDAS-4 parameters have minimum values of 1.47 and 1.08 at 50 KHz and the SADAS-5 and SANDAS-5 parameters have minimum values of 2.76 and 2.04. As will be seen later, this is not large enough when unbalance effects on the high frequency parameters are considered for making a judgment as to the health of the bearing just based on these two parameters alone.

The most successful processed parameters for detecting the ball defect were those non-spectrum parameters associated with the amplitude distribution of the signal, namely SEACOST-1 and TCCFR-2. Figure 63 shows the increase in the 3 σ spike voltage due to the ball defect and Figure 64 shows the change in the count distribution at 125 KHz. These parameters are not significantly affected by ball side-spin. The parameter TCCFR-1 did not change significantly at any frequency since the count rate up to approximately the 4 σ threshold seemed to remain relatively constant for baseline and fault data. The minimum value of SEACOST-1 for the two transducers at 80 KHz was found to be 7.4 and the minimum value of TCCFR-2 for the two transducers at 125 KHz was found to be 7.7. Considering the amplitude distribution of the spikes in the ball defect fault data, 5 σ spike data would probably show a more profound increase but no processing circuitry was available for making 5 σ spike energy measurements at the time of this testing.

One final note on the ball defect data. The SADAS plots show a spectrum line at approximately 34 Hz on most of the ball defect plots which was not present in the baseline data. This spectral line is the cage frequency with respect to the outer race and is an indication that the two-piece cage was not reassembled as well as thought. Since this line was not supposed to be there, it was not considered in the calculation of the SADAS-4 data. If it had, it would have erroneously made the SADAS-4 data look better than it actually was. Also 60 Hz powerline signal and its harmonics got into the ball defect SADAS plots. These also were not considered in the calculation of the SADAS-4 data.

In order to determine the effect unbalancing has on the ball defect detectability, the processed parameters determined for the ball defect were recalculated assuming the unbalance data to be part of the baseline data. The results are shown in Figures 65 through 68. As can be seen from the plots the SADAS-4 and 5 and SANDAS-4 and 5 are generally less than unity which shows they would not be good parameters to choose, in this case, for making a decision as to the condition of the bearing.

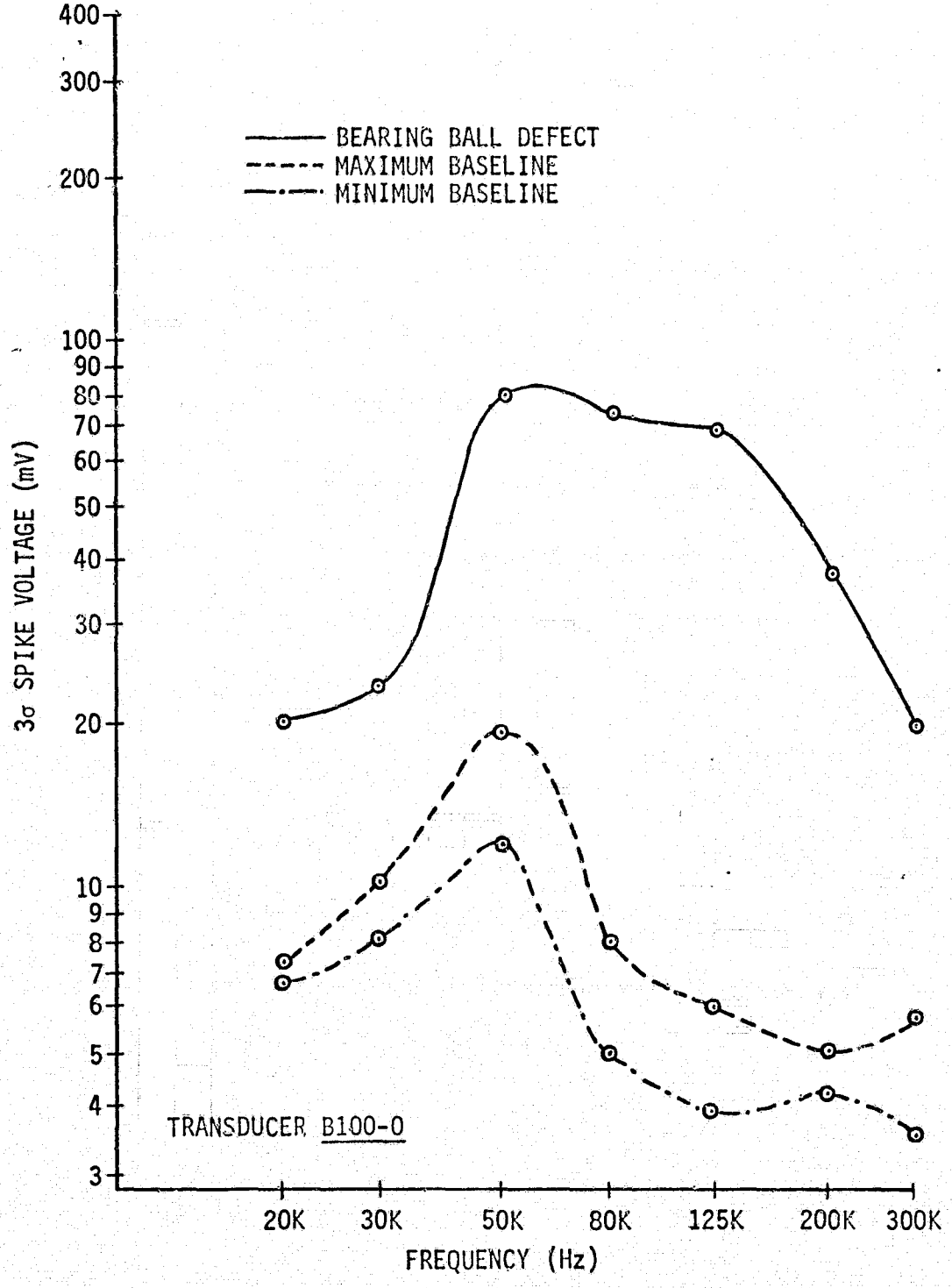

FIGURE 63 3σ SPIKE DATA FOR TRW GLOBE 19A532 FAN

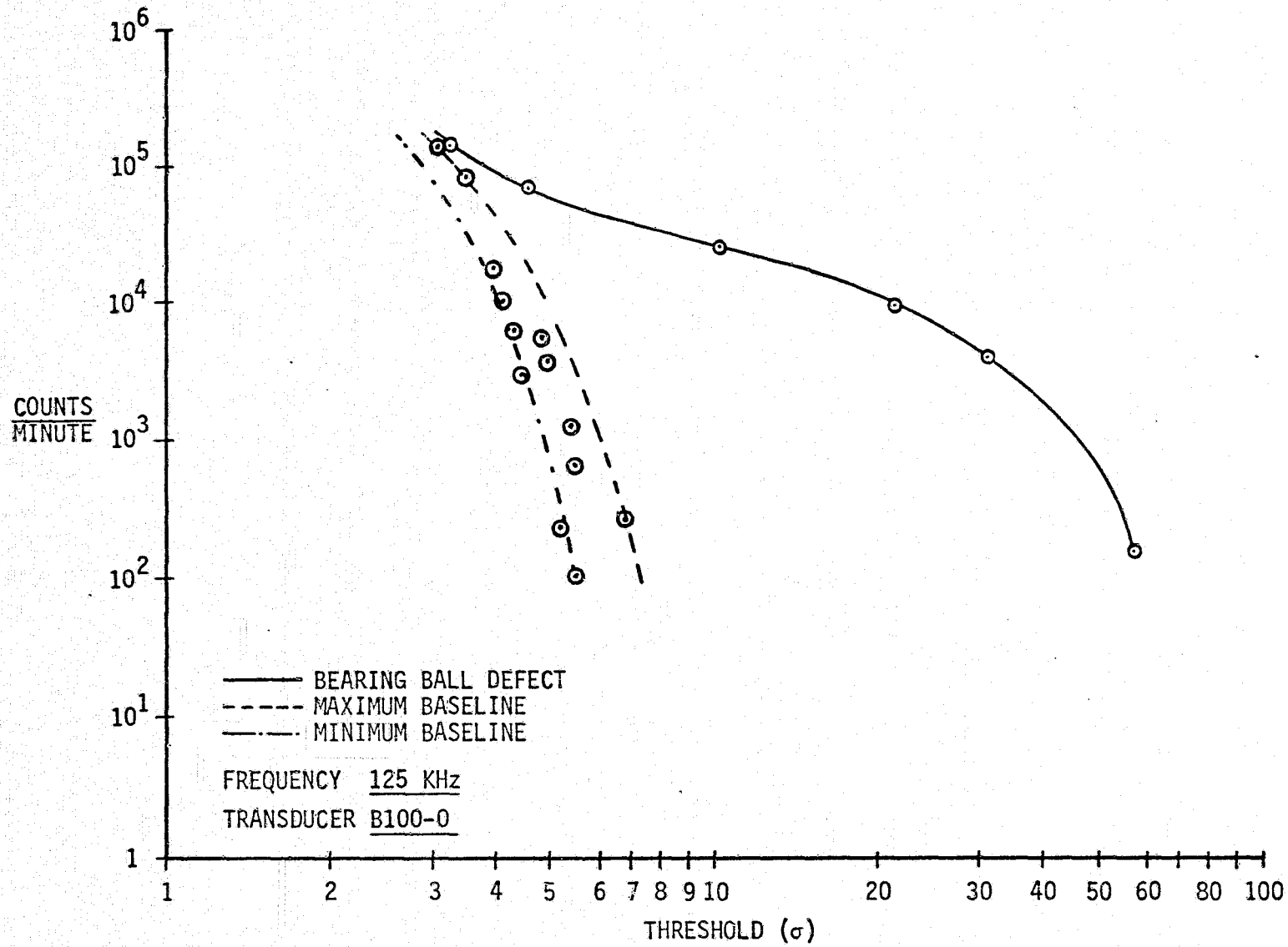

FIGURE 64 COUNT DATA FOR TRW GLOBE 19A532 FAN

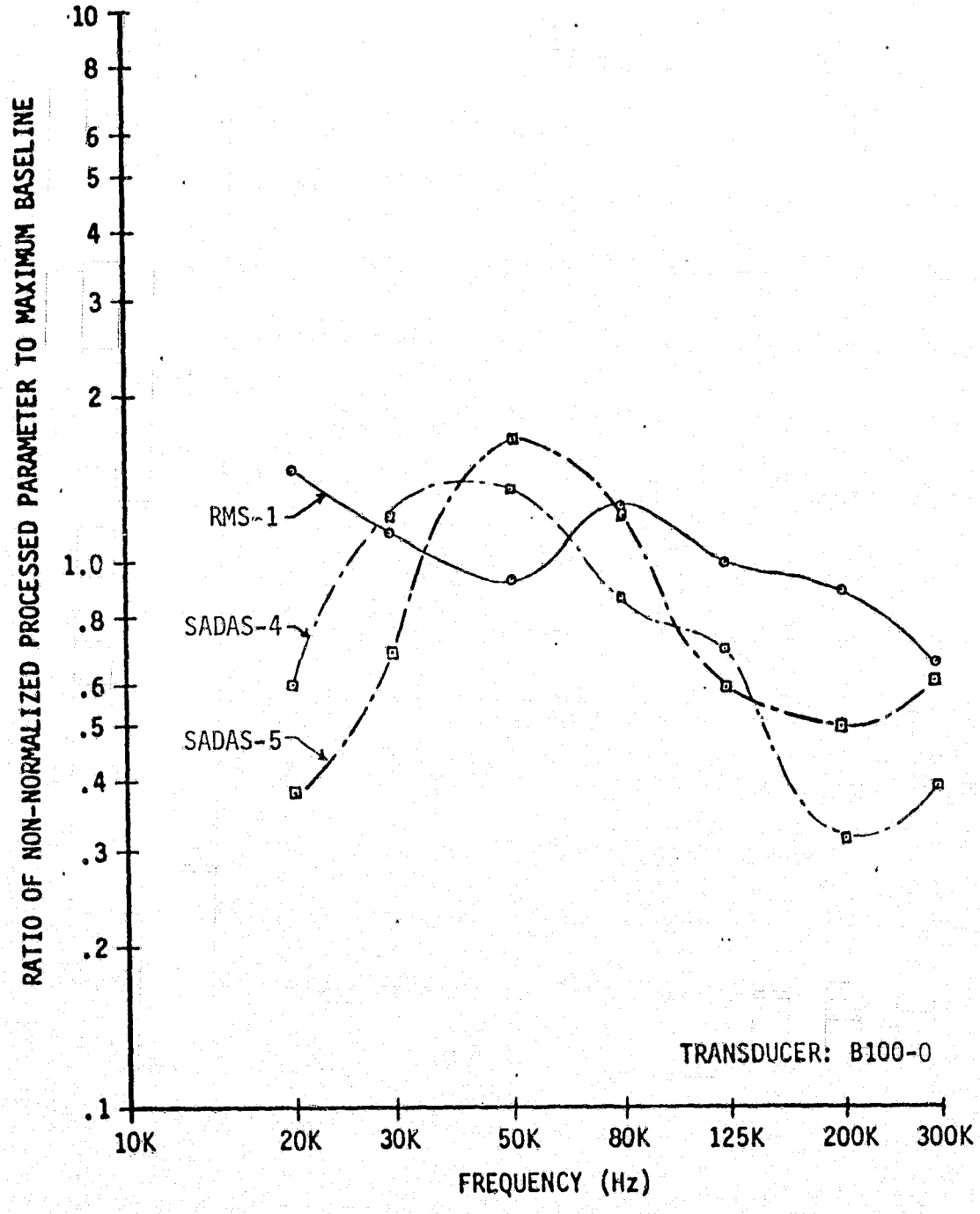

FIG. 65 NON-NORMALIZED PROCESSED PARAMETER CHANGES DUE TO BEARING BALL DEFECT IN TRW GLOBE 19A532 FAN ASSUMING UNBALANCE RESULTS PART OF BASELINE

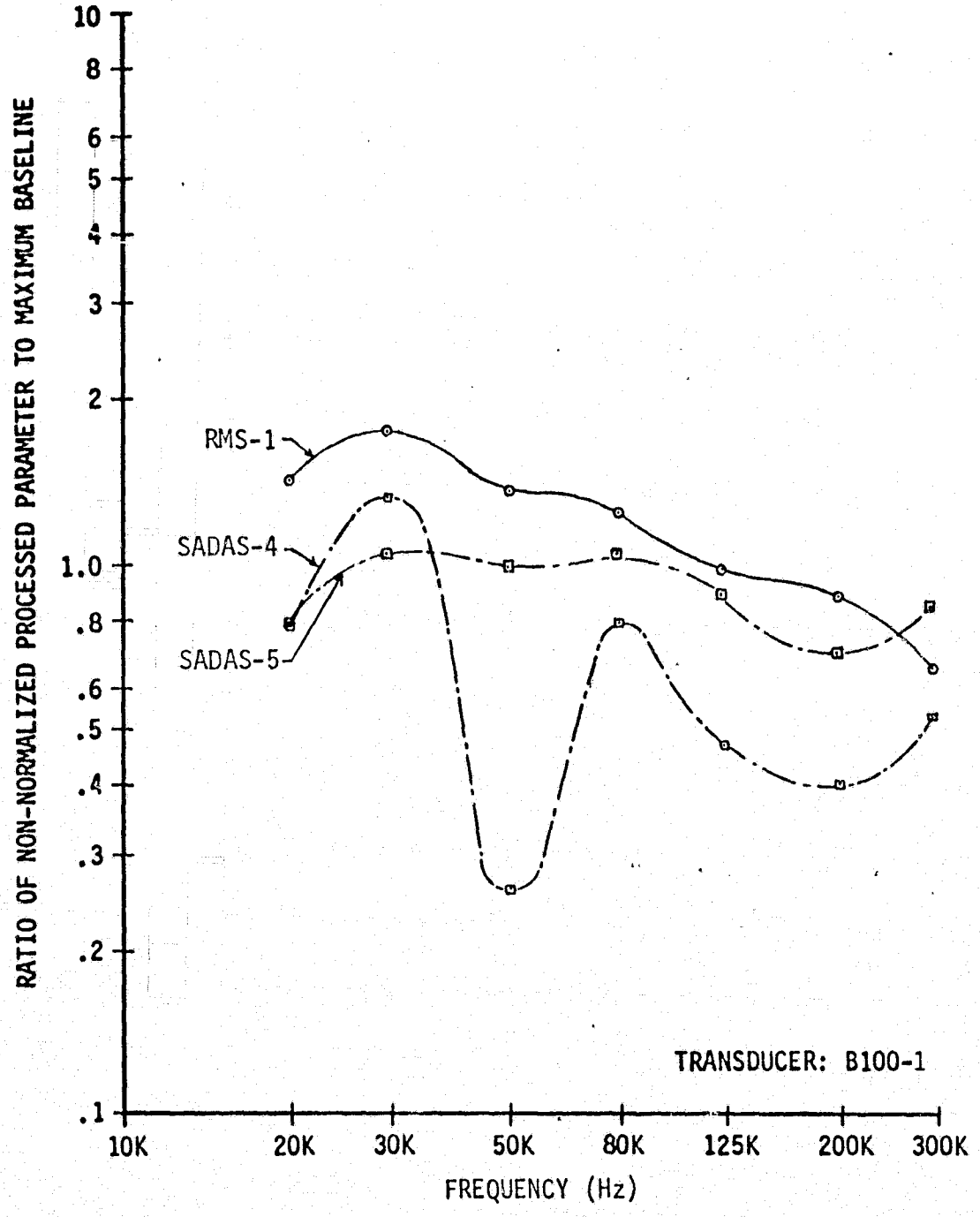

FIG. 66 NON-NORMALIZED PROCESSED PARAMETER CHANGES DUE TO BEARING BALL DEFECT IN TRW GLOBE 19A532 FAN ASSUMING UNBALANCE RESULTS PART OF BASELINE

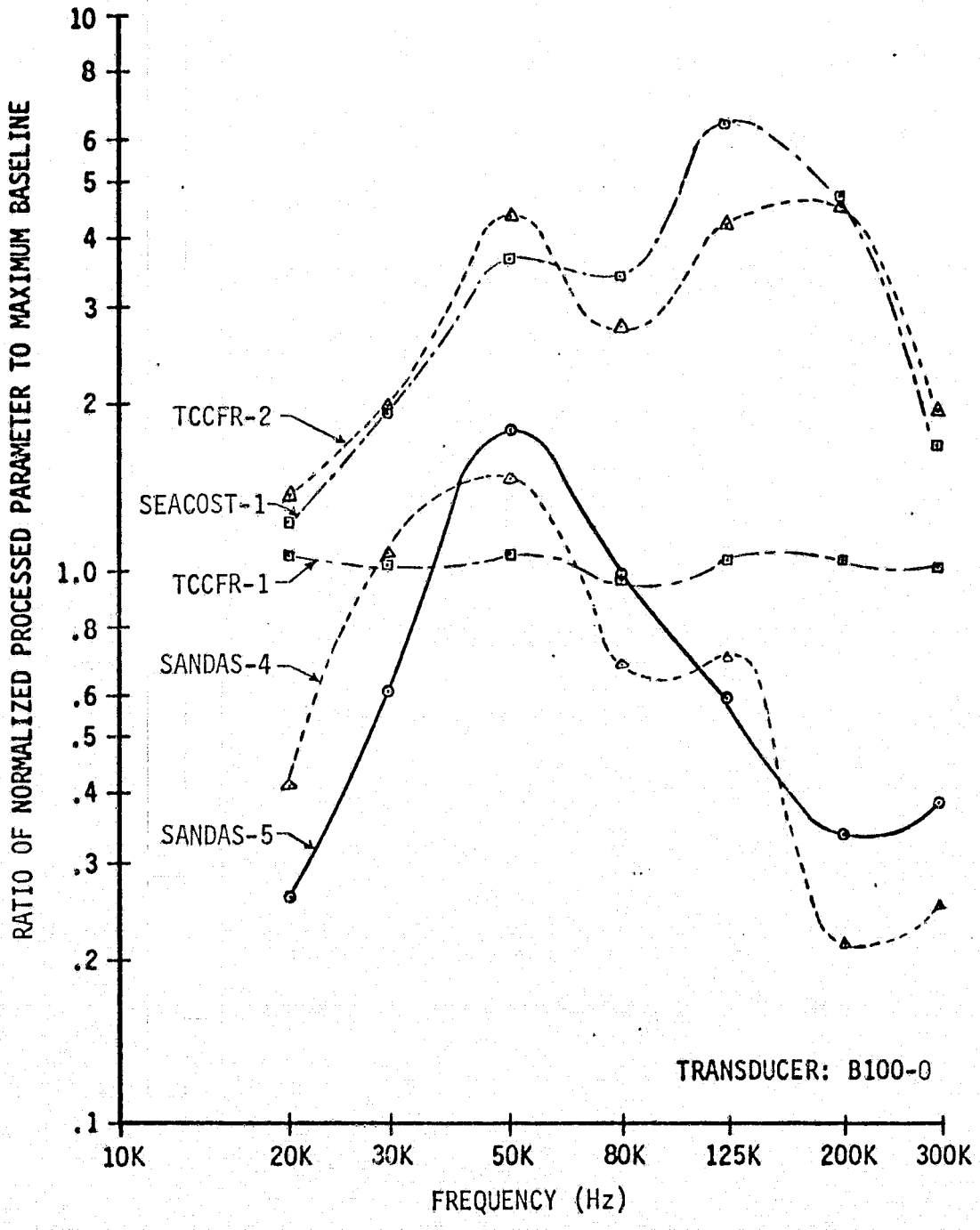

FIG. 67 NORMALIZED PROCESSED PARAMETER CHANGES DUE TO BEARING BALL DEFECT IN TRW GLOBE 19A532 FAN ASSUMING UNBALANCE RESULTS PART OF BASELINE

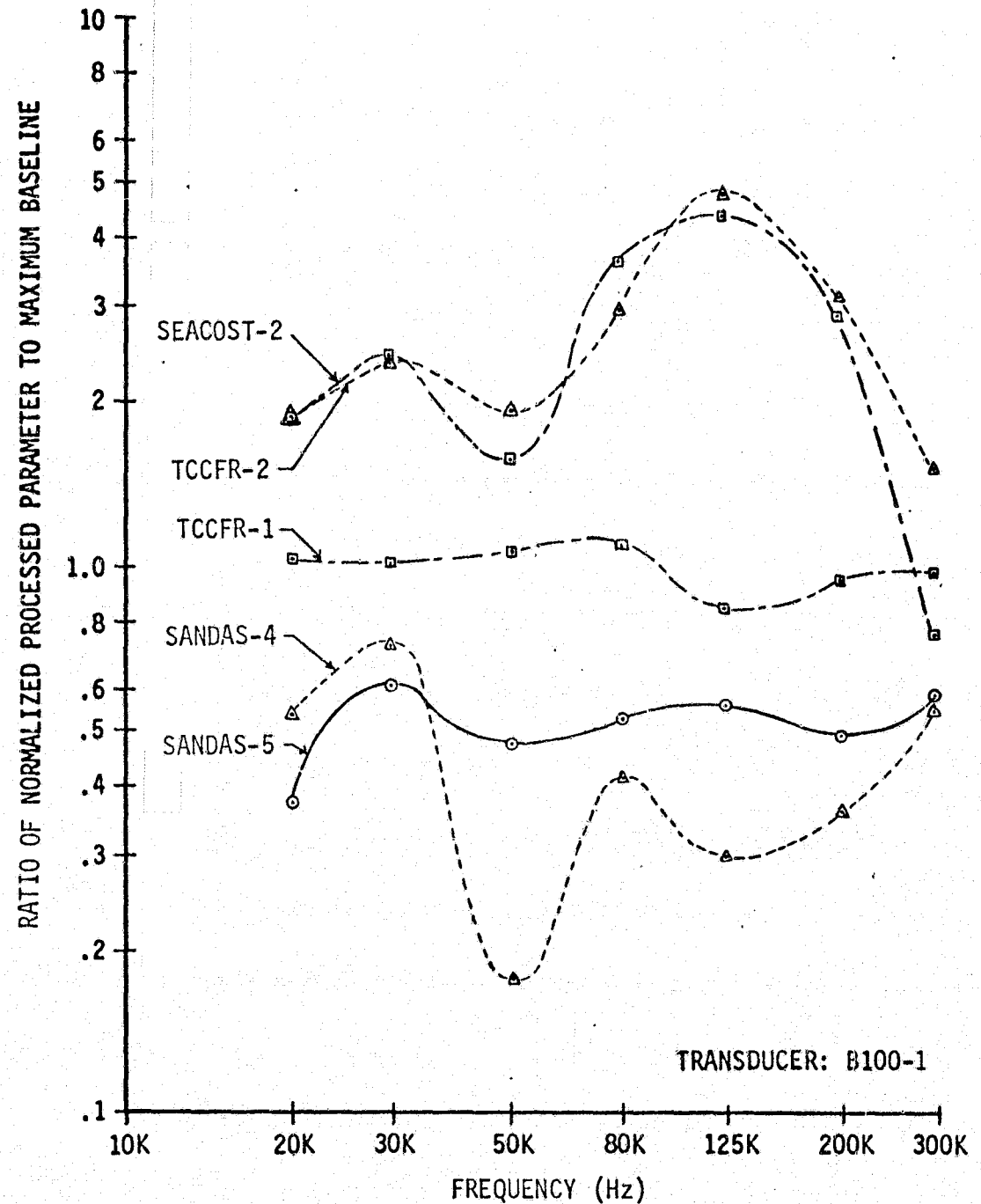

FIG. 68 NORMALIZED PROCESSED PARAMETER CHANGES DUE TO BEARING BALL DEFECT IN TRW GLOBE 19A532 FAN ASSUMING UNBALANCE RESULTS PART OF BASELINE

However, the SEACOST-1 and TCCFR-2 parameters do provide good defect detectability, having minimum values of 4.3 and 4.2 at 125 KHz respectively.

Dynamic Air Engineering C050L Fan

The inner race defect in the bearing was expected to generate a train of narrow vibration/acoustic pulses with a repetitive frequency equal to the inner race ball passing frequency of 1731 - 1735 Hz.

The bearing defect could not be detected with any significant degree of certainty by an examination of the low frequency baseband vibration/acoustic spectrum, as is evident in Figure 69. Notice that the spectral line associated with the inner race ball passing frequency did not exceed the maximum baseline value. However, the defect was detected using the high frequency techniques. Figures 70 and 71 show the high frequency processed parameters for the bearing inner race defect. The most successful processed parameters for detecting the inner race defect were the SADAS parameters, and optimum detection occurred at 50 KHz. The SADAS plot for this bandpass frequency is shown in Figure 72. The values of these parameters at this frequency are given below.

Parameter	Ratio
SADAS-2	15.8
SADAS-5	20.5
SANDAS-2	5.1
SANDAS-5	6.6

The normalized non-spectrum parameters associated with the amplitude distribution of the signal, namely SEACOST-1, TCCFR-1, and TCCFR-2, were very poor at detecting the defect. The maximum value achieved by any of these parameters was 1.43 for SEACOST-1 at 80 KHz. The baseline spike distribution for this fan is normal for a good ball bearing and not corrupted by an outside signal source. This was not the case for the Micropump Pump, discussed in the next section, where turbulent water flow resulted in an abnormal spike distribution. For that pump this abnormal spike distribution made it difficult for the normalized non-spectrum parameters to detect the induced bearing fault. Since this was not the case for the Dynamic Air Engineering fan, the reaction of the balls against the outer race after striking the inner race defect in this small of a bearing must not generate very large amplitude pulses. Since this is required for the normalized non-spectrum parameters to be effective, these parameters will probably not be of much use for detecting small inner race defects in the small bearings associated with aircraft type fans and pumps.

Micropump 10-71-316-1367 Pump

The multiple defects in the faulted original bearing, as a result of the brinelling caused by the 13,350 newton tensile load, were expected to generate multiple trains of relatively wide vibration/acoustic pulses with repetitive frequencies equal to the outer race ball passing frequency of 529.1 - 534.1 Hz, the ball frequency of 737.3 - 744.3 Hz, and the inner race ball passing frequency of 825.3 - 833.1 Hz. Unlike the small, spall simulated defects which were introduced into the three previous test items, the relatively large brinelled multiple defect introduced into the original

DYNAMIC AIR ENGINEERING

TEST ITEM	COSOL FAN
PLOT NO.	12
TRANSDUCER	B100-9

CONTROLLED TEST PARAMETERS	
VOLTAGE	115
P.S. FREQ.	400.0
FLOW RATE	1.89×10^{-2} (40.0)

VARIABLE TEST PARAMETERS		
	BASELINE	FAULT
DATE	6/8 - 6/13	6/24
I	2.01 - 2.03	1.99
ϕ<	.140 - .175	.157
PWR	228 - 231	226
RPM	23440 - 23490	23460
ΔP	4200 - 4430	4430
TEMP	295 - 297	296
BARO	101000 - 101590	101800

PROCESSING CHANNEL PARAMETERS	
INPUT RESISTANCE	—
AMPLIFIER GAINS (DB)	
A_1	20
A_2	—
A_3	—
FILTER FREQUENCIES (KHZ)	
BAND PASS	—
HIGH PASS	0.75
LOW PASS	—

SPECTRUM ANALYZER PARAMETERS		
	BASELINE	FAULT
INPUT V. (MV)	66-755	144

GAIN SETTINGS (0 DB REF)
ANALYZER GAIN 20
INPUT ATTEN. 1.0
INTEGRATION
LINEAR
32 SUMS PER BIN
COSINE WEIGHT
D. C. COUPLE
INTERNAL SAMPLE

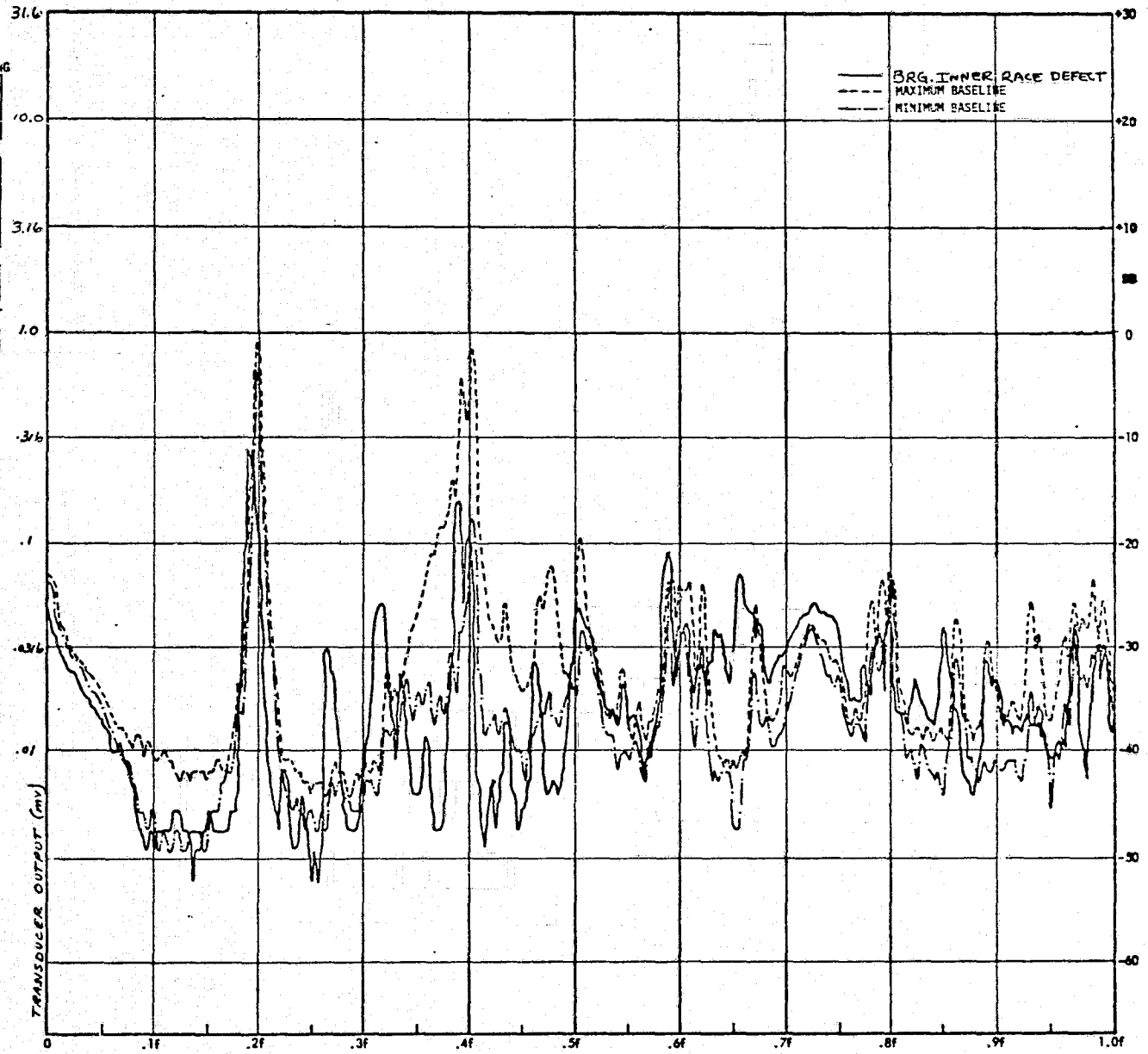

FIG. 69

FREQUENCY SPECTRUM FOR DYNAMIC AIR ENGINEERING COSOL FAN

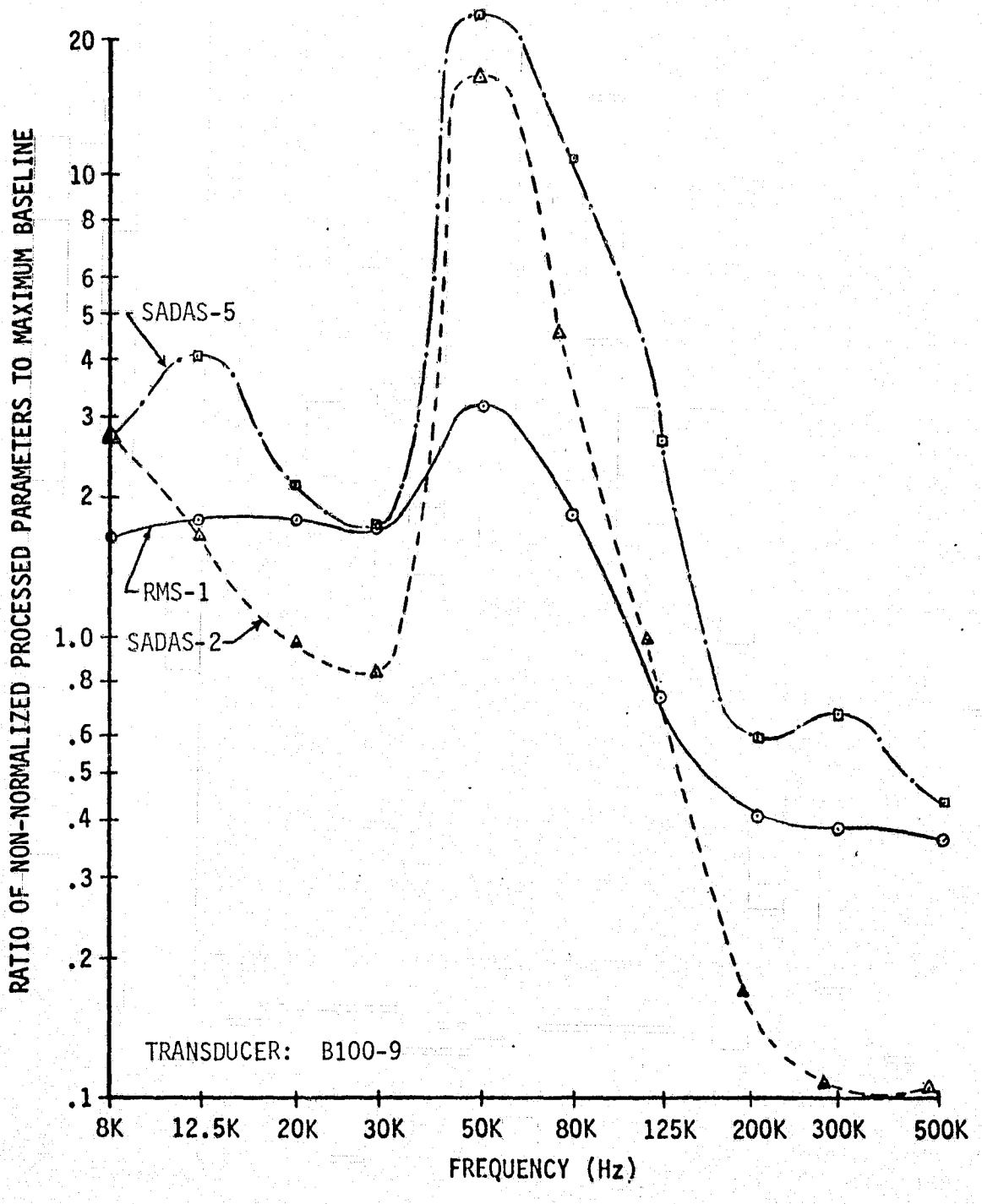

FIG. 70 NON-NORMALIZED PARAMETER CHANGES DUE TO BEARING INNER RACE FLAW IN DYNAMIC AIR ENGINEERING C050L FAN

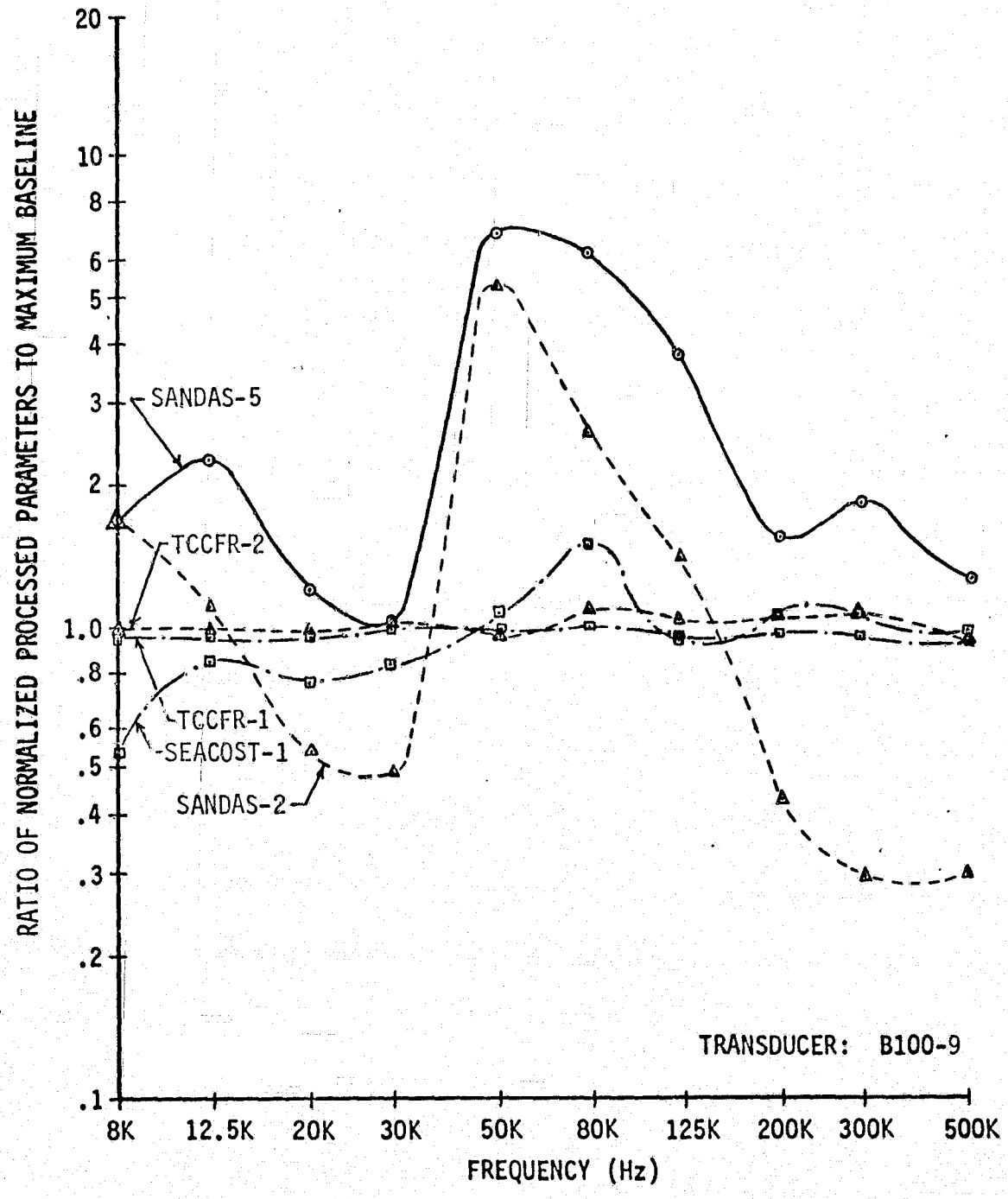

FIG. 71 NORMALIZED PROCESSED PARAMETER CHANGES DUE TO BEARING INNER RACE FLAW IN DYNAMIC AIR ENGINEERING C05OL FAN

DYNAMIC AIR ENGINEERING

TEST ITEM	COSOL FAN
PLOT NO.	35
TRANSDUCER	B100-9

CONTROLLED TEST PARAMETERS	
VOLTAGE	115
P.S. FREQ.	400.0
FLOW RATE	1.89×10^{-2} (40.0)

VARIABLE TEST PARAMETERS	BASELINE	FAULT
DATE	6/8 - 6/13	6/24
I	2.01 - 2.03	1.99
ΔP	.140 - .175	.157
PWR	228 - 231	226
RPM	23440 - 23490	23460
ΔP	4280 - 4430	4430
TEMP	295 - 297	296
BARO	101000 - 101500	101800

PROCESSING CHANNEL PARAMETERS	
INPUT RESISTANCE	22KΩ
AMPLIFIER GAINS (DB)	
A_1	20
A_2	40
A_3	—
FILTER FREQUENCIES (KHZ)	
BAND PASS	50
HIGH PASS	50
LOW PASS	2

SPECTRUM ANALYZER PARAMETERS	BASELINE	FAULT
INPUT V. (HV)	116-155	765
GAIN SETTINGS (0 DB REF)		
ANALYZER GAIN	10	
INPUT ATTEN.	20	
INTEGRATION		
LINEAR		
32 SUMS PER BIN		
COSINE WEIGHT		
D. C. COUPLE		
INTERNAL SAMPLE		

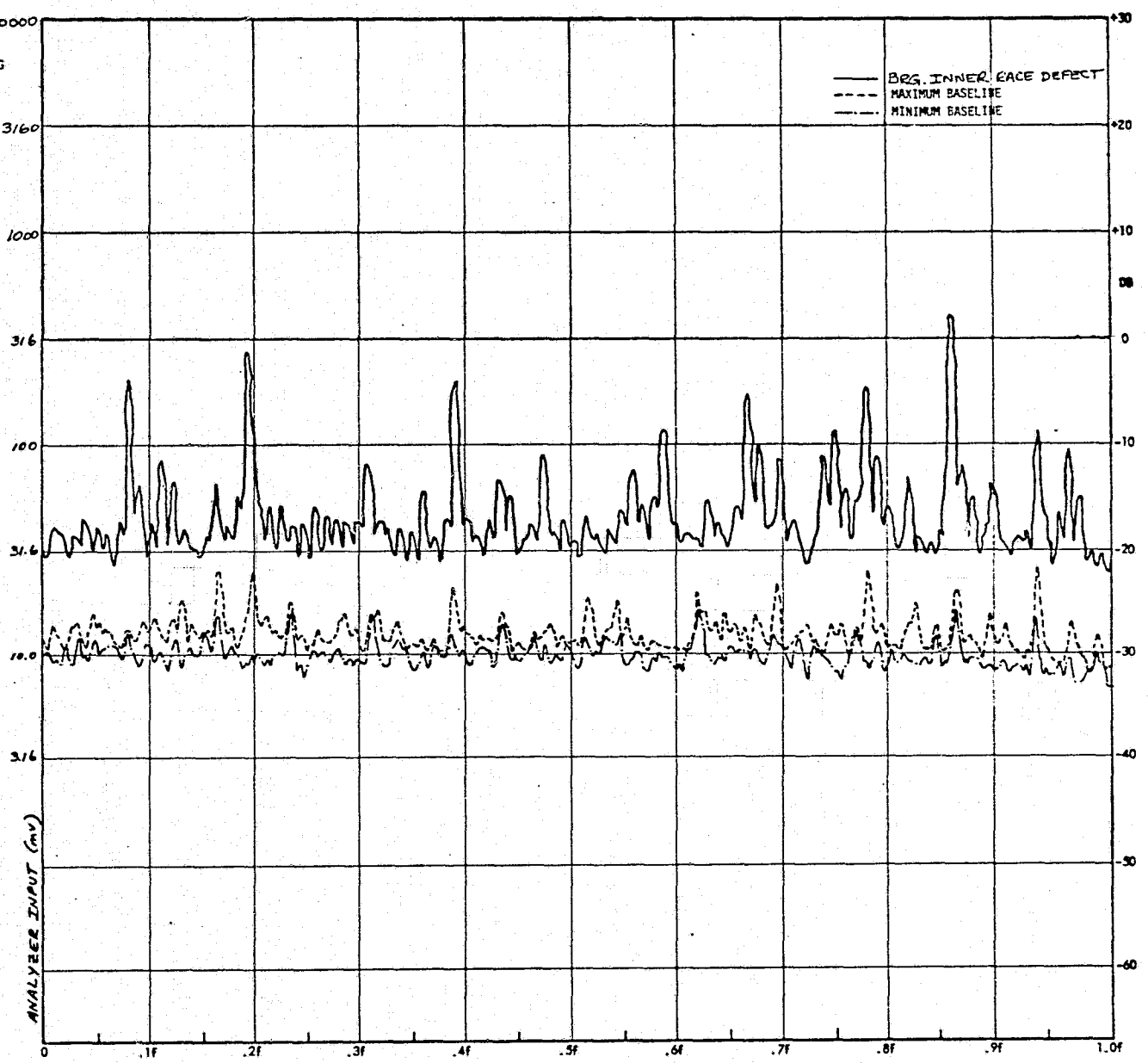

FIG. 72

FREQUENCY SPECTRUM FOR DYNAMIC AIR ENGINEERING COSOL FAN

bearing could easily have been detected by an examination of the low frequency baseband vibration/acoustic spectrum. However, the multiple defect did not appear as increases in the fundamental spectral lines associated with the ball passing frequencies. Instead it appeared as increases in the spectral lines associated with ball bearing non-linear theory vibration orders, with multiples of f_s, shaft frequency, and with multiples of f_{ci}, cage with respect to inner race frequency. This can readily be seen in Figure 73. Ball bearing non-linear theory vibration orders result from waviness in the inner and outer race and are given by $nf_{ci} \pm f_{co}$ for inner race waviness and $(n \pm 1) f_{co}$ for outer race waviness. "n" in these equations is an index number and is equal to 1, 2, 3, ... A list of these cage associated frequencies is given in Table XXIII.

The multiple defect also resulted in increased high frequency signal levels, as shown in Figure 74. However, the defect did not appear as increases in the SADAS fundamental spectral lines associated with the outer race ball passing frequency, 529.1 - 534.1 Hz or the inner race ball passing frequency, 825.3 - 833.1 Hz, as expected. They did, however, appear as an increase in the SADAS fundamental spectral line associated with the ball frequency, 737.3 - 744.3 Hz. Also, like the low frequency vibration spectrum, the defect appeared as increases in the SADAS spectral lines associated with ball bearing non-linear theory vibration orders, with multiples of f_s, shaft frequency, and with multiples of f_{ci}, cage with respect to inner race frequency.

A summary of the high frequency results is shown in Figures 75 and 76. Figure 75 shows non-normalized processed parameters for transducer B100 - S.N. 5. Note that the defect resulted in a greater than 20:1 increase in high frequency RMS signal level for all frequencies from 20 KHz to 125 KHz. Optimum defect detectability over the frequency range from 20 KHz to 300 KHz for all three non-normalized processed parameters occurs at 125 KHz. At this frequency the SADAS-6 parameter had a maximum value of 120.

Normalized processed parameters are shown in Figure 76. For all these parameters SANDAS-6 gave the greatest defect detectability, again at 125 KHz, where it was equal to 4.2. The non-spectrum parameters associated with the amplitude distribution of the signal, namely SEACOST-1, TCCFR-1, and TCCFR-2 did not provide good defect detectability. This is due to the following two factors:

A. The brinelling of the bearing causes a smooth contour-fault in contrast with the sharp edges which result from spalling. The smooth contour generates less high amplitude spikes in relation to the increase in overall RMS level.

B. Turbulent flow of the water in the pump generates a very spiky background signal which tends to considerably increase the baseline for this type of parameter. Thus, any increase in the spike level relative to the overall increase in RMS level caused by the bad bearing has a much reduced effect.

TEST ITEM	Micropump Model 10-71-316-1367 Centrifugal Pump
PLOT NO.	7
TRANSDUCER	B100-5

CONTROLLED TEST PARAMETERS	
VOLTAGE	115
P.S. FREQ.	400.0
FLOW RATE	7.5×10^{-5} (1.2)

VARIABLE TEST PARAMETERS	BASELINE	FAULT
DATE	4/23,5/10	5/31
I	.677	.699
ϕ_L	.384-.419	.384
PWR	71.1-72.2	74.5
RPM	10240-10250	10160
P_S	6900	6900
P_D	162000-165000	165000
ΔP	155000-158000	158000
TEMP	295-297	295
BARO	100900-101900	101300

PROCESSING CHANNEL PARAMETERS	
INPUT RESISTANCE	—
AMPLIFIER GAINS (DB)	
A_1	20
A_2	—
A_3	—
FILTER FREQUENCIES (KHZ)	
BAND PASS	—
HIGH PASS	—
LOW PASS	1

SPECTRUM ANALYZER PARAMETERS	BASELINE	FAULT
INPUT V. (MV)	19-25	60
GAIN SETTINGS (0 DB REF)		
ANALYZER GAIN	10	
INPUT ATTEN.	11	
INTEGRATION		
LINEAR 32ε/BIN COSINE WEIGHT	D.C. COUPLE INTERNAL SAMPLE	

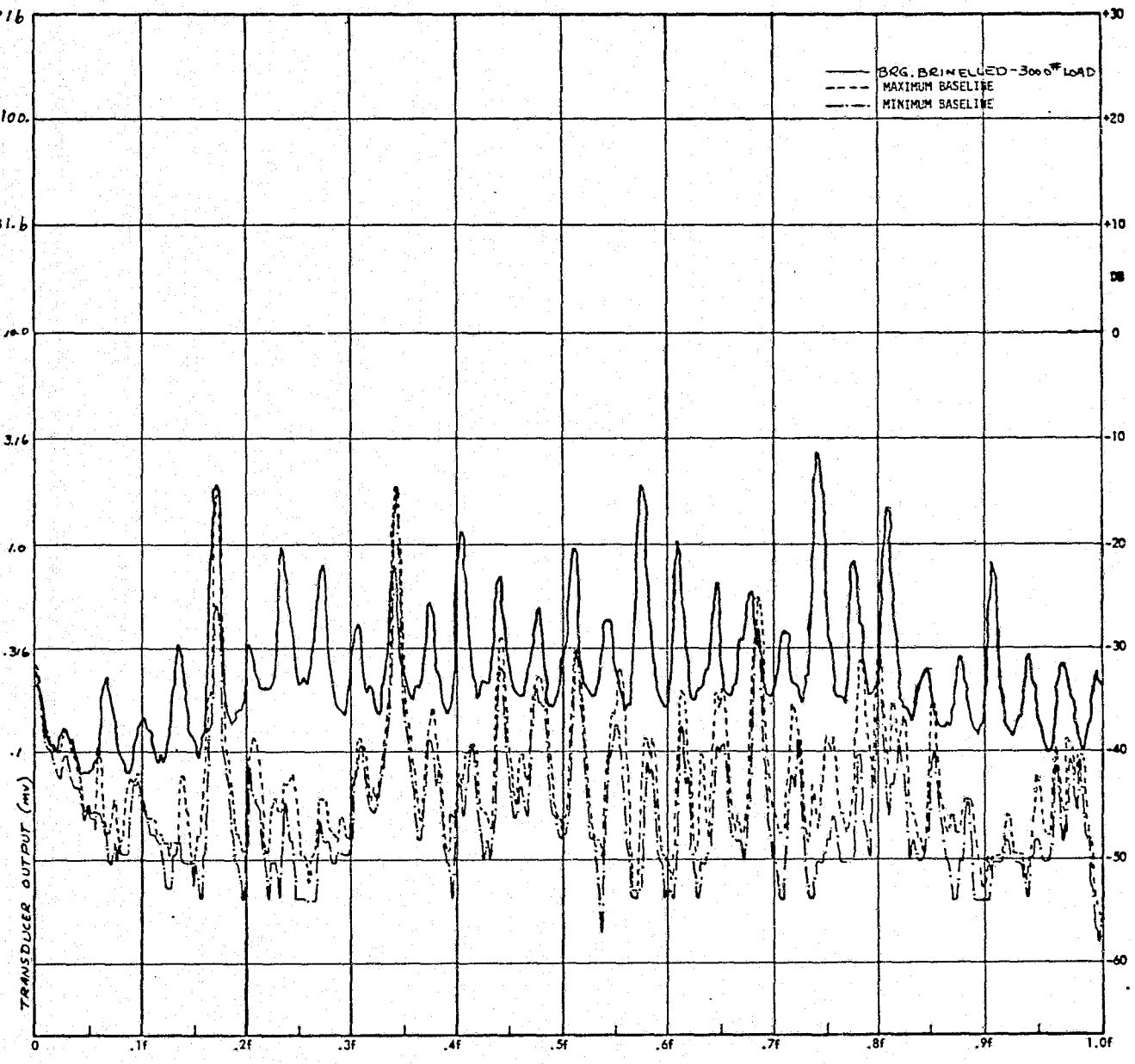

FIG. 73 FREQUENCY SPECTRUM FOR MICROPUMP 10-71-316-1367 PUMP

TABLE XXIII - BEARING CAGE FREQUENCIES ASSOCIATED WITH MICROPUMP PUMP (0 - 1000 Hz)

f_s = 169.3 - 170.9 Hz : f_{co} = 66.2 - 66.8 Hz : f_{ci} = 103.1 - 104.1 Hz

	Freq. (Hz)		Freq. (Hz)
$f_{ci} - f_{co}$	36.9 - 37.3	$6f_{ci} - f_{co}$	552.4 - 557.8
f_{co}	66.2 - 66.8	$5f_{ci} + f_{co}$	581.7 - 587.3
f_{ci}	103.1 - 104.1	$9f_{co}$	595.8 - 601.2
$2f_{co}$	132.4 - 133.6	$6f_{ci}$	618.6 - 624.6
$2f_{ci} - f_{co}$	140.0 - 141.4	$7f_{ci} - f_{co}$	655.5 - 661.9
$f_{ci} + f_{co}$	169.3 - 170.9	$10f_{co}$	662.0 - 668.0
$3f_{co}$	198.6 - 200.4	$6f_{ci} + f_{co}$	684.8 - 691.4
$2f_{ci}$	206.2 - 208.2	$7f_{ci}$	721.7 - 728.7
$3f_{ci} - f_{co}$	243.1 - 245.5	$11f_{co}$	728.2 - 734.8
$4f_{co}$	264.8 - 267.2	$8f_{ci} - f_{co}$	758.6 - 766.0
$2f_{ci} + f_{co}$	272.4 - 275.0	$7f_{ci} + f_{co}$	787.9 - 795.5
$3f_{ci}$	309.3 - 312.3	$12f_{co}$	794.4 - 801.6
$5f_{co}$	331.0 - 334.0	$8f_{ci}$	824.8 - 832.8
$4f_{ci} - f_{co}$	346.2 - 349.6	$13f_{co}$	860.6 - 868.4
$3f_{ci} + f_{co}$	375.5 - 379.1	$9f_{ci} - f_{co}$	861.7 - 870.1
$6f_{co}$	397.2 - 400.8	$8f_{ci} + f_{co}$	891.0 - 899.6
$4f_{ci}$	412.4 - 416.4	$14f_{co}$	926.8 - 935.2
$5f_{ci} - f_{co}$	449.3 - 453.7	$9f_{ci}$	927.9 - 936.9
$7f_{co}$	463.4 - 467.6	$10f_{ci} - f_{co}$	964.8 - 974.8
$4f_{ci} + f_{co}$	478.6 - 483.2	$15f_{co}$	993.0 - 1002
$5f_{ci}$	515.5 - 520.5	$9f_{ci} + f_{co}$	994.1 - 1003.7
$8f_{co}$	529.6 - 534.4		

TEST ITEM	Micropump Model 10-71-316-1367 Centrifugal Pump
PLOT NO.	25
TRANSDUCER	B/00-5

CONTROLLED TEST PARAMETERS	
VOLTAGE	115
P.S. FREQ.	400.0
FLOW RATE	7.5×10^{-5} (1.2)

VARIABLE TEST PARAMETERS	BASELINE	FAULT
DATE	4/23,5/10	5/31
I	.677	.699
ϕ_L	.384-.419	.384
PWR	71.1-72.2	74.5
RPM	10240-10250	10160
P_S	6900	6900
P_D	162000-165000	165000
ΔP	155000-158000	158000
TEMP	295-297	295
BARO	100900-101900	10/300

PROCESSING CHANNEL PARAMETERS	
INPUT RESISTANCE	22Kn
AMPLIFIER GAINS (DB)	
A_1	40
A_2	—
A_3	20
FILTER FREQUENCIES (KHZ)	
BAND PASS	125
HIGH PASS	50
LOW PASS	1

SPECTRUM ANALYZER PARAMETERS	BASELINE	FAULT
INPUT V. (MV)	5	170
GAIN SETTINGS (0 DB REF)		
ANALYZER GAIN	20	
INPUT ATTEN.	0	
INTEGRATION		
LINEAR 32E/BIN COSINE WEIGHT	D.C. COUPLE INTERNAL SAMPLE	

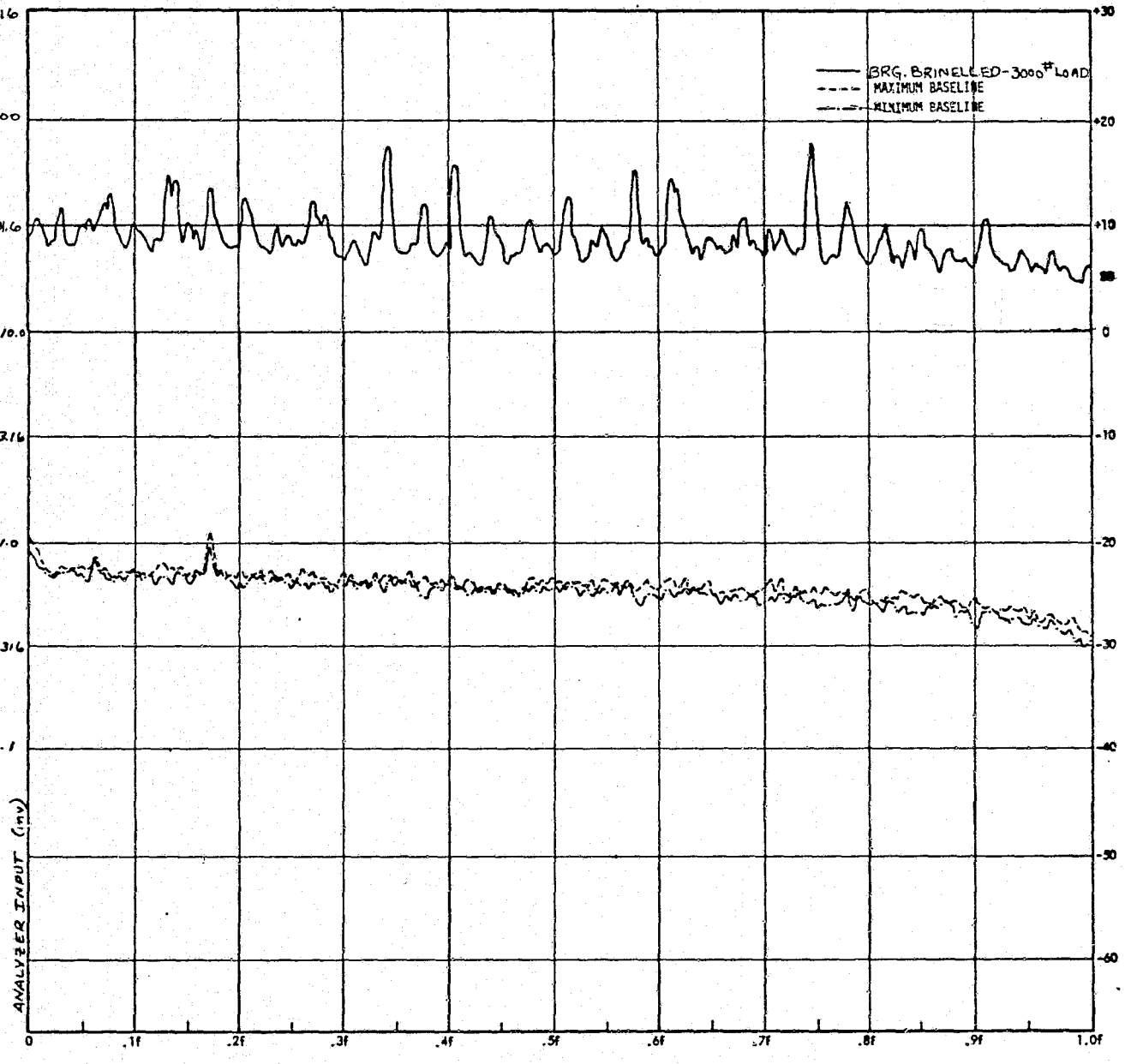

FIG. 74 FREQUENCY SPECTRUM FOR MICROPUMP 10-71-316-1367 PUMP

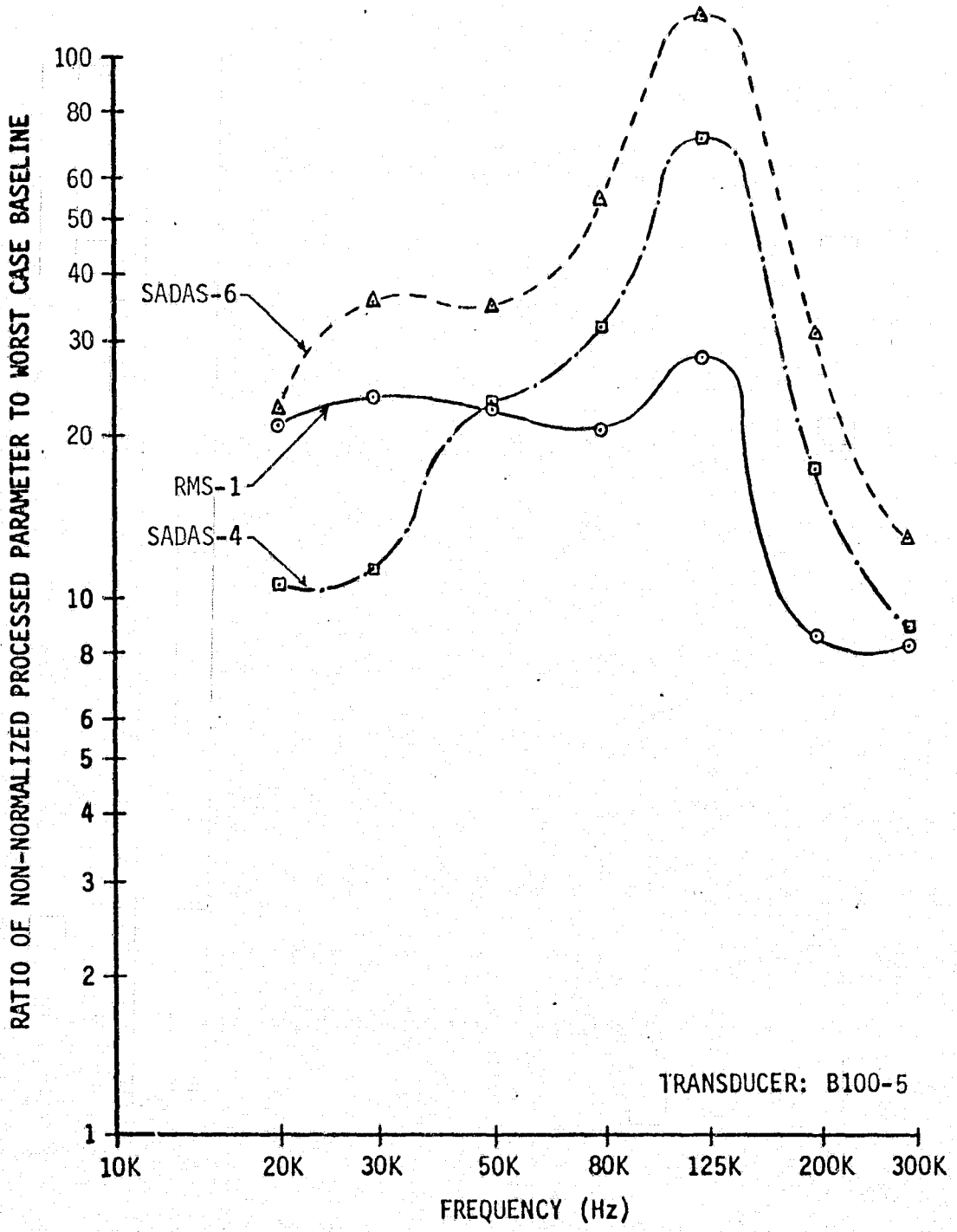

FIG. 75 NON-NORMALIZED PROCESSED PARAMETER CHANGES DUE TO BRINELLING ORIGINAL BEARING BY LOADING IT TO 3000 POUNDS - MICROPUMP 10-71-316-1367 PUMP

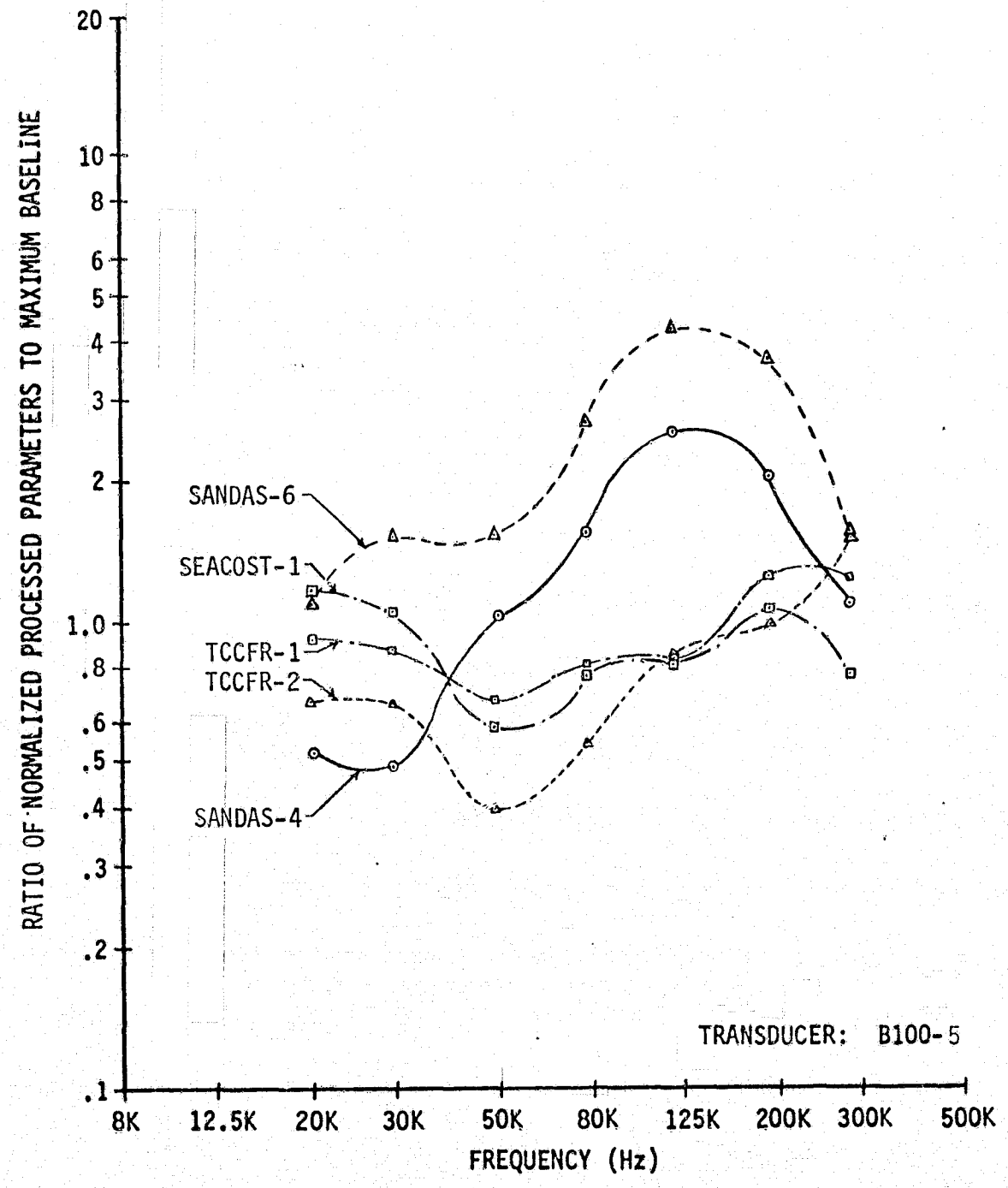

FIG. 76 NORMALIZED PROCESSED PARAMETER CHANGES DUE TO BRINELLING ORIGINAL BEARING BY LOADING IT TO 3000 POUNDS-MICROPUMP 10-71-316-1367 PUMP

Since the purpose of testing the first replacement bearing, loaded to 4,450 Newtons, was just to determine if this small of a brinelled defect could be detected, no baseline data was collected, nor was any broadband RMS, spike, or count fault data taken. The smaller amount of brinelling, which was introduced into the first replacement bearing, resulted in not being able to detect the defect, with any significant degree of certainty, by a comparison of the low frequency baseband vibration/acoustic spectrum with the original bearing baseline data. Unfortunately the defect also did not show up with any significant degree of certainty at frequencies greater than 30 KHz. However, baseband spectrum plots which were taken for this defect showed a large increase in RMS signal level between 2 KHz and 19 KHz when compared with the original bearing baseline data. SADAS plots were made with the bandpass filter's center frequency set at frequencies ranging from 2 KHz to 20 KHz. One such plot is shown in Figure 77 for a center frequency of 8 KHz. The plot shows large spectral lines at the inner and outer race ball passing frequencies, indicating this range of frequencies is a better choice for detecting the brinelled defect. A comparison of this data with the second replacement bearing baseline data was made and the results are shown in Figure 78. SADAS-6 was the best non-normalized parameter for detecting this defect and was greater than 10:1 for center frequencies from 5 to 12.5 KHz.

The small amount of brinelling, which was introduced into the second replacement bearing, again resulted in not being able to detect the defect, with any significant degree of certainty, by an examination of the low frequency vibration/acoustic spectrum, as is evident in Figure 79. The defect was detected for the range of high frequencies established for the first replacement bearing using the high frequency processing techniques. A typical SADAS plot for a bandpass frequency of 8 KHz is shown in Figure 80. The summarized data is shown in Figures 81 and 82. Figure 81 shows the non-normalized processed parameters. As for the first two cases, the SADAS-6 parameter provides the greatest defect detectability. This parameter has a maximum of 11.6 at 12.5 KHz. The SADAS plots for this bearing defect were unlike those obtained for the first replacement bearing. Unlike that bearing, where major SADAS spectral lines appeared at the inner and outer race ball pass frequencies, the SADAS plots for this defect were more like reduced versions of the plots obtained at higher frequencies for the original bearing which was more severely brinelled. The normalized processed parameters are shown in Figure 82. Again, SANDAS-6 gave the greatest defect detectability with a maximum of 3.0 at 20 KHz. The SEACOST-1 parameter was a much better indicator of the defect than it was at higher frequencies, having a maximum of 2.8 at 8 KHz. The improved performance of SEACOST-1 at these lower frequencies is probably due to the fact that turbulent flow in the pump generates a less spikey background signal at these lower frequencies.

Hydrokinetics 10461 Pump

For the four other items tested during the course of this study, the fault which was originally introduced into one of the test item's bearings was not expected to, and did not change significantly during the several hour period during which fault data was collected. Thus, there was good repeatability

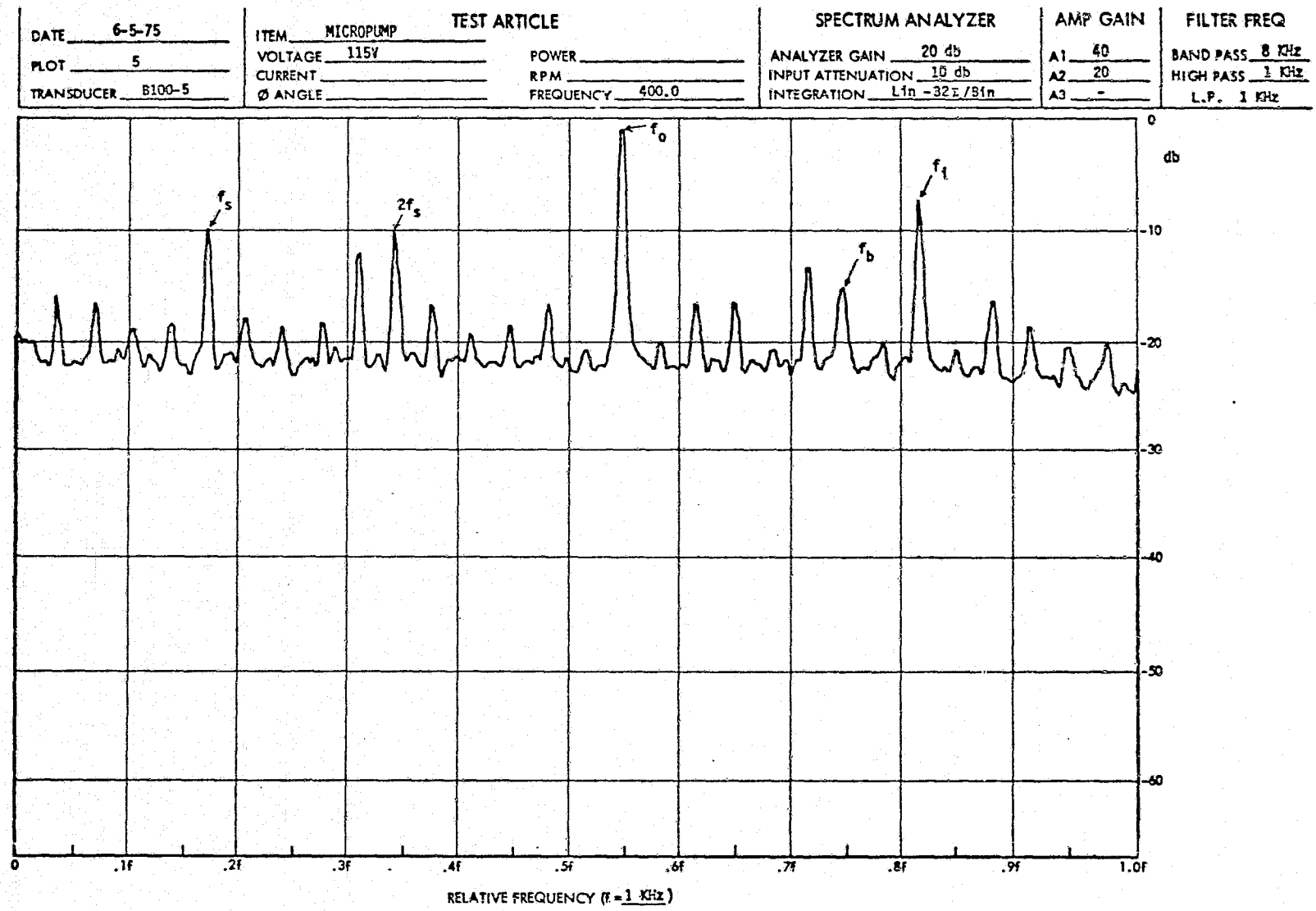

FIG. 77 FREQUENCY SPECTRUM FOR MICROPUMP 10-71-316-1367 PUMP-BRINELLED FIRST REPLACEMENT BEARING

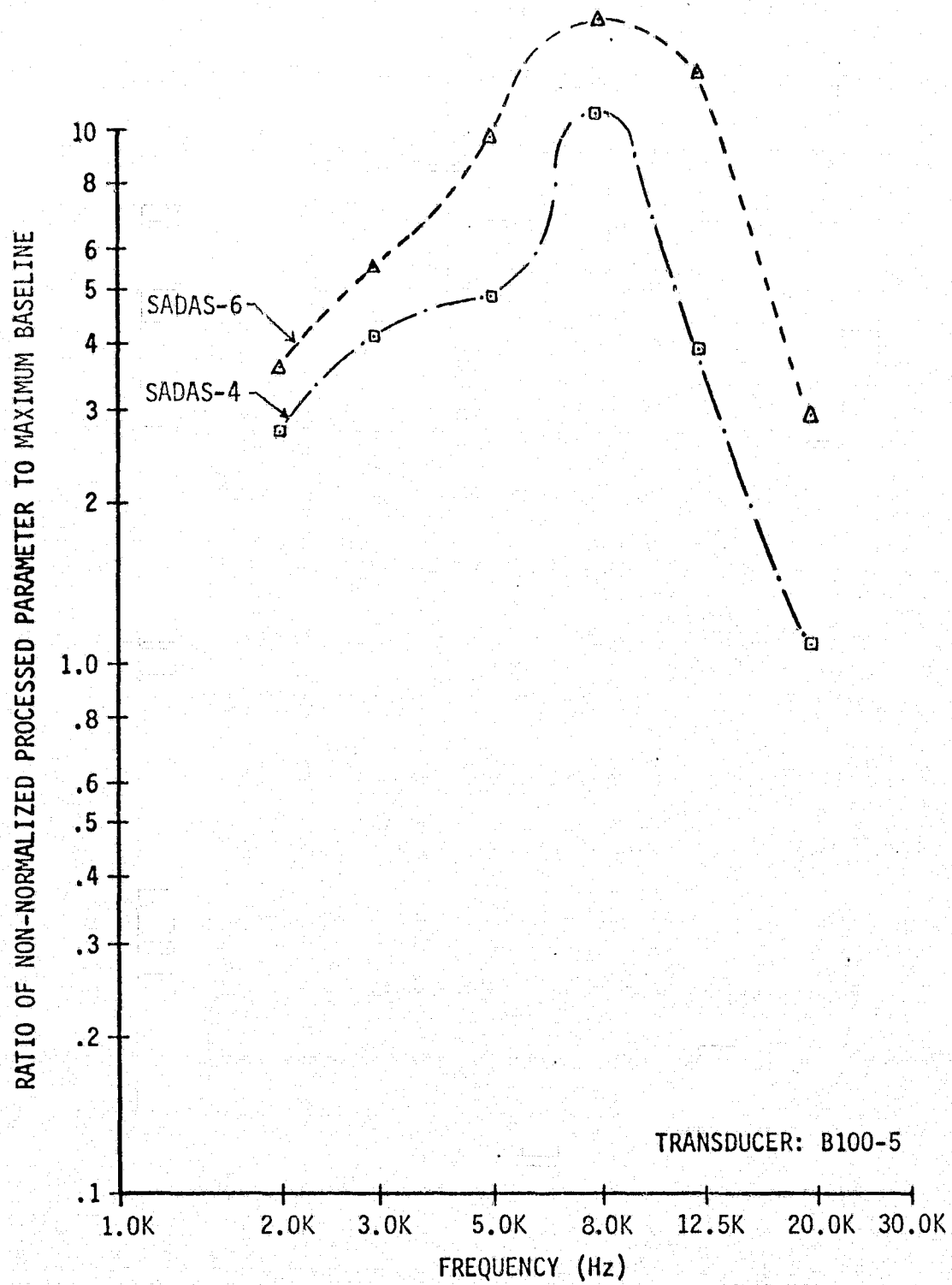

FIG. 78 NON-NORMALIZED PROCESSED PARAMETER CHANGES DUE TO BRINELLING FIRST REPLACEMENT BEARING BY LOADING IT TO 1000 POUNDS - COMPARISON WITH SECOND REPLACEMENT BEARING BASELINE - MICROPUMP 10-71-316-1367 PUMP

TEST ITEM	Micropump Model 10-71-316-1367 Centrifugal Pump
PLOT NO.	56
TRANSDUCER	B100-5

CONTROLLED TEST PARAMETERS	
VOLTAGE	115
P.S. FREQ.	400.0
FLOW RATE	7.5×10^{-5} (1.2)

VARIABLE TEST PARAMETERS	BASELINE	FAULT
DATE	6/18-6/19	6/23
I	.622	.630
$\phi \angle$	.384	.384
PWR	66.3	67.2
RPM	10240-10260	10240
P_S	6900	6900
P_D	165000	165000
ΔP	158000	158000
TEMP	297	297
BARO	101300-101400	101600

PROCESSING CHANNEL PARAMETERS	
INPUT RESISTANCE	—
AMPLIFIER GAINS (DB)	
A_1	20
A_2	—
A_3	—
FILTER FREQUENCIES (KHZ)	
BAND PASS	—
HIGH PASS	—
LOW PASS	1

SPECTRUM ANALYZER PARAMETERS	BASELINE	FAULT
INPUT V (MV)	12.4-19	15.2-16.5
GAIN SETTINGS (0 DB REF)		
ANALYZER GAIN	10	
INPUT ATTEN.	11	
INTEGRATION		
LINEAR 32E/BIN COSINE WEIGHT	D.C. COUPLE INTERNAL SAMPLE	

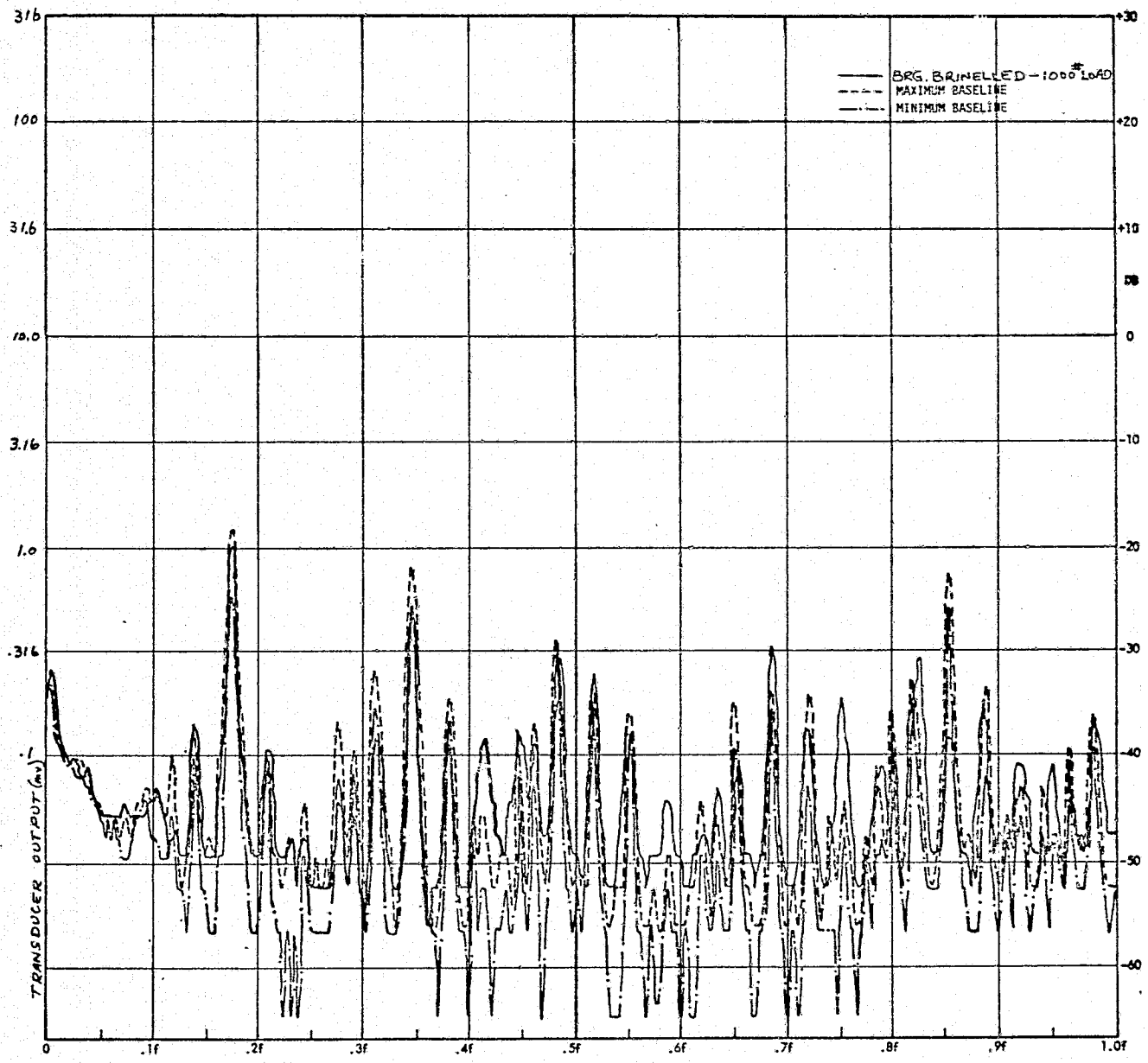

FIG. 79 FREQUENCY SPECTRUM FOR MICROPUMP 10-71-316-1367 PUMP

TEST ITEM	Micropump Model 10-71-316-1367 Centrifugal Pump
PLOT NO.	64
TRANSDUCER	6100-5

CONTROLLED TEST PARAMETERS	
VOLTAGE	115
P.S. FREQ.	400.0
FLOW RATE	7.5×10^{-5} (1.2)

VARIABLE TEST PARAMETERS	BASELINE	FAULT
DATE	6/18-6/19	6/23
I	.622	.630
$\phi\angle$	.384	.384
PWR	66.3	67.2
RPM	10240-10260	10240
P_S	6930	6900
P_D	165000	165000
ΔP	158000	158000
TEMP	297	297
BARO	101300-101400	101600

PROCESSING CHANNEL PARAMETERS	
INPUT RESISTANCE	—
AMPLIFIER GAINS (DB)	
A_1	40
A_2	20
A_3	—
FILTER FREQUENCIES (KHZ)	
BAND PASS	8
HIGH PASS	1
LOW PASS	1

SPECTRUM ANALYZER PARAMETERS	BASELINE	FAULT
INPUT V (MV)	5.7-9	43-60

GAIN SETTINGS (0 DB REF)

ANALYZER GAIN 10

INPUT ATTEN. 0

INTEGRATION

LINEAR 32Σ/BIN COSINE WEIGHT

D.C. COUPLE INTERNAL SAMPLE

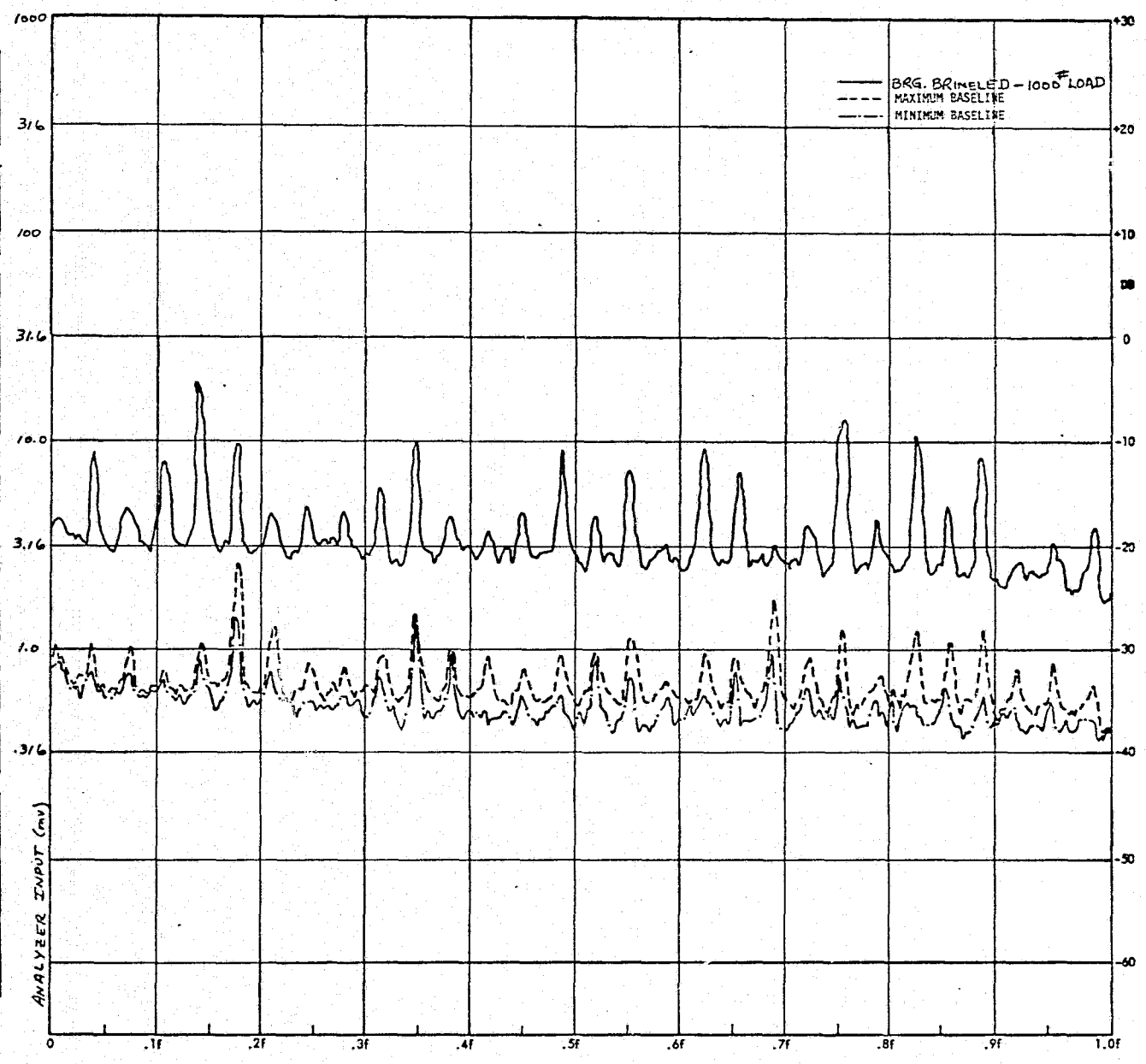

FIG. 80 FREQUENCY SPECTRUM FOR MICROPUMP 10-71-316-1367 PUMP

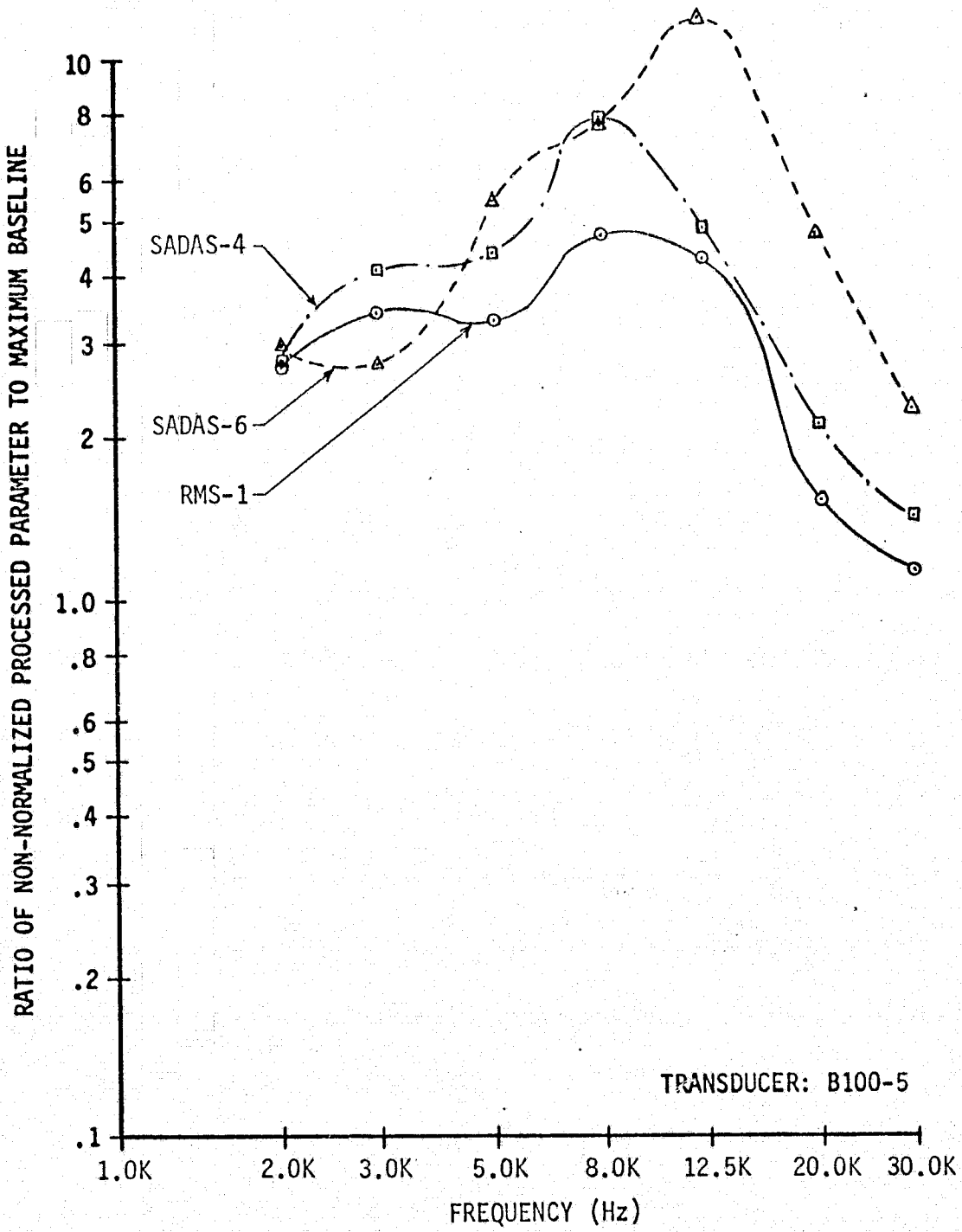

FIG. 81 NON-NORMALIZED PROCESSED PARAMETER CHANGES DUE TO BRINELLING SECOND REPLACEMENT BEARING BY LOADING IT TO 1000 POUNDS - MICROPUMP 10-71-316-1367 PUMP

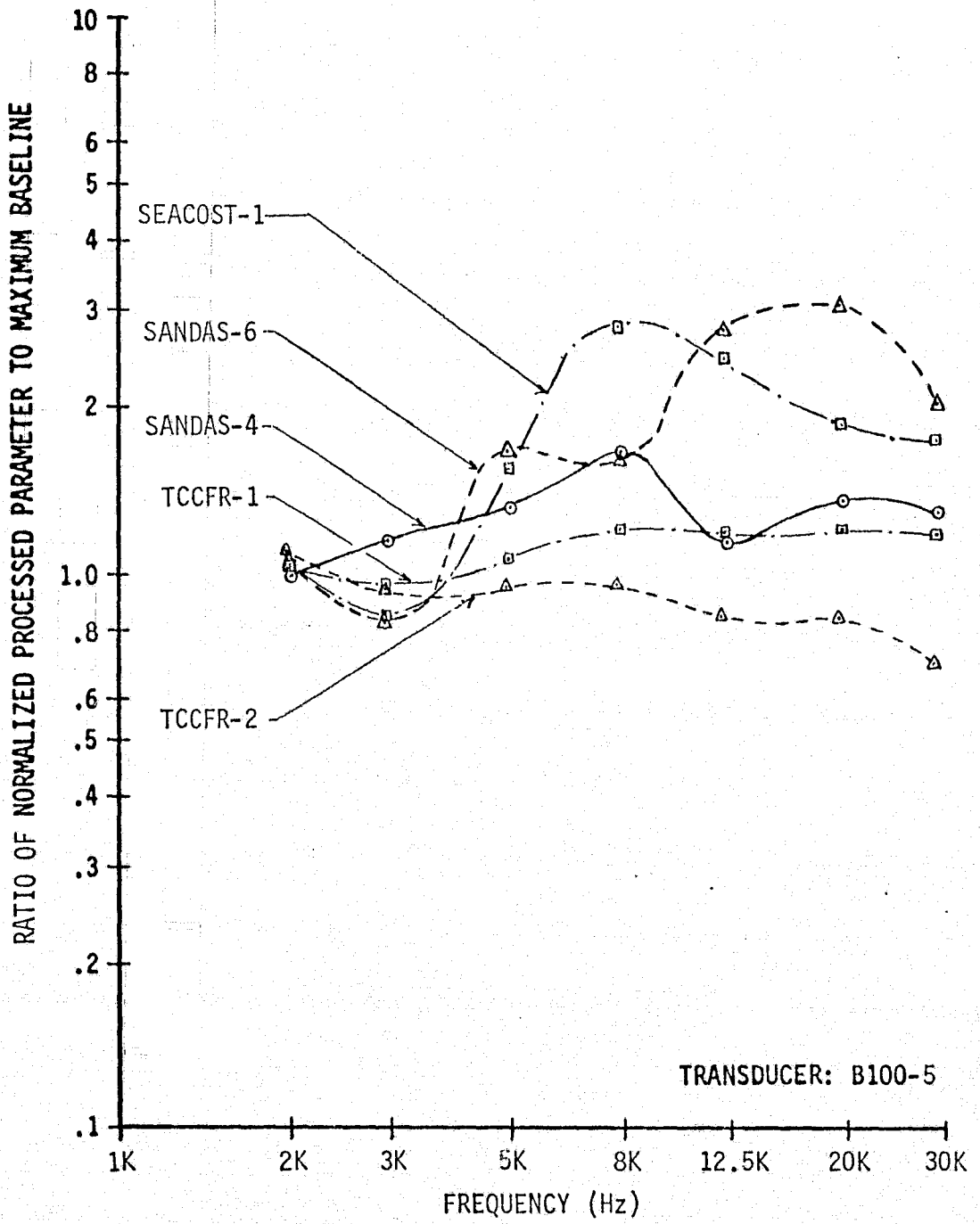

FIG. 82 NORMALIZED PROCESSED PARAMETER CHANGES DUE TO BRINELLING SECOND REPLACEMENT BEARING BY LOADING IT TO 1000 POUNDS - MICROPUMP 10-71-316-1367 PUMP

between data collected at the beginning and the end of the test period. However, since it was decided to introduce a dry bearing in the Hydrokinetic pump, fault conditions were expected to change considerably during the several hour period needed to process the fault data. Because of this, it was decided to run the Hydrokinetics pump for only a few minutes, during which it was hoped the fault conditions would remain relatively stable, and tape record the transducers' signals. The tape recorded data could then be replayed for each of the processing equipment configurations. A block diagram of the tape recording setup is shown in Figure 83. The tape recorder record/reproduce gains were adjusted to unity for all channels. This provided unity gain for all data except for the Direct 2 (D-2) channel which had a gain of 20 db. During some tests this channel was switched to have a high pass filter of 150 KHz and a gain of 40 db to improve the signal-to-noise ratio for the higher frequencies. Before the fault was introduced into the pump, twelve pairs of broadband spectrum data plots were made from both real-time data and recorded data. Comparison of the spectrum plots was always within $\pm$ 1 db and usually within $\pm$ 0.25 db.

For the initial fault test run on 8-5-75, which was made with the water lubricated bearing, data was taken after approximately 1.5 minutes of pump operation stabilization. The equipment was set up as in Figure 83 with switch S1 in the 22KΩ position. After 1.5 minutes of recording, switch S1 was placed in the open position and data recorded for an additional 1.5 minutes. After this, switch S1 was placed in the 22KΩ position, the high pass filter was changed from 85 KHz to 150 KHz, and the gain of amplifier A2 switched to 40 db. Data under these conditions was also taken for 1.5 minutes, and then the pump turned off so that the total pump run time was 6 minutes. On 8-11-75 the pump was run for six runs for a total of 72 minutes, with the longest continuous run lasting for 30 minutes. During this time, data was tape recorded for each of the runs at random times and for random intervals, for a total data record of 7.7 minutes. For most of this data recording the equipment configuration was like that shown in Figure 83. During the second test run for this day, with the bearing still in a corroded condition, switch S1 was placed in the open position, which was the configuration for which most baseline baseband spectrum data and 8 KHz and 12.5 KHz bandpass data was taken. Thus, corroded bearing fault data was available for baseband spectrum, and 8 KHz and 12.5 KHz bandpass data analysis. For the last run, with the bearing experiencing internal clearance problems, switch S1 was in the 22KΩ position. Thus, fault data for baseband spectrum, and 8 KHz and 12.5 KHz bandpass data analysis was not recorded.

The initial concept of having a dry bearing as the faulted condition was expected to cause an increase in bearing friction which would cause an increase in the overall RMS signal level. If the bearing's rolling surfaces remained defect-free during the duration of the test, it was expected that the SADAS plots would not show any significant spectral lines at the ball passing frequencies, and that these plots would tend to be flatter since the increased bearing friction signal would represent a larger portion of the total acoustic signal from the pump. Similarly it was expected that the amplitude distribution parameters, count and 3 σ spike data, would probably decrease since the Gaussion distributed bearing friction signal would represent a larger portion of the total acoustic signal from the pump. With water lubrication in the bearing it was not known if the bearing would behave similar to a dry bearing or to a grease lubricated bearing.

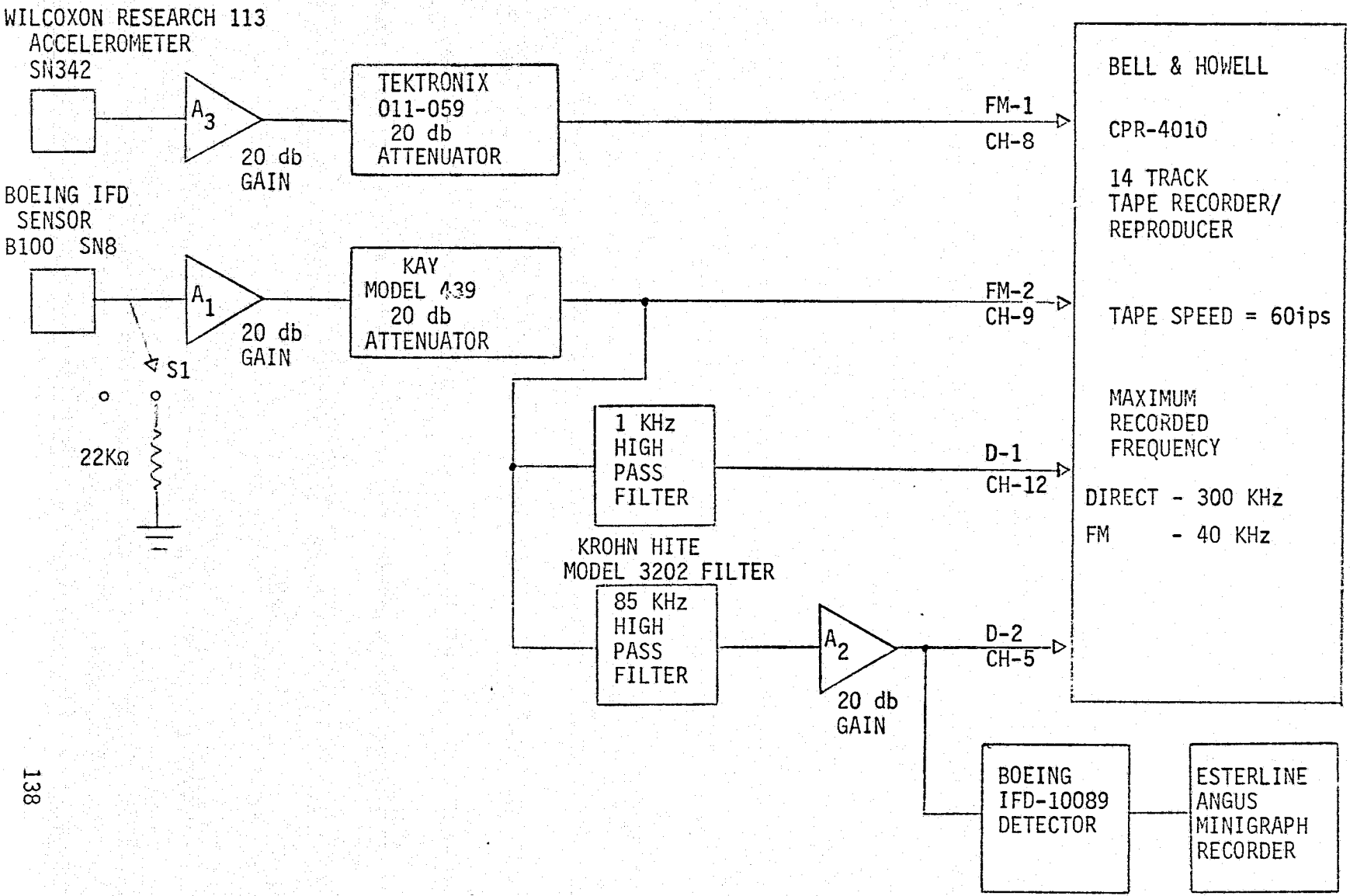

FIGURE 83 - TEST SETUP FOR TAPE RECORDING HYDROKINETICS 10461 PUMP FAULT DATA

A typical SADAS plot for the water lubricated bearing is shown in Figure 84. Figures 85 and 86 show the high frequency processed parameters. As can be seen in these figures, the water lubricated bearing defect could not be detected with any significant degree of certainty by any high frequency processed parameter. Probably the most significant reason for the high frequency parameters not being able to detect this fault was due to the very large spikey background signal generated by the turbulent flow of water in the pump. A rough measure of the effects of this background signal can be determined by comparing the baseline results with those obtained from the Dynamic Air Engineering centrifugal fan. This fan operated at close to the same speed as the Hydrokinetics pump and used similar bearings. Thus rough differences between signals from the two items would be due to differences in air and water effects. From 8 KHz to 80 KHz the Hydrokinetics pump RMS signal ranged from 1.65 to 20.7 times the RMS signal from the Dynamic Air Engineering fan. The RMS signal from both items became roughly the same for frequencies from 125 KHz to 500 KHz but the 3 σ spike level was a minimum of 5.1 times greater for the Hydrokinetics pump over this frequency range. Also at 30 KHz, where the RMS level from the Hydrokinetics pump was only 1.65 times that for the Dynamic Air Engineering fan, the 3 σ spike level was 2.8 times greater. Thus, it is probable that the signal from the water lubricated bearing would have had to be significantly greater than that from the grease lubricated bearing in order to generate an appreciable increase in the high frequency processed parameters.

The results of the low frequency data evaluation are shown in Table XXIV. The only low frequency vibration parameter which showed a significant increase due to the water lubricated bearing fault was SABVS-5 which represents the change in the outer race ball passing frequency spectral line, (1010-1015 Hz). This is evident in the baseband vibration spectrum shown in Figure 87. The SABVS-5 parameter increased to more than twice its worst case baseline value and was the only measured parameter which showed a significant increase. Evidently the water lubrication of the bearing resulted in increased vibration at the outer race ball passing frequency, a phenomena which was not experienced in any of the other four test items.

Figure 88 is a plot of the outer race ball passing frequency spectral line amplitude versus time. The plot was made by processing the output of the FM-1 channel from the tape recorder through the SAICOR SAI-52B Spectrum Analyzer which was used like a wave analyzer. The time axis represents pump running time starting from the time the first fault was introduced. The first segment from 50 to 350 seconds is for the initial bearing fault of water lubrication.

Corrosion in the faulted bearing was expected to generate multiple trains of acoustic pulses with repetitive frequencies equal to the outer race ball passing frequency of 1010 - 1015 Hz, the ball frequency of 1343 - 1350 Hz, and the inner race ball passing frequency of 1705 - 1713 Hz. This was evident in the SADAS plots for bandpass frequencies of 20 KHz and greater. A sample plot is shown in Figure 89 for a 300 KHz bandpass frequency. Figures 90 and 91 show the high frequency processed parameters for the corroded bearing defect. The increase in the spectral line amplitudes were not as significant as the overall increase in RMS level, however, as

TEST ITEM	HYDROKINETIC 10461 PUMP
PLOT NO.	47
TRANSDUCER	8100-8

CONTROLLED TEST PARAMETERS	
VOLTAGE	115
P.S. FREQ.	400.0
FLOW RATE	7.5×10^{-5} (1.2)

VARIABLE TEST PARAMETERS	BASELINE	FAULT
DATE	7/19-7/22	8/5
I	3.2-3.5	3.3
ϕ<	.035	.035
PWR	368-402	379
RPM	23270-23340	23290
P_S	6900	6900
P_D	652000 - 655000	652000
ΔP	645000 - 648000	645000
TEMP	296-298	296
BARO	101500 - 101700	101700

PROCESSING CHANNEL PARAMETERS	
INPUT RESISTANCE	22KΩ
AMPLIFIER GAINS (DB)	
A_1	20
A_2	20
A_3	20
FILTER FREQUENCIES (KHZ)	
BAND PASS	300
HIGH PASS	200
LOW PASS	2

SPECTRUM ANALYZER PARAMETERS	BASELINE	FAULT
INPUT V (MV)	35-44	26-33
GAIN SETTINGS (0 DB REF)		
ANALYZER GAIN	10	
INPUT ATTEN.	20	
INTEGRATION		
LINEAR 32ε/BIN COSINE WEIGHT	D.C. COUPLE INTERNAL SAMPLE	

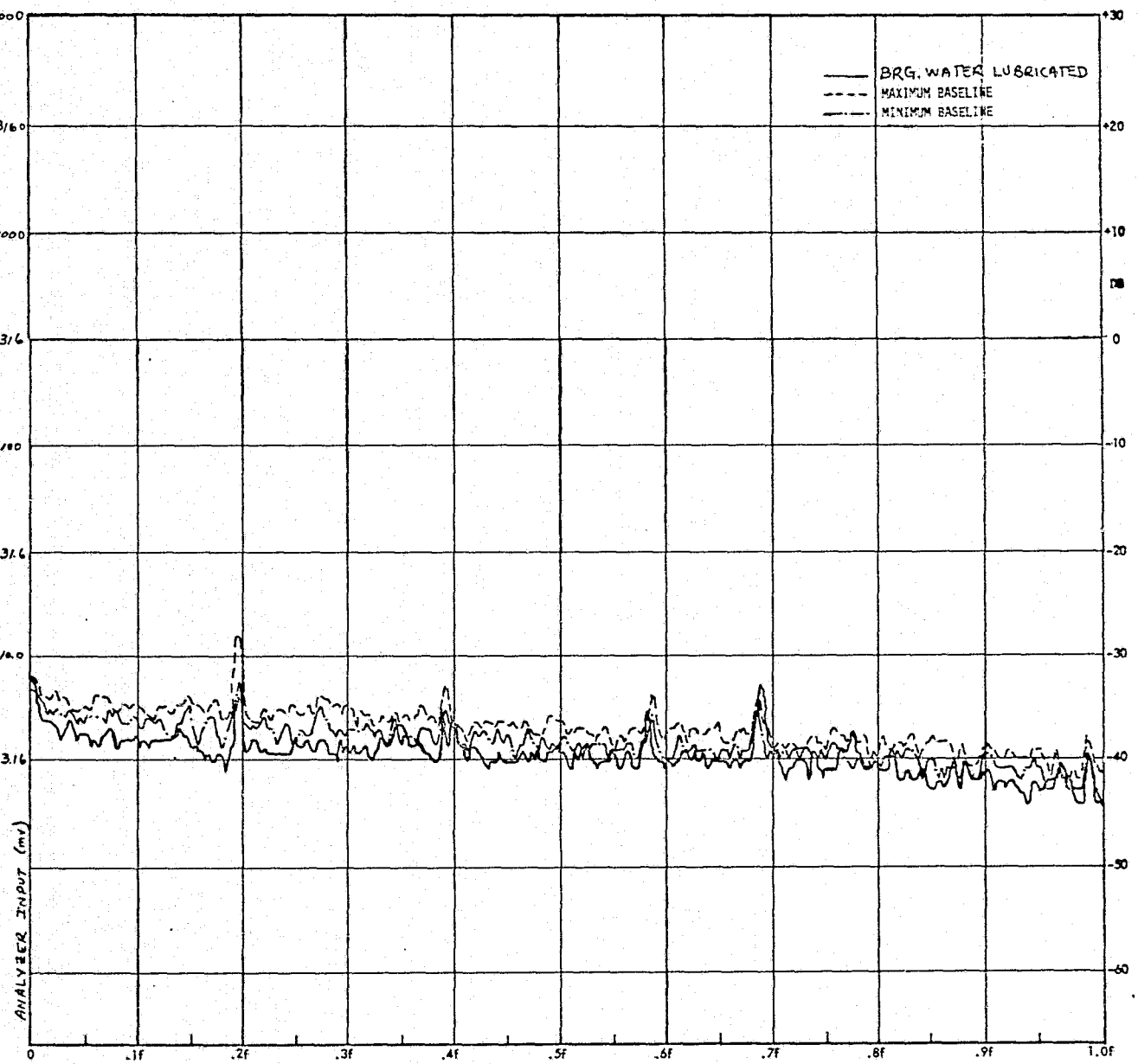

FIG. 84 FREQUENCY SPECTRUM FOR HYDROKINETICS 10461 PUMP

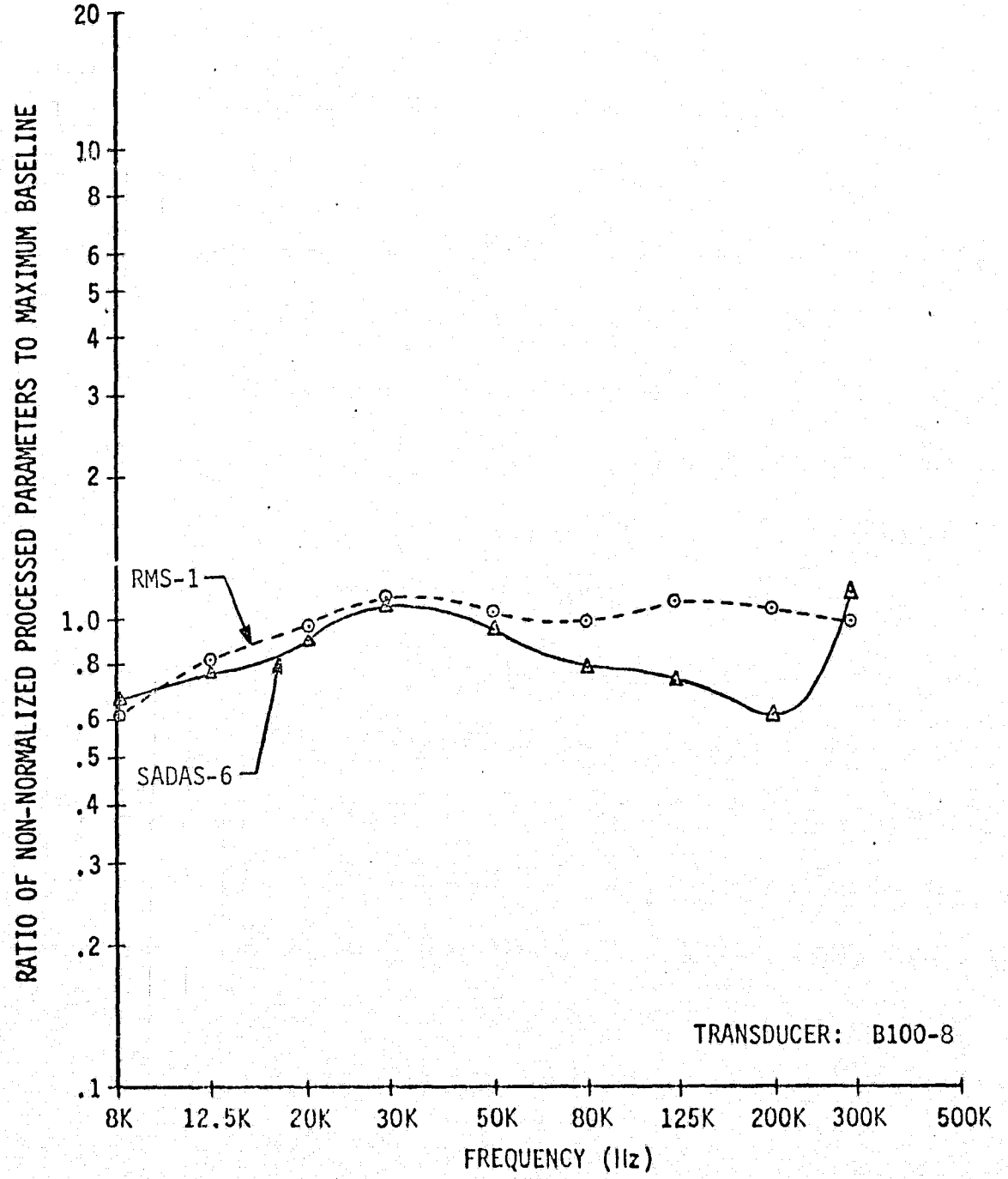

FIG. 85 NON-NORMALIZED PARAMETER CHANGES DUE TO WATER LUBRICATED BEARING - HYDROKINETICS 10461 PUMP

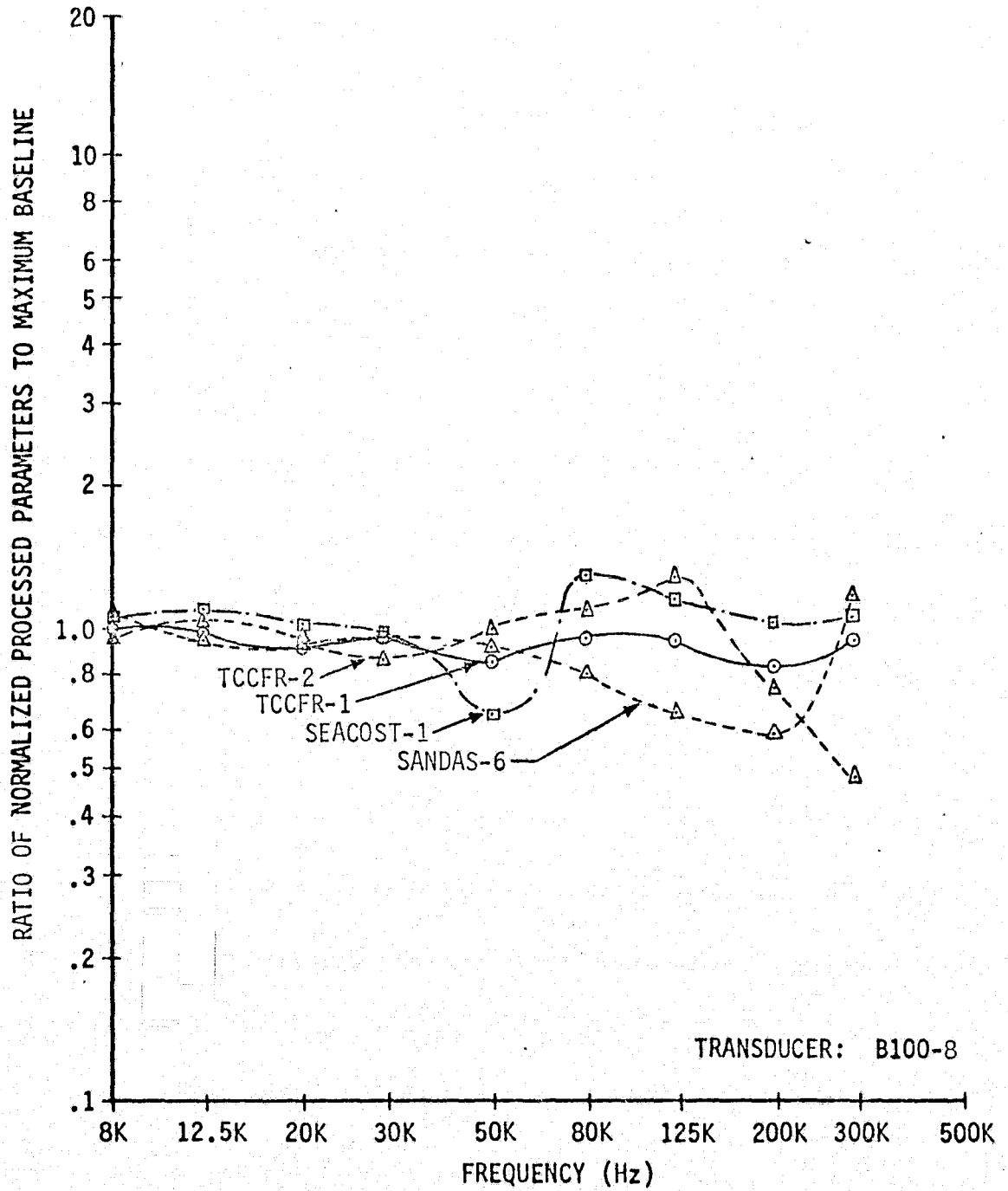

FIG. 86 NORMALIZED PROCESSED PARAMETER CHANGES DUE TO WATER LUBRICATED BEARING - HYDROKINETICS 10461 PUMP

TABLE XXIV. LOW FREQUENCY TEST RESULTS FOR THE HYDROKINETICS 10461 PUMP

TRANSDUCER: WR 113, S.N. 342

PROCESSED PARAMETER	38SSTX2K5G32 BALL BEARING CONDITION			
	WATER LUBRICATED	CORRODED		INTERNAL CLEARANCES REDUCED
		#1	#2	
SABVS-5	2.02	4.81	9.01	84.06
SABVS-6	.43	.56	1.06	9.96
BVRMS-1	.69	.56	.94	10.25

TEST ITEM	HYDROKINETIC 10461 PUMP
PLOT NO.	3
TRANSDUCER	342

CONTROLLED TEST PARAMETERS	
VOLTAGE	115
P.S. FREQ.	400.0
FLOW RATE	7.5×10^{-5} (1.2)

VARIABLE TEST PARAMETERS	BASELINE	FAULT
DATE	7/19-7/22	8/5
I	3.2-3.5	3.3
ϕ<	.035	.035
PWR	368-402	379
RPM	23270-23340	23290
P_S	6900	6900
P_D	652000 - 655000	652000
ΔP	645000 - 648000	645000
TEMP	296-298	296
BARO	101500 - 101700	101700

PROCESSING CHANNEL PARAMETERS	
INPUT RESISTANCE	—
AMPLIFIER GAINS (DB)	
A_1	20
A_2	—
A_3	—
FILTER FREQUENCIES (KHZ)	
BAND PASS	—
HIGH PASS	—
LOW PASS	2

SPECTRUM ANALYZER PARAMETERS	BASELINE	FAULT
INPUT V (MV)	400-800	420-550

GAIN SETTINGS (0 DB REF)	
ANALYZER GAIN	10
INPUT ATTEN.	34.1

INTEGRATION
LINEAR 32ε/BIN COSINE WEIGHT
D.C. COUPLE INTERNAL SAMPLE

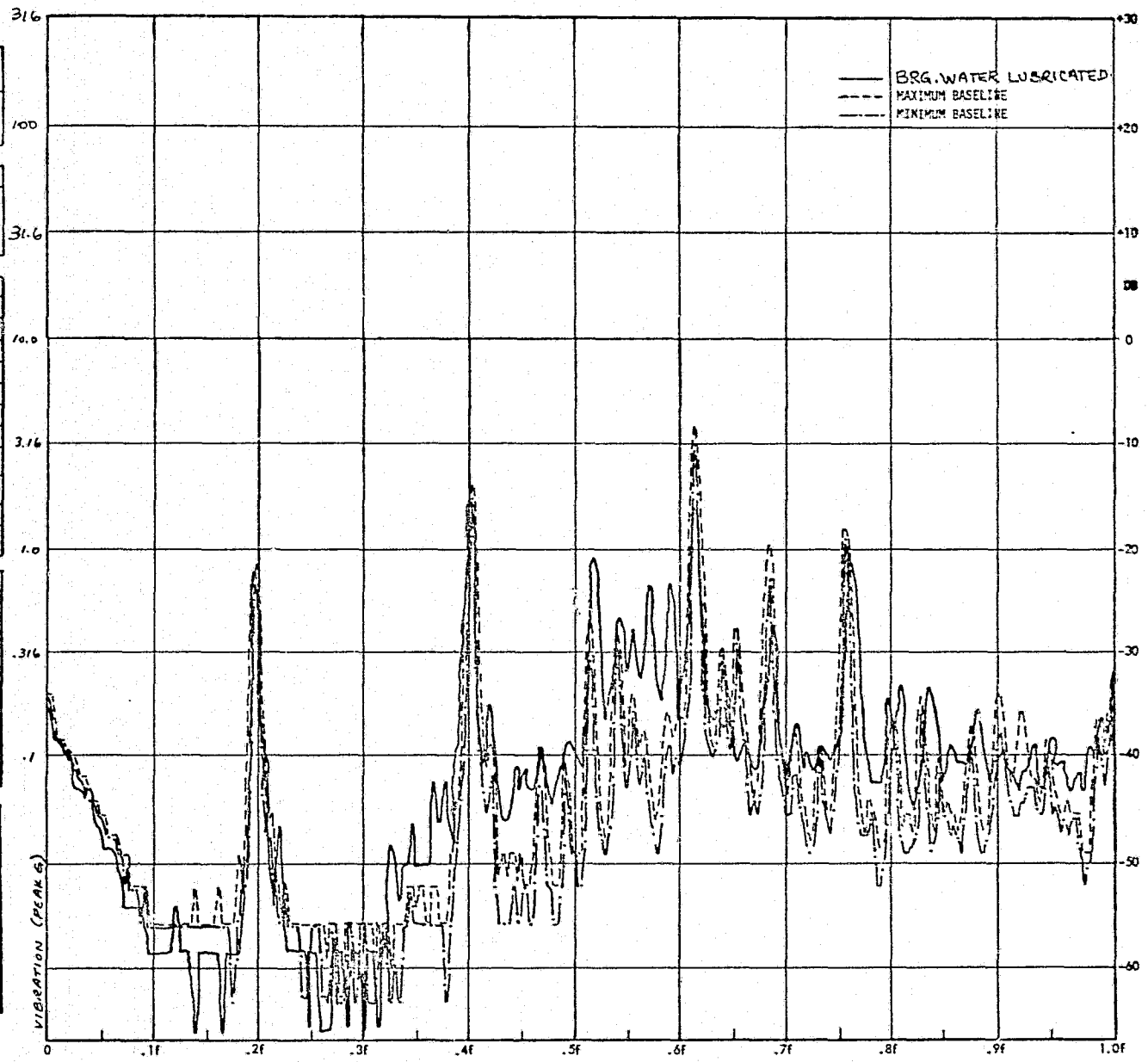

FIG. 87 FREQUENCY SPECTRUM FOR HYDROKINETICS 10461 PUMP

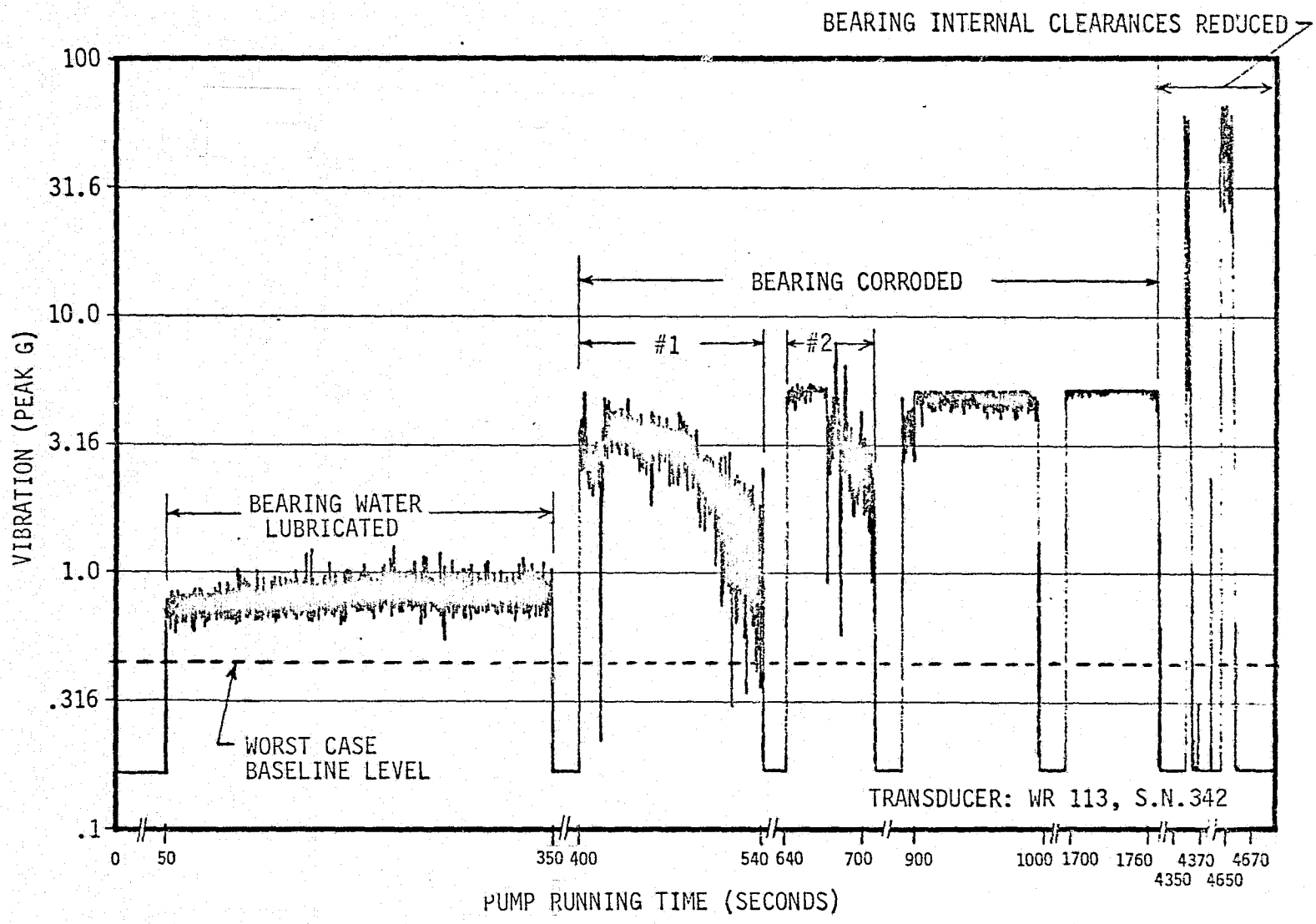

FIG. 88 OUTER RACE BALL PASSING FREQUENCY SPECTRAL LINE AMPLITUDE VS. PUMP RUNNING TIME FROM FAULT INITIATION

TEST ITEM	HYDROKINETIC 10461 PUMP
PLOT NO.	47
TRANSDUCER	B100-8

CONTROLLED TEST PARAMETERS	
VOLTAGE	115
P.S. FREQ.	400.0
FLOW RATE	7.5×10^{-5} (1.2)

VARIABLE TEST PARAMETERS	BASELINE	FAULT
DATE	7/19-7/22	8/11
I	3.2-3.5	3.4
$\phi <$	.035	.035
PWR	368-402	391
RPM	23270-23340	23390
P_S	6900	6900
P_D	652000 - 655000	652000
ΔP	645000 - 648000	645000
TEMP	296-298	297
BARO	101500 - 101700	101600

PROCESSING CHANNEL PARAMETERS	
INPUT RESISTANCE	22Kn
AMPLIFIER GAINS (DB)	
A_1	20
A_2	20
A_3	20
FILTER FREQUENCIES (KHZ)	
BAND PASS	300
HIGH PASS	200
LOW PASS	2

SPECTRUM ANALYZER PARAMETERS	BASELINE	FAULT
INPUT V (MV)	35-44	50-90
GAIN SETTINGS (0 DB REF)		
ANALYZER GAIN	10	
INPUT ATTEN.	20	
INTEGRATION		
LINEAR	D.C. COUPLE	
32E/BIN	INTERNAL SAMPLE	
COSINE WEIGHT		

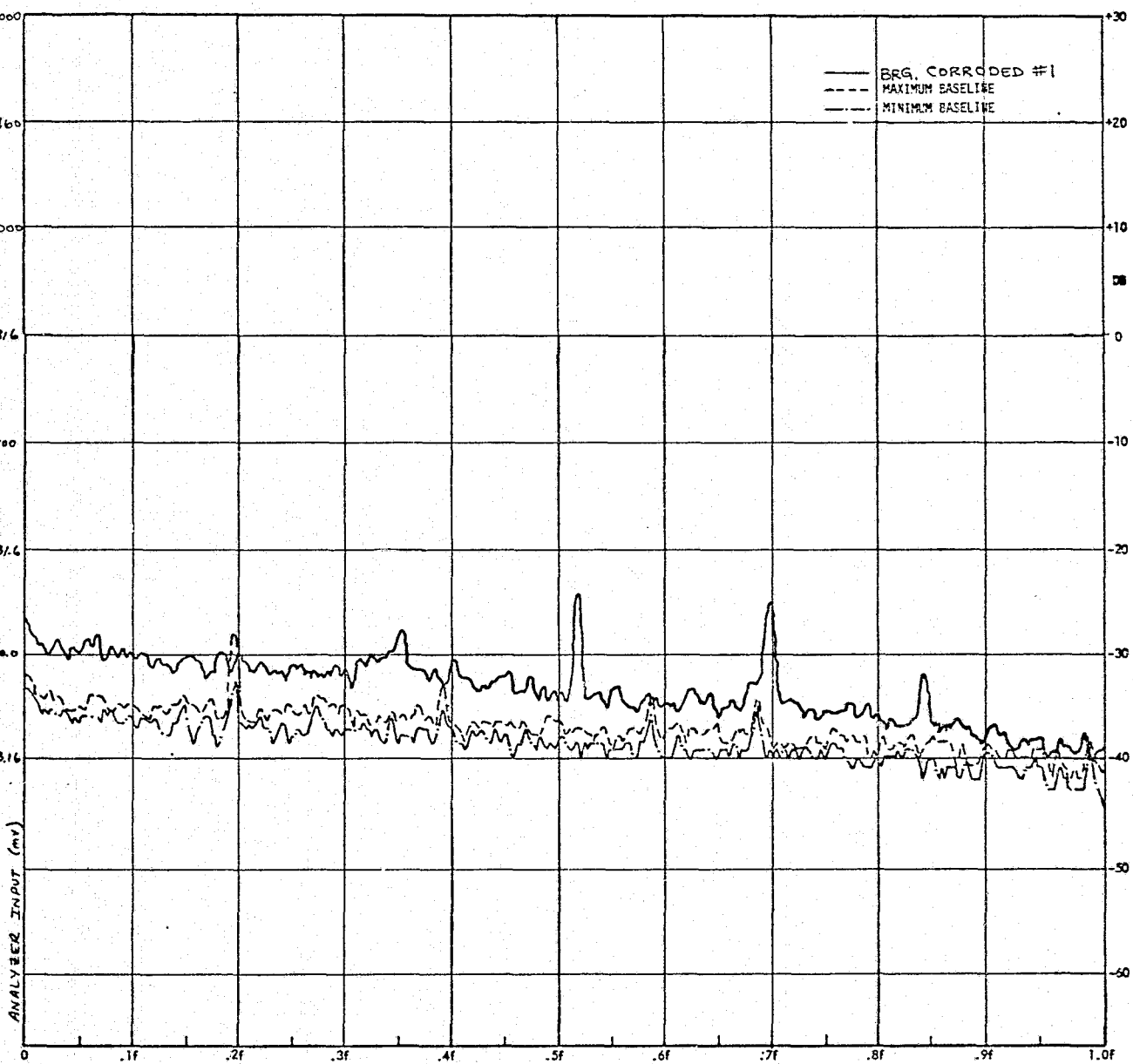

FIG. 89 FREQUENCY SPECTRUM FOR HYDROKINETICS 10461 PUMP

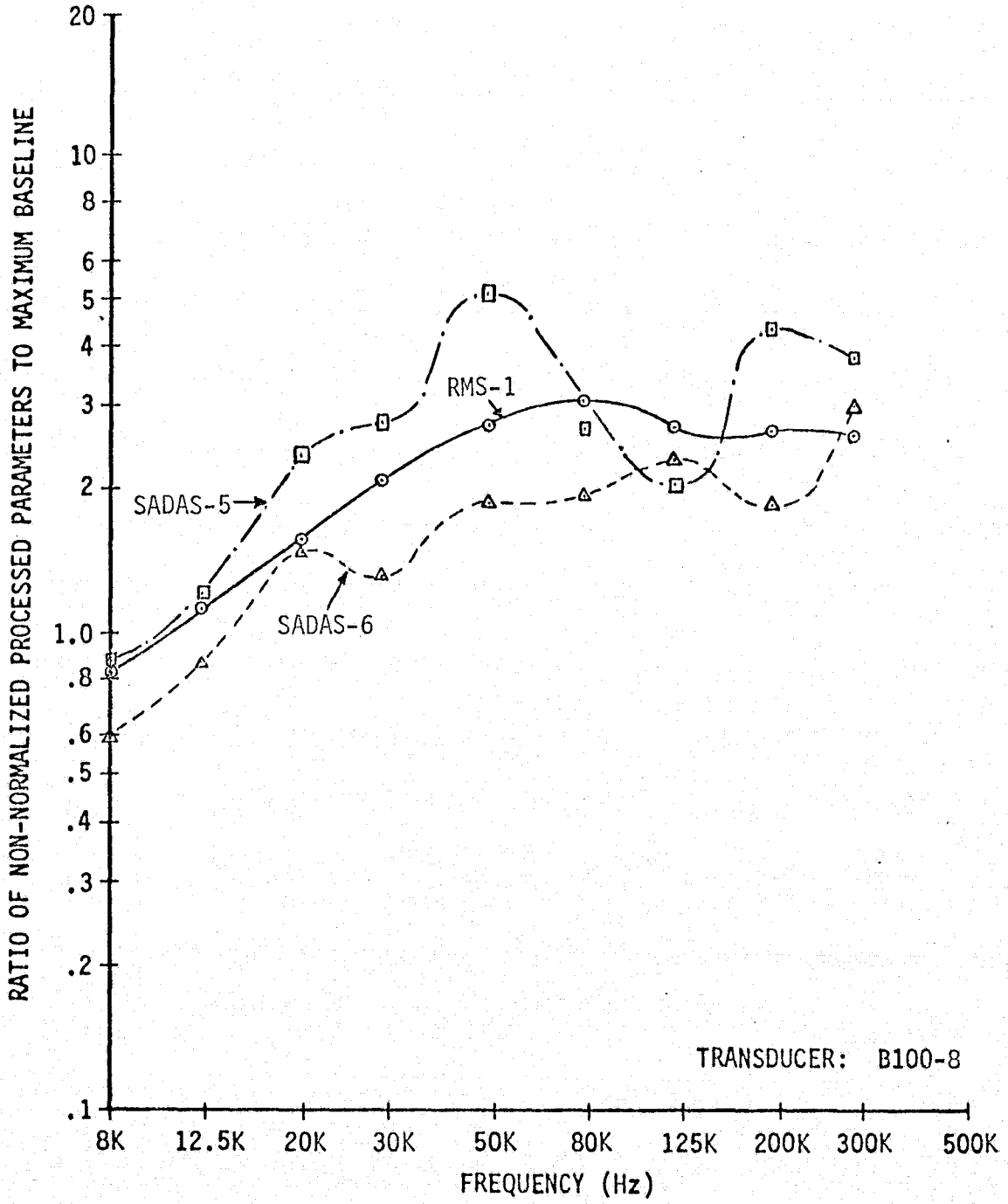

FIG. 90 NON-NORMALIZED PARAMETER CHANGES DUE TO CORRODED BEARING - HYDROKINETICS 10461 PUMP

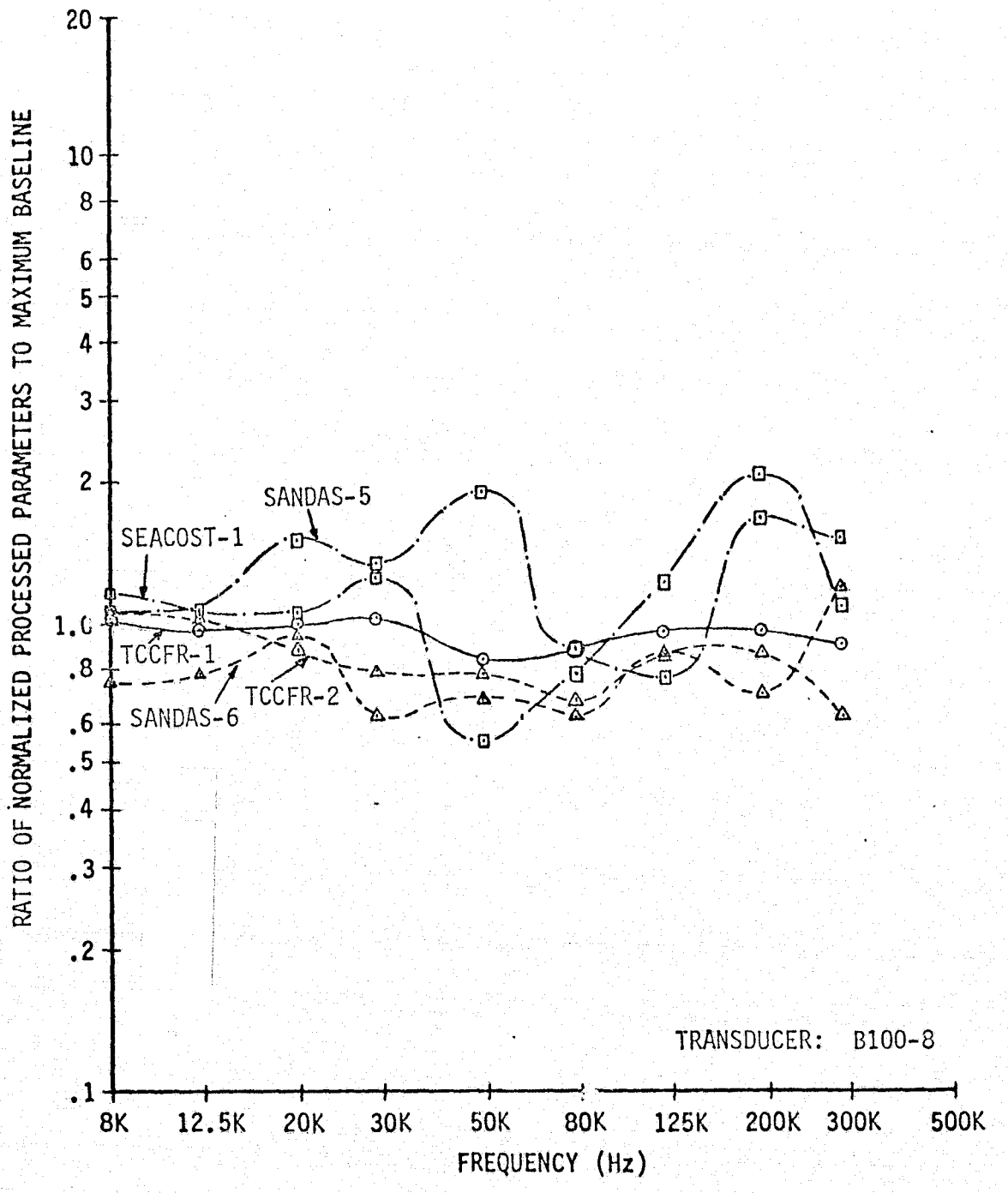

FIG. 91 NORMALIZED PROCESSED PARAMETER CHANGES DUE TO CORRODED BEARING - HYDROKINETICS 10461 PUMP

noted by the low values for the normalized spectrum analysis parameters, SANDAS-5 and SANDAS-6. The maximum value for these parameters occurred at 50 KHz and was equal to 1.89. In comparison, the high frequency RMS level increased greater than 2.59 for all frequencies from 50 KHz to 300 KHz. The most successful high frequency parameter at detecting this defect was SADAS-5 which had a value of 5.16 at 50 KHz.

Corroded bearing data was processed for two different time intervals with respect to the pump running time. The first interval was for a pump running time between 400 and 540 seconds. During this time, identified in the data as Bearing Corroded #1, the 22KΩ resistor was switched in, and 20 KHz to 300 KHz data processed. The second interval was for a pump running time between 640 and 710 seconds, identified in the data as Bearing Corroded #2. During this time, the 22KΩ resistor was switched out, and broadband spectrum and 8 to 12.5 KHz data processed.

The results of the low frequency data evaluation are shown in Table XXIV and Figure 88. Again the only low frequency vibration parameter which showed a significant increase due to the corroded bearing fault was SABVS-5 which increased by a factor of 4.81 for the initial interval, as evident by the baseband vibration spectrum shown in Figure 92, and 9.01 for the second interval. The equivalent high frequency parameter of SABVS-5 is SADAS-5, which at 50 KHz showed a similar increase.

When the bearing experienced reduced internal clearances, it was expected that the increased bearing friction would result in an increase in the overall high frequency RMS level. This turned out to be the case, with the RMS signal level having a maximum increase of 5.96 at 200 KHz. Figures 93 and 94 show the high frequency processed parameters for the bearing's reduced internal clearances. The best overall high frequency results were at 300 KHz, as shown by the SADAS plot in Figure 95, for the spectral analysis parameters and are as follows:

SADAS-5	25.94
SADAS-6	20.11
SANDAS-5	4.62
SANDAS-6	3.59

The normalized non-spectrum parameters associated with the amplitude distribution of the signal, namely TCCFR-1 and TCCFR-2, were very poor in detecting this defect as they were in detecting the previous two defects. SEACOST-1 data could not be processed for this defect because of the limited data sample, but it is mathematically tied to the TCCFR parameters and probably would not have shown any significant increase. This was also the case for the two previous defects. The most likely cause for the failure of these parameters to detect the defect is due to the high spike level generated by the turbulent flow of water in the pump which increases the baseline condition and makes it difficult to detect acoustic spikes generated by the defective bearing. The most successful parameter at detecting this defect, however, was the low frequency vibration parameter SABVS-5, as might have been expected by the high pitched sound which was generated when this trouble occurred. As shown in Table XXIV, Figure 88 and Figure 96, this parameter had a value of 84.06 which was more than triple the maximum increase in any

TEST ITEM	HYDROKINETIC 10461 PUMP
PLOT NO.	3
TRANSDUCER	342

CONTROLLED TEST PARAMETERS	
VOLTAGE	115
P.S. FREQ.	400.0
FLOW RATE	7.5×10^{-5} (1.2)

VARIABLE TEST PARAMETERS	BASELINE	FAULT
DATE	7/19-7/22	8/11
I	3.2-3.5	3.4
ϕ<	.035	.035
PWR	368-402	391
RPM	23270-23340	23390
P_S	6900	6900
P_D	652000 - 655000	652000
ΔP	645000 - 648000	645000
TEMP	296-298	297
BARO	101500 - 101700	101600

PROCESSING CHANNEL PARAMETERS	
INPUT RESISTANCE	—
AMPLIFIER GAINS (DB)	
A_1	20
A_2	—
A_3	—
FILTER FREQUENCIES (KHZ)	
BAND PASS	—
HIGH PASS	—
LOW PASS	2

SPECTRUM ANALYZER PARAMETERS	BASELINE	FAULT
INPUT V (MV)	400-800	380-450
GAIN SETTINGS (0 DB REF)		
ANALYZER GAIN	10	
INPUT ATTEN.	34.1	
INTEGRATION		
LINEAR	D.C. COUPLE	
32t/BIN	INTERNAL SAMPLE	
COSINE WEIGHT		

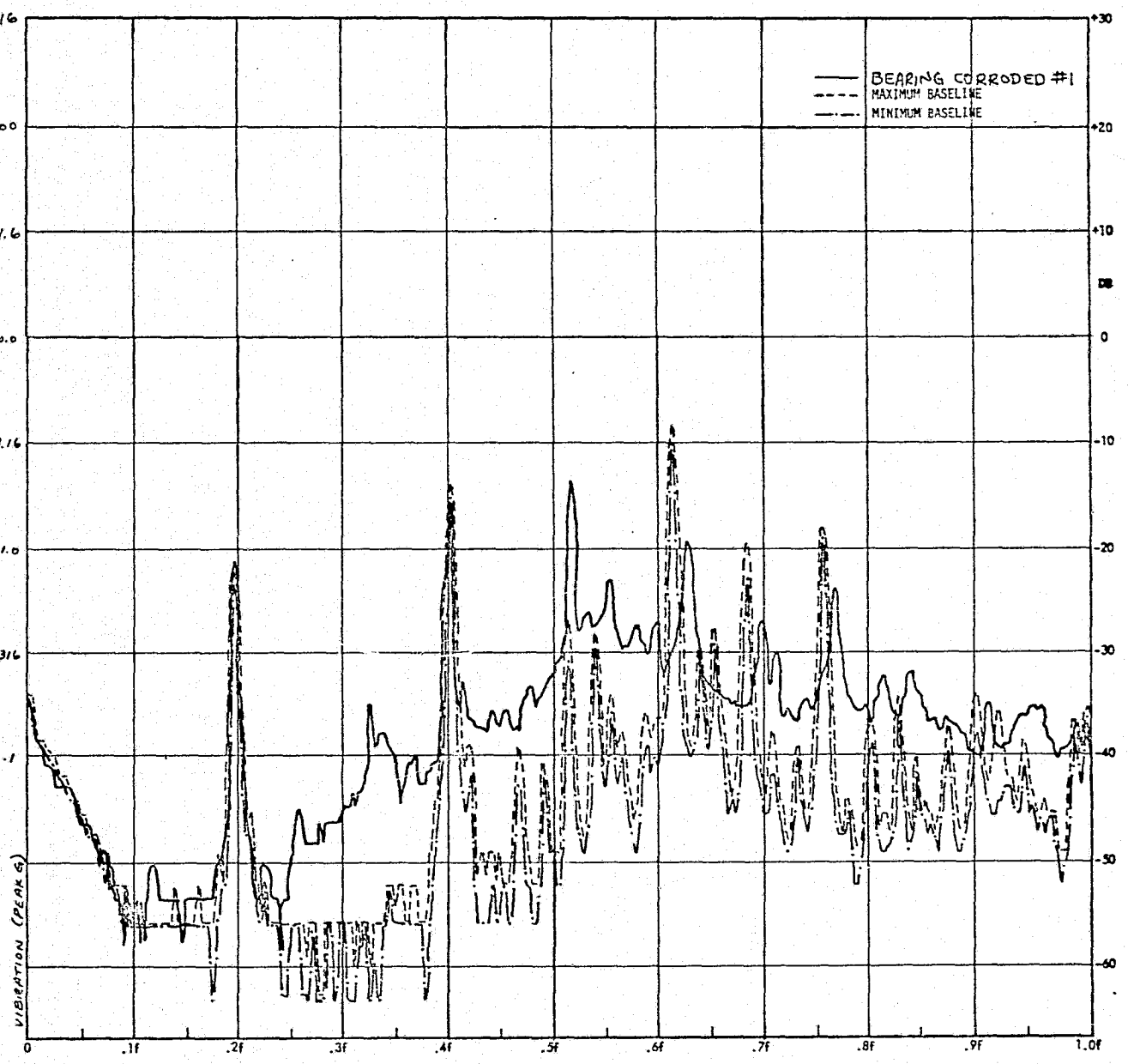

FIG. 92 FREQUENCY SPECTRUM FOR HYDROKINETICS 10461 PUMP

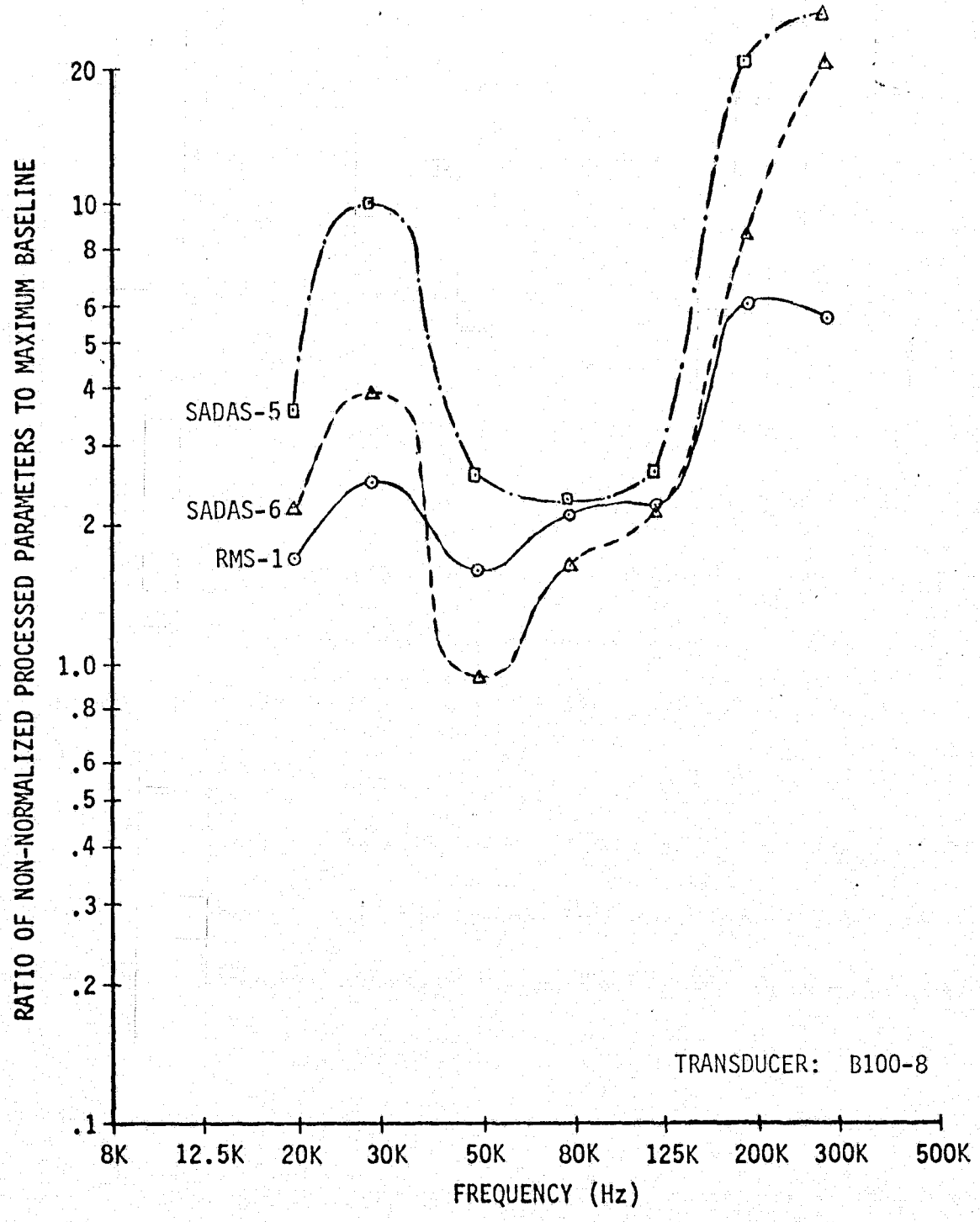

FIG. 93 NON-NORMALIZED PARAMETER CHANGES DUE TO BEARING INTERNAL CLEARANCES REDUCED - HYDROKINETICS 10461 PUMP

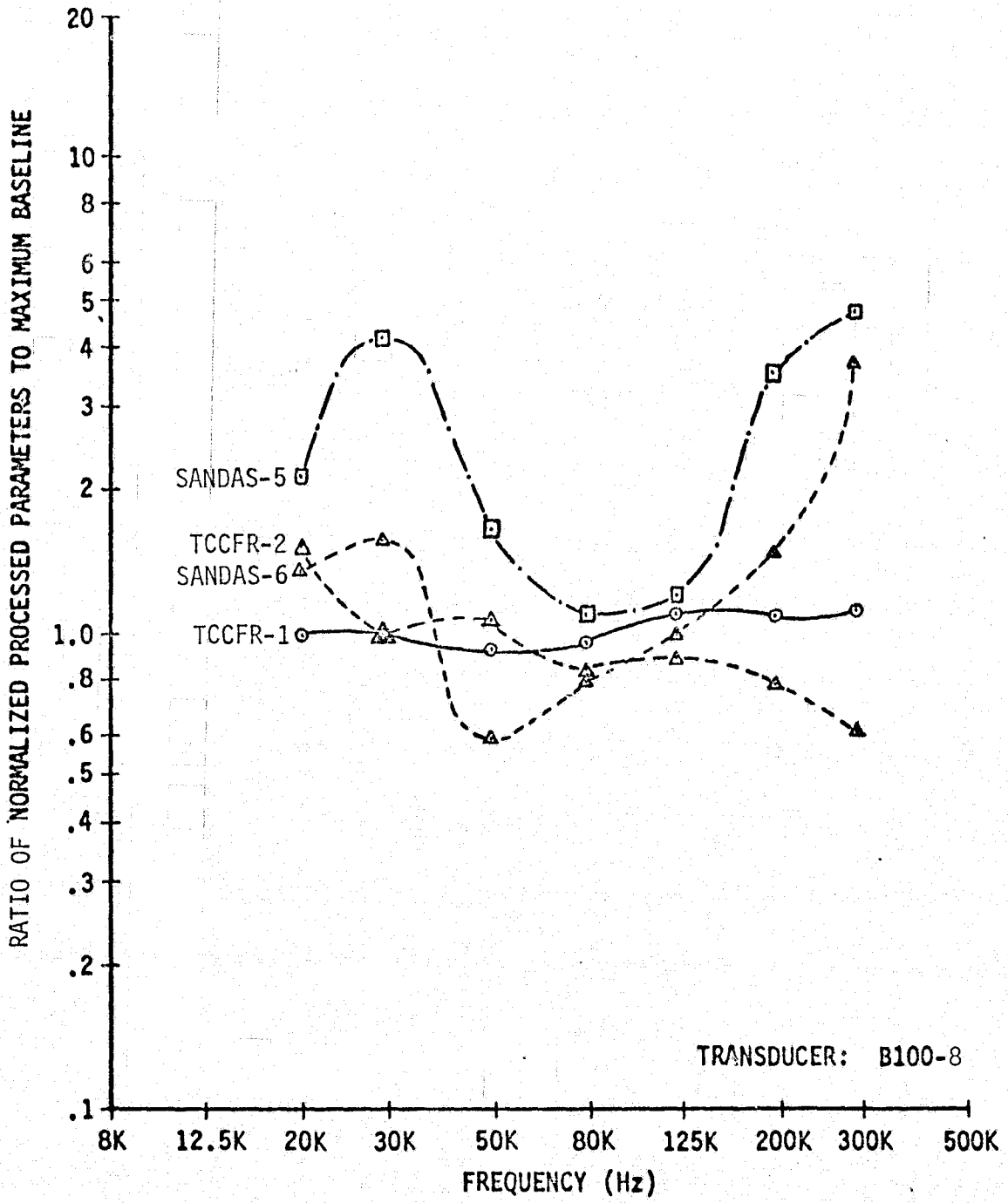

FIG. 94 NORMALIZED PROCESSED PARAMETER CHANGES DUE TO BEARING INTERNAL CLEARANCES REDUCED - HYDROKINETICS 10461 PUMP

TEST ITEM	HYDROKINETIC 10461 PUMP
PLOT NO.	47
TRANSDUCER	8100-8

CONTROLLED TEST PARAMETERS	
VOLTAGE	115
P.S. FREQ.	400.0
FLOW RATE	7.5×10^{-5} (1.2)

VARIABLE TEST PARAMETERS	BASELINE	FAULT
DATE	7/19-7/22	8/11
I	3.2-3.5	—
ϕ<	.035	—
PWR	368-402	—
RPM	23270-23340	22620
P_S	6900	6900
P_D	652000 - 655000	61400
ΔP	645000 - 648000	607000
TEMP	295-298	297
BARO	101870 - 101700	101600

PROCESSING CHANNEL PARAMETERS	
INPUT RESISTANCE	22KΩ
AMPLIFIER GAINS (DB)	
A_1	20
A_2	20
A_3	20
FILTER FREQUENCIES (KHZ)	
BAND PASS	300
HIGH PASS	200
LOW PASS	2

SPECTRUM ANALYZER PARAMETERS	BASELINE	FAULT
INPUT V (MV)	35-44	300-450
GAIN SETTINGS (0 DB REF)		
ANALYZER GAIN	10	
INPUT ATTEN.	20	
INTEGRATION		
LINEAR	D.C. COUPLE	
32ℓ/BIN	INTERNAL SAMPLE	
COSINE WEIGHT		

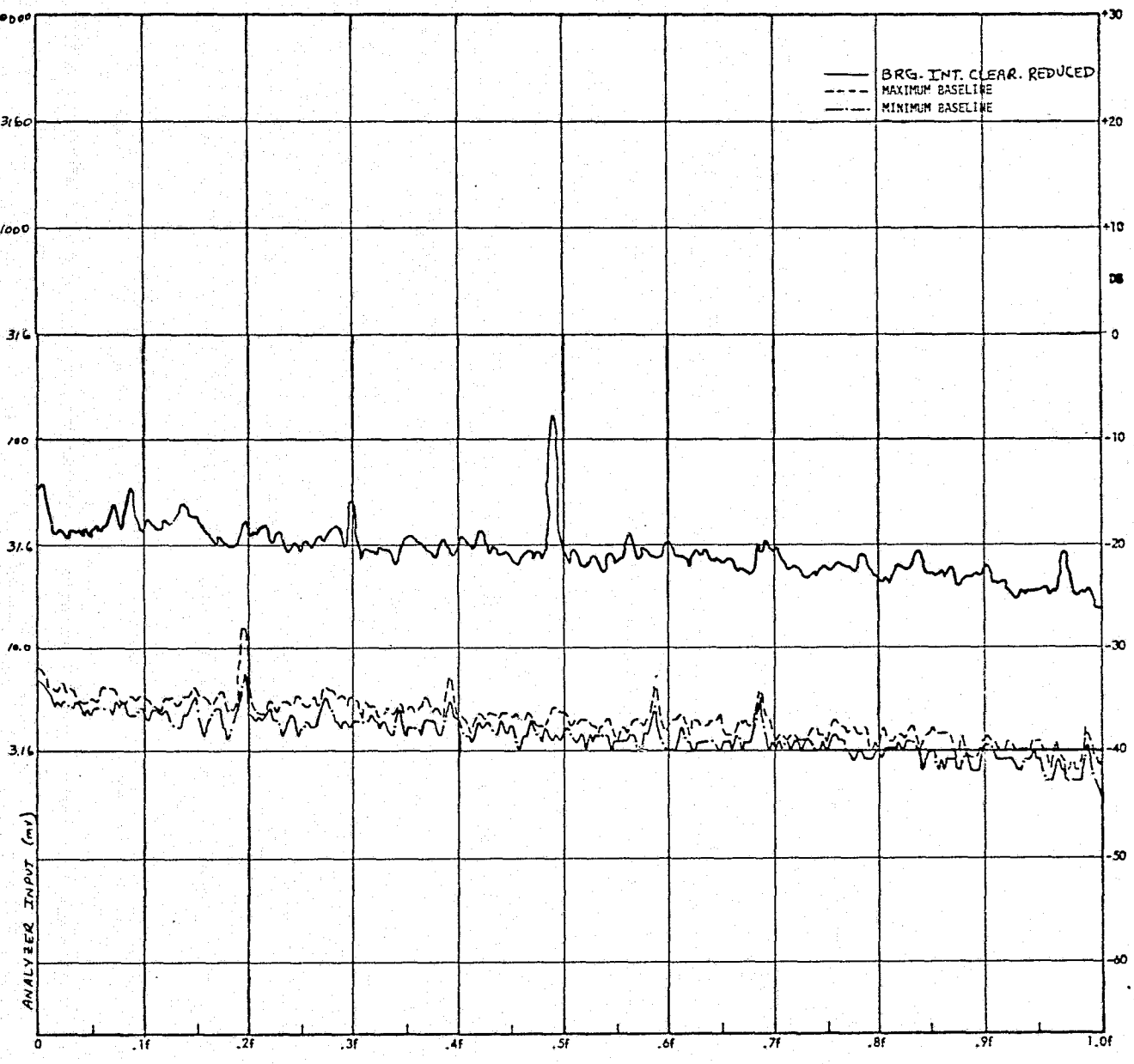

FIG. 95 FREQUENCY SPECTRUM FOR HYDROKINETICS 10461 PUMP

TEST ITEM	HYDROKINETIC 10461 PUMP
PLOT NO.	3
TRANSDUCER	342

CONTROLLED TEST PARAMETERS	
VOLTAGE	115
P. S. FREQ.	400.0
FLOW RATE	7.5×10^{-5} (1.2)

VARIABLE TEST PARAMETERS	BASELINE	FAULT
DATE	7/19-7/22	8-11
I	3.2-3.5	—
ϕ<	.035	—
PWR	348-402	—
PPM	23370-23340	22620
P_S	6900	6900
P_D	652000 - 655000	614000
ΔP	645000 - 646000	607000
TEMP	296-298	297
BARO	101500 - 101700	101600

PROCESSING CHANNEL PARAMETERS	
INPUT RESISTANCE	—
AMPLIFIER GAINS (DB)	
A_1	20
A_2	—
A_3	—
FILTER FREQUENCIES (KHZ)	
BAND PASS	—
HIGH PASS	—
LOW PASS	2

SPECTRUM ANALYZER PARAMETERS	BASELINE	FAULT
INPUT V (MV)	400-800	4000-8200
GAIN SETTINGS (0 DB REF)		
ANALYZER GAIN	20	
INPUT ATTEN.	34.1	
INTEGRATION		
LINEAR	D.C. COUPLE	
32ε/BIN	INTERNAL SAMPLE	
COSINE WEIGHT		

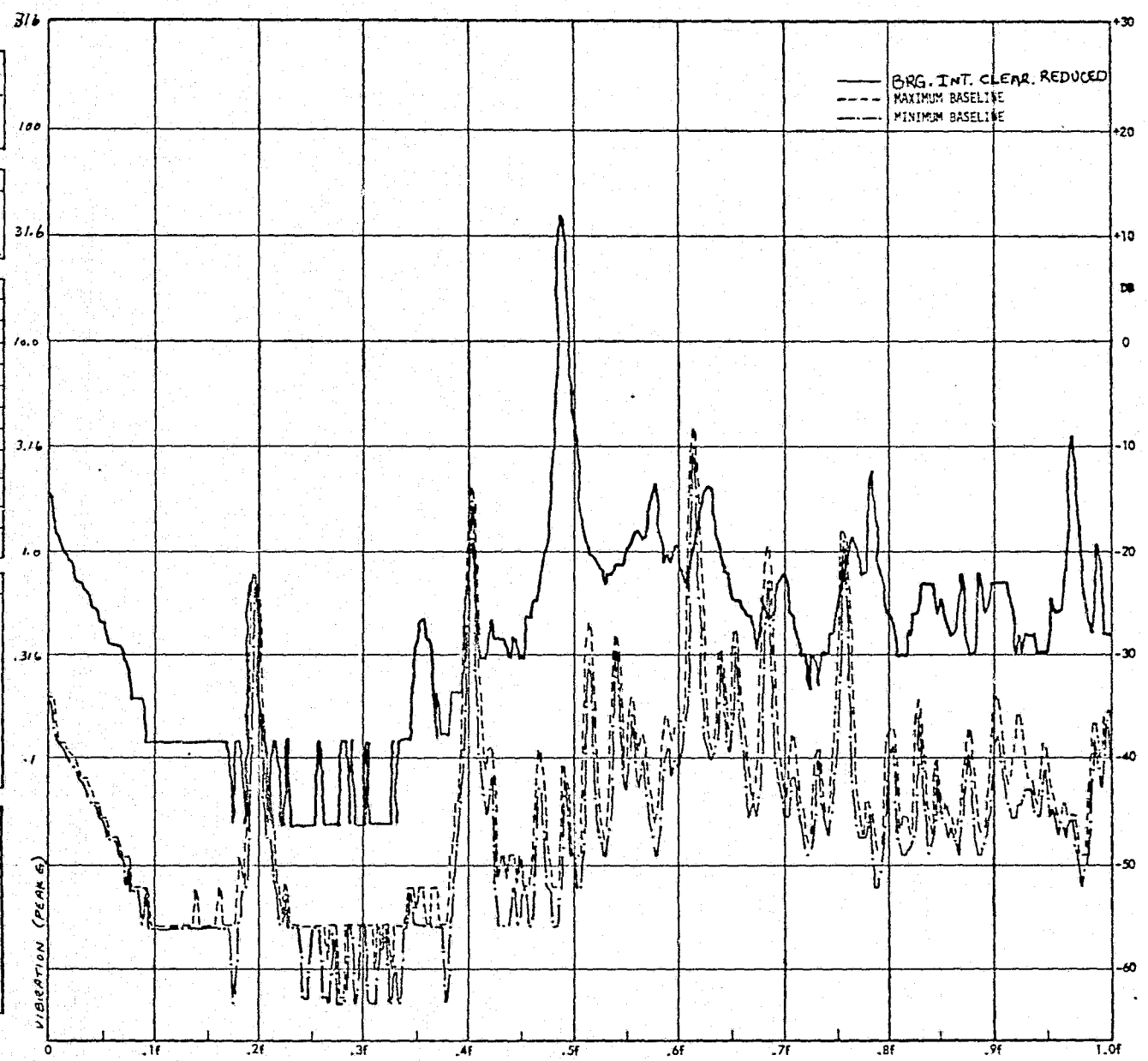

FIG. 96 FREQUENCY SPECTRUM FOR HYDROKINETICS 10461 PUMP

high frequency parameter. Even the low frequency vibration RMS level increased by a factor of 10.25 which was 72% greater than the increase in RMS level at any bandpass frequency.

DATA ASSESSMENT (Reference paragraph 3.2.6 of SOW)

An examination of the results obtained in the preceding paragraph indicates the following requirements for electronic instrumentation which would provide a high probability of detecting incipient defects on environmental control system components.

1. Spectrum analysis of both the low frequency vibration signal and the detected high frequency bandpass acoustic signal are required.

2. Amplitude distribution measurements of the high frequency bandpass acoustic signal are required in addition to the spectrum analysis.

3. Processing for more than a single pass band of high frequencies is required.

For the ten defects examined during this study, a family of statistical parameters which would have been successful in detecting them all with at least a margin of 2:1 over the maximum baseline values would have been:

1. Amplitudes of the baseband vibration spectral lines associated with f_s and f_o.

2. Amplitude of the maximum detected high frequency bandpass spectral line located between the spread of frequencies associated with the components bearing's three major ball passing frequencies, (SADAS-6) for five bandpass frequencies, 8, 20, 50, 125 and 300 KHz.

3. Amplitude of the 3σ spike signal (SEACOST-1) for the five bandpass frequencies in 2.

The results which would have been achieved using these parameters are shown in Table I in the RESULTS paragraph.

A conceptual drawing of a proposed portable instrument, which utilizes all these parameters for detecting incipient defects in rotating machinery is shown in Figure 97. Table XXV provides a list of the instrument's control functions. The instrument has the spectral analysis flexibility of determining the SADAS-5 parameter, in addition to the SADAS-6 parameter, which allows for more detailed detection at the expense of a longer operation time. The drawing shown in Figure 97 shows the major operating controls and indicators. Other indicators such as a calibration/check switch and a battery condition indicator would be included. The instrument could be housed in a 14" x 12" x 12" case and operate off self-contained rechargeable batteries.

The philosophy behind the design of the vibration/acoustic processing instrument would be for the operation to be similar to that of an ordinary electronic tube tester. The operator would just have to make a connection to the

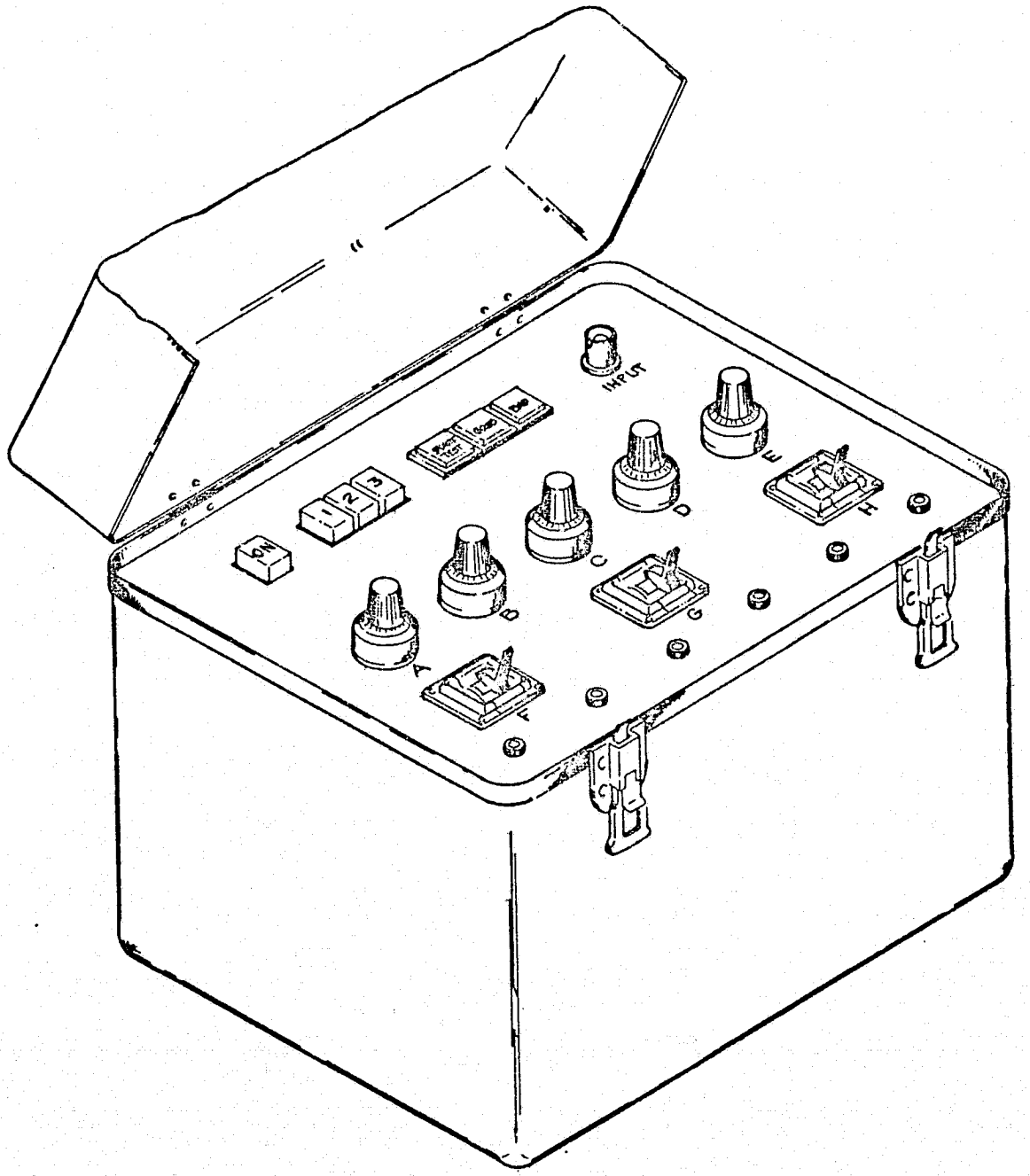

FIG. 97 PORTABLE VIBRATION/ACOUSTIC COMPONENT HEALTH MONITORING INSTRUMENT

TABLE XXV - PROPOSED PORTABLE VIBRATION/ACOUSTIC PROCESSING INSTRUMENT CONTROL FUNCTIONS

Top Row	
ON-OFF SWITCH	Push to turn instrument on and off
TEST SWITCHES	
Switch No. 1	Push to test for RMS signal level exceeding threshold level
Switch No. 2	Push to test for spike energy signal level exceeding threshold level
Switch No. 3	Push to test for a peak spectral line exceeding threshold level
INDICATORS	
START TEST	Push to clear memories and start new test. Light goes on when test starts and off when it is completed.
GOOD	Green light indicates no incipient defect in ECS component under test. On when test switch down.
BAD	Red light indicates an incipient defect in ECS component under test. On when test switch down.
INPUT	Input BNC connector for making connection with sensor cable
Second Row	
POTENTIOMETER A	Sets threshold level for RMS signal
POTENTIOMETER B	Sets threshold level for spike energy signal
POTENTIOMETER C	Sets threshold level for the maximum spectral line in the range of frequencies swept over
POTENTIOMETER D	Sets lower relative sweep frequency for the spectrum analysis
POTENTIOMETER E	Sets upper relative sweep frequency for the spectrum analysis
Third Row	
SWITCH F	Sets frequency band configuration. This switch will set up all filter and input resistance configurations. Thus for low frequency vibration processing it will set up a low pass filter, high input impedance configuration, whereas for high frequencies processing it will set up the appropriate band-pass and lower input resistance configuration.
SWITCH G	Sets coarse circuit gain. This switch will set the circuit gain in 10 db or 20 db steps to the high gains needed for slow speed ECS components or the low gains needed for high speed components.
SWITCH H	Sets spectrum analysis frequency band and analyzing bandwidth
Bottom Row	
TEST PINS	
1	Input signal after amplifying and filtering
2	Envelope detected signal
3	RMS signal output
4	Spike signal output
5	Peak spectral line output
6	Ground

sensor cable from the ECS component he is monitoring, refer to a table in the cover of the instrument for control settings, set the controls, push the START TEST button, wait no more than a minute while processing is taking place while observing the GOOD/BAD indicator to observe if an incipient failure is present in the machine. Thus no operator data assessment is required. In most cases the operator will have to repeat this operation with different control settings to guarantee optimum detectability of the incipient defects. A typical operating sequence may be as follows:

A. Check low frequency vibration RMS level and amplitudes of the baseband vibration spectral lines associated with f_s and f_o.

1. Push ON switch down.

2. Push Switches 1 and 3 down.

3. Set potentiometers A and C to positions determined from previous baseline runs.

4. Set switch H and potentiometers D and E to sweep pass frequency f_s plus a guard band because of inexact knowledge of actual value of f_s.

5. Set switch F to low frequency position and switch G to gain determined from previous baseline runs.

6. Push START TEST and observe GOOD/BAD indicator. If the BAD indicator should go on during the course of the test it will stay on until the START TEST button is pushed again.

7. After START TEST light goes out, indicating that particular test is over, reset potentiometer C to a new threshold level, and switch H and potentiometers D and E to sweep pass frequency f_o plus a guard band.

8. Push START TEST and observe GOOD/BAD indicator for defect.

B. Check for the amplitude of the maximum detected high frequency band pass spectral line located between the bearing's three major ball passing frequencies plus RMS and 3σ spike levels for five bandpass frequencies.

1. After START TEST light goes out for low frequency checks, push switch 2 down.

2. Set potentiometers A, B, C to positions determined from previous runs.

3. Set Switch H and potentiometers D and E to sweep pass bearing frequencies f_o, f_b, and f_i plus a guard band because of inexact knowledge of the exact value of these frequencies.

4. Set Switch F to 8 KHz bandpass and Switch G to gain determined from previous baseline runs.

5. Push START TEST and observe GOOD/BAD indicator for defect.

6. After START TEST light goes out, reset potentiometer A, B, and C; set Switch F to 20 KHz and Switch G to gain determined from previous baseline runs.

7. Push START TEST and observe GOOD/BAD indicator for defect.

8. Repeat steps 6 and 7 for 50, 125, and 300 KHz.

A block diagram of the portable instrument is shown in Figure 98. The IFD sensor is connected to the Input jack. A Calibrate and Check circuit provides a convenient test signal for the calibration and checkout of the instrument. The switch S_F is controlled by the F function switch shown in Table XXV. The S_F positions shown in Figure 98 are for high frequency bandpass operation. The other positions of S_F are for low frequency operation. The input signal can be switched to a high frequency, low noise, low input impedance preamplifier followed by a set of high pass filters or to a low frequency, high impedance preamplifier. The high pass filter selection is also controlled by Switch F. The output from one of the preamplifiers is fed to a variable gain amplifier whose gain can be varied in 10 db steps by Switch G. The high frequency signal from the variable gain amplifier is bandpass filtered and fed to three analyzer circuits. The top analyzer circuit is for determining the 3σ spike level. The output of the AGC circuit has an approximately constant RMS level. The Spike Threshold Detector has a fixed threshold level and only passes that portion of the input signal which exceeds the threshold level, referencing this signal to zero volts. The output of the spike threshold detector is integrated by an exponential integrator and compared against a fixed threshold, set by potentiometer B, in Comparator #2. The center analyzer circuit is for determining the RMS level and consists of an RMS detector, exponential integrator and comparator #1, which compares the output of the integrator with a fixed threshold set by potentiometer A. The bottom analyzer circuit is for performing the SADAS function. A precision detector detects the bandpass signal. The output of this detector is low pass filtered, controlled by Switch H, to eliminate aliasing errors and fed to a mixer. A swept local oscillator, controlled by Switch H and potentiometers D and E, also feeds the mixer. Switch H will select the basic frequency band and potentiometers D and E will set up frequency limits within that frequency band between which the spectrum analysis is done. One set of frequency ranges and analyzer bandwidths which could be used are shown below.

Band No.	Frequency Range (Hz)	Analyzer Bandwidth (Hz)
1	10-40	.58
2	20-80	.82
3	40-160	1.15
4	80-320	1.64
5	160-640	2.31
6	320-1280	3.27
7	640-2560	4.63
8	1280-5120	6.54

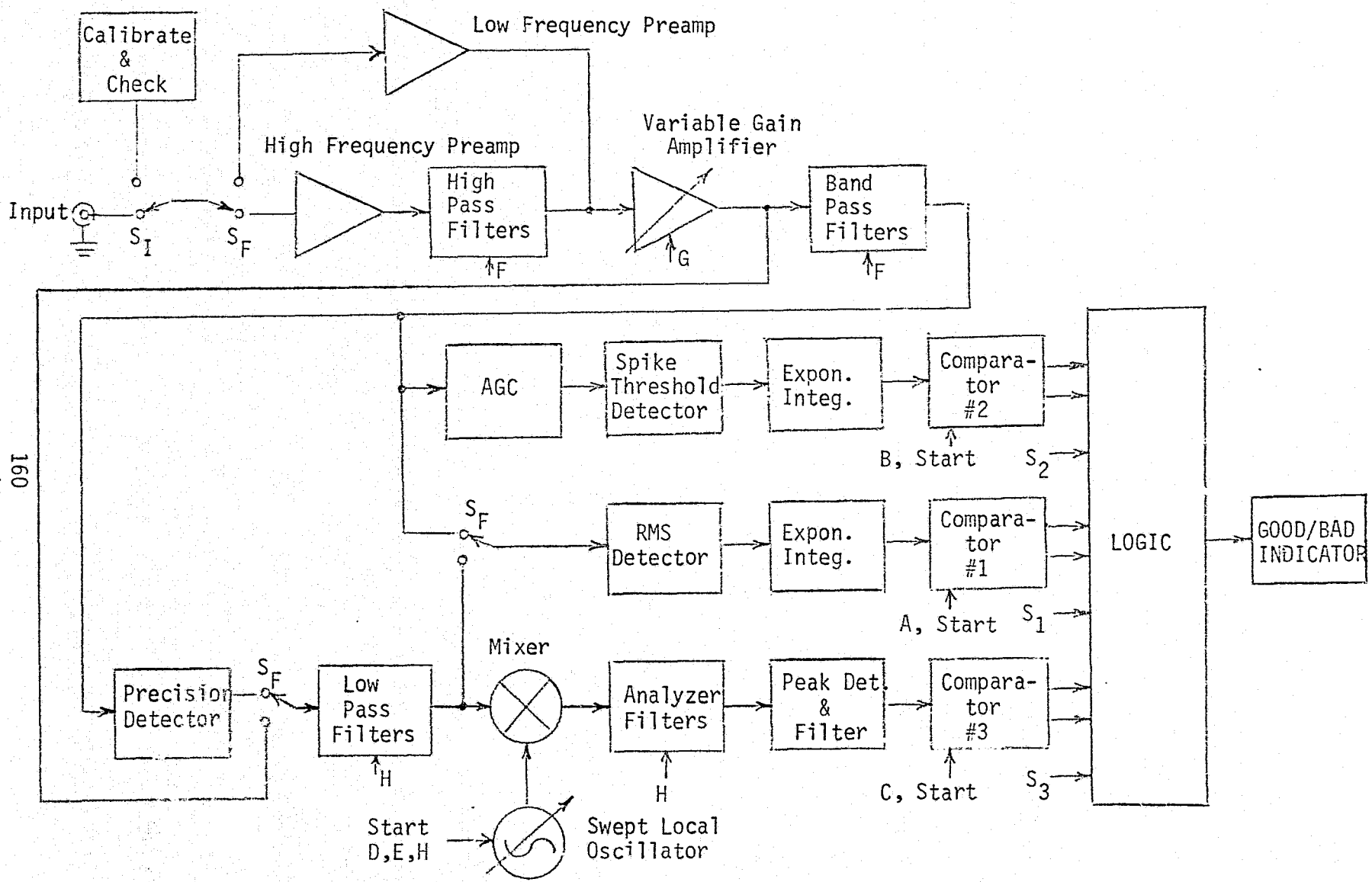

FIGURE 98. PROPOSED PORTABLE VIBRATION/ACOUSTIC PROCESSING INSTRUMENT

The analyzer bandwidths shown above are minimum for a spectrum analysis taking place over a worst case 2-to-1 frequency range and a 1-minute measurement time. Wider analyzer bandwidths or smaller frequency ranges would allow either shorter measurement times or more statistically stable measured data at the expense of defect detectability. The resulting difference signal from the mixer is swept pass the analyzer filters selected by Switch H, to perform the spectrum analysis. The peak detector and filter detects the maximum spectral line amplitude over the frequency band swept by the local oscillator and compares it against a fixed threshold set by potentiometer C in comparator #3. The switches S_1, S_2, and S_3, when operated, allow the comparators to energize the BAD indicator if their thresholds are exceeded.

The RMS and spectrum analyzer circuits are also used for measuring the RMS and spectrum of the low frequency signal when switch S_F is opposite the position shown.

REFERENCES AND BIBLIOGRAPHY

1. Rotron Aximax 2-464-YS Vaneaxial Fan Final Report, IFD Group, Boeing Aerospace Company, Houston, Texas

2. TRW Globe 19A532 Fan Final Report, IFD Group, Boeing Aerospace Company, Houston, Texas

3. Micropump 10-71-316-1367 Pump Final Report, IFD Group, Boeing Aerospace Company, Houston, Texas

4. Dynamic Air Engineering C05OL Centrifugal Fan Final Report, IFD Group, Boeing Aerospace Company, Houston, Texas

5. Hydrokinetics 10461 Pump Final Report, IFD Group, Boeing Aerospace Company, Houston, Texas

6. R. James, B. Reber, B. Baird, W. Neale, "Application of High Frequency Acoustic Techniques for Predictive Maintenance in a Petrochemical Plant," 28th Annual Petroleum Mechanical Engineering Conference, Los Angeles, Calif., 17-20 September 1973